CYTOPLASMIC LIPID DROPLETS IN METABOLIC DISEASE

by

Alyssa S. Zembroski

A Dissertation

Submitted to the Faculty of Purdue University

In Partial Fulfillment of the Requirements for the degree of

Doctor of Philosophy

Department of Nutrition Science

West Lafayette, Indiana

May 2021

To my parents

ACKNOWLEDGMENTS

TABLE OF CONTENTS

LIST OF TABLES

LIST OF FIGURES

ABBREVIATIONS

17β-HSD13	17β-hydroxysteroid dehydrogenase 13
ABHD5	1-acylglycerol-3-phosphate O-acyltransferase ABHD5
ACAT	acyl-CoA:cholesterol acyltransferase
ACC	acetyl-CoA carboxylase
ACS	acyl-CoA synthetase
AGPAT	1-acyl-glycerol-3-phosphate acyltransferase
AMPK	AMP-activated protein kinase
APO	apolipoprotein
ATGL	adipose triglyceride lipase
ATP	adenosine triphosphate
BCAA	branched chain amino acid
CANX	calnexin
CE	cholesteryl ester
CES	carboxylesterase
CCT1	CTP:phosphocholine cytidylyltransferase 1
CD36	fatty acid translocase
CGI-58	comparative gene identification-58
CHO	Chinese hamster ovary
CIDE	cell death-inducing DNA fragmentation factor alpha-like effector
CLD	cytoplasmic lipid droplet
CM	chylomicron
COX	cyclooxygenase
CPT	carnitine palmitoyltransferase
CVD	cardiovascular disease
DAG	diacylglycerol
DAVID	The Database for Annotation, Visualization, and Integrated Discovery
DGAT	diacylglycerol O-acyltransferase
DIO	diet-induced obese
EMT	epithelial-mesenchymal transition

ER	endoplasmic reticulum
ERAD	endoplasmic reticulum-associated degradation
ESI	electrospray ionization
ETC	electron transport chain
FA	fatty acid
FABP	fatty acid binding protein
FAO	fatty acid oxidation
FASN	fatty acid synthase
FF	floating fraction
FIT2	fat storage inducing transmembrane protein 2
FXR	farnesoid X receptor
GAPDH	glyceraldehyde 3-phosphate dehydrogenase
G3P	glycerol-3-phosphate
GLP-1	glucagon-like peptide-1
GLP-2	glucagon-like peptide-2
GO_BP	Gene Ontology Biological Process
GOrilla	Gene Ontology Enrichment Analysis and Visualization Tool
GPAT	glycerol-3-phosphate acyltransferase
HDL	high-density lipoprotein
HMGCS1	hydroxymethylglutaryl-CoA synthase, cytoplasmic
HNRNP	heterogeneous nuclear ribonucleoprotein
HSL	hormone sensitive lipase
ICAT	isotope-coded affinity tags
IAP	intestinal alkaline phosphatase
iTRAQ	isobaric tag for absolute and relative quantification
KEGG	Kyoto Encyclopedia of Genes and Genomes
LAL	lysosomal acid lipase
LC-MS/MS	liquid chromatography tandem mass spectrometry
LDL	low-density lipoprotein
LFQ	label-free quantification
LPL	lipoprotein lipase

LXR	liver X receptor
m/z	mass-to-charge
MAFLD	metabolic associated fatty liver disease
MAG	monoacylglycerol
MALDI	matrix-assisted laser desorption/ionization
MetS	metabolic syndrome
MGAT	acyl-CoA:monoacylglycerol acyltransferase
MGL	monoacylglycerol lipase
MRM	multiple reaction monitoring
MS	mass spectrometry
MS/MS	tandem mass spectrometry
MTTP	microsomal triglyceride transport protein
NAFLD	non-alcoholic fatty liver disease
NASH	non-alcoholic steatohepatitis
NEFA	non-esterified fatty acid
NMR	nuclear magnetic resonance
NSDHL	sterol-4-alpha-carboxylate 3-dehydrogenase, decarboxylating
PCTV	pre-chylomicron transport vesicle
PCYT1A	choline-phosphate cytidylyltransferase A
PG	prostaglandin
PKCζ	protein kinase C zeta
PL	phospholipid
PLA2	phospholipase A2
PLIN	perilipin
PNPLA2	patatin-like phospholipase domain-containing protein 2
PNPLA3	patatin-like phospholipase domain-containing 3
PPAR	peroxisome proliferator-activated receptor
PTM	post-translational modification
PYY	peptide YY
ROS	reactive oxygen species
SAR1B	GTP-binding protein SAR1b

SCD	stearoyl-CoA desaturase
SEC13	protein SEC13 homolog
SEC24C	protein transport protein Sec24C
SILAC	stable isotope labeling of amino acids in cell culture
SQLE	squalene monooxygenase
Sr	serine-arginine-rich
SREBP	sterol response element binding protein
SVIP	small VCP/p97 interacting protein
TAG	triacylglycerol
TCA	tricarboxylic acid
TEM	transmission electron microscopy
TGH	triacylglycerol hydrolase
TMT	tandem mass tag
TRL	triglyceride-rich lipoprotein
UPR	unfolded protein response
VEGF	vascular endothelial growth factor
VAMP7	vesicle-associated membrane protein 7
VLDL	very low-density lipoprotein
WCL	whole cell lysate

ABSTRACT

Metabolic diseases associated with conditions of the metabolic syndrome (MetS) are on the rise in the United States. MetS develops as a consequence of dysfunctional nutrient metabolism, leading to hypertriglyceridemia, insulin resistance, and obesity. These conditions contribute to the development of more serious diseases such as Type 2 diabetes, cardiovascular disease, non-alcoholic/metabolic associated fatty liver disease (NAFLD/MAFLD), and cancer. Therefore, it is important to understand the cellular and molecular factors contributing to metabolic dysfunction and disease progression. A common feature of metabolic disease and its contributing conditions is abnormal lipid metabolism, specifically the accumulation of neutral lipid in cellular cytoplasmic lipid droplets (CLDs). The objective of this dissertation is to examine the role of cytoplasmic lipid droplets in metabolic disease.

First, we investigated CLDs in metastatic breast cancer. CLD accumulation in breast cancer cells is positively associated with cancer aggressiveness; however, the functional consequence of this phenomenon is unclear. The function of CLDs is often reflected by their associated proteins, which regulate both cellular and CLD metabolism. However, the proteome of CLDs in metastatic breast cancer cells has not been described. In this study, we characterized the proteome of CLDs in the human metastatic breast cancer cell line, MCF10CA1a, for the first time. We identified a novel CLD proteome with both similarities and differences to CLDs of other cell types. Overall, this study is the first to analyze the proteins associated with CLDs in metastatic breast cancer cells and in turn produced a hypothesis-generating list of potential proteins involved breast cancer metastasis that can be applied to future studies in order to define the role of CLDs and their proteins in breast cancer metabolism.

Next, we investigated the characteristics and proteome of CLDs in enterocytes of the proximal, middle, and distal regions of the small intestine in the response to dietary fat. Enterocytes of all three regions of the small intestine are capable of packaging and secreting dietary fat on chylomicrons to contribute to blood triacylglycerol (TAG) levels, although to different extents. All regions can also store dietary fat in CLDs, however whether CLDs serve different roles or are differentially metabolized in each region is not clear. Further, obesity has been shown to influence the rate at which dietary fat is absorbed and stored in the middle region of the small intestine, however, whether obesity influences dietary fat storage in the other regions is not known.

Therefore, we examined the effect of intestine region and obesity on the characteristics and proteome of CLDs in the proximal, middle, and distal regions of the small intestine in response to dietary fat to determine potential differences in lipid processing, storage, or CLD metabolism. We found dietary fat storage and CLD proteins varied in each region of the small intestine in lean and diet-induced obese mice, which may indicate differences in dietary fat processing or CLD metabolism in each intestine region. Overall, this study helped to characterize the dynamics of dietary fat absorption along the length of the small intestine and provides insight as to how the process of dietary fat absorption or enterocyte lipid metabolism may be altered in obesity.

Third, we investigated the molecular mechanisms of intestinal lipid mobilization by the enteroendocrine hormone, glucagon-like peptide-2 (GLP-2). GLP-2 has been shown to briefly stimulate the secretion of TAG in chylomicrons from the small intestine hours after the consumption of dietary fat, contributing to blood TAG concentrations. Multiple intestinal TAG pools are potentially mobilized by GLP-2, including those in the lamina propria or lymphatics. However, the exact pool mobilized is not clear. Therefore, we assessed the presence and size of CLDs in human enterocytes as well as the proteome of intestine biopsies to identify the TAG storage pool mobilized by GLP-2 and/or the molecular mediators of GLP-2's effects on TAG mobilization. We identified no differences in CLD characteristics in GLP-2 biopsies compared to placebo, supporting a role for GLP-2 in mobilizing TAG pools outside of enterocytes. Further, we identified several proteins potentially involved in mediating the intestinal response to GLP-2. Overall, this study helped characterize the effect of a novel physiological stimulus on intestinal TAG secretion which has implications in the development of treatment strategies to reduce hyperlipidemia and prevent cardiovascular disease.

Last, we identified and compared the tissue proteome and phosphoproteome of liver in obesity-associated hepatosteatosis to that of lean liver in the postprandial state. The liver plays a central role in the maintenance of systemic nutrient homeostasis during both the fasted and fed states by tightly regulating its cellular metabolic pathways. During obesity, development of hepatosteatosis alters hepatic nutrient utilization, contributing to metabolic dysfunction. The molecular factors that contribute to this metabolic dysfunction, particularly in the fed state, are unclear. Therefore, we performed proteome and phosphoproteome analysis of liver from DIO compared to lean mice in the postprandial state after a lipid meal in order to determine the effect of obesity-associated hepatosteatosis on the liver proteome during the postprandial state. We

identified significant differences in the relative levels of proteins involved in major nutrient metabolic pathways in livers of obese compared to lean mice, indicating changes in hepatic nutrient utilization in obese mice in the postprandial state. Overall, this study helped characterize the liver proteome and phosphoproteome of DIO and lean mice in a controlled postprandial state and uncovered potentially disrupted metabolic pathways contributing to the disorders present in obesity-associated hepatosteatosis.

The four research projects included in this dissertation apply proteomic methods to understand the role of CLDs in metabolic disease. Proteomics is used to characterize the molecular landscape of an experimental model, and we capitalize on the untargeted nature of proteomics in these projects to generate protein datasets that contain numerous candidate proteins contributing to metabolic disease. This research expands our knowledge about the CLD proteome in metastatic breast cancer and in enterocytes during the process of dietary fat absorption in lean and obese states, as well as the liver proteome during obesity-associated hepatosteatosis. As proteins are the core constituents of metabolic pathways in the form of enzymes, transcription factors, and regulatory proteins, identifying the proteome of CLDs and tissues offers a large-scale untargeted molecular view of cellular components that may contribute to metabolic abnormalities and disease. The identification of these factors will allow for the development of targeted therapies modulating cellular lipid storage and its associated consequences present in metabolic disease.

CHAPTER 1 INTRODUCTION

1.1 Metabolic disease and its impact on health

The incidence of metabolic diseases such as Type 2 diabetes, cardiovascular disease (CVD), and non-alcoholic fatty liver disease (NAFLD) (recently termed metabolic associated fatty liver disease/MAFLD [1]) is on the rise in the United States, therefore, understanding how these diseases develop and persist is crucial for their prevention and treatment. Metabolic diseases often develop due to conditions associated with the metabolic syndrome (MetS) [2], which result from abnormal or disrupted metabolic pathways and nutrient utilization. The conditions comprising MetS include obesity, hyperglycemia, hypertriglyceridemia, low high-density lipoprotein (HDL) cholesterol, and high blood pressure [2], with insulin resistance a major driving factor for many of these conditions [3]. It is estimated that greater than one-third of the United States adult population has MetS [4], consistent with the prevalence of adult obesity [5]. As the rate of MetS continues to increase, it is important to understand how its associated conditions contribute to metabolic disease for improved treatment or prevention.

A common theme of metabolic disease is disrupted lipid metabolism. For example, insulin resistance in adipose tissue leads to uncontrolled lipolysis and excess release of non-esterified fatty acids (NEFAs) in circulation. Excess NEFAs are taken up and stored by multiple cell types, contributing to ectopic lipid accumulation [6]. For example, an increase in hepatic lipid substrates increases the amount of triacylglycerol (TAG) synthesized, secreted in very low-density lipoproteins (VLDL), and stored [7]. Further, imbalanced hepatic TAG storage and secretion can lead to lipid accumulation and NAFLD [7]. In addition, chylomicron (CM) secretion from the intestine is also elevated in insulin resistance [8], further increasing blood TAG and cholesterol levels. Excess blood TAG and cholesterol can deposit in arteries and be taken up by macrophages leading to foam cell formation and inflammation, contributing to atherosclerosis and CVD [9]. Finally, a characteristic feature of cancer metabolism is abnormal activity of lipid-related pathways including increased de novo fatty acid (FA) synthesis, fatty acid oxidation (FAO), and TAG storage [10]. Therefore, it is important to understand how lipid metabolism is regulated and how it contributes to metabolic disorders.

1.2 Cytoplasmic lipid droplets (CLDs)

One aspect of lipid metabolism that plays a role in metabolic disease is the storage of cellular lipid in cytoplasmic lipid droplets (CLDs) [11]. CLDs form in almost every cell type as a part of normal cell metabolism and serve as a readily available pool of FA substrate for cellular energy or building needs. However, too much lipid storage in CLDs can be detrimental to cell types that do not typically store large amounts of lipid, resulting in lipotoxicity and negative consequences. In fact, whether the formation of CLDs is a cause or consequence of metabolic disease is still in question. Much progress has been made to understand CLD biology and metabolism in recent years [12]. Collectively, these studies have revealed a fascinating dynamic organelle that, as a key feature of many disorders [13, 14], serves as an attractive target to mitigate or prevent metabolic disease by modulating cellular lipid storage.

1.2.1 General role of CLDs

The major role of CLDs in all cell types is to safely store excess cellular lipid in the form of TAG or cholesteryl esters (CE). By doing so, CLDs protect the cell from lipotoxicity as well as retain energy-dense FA which upon CLD mobilization act as substrate for the synthesis of cellular components and/or provide cellular energy through FAO during times of need. As such, CLDs maintain cellular lipid homeostasis and are therefore key players in the cause or consequence of disrupted lipid metabolism and metabolic disease.

CLD formation is a multistep process [15]. The first step in CLD formation is TAG and CE synthesis, which occurs at the endoplasmic reticulum (ER) membrane using substrates produced inside the cell or those taken up from the circulation. Next, TAG accumulates within the ER bilayer creating a lipid lens that buds from the ER into the cytosol upon reaching a certain size. CLD growth is then facilitated by the localization of TAG synthesis enzymes to the CLD surface or by connections with the ER. Proteins target to CLDs by two defined mechanisms and have many roles within CLD, lipid, and cellular metabolism. Lastly, CLD breakdown is catalyzed by lipolysis which releases FA destined for various fates. The dynamic existence of CLDs demonstrates different aspects of how they may influence or contribute to metabolic dysfunction.

1.2.2 CLD composition

1.2.2.1 Source of lipid

1.2.2.1.1 Intracellular sources

TAG and CE stored in CLDs is synthesized from intra- and/or extracellular sources. Intracellular sources include *de novo*-synthesized FA, cholesterol and glycerol. *De novo* FA or cholesterol synthesis is stimulated by acetyl-CoA substrate from the catabolism of excess cellular carbohydrates and amino acids. The product of *de novo* FA synthesis, palmitate, can be modified into other FA species by elongase or desaturase enzymes such as ELOVL fatty acid elongase 6 [16] and stearoyl-CoA desaturase 1 [17]. Cholesterol is synthesized through the mevalonate pathway by the rate-limiting enzyme, HMG-CoA reductase [18]. Finally, cellular glycerol originates as a by-product of glycolysis, glycerol-3-phosphate (G3P) [19].

1.2.2.1.2 Extracellular sources

Extracellular sources of lipid include FA and cholesterol delivered to cells by lipoproteins or circulating NEFA and glycerol. Lipoproteins including VLDL originating from the liver and CMs from the small intestine carry and deliver TAG and cholesterol to cells. TAG in lipoproteins is hydrolyzed at the cell surface by lipoprotein lipase (LPL), releasing FA that are taken up into cells [20]. Low-density lipoproteins (LDL), the lipoprotein responsible for the majority of cholesterol transport in humans, delivers cholesterol to cells through LDL-receptor-mediated uptake and subsequent degradation [21]. Circulating NEFA and glycerol originate from adipose tissue lipolysis, which is activated by catecholamines during fasting and is elevated during insulin resistance [22].

1.2.2.2 Triacylglycerol and cholesterol synthesis

1.2.2.2.1 Glycerol-3-phosphate pathway of triacylglycerol (TAG) synthesis

TAG is synthesized at the ER membrane by two potential mechanisms: the G3P pathway or the acyl-CoA:monoacylglycerol acyltransferase (MGAT) pathway [23]. Although both pathways have distinct substrate and enzyme components, they share the same final rate-limiting step. The G3P pathway is the predominant TAG synthesis pathway in most cell types [24]. The

first step of the G3P pathway is the addition of a fatty-acyl CoA to G3P by glycerol-3-phosphate acyltransferases (GPAT). The second fatty-acyl CoA is added by 1-acyl-glycerol-3-phosphate acyltransferases (AGPAT). The third and final fatty-acyl CoA is added by diacylglycerol acyltransferases (DGAT). DGAT1 and 2 catalyze the rate-limiting step in TAG synthesis, and these enzymes are imperative for maintaining systemic lipid homeostasis [23]. Although both DGAT enzymes are individually important for TAG synthesis, they are members of different gene families, display different ER membrane topology, and prefer different FA substrates [23]. For example, DGAT1 is a transmembrane protein [25, 26] and shows greater activity towards exogenous FA, while DGAT2 has two transmembrane domains and interacts with CLDs through its C-terminal region [27] and shows greater activity towards endogenous FA [28].

1.2.2.2.2 Acyl-CoA:monoacylglycerol acyltransferase (MGAT) pathway of TAG synthesis

The MGAT pathway supplies the majority of TAG synthesis in enterocytes, the absorptive cells of the small intestine [29]. The first step of the MGAT pathway is the addition of a fatty acyl-CoA to *sn*-2 monoacylglycerol (MAG), which is the major product of dietary fat digestion in the intestinal lumen and is therefore present at high concentrations. The next and final step in the MGAT pathway is addition of a fatty acyl-CoA to diacylglycerol (DAG) catalyzed by DGAT1 or 2, similar to the G3P pathway. DGAT1 and DGAT2 differentially partition TAG in murine enterocytes during the process dietary fat absorption [30]. For example, DGAT1 synthesizes TAG used for the formation of ER luminal lipid droplets and large CMs, while DGAT2 synthesizes TAG used for the formation of nascent CMs for secretion as well as TAG for storage in CLDs [30].

1.2.2.2.3 Cholesteryl ester (CE) synthesis

CE are synthesized at the ER membrane by the esterification of fatty-acyl CoA to cholesterol by acyl-CoA:cholesterol acyltransferase (ACAT) 1 or 2 [31]. Although the predominant neutral lipid stored in CLDs in most cell types is TAG, CE is commonly stored in cell types active in steroid hormone synthesis [32].

1.2.3 CLD formation

Newly synthesized TAG and CE accumulates within the ER bilayer to stimulate CLD formation. CLD formation is a series of steps composed of nucleation, growth, budding, and detachment from the ER (Figure 1-1) [33]. Many recent studies have revealed an important role for ER membrane physics, lipid, and protein composition for initiating and maintaining CLD formation, revealing a complex system of factors influencing this process [34, 35].

1.2.3.1 Budding from the endoplasmic reticulum

The lipid composition of the ER is a major determinant of CLD formation and budding by regulating membrane surface tension. Phospholipids (PL) in the ER with a positive curvature, such as lyso-phosphatidylcholine, favor CLD budding by decreasing ER surface tension, while lipids with a negative curvature, such as DAG and phosphatidylethanolamine, inhibit budding by increasing ER surface tension [36, 37]. Specific proteins within the ER have been shown to regulate the lipid composition of the ER membrane. For example, the putative lipid phosphatase fat storage inducing transmembrane protein 2 (FIT2) localizes to regions of the ER where CLDs form and controls local DAG concentration [36], creating a favorable environment for CLD formation and budding. In support of this, lack of *Fit2* in mice inhibits CLD budding from the ER membrane in enterocytes [38]. In addition to ER membrane lipid composition regulating CLD budding, the concentration of PL in the ER membrane is also important. Budding of CLDs into the cytosol requires an adequate amount of PL on the outer face of the ER membrane to decrease surface tension and allow CLD emergence from the ER [39]. Therefore, regulation of ER membrane surface tension conferred by its intrinsic lipid species is an important factor contributing to CLD formation.

Although CLD formation appears to rely heavily on the intrinsic properties of the ER, several proteins have been shown to facilitate CLD formation and budding. The major protein implicated in this process is seipin, which moves within the ER [40, 41]. Seipin senses regions of CLD formation in the ER due to packing defects in the ER membrane [42], and specifically localizes to ER membrane tubules which are regions favorable for CLD formation [43]. Seipin facilitates CLD formation by maintaining CLD-ER contacts and allows for the addition of TAG from the ER membrane to nascent CLDs through membrane "necks", thereby preventing CLD

ripening [40, 44]. Seipin interacts with multiple proteins in the ER [44, 45], suggesting that seipin may not work alone but in conjunction with protein complexes. In fact, other proteins are implicated in CLD formation due to their ability to maintain CLD-ER contacts [46, 47]. Deficiency or mutations in the seipin gene cause Berardinelli-Seip congenital lipodystrophy [48], confirming a core role for seipin in proper CLD formation and cellular lipid storage.

1.2.3.2 CLD growth

CLDs can grow by reattachment to the ER and migration of TAG synthesis enzymes to the CLD surface, coalescence, and by lipid transfer between CLDs. TAG synthesis enzymes of the G3P pathway have been shown to relocalize from the ER to CLDs through membrane bridges generated by the action of ARF1/COP1 proteins [49, 50]. This population of large CLDs is termed expanding lipid droplets, as opposed to small CLDs which do not harbor TAG synthesis enzymes [49]. In contrast to the complete relocalization of TAG synthesis enzymes to CLDs, DGAT2 has been shown to contact CLDs through its C-terminal region while its transmembrane regions stay in the ER [27]. Similarly, certain populations of CLDs isolated from Chinese hamster ovary K2 (CHO K2) cells have been shown to synthesize TAG and PL in the absence of ER membrane [51], suggesting connection to the ER may not be required for CLD expansion.

Another mechanism responsible for CLD growth is the transfer of TAG from smaller to larger CLDs [52]. This process is mediated by CLD-CLD contacts established by cell death-inducing DNA fragmentation factor alpha-like effector (CIDE) proteins [53]. The three CIDE proteins, CIDEA, CIDEB, and CIDEC have been shown to regulate lipid metabolism in multiple tissues and may contribute to the development of metabolic disease due to their role in regulating lipid storage [53].

The stability of growing CLDs is maintained by the replenishment of the outer PL monolayer. The enzyme responsible for providing PL to growing CLDs is CTP:phosphocholine cytidylyltransferase 1 (CCT1), the rate-limiting enzyme in phosphatidylcholine synthesis. CCT1 senses inadequate phosphatidylcholine levels in the growing CLD monolayer [54] and upon association with CLDs [55] or the nuclear envelope [56] is activated for phosphatidylcholine synthesis. Maintenance of CLD PL concentration by CCT1 is necessary to regulate CLD size and prevent CLD coalescence [57].

1.2.4 CLD proteins

The proteins that associate with CLDs not only play integral roles in CLD and lipid metabolism but also hold novel cellular functions and are implicated in multiple metabolic diseases [14]. Much like the dynamic nature of CLDs, the CLD proteome is diverse and modified based on cell type, metabolic state, and even differs between CLD populations within a cell [51, 58]. Proteomic studies of CLDs in multiple cell types have uncovered commonly identified CLD proteins that have suggested unconventional roles for CLDs besides simply TAG storage [59, 60]. Although the function of the vast majority of CLD proteins has yet to be studied, the proteome of CLDs provides insight as to the functional roles of CLDs in cell metabolism as well as how CLDs and their proteins may contribute to disrupted metabolism in metabolic disease.

1.2.4.1 Protein association with CLDs: Class I and Class II proteins

Unlike other cellular proteins that associate with organelles based on specific targeting sequences [61], no protein targeting sequence specific to CLDs has been identified. Instead, characteristic structural features of CLD proteins have led to their grouping based on their mechanism of association with CLDs [62]. The first group of CLD proteins is Class I proteins, which contain a hydrophobic hairpin loop that is embedded in membranes. The majority of these proteins originate from the ER and associate with CLDs either during their formation or through membrane bridges connecting ER and CLDs [49]. What determines which Class I proteins will reside on CLDs is not clear; however the unique structural features of the CLD PL monolayer may allow for the transfer of only certain monotopic proteins [63], and ER-associated degradation (ERAD) of proteins may also play a role [64, 65]. The second group of CLD proteins is Class II proteins, which originate from the cytosol and contain amphipathic helices. The mechanism of Class II protein targeting to the CLD has recently been defined [66]. Proteins with amphipathic helices sense packing defects in the CLD monolayer, which exposes the neutral lipid core of CLDs and determines protein binding affinity [66, 67]. This binding affinity may act as a source of regulation for the CLD proteome, as Class II proteins with a stronger attachment to CLDs are less likely to be removed by molecular crowding at the CLD surface [66, 68].

1.2.4.2 Types and roles of CLD proteins

The proteins that associate with CLDs can be categorized into several groups, as they are consistently identified in CLD proteomic studies of multiple cell types and organisms [14, 59]. The major group are those proteins involved in CLD maintenance and metabolism, including the Perilipin (PLIN) family of proteins, TAG and PL synthesis enzymes, and lipolytic enzymes [14]. In addition, proteins mediating CLD connections to other organelles including the ER and mitochondria are also key players in the utilization or deposition of lipid substrates stored in CLDs [69]. These proteins play a core role in the regulation of CLD metabolism and by doing so are imperative for the maintenance of cellular lipid storage. Other groups of proteins include histones, proteins involved in cell signaling or trafficking, ribosomal proteins, and those involved in protein degradation [59]. The identification of proteins involved in cellular functions outside of lipid metabolism suggests CLDs serve many roles in addition to lipid storage.

1.2.4.2.1 Perilipins

The most well studied CLD-associated proteins are the PLINs, which surround CLDs and are recognized to protect CLDs from lipolytic breakdown [70]. PLINs associate with the PL monolayer of CLDs through amphipathic helices composed of 11-mer repeats [71, 72], and can replace each other on the CLD surface over time [72]. The first PLIN discovered, PLIN1, was identified in adipocytes as responsible for initiating the lipolytic cascade upon phosphorylation by protein kinase A due to its release of the sequestered co-activator for ATGL, comparative gene identification-58 (CGI-58) [73, 74]. Subsequent studies have identified several other PLIN species (PLIN2-PLIN5) which serve similar but distinct roles. For example, PLIN1 is expressed only in adipocytes, is regulated by phosphorylation to control lipolysis, and promotes TAG storage [75]. On the other hand, PLIN2, which is widely expressed, protects from lipolysis simply by serving as a barrier between lipolytic enzymes and the TAG core of CLDs [76]. Another widely expressed PLIN is PLIN3; however, its function at the CLD is not completely understood. PLIN3 is an exchangeable CLD protein that normally resides in the cytosol but associates with CLDs when CLDs are present in the early stages of fat storage [77, 78]. Although PLIN3 has not directly been shown to prevent lipolysis [70], its association with nascent CLDs and eventual replacement with PLIN2 and PLIN1 in adipocytes for example [77] suggests it stabilizes newly formed CLDs. In

contrast to PLIN1-3, PLIN4 is less well studied. PLIN4 is expressed in white adipocytes [77], and in lower levels in cardio and skeletal myocytes [79]. PLIN4 contains a very large amphipathic helix suited to bind directly to TAG in CLDs in the absence of adequate phosphatidylcholine levels [80], suggesting it may stabilize CLDs when PL is limiting, for example during CLD growth. Further studies are required to determine the role of PLIN4 in CLD maintenance. Lastly, PLIN5 is expressed in highly oxidative cell types such as myocytes and brown adipose tissue as it regulates the association of CLDs with mitochondria and the utilization of FA for FAO [81]. PLIN5 has recently been shown to interact with ATGL and mediate lipolysis in hepatocytes [82] and bind to and transport monounsaturated FA to the nucleus to stimulate PPARα gene expression through activation of the transcriptional regulator sirtuin 1 [83]. Since every CLD houses at least one PLIN species [70], PLINs are crucial CLD-associated proteins that maintain and regulate cellular TAG storage.

1.2.4.2.2 Lipid metabolism enzymes

Enzymes involved in the synthesis and breakdown of neutral lipid stored in CLDs as well as maintenance of the outer PL monolayer are common and well-studied CLD-associated proteins [59]. These include proteins involved in TAG synthesis (GPAT, AGPAT, DGAT, ACSL), TAG breakdown (ATGL, HSL, CGI-58), cholesterol synthesis (NSDHL, LSS), and PL synthesis (CCT1, LPCAT) [60, 65]. Because CLDs must be formed and broken down upon fluctuating cellular signals [58], the presence of enzymes involved in multiple aspects of lipid metabolism on CLDs reflects the dynamic nature and primary role of CLDs in regulating and maintaining cellular lipid storage.

1.2.4.2.3 Proteins mediating connections to organelles

CLDs interact with multiple cellular organelles, including the ER, mitochondria, peroxisomes, lysosomes, and Golgi [69, 84]. These interactions are in part reflected by the identification of organelle-specific proteins on CLDs that are either required for CLD-organelle interactions or are artifacts of contamination due to the close associations of CLDs and organelles. CLDs can associate with other organelles by protein tethers, protein-protein interactions, or by moving along microtubules [85], which allows for the transfer of lipids or proteins between them

depending on cell demand. For example, in COS-7 fibroblast cells, the majority of CLD-organelle interactions occurred with the ER [84], consistent with its important role in CLD biogenesis and growth. However, CLD contacts shifted to mitochondria upon cell starvation in order to facilitate FA transfer for FAO and energy production [84], suggesting that modifying CLD-organelle contacts helps cells respond to stressful environments. One protein that mediates contacts between CLDs and the mitochondria is PLIN5, which regulates the use of CLD FAs for oxidation [81, 86, 87]. Interestingly, PLIN5 also mediates contacts between mitochondria and CLDs for energy production required for TAG synthesis and CLD expansion in brown adipocytes [88]. Overall, CLD-organelle interactions are an important aspect of cell metabolism; however, future studies are required to identify additional molecular mediators of these dynamic interactions.

1.2.4.2.4 Proteins to regulate gene expression

One unique role of CLDs is to regulate gene expression by sequestering histones and transcription factors on their surface. For example, excess histones in *Drosophila melanogaster* embryos accumulate on CLDs and are transferred to the nucleus when needed for growth and development [89, 90]. Although histones are commonly identified in CLD proteomes of multiple cell types and organisms [59], whether a similar phenomenon also occurs in mammalian cells has not been confirmed. In addition to sequestering histones, CLDs influence gene expression by storing or releasing transcription factors upon specific cellular signals [91]. For example, in human macrophages, the MLX family of transcription factors are sequestered on CLDs in response to glucose stimulation, preventing the transcription of genes involved in nutrient metabolism [91]. In fact, inhibiting MLX transcriptional activity modulated glucose uptake, suggesting CLDs can influence cellular metabolic responses to external stimuli by regulating gene expression through protein storage. Therefore, the ability of CLDs to store histones and transcription factors until they are needed suggests CLDs may be a target to modulate gene expression and associated metabolic consequences.

1.2.4.2.5 Proteins targeted for degradation

In addition to protein storage, CLDs are also involved in protein degradation. Several proteins involved in protein ubiquitination and proteasomal degradation have been identified on

CLDs [65], suggesting CLDs contribute to cellular protein control. In fact, certain proteins target to CLDs for their degradation after removal from the ER [92, 93]. One example is apolipoprotein (APO)B-100, which translocates to CLDs from the ER for its proteasomal degradation in Huh7 human hepatocellular carcinoma cells [94, 95]. CLDs therefore play an unanticipated role in protein quality control, which is important during times of ER stress to help facilitate the cellular response and restore ER homeostasis [96].

1.2.4.2.6 Proteins with functional roles—inflammatory signaling

Proteins that reside on CLDs may also serve a functional role instead of being stored or degraded, such as those involved in lipid metabolism as described above. Another example of proteins that serve a functional role on CLDs include those involved in inflammatory eicosanoid signaling such as phospholipase A2 and cyclooxygenase (COX)-1 [97]. Phospholipase A2, which catalyzes the initiating step in prostaglandin synthesis by releasing arachidonic acid from PL membranes [98], localizes to CLDs in IEC-6 rat intestinal epithelial cells [99]. Consistently, CLD accumulation in these cells was associated with arachidonic acid release and prostaglandin (PG) E_2 synthesis. Similarly, COX-2 localizes to CLDs in Caco-2 cells, a model of human colon adenocarcinoma, where it synthesizes PGE_2 and contributes to cell proliferation [100]. Therefore, CLDs partake in inflammatory signaling by not only serving as a docking place for eicosanoid synthesis enzymes but also by providing lipid substrate to potentiate these pathways [101].

1.2.4.2.7 Proteins mediating the immune response

CLD proteins are also involved in the cellular immune response. For example, CLD proteins isolated from livers of mice treated with lipopolysaccharide or mice with sepsis demonstrated antibacterial activity [102]. These antibacterial proteins may transfer from CLDs to bacteria through close associations, as CLDs in *Escherichia coli*-infected macrophages appeared to interact with the bacteria. Several proteins were identified as key mediators of the anti-bacterial response in macrophages, including cathelicidin [102]. Therefore, CLDs may contribute to cellular protection against bacterial infection by housing antibacterial proteins. Some anti-bacterial activity of CLD proteins may be conferred by histones [103]. Histones on CLDs in *Drosophila* confer defense against bacteria and are released from CLDs in response to lipopolysaccharide or

lipoteichoic acid treatment in order to initiate their bactericidal activity [103]. Similarly, the presence of histone H-1 on CLDs in murine livers was increased in response to lipopolysaccharide infection and is also released from CLDs upon exposure to lipopolysaccharide [103]. These results suggest that CLDs play an unappreciated role in innate immunity and may serve as targets to modulate the cellular immune response.

1.2.5 CLD breakdown

CLDs are generally broken down when there is a cellular need for FA, for example during fasting states. CLD breakdown is catalyzed by either cytoplasmic or lysosomal TAG lipolysis, the latter termed lipophagy [104]. Each pathway has different mechanisms and enzymes involved; however, both result in the catabolism of CLDs and release of stored FA. FA released from CLD storage are used for various cell processes depending on the metabolic state and needs of the cell. The ability of CLDs to be synthesized and broken down rapidly contributes to their dynamic nature and adaptability to changing cellular conditions.

1.2.5.1 Cytoplasmic TAG lipolysis

Although most cell types are thought to utilize cytoplasmic TAG lipolysis for CLD breakdown, this pathway has been most studied in adipocytes, the main fat storage cells of the body [105]. Cytoplasmic TAG lipolysis occurs upon the association and activation of lipolytic enzymes on the CLD surface [105]. The first enzyme in this pathway is adipose triglyceride lipase (ATGL), which hydrolyzes a FA from TAG releasing DAG. The activity of ATGL is regulated via interaction with its coactivator CGI-58, which enhances ATGL activity [106]. In adipocytes in basal conditions, CGI-58 associates with PLIN1 on the CLD surface, preventing ATGL activation. Upon lipolytic stimulation, phosphorylation of PLIN1 releases CGI-58, allowing it to associate with and activate ATGL to initiate lipolysis [74]. The essential action of CGI-58 in ATGL activation and the lipolytic cascade is apparent in Chanarin-Dorfman Syndrome, or neutral lipid storage disease, which is characterized by abnormal accumulation of lipid in multiple cell types due to mutations in the *CGI-58* gene and lack of lipolytic TAG breakdown [106-108]. After the lipolytic action of ATGL, DAG is hydrolyzed to FA and MAG by hormone sensitive lipase (HSL). HSL is activated by phosphorylation in the cytosol and subsequent association with CLDs [109].

31

The final step in the cytoplasmic TAG lipolysis pathway is catalyzed by monoacylglycerol lipase (MGL), releasing FA and glycerol [105]. In addition to MAG hydrolysis, MGL also hydrolyzes the endocannabinoid 2-arachidonoylglycerol, therefore contributing to the regulation of endocannabinoid signaling [110].

1.2.5.2 Lysosomal TAG lipolysis

Lysosomal TAG lipolysis, or lipophagy, takes place in lysosomes and is catalyzed by lysosomal acid lipase (LAL) [111, 112]. The process of lipophagy begins with the partial or entire engulfment of a CLD by an autophagosome, which then fuses with a lysosome containing LAL. LAL then hydrolyses TAG or CE to release FA and cholesterol [113]. Lipophagy is an important aspect of CLD breakdown in cell types that store large amounts of lipid, including hepatocytes and enterocytes. Interestingly, it was recently shown that TAG in CLDs can be directly transferred to lysosomes for breakdown in hepatocytes [114], suggesting other unique mechanisms of CLD breakdown exist in the liver. In enterocytes, defective lipophagy contributes to the accumulation and defective mobilization of CLDs in *Dgat1*$^{-/-}$ mice [115]. Defective lipophagy contributes to Wolman disease/cholesteryl ester storage disease, which is the accumulation of TAG and CE due to loss of or defects in LAL function [116], and also contributes to multiple other metabolic disorders [117]. Therefore, lysosomal TAG lipolysis is an important aspect maintaining cellular lipid homeostasis.

1.2.5.3 Interrelationship between cytoplasmic and lysosomal TAG lipolysis

Lysosomal TAG lipolysis and cytoplasmic TAG lipolysis have been shown to be interrelated in the liver, with ATGL working upstream of lipophagy. For example, lipophagy acts on smaller CLDs that result from ATGL-mediated breakdown of large CLDs in murine hepatocytes [118]. In addition, ATGL-mediated lipolysis promotes autophagy by initiating SIRT1 activity in murine hepatocytes, which activates autophagic machinery and related transcription factors [119]. These results suggest that both pathways of CLD breakdown are not mutually exclusive in hepatocytes and may depend on each other to catalyze efficient CLD breakdown.

1.2.6 Fates of fatty acids stored in CLDs

FA stored in CLDs are used for multiple metabolic processes depending on the function and metabolic state of the cell. For example, the utilization of stored lipid in highly oxidative and energy-demanding cell types such as cardiomyocytes is different than the repurposing of stored lipid in secretory cell types including enterocytes and hepatocytes. In addition to providing substrate for core cellular functions, FA released from CLDs serve as signaling molecules that regulate gene transcription and lipid signaling pathways. Therefore, modulating cellular lipid storage in CLDs can have many downstream effects that may either contribute to or ameliorate metabolic disease.

1.2.6.1 Fatty acid oxidation (FAO)

FAs stored in CLDs provide a readily available source of substrate for FAO to produce cellular energy in the form of adenosine triphosphate (ATP). FAO is often active when cellular energy stores are low, such as during fasting, but also provides the majority of cellular energy for highly oxidative and energy-demanding cell types including cardio- and skeletal myocytes on a regular basis. An additional role of FAO during fasting in hepatocytes is the partial oxidation of FA to ketone bodies, which are secreted into circulation and serve as an alternative cellular energy source when glucose levels are low [120]. The majority of FAO occurs in the mitochondria through a series of steps [121]. First, FA enter the mitochondria by carnitine-facilitated transport by carnitine palmitoyltransferase (CPT) 1 and 2. Within the mitochondria, a cyclical sequence of reactions catabolizes FA to acetyl-CoA, which is then shuttled into the tricarboxylic acid (TCA) cycle to produce reducing agents for oxidative phosphorylation and ATP synthesis [121]. CLDs are therefore a valuable cellular energy resource needed to power the fluctuating energy demands of the cell.

The expression of genes involved in FAO are transcriptionally regulated by peroxisome proliferator-activated receptor (PPAR) α, a ligand-activated transcription factor of the PPAR family that controls genes involved in lipid metabolism in a variety of cell types, most notably those with high oxidative capacity [122]. FA are specifically directed to PPARα by ATGL-mediated CLD lipolysis [123-125]. Deficiency of ATGL in cardiomyocytes, whose predominant energy source is FA through FAO [126], leads to massive lipid accumulation, mitochondrial

disfunction, and cardiac abnormalities due to lack of PPARα activation and decreased expression of FAO genes [124]. Therefore, ATGL-mediated CLD-lipolysis and activation of PPARα and FAO is imperative for cardiometabolic health and maintenance of cellular lipid homeostasis.

Another highly oxidative cell type that utilizes FA stored in CLDs for FAO is Type I skeletal muscle fibers [127]. In Type I skeletal muscle fibers, CLDs are found in close proximity with mitochondria [128] and FA in CLDs are oxidized during exercise [129-131]. Consistently, ATGL levels are increased during exercise likely powering CLD lipolysis for FA utilization in FAO [132, 133]. Although an elevated number of CLDs are present in myocytes of trained athletes, presumably an adaptation to their elevated energy requirement, CLDs also accumulate in myocytes of patients with insulin resistance and Type II diabetes [127], suggesting intramuscular CLDs are not always beneficial. This paradigm, called the "athlete's paradox," is in part due to increased efficiency of CLD utilization and greater CLD-mitochondrial contacts in myocytes of athletes, while CLDs in patients with Type II diabetes are less lipolytically active [134]. Overall, the ability to oxidize FA stored in CLDs in myocytes contributes to the high energy requirements of skeletal muscle, especially during exercise, but may also contribute to disease when the efficiency of CLD utilization decreases.

1.2.6.2 Signaling

FA released from CLD breakdown can also be used as signaling molecules [135]. For example, liberated FA can bind to and activate PPAR transcription factors, in turn regulating the expression of genes involved in nutrient metabolism as described above for PPARα [122]. Other members of the PPAR family include PPARβ/δ and PPARγ, and each regulate a different set of genes. For example, PPARβ/δ regulates genes involved in catabolic nutrient pathways, similar to PPARα [136], while PPARγ regulates the expression of genes involved in lipid anabolism and adipocyte differentiation [137]. Because of their ability to regulate gene expression of key factors in nutrient metabolism, pharmacological agonists of PPARs are used as a treatment for conditions associated with MetS. For example, thiazolidinediones target PPARγ to treat Type II diabetes and insulin resistance, whereas fibrates target PPARα to stimulate lipid catabolism [138]. Because FA are generally stored in CLDs before they are utilized [139, 140], modulating CLD breakdown may serve as a therapeutic target to control gene expression and nutrient metabolism.

FA within CLDs can also participate in lipid signaling pathways, including eicosanoid synthesis (as described in Section 1.2.4.2.6). It is possible that certain cell types store a greater proportion of inflammatory lipid species, such as arachidonic acid, in CLDs, making CLDs a central hub for prostaglandin synthesis and signaling [101]. For example, mast cells readily package arachidonic acid in CLDs [141, 142]. Whether arachidonic acid in CLDs is stored in the neutral lipid core or phospholipid monolayer is not currently clear; however several hypotheses exist for how arachidonic acid in mast cell CLDs potentiates eicosanoid synthesis [101].

1.2.6.3 Lipoprotein synthesis

CLDs in hepatocytes and enterocytes serve as substrate for VLDL and CM synthesis, respectively. In hepatocytes, lipid stored in CLDs during times of lipid excess is repackaged into VLDL and secreted into circulation during fasting to deliver FA to tissues in need [140]. In enterocytes during the process of dietary fat absorption, excess dietary lipid not immediately packaged and secreted in CMs is transiently stored in CLDs, which are mobilized at later times and used for CM synthesis [143]. CLD turnover in the major cell types regulating blood TAG concentrations is therefore critical for cellular and systemic lipid homeostasis.

1.2.6.3.1 VLDL secretion in hepatocytes

CLDs in hepatocytes serve as substrate for VLDL synthesis to provide systemic tissues with FA necessary for cellular energy during times of low nutrient availability, such as during fasting. Although hepatocytes can obtain FA from both extracellular and intracellular mechanisms (see Section 1.2.2.1), FA must be first packaged into TAG and CLDs before they are utilized for VLDL synthesis [144, 145]. Because the liver is a major metabolic organ involved in many lipid metabolic pathways, the utilization of cellular lipid specifically for a certain cell process must be regulated by enzyme specificity or modification [146]. Consistently, triacylglycerol hydrolase/carboxylesterase 1 (TGH/CES1) has been identified as the enzyme responsible for mobilization of hepatocyte lipid stores for VLDL assembly [147, 148]. Overexpression of TGH increases VLDL secretion and decreases intracellular TAG stores [148], while loss of TGH led to reduced lipid transfer and lipid accumulation [149], decreased VLDL secretion [150-152], and protected against hepatosteatosis and non-alcoholic steatohepatitis (NASH) [153]. Therefore,

TGH is integral to hepatocyte lipid homeostasis by mediating the balance between TAG storage and secretion and may serve as a potential therapeutic target to modulate blood TAG concentrations [146]. This is an important concept, as imbalanced TAG storage and secretion can lead to NAFLD and perpetuate the conditions present in MetS, discussed below in Section 1.3.1.

1.2.6.3.2 CM secretion in enterocytes

CLDs accumulate in enterocytes as a mechanism to mediate the postprandial triglyceridemic response by regulating the rate of CM secretion, as well as to protect the cell from lipotoxicity [154]. Enterocyte CLDs form in response to large amounts of dietary fat [155], suggesting CLDs serve as an overflow pool of TAG that surpasses the amount that can be packaged and secreted in CMs at one time. Consistently, TAG stored in CLDs is mobilized over time, as enterocyte CLDs gradually decrease in size and are mostly absent by twelve hours after a lipid challenge in mice [155]. Although the exact fate of TAG stored in enterocyte CLDs is uncertain, it is generally accepted that they are utilized for CM synthesis and secretion between meals or during fasting. In fact, certain physiological stimuli have been shown to stimulate the mobilization of intestinal TAG stores hours after consumption of dietary fat [154], including glucose [156-159], sham fat feeding [160], a subsequent meal [161], and the enteroendocrine hormone glucagon-like peptide-2 (GLP-2) [162]. Administration of these factors results in an increase in blood TAG concentrations hours after the postprandial triglyceridemic response, pointing to the utilization of TAG stored in CLDs for CM secretion (discussed in Section 1.3.2.6).

Despite these observations, the lipolytic enzyme responsible for mobilizing CLDs for CM synthesis has not been identified. Loss of enzymes involved in cytoplasmic TAG lipolysis including ATGL and HSL does not alter intestinal TAG secretion [125, 163, 164]. However, lack of MGL or ATGL's coactivator CGI-58 results in reduced TAG secretion [165, 166], suggesting a potential role in CLD lipolysis. Other candidate enzymes responsible for CLD mobilization in enterocytes include the CES family of proteins, which regulate VLDL assembly in hepatocytes [167]. Multiple CES enzymes were recently identified as highly expressed and active in specific regions of the small intestine in mice [168], and have been shown to influence multiple aspects of intestinal lipid metabolism [169, 170]. Therefore, CES enzymes are promising potential factors controlling the utilization of enterocyte lipid stores for CM secretion, similar to their function in the liver.

Lipophagy may also contribute to the mobilization of CLDs for CM synthesis. For example, a defect in the lysosomal breakdown of TAG in enterocytes of *Dgat1*^{-/-} mice contributes in part to delayed CLD mobilization and reduced rate of intestinal TAG secretion [115]. In addition, autophagy is activated in enterocytes in response to a lipid meal in mice and upon exposure to lipid micelles in Caco-2 cells [171]. Inhibiting autophagy in Caco-2 cells results in the accumulation of CLDs and a decrease in APOB-48 secretion [171]. These results suggest lipophagy contributes to lipid homeostasis in enterocytes by catabolizing CLDs for use in CM synthesis and therefore may be an important contributing factor to the regulation of blood TAG concentrations.

1.3 CLDs and their role in metabolic disease

CLDs contribute to metabolic disease when they no longer maintain cellular lipid homeostasis but instead perpetuate disrupted cellular metabolism. Several metabolic diseases are defined by cellular lipid accumulation, including NAFLD [172], multiple types of cancer [173], and atherosclerotic CVD [174]. However, a major question in the field is whether CLDs contribute to or are a consequence of disrupted cellular metabolism and development of metabolic disease. This is difficult to define since multiple factors contribute to cellular lipid accumulation. Because CLDs play an integral role in the pathogenesis of NAFLD, cancer, and CVD, understanding how CLDs accumulate and what their role is in each disease state is imperative in developing therapeutic targets and treatment strategies.

1.3.1 CLDs and non-alcoholic fatty liver disease (NAFLD)

NAFLD (or MAFLD [1]) encompasses a spectrum of liver disorders developing from hepatocyte lipid accumulation. The first stage in NAFLD is simple steatosis defined as greater than five percent of liver weight composed of fat [175]. Hepatosteatosis can develop into more serious conditions such as non-alcoholic steatohepatitis (NASH), with the onset of liver inflammation and fibrosis. NASH can worsen and ultimately result in cirrhosis, hepatocellular carcinoma, and liver failure, making NAFLD a major cause of liver transplant in the United States [176]. The incidence of NAFLD is high, affecting about 25% of the worldwide population [177]. Commonly considered the hepatic manifestation of MetS, NAFLD is a feature of obesity and insulin resistance [177, 178] and is a risk factor for CVD and Type II diabetes [178, 179]. Therefore, understanding the

characteristics and contributing factors to NAFLD is key to preventing its development and/or progression.

CLD accumulation in the liver during NAFLD arises from an imbalance in lipid storage and secretion due to disrupted metabolic pathways and improper cell signaling often present during insulin resistance [172]. Under normal conditions in the fed state, insulin promotes lipogenesis and TAG storage in hepatocytes, while inhibiting the turnover of CLDs for VLDL synthesis [145]. During the fasting state, TAG stored in CLDs is used for VLDL synthesis and secretion to provide systemic tissues with FA, and FAO is also activated to provide cellular energy and/or ketones [7]. However, during insulin resistance, elevated levels of FA substrates are present in hepatocytes [172]. This is due to the acquisition of excess circulating NEFA from uncontrolled adipocyte lipolysis, and elevated *de novo* FA synthesis from heightened glucose catabolism and acetyl-CoA production [180]. These excess FA are packaged into TAG and stored in CLDs, contributing to lipid accumulation. Excess CLDs provide substrate for VLDL synthesis in the absence of fasting due to loss of insulin-mediated control of VLDL secretion [7], contributing to hyperlipidemia. The degree of lipid accumulation in hepatocytes is not able to be overcome by lipid catabolism or secretion, perpetuating a state of lipotoxicity. This lipid overload contributes to ER stress, overproduction of reactive oxygen species (ROS) from elevated compensatory FAO, and inflammation [181], leading to a state of overall metabolic dysfunction and disease development. Because CLDs serve other roles in NAFLD in addition to lipid storage [182], targeting CLD metabolism and its regulation is a promising strategy to prevent or treat NAFLD and its associated disorders.

1.3.1.1 CLD proteins contributing to NAFLD

1.3.1.1.1 PLIN2

Several CLD proteins in hepatocytes have been shown to contribute to NAFLD [14]. For example, PLIN2 is upregulated in NAFLD, consistent with an increase in CLDs [183]. PLIN2 on hepatocyte CLDs contributes to lipid accumulation, as the PLIN family of proteins are thought to protect CLDs from lipolysis [70]. Consistently, overexpression of PLIN2 increases CLD formation and cellular TAG content [76, 184, 185]. Further, transfection of PLIN2 in human embryonic kidney HEK293 cells increases CLD accumulation by preventing the association of ATGL with

CLDs and decreasing lipolysis [76], and also prevents autophagy when overexpressed in McArdle RH 7777 rat hepatoma cells [186]. Consistently, lack of PLIN2 increases ATGL association with CLDs in HEK293 cells [76] and increases autophagic breakdown of CLDs in McArdle RH 7777 cells [186]. Therefore, PLIN2 regulates CLD turnover, suggesting it plays a core role in hepatic lipid homeostasis.

Although promoting TAG storage in CLDs generally protects from lipotoxicity and its negative cellular consequences [187], PLIN2 on CLDs contributes to NAFLD by maintaining the TAG storage pool and promoting excess lipid storage. For example, mice lacking *Plin2* are protected from hepatosteatosis due to lack of CLD accumulation [188-192]. PLIN2 may stimulate CLD formation and TAG accumulation be inhibiting CLD breakdown or by regulating sterol response element binding protein (SREBP) transcriptional activity and promoting the expression of genes involved in lipogenesis [189, 191]. Further, preventing CLD breakdown reduces the catabolism of FA through FAO or their utilization for VLDL secretion, maintaining a high cellular lipid concentration. Preventing CLD breakdown also reduces the ability of FA to signal through PPAR transcription factors, which may influence homeostatic cell sensing mechanisms and alter gene expression. As ATGL associates with CLDs in the absence of PLIN2 [76], and directs FA hydrolyzed from CLDs to FAO by activating PPARα gene expression [123], PLIN2 may prevent CLD and PPARα-mediated FA catabolism in turn promoting storage and NAFLD progression. Consistently, knockdown of *PLIN2* in McA-RH7777 cells decreased CLD accumulation and increased FAO [184]. On the other hand, $Plin2^{-/-}$ mice on a Western diet display decreased mRNA levels of *PPARα* and *Cpt1a* [189], suggesting a different mechanism may exist. Despite a role for PLIN2 in mediating the development of NAFLD, how PLIN2 is regulated in not clear. Nonetheless, PLIN2 may serve as a molecular target to ameliorate NAFLD by modulating its ability to maintain TAG storage in hepatocyte CLDs.

1.3.1.1.2 CIDE proteins

Another protein supporting TAG storage in hepatocyte CLDs during NAFLD is the CIDE family of proteins involved in CLD fusion and growth (see Section 1.2.3.2). CIDEA, CIDEB, and CIDEC are enriched at CLD-CLD contact sites in human hepatocyte carcinoma HepG2 cells to facilitate lipid exchange and the growth of large CLDs [193]. The expression of CIDE proteins is increased in murine liver during obesity-associated hepatosteatosis [193-196] and in response to

high fat feeding [196], consistent with their role in promoting TAG storage. In fact, loss or knockdown of CIDE proteins confers protection from hepatosteatosis and decreases hepatocyte TAG accumulation [193, 194, 196, 197]. The mechanisms of this protection may be due to several reasons. First, the formation of large CLDs catalyzed by CIDE proteins promotes steady TAG storage, as large CLDs are less likely to be broken down by lipases due to a reduced surface area to volume ratio [52, 58]. Second, CIDE proteins may regulate other aspects of hepatocyte lipid metabolism in addition to storage. For example, CIDEB was recently shown to regulate SREBP transcriptional activity by promoting its transport from the ER to the Golgi for processing and activation [198]. SREBP transcription factors control the expression of genes involved in lipogenesis and cholesterol homeostasis [199]; therefore, CIDEB may contribute to hepatosteatosis by stimulating lipid synthesis through SREBP transcriptional activity. In addition, CIDEB is involved in the lipidation and transport of VLDL particles in the liver by mediating the transfer of FA released by CLD lipolysis to VLDL secretion through connection with the ER [200, 201] and by interacting with APOB-100 and promoting VLDL transport vesicle budding [202]. It is possible that CIDEB accumulation on CLDs in NAFLD may facilitate elevated VLDL secretion during insulin resistance, however, it's contribution to VLDL secretion during NAFLD has not been investigated.

1.3.1.1.3 PNPLA3

One CLD protein in particular has a strong correlation with NAFLD: patatin-like phospholipase domain-containing 3 (PNPLA3) [203]. Specifically, the I148M polymorphism in the human *PNPLA3* gene is strongly associated with hepatic TAG accumulation [203-205]. PNPLA3 localizes to ER membranes as well as CLDs [206-209] and its expression is induced in hepatocytes of mice fed a Western diet [210], suggesting it regulates lipid metabolism or storage. However, the function of PNPLA3 is generally unknown [211]. PNPLA3 is closely related to the lipolytic enzyme PNPLA2/ATGL, suggesting TAG accumulation may be due to defective lipolytic function of the I148M gene variant. In fact, multiple studies have identified PNPLA3 to have lipid hydrolase activity [207, 212]. In McA-RH 7777 cells, overexpressing mutant PNPLA3 resulted in lower APOB-100 secretion and increased TAG accumulation [206], consistent with lack of hydrolase activity. However, a different study instead identified PNPLA3 as a lysophosphatidic acid acyltransferase that stimulates TAG and PL synthesis, and had low TAG hydrolase activity

[208]. This led to the hypothesis that the I148M mutant of PNPLA3 instead confers gain of function leading to increased TAG accumulation. Observed differences in the function of PNPLA3 may be due to the use of different cell types, culture conditions, and cell treatments; therefore, conflicting reports make it difficult to distinguish the molecular mechanisms of the role of PNPLA3 in NAFLD.

1.3.1.1.4 17β-HSD13

Lastly, 17β-hydroxysteroid dehydrogenase 13 (17β-HSD13) has also been identified as a hepatic CLD-associated protein associated with NAFLD [211]. 17β-HSD13 is expressed at higher levels in livers of patients with NASH [213], in livers of *db/db* mice and mice fed a high fat diet [214], and in the CLD fraction isolated from livers of patients with steatosis compared to those without steatosis [214]. Interestingly, splice variants of the 17β-HSD13 gene are associated with protection from NAFLD and NASH [215, 216]. Although the localization of 17β-HSD13 on CLDs has been confirmed in multiple hepatocyte models, including HepG2 cells [213, 215], Huh7 cells [214], and human liver samples [214], the role of 17β-HSD13 in NAFLD is not clear. 17β-HSD13 is part of the 17β-HSD family of enzymes involved in steroid and sex hormone metabolism [217], however loss of 17β-HSD13 in mice does not influence reproductive function or sex steroids [218]. Instead, 17β-HSD13 has been shown to have retinol dehydrogenase activity on CLDs [213], suggesting it may contribute to cellular retinoid signaling [219]. In addition, 17β-HSD13 promotes lipogenesis, as overexpression of 17β-HSD13 in HepG2 and Huh7 cells led to CLD accumulation [214]. However, loss of 17β-HSD13 does not completely prevent liver lipid accumulation, as mice lacking 17β-HSD13 develop hepatosteatosis and liver inflammation over time [218]. Future studies are required to determine how 17β-HSD13 on CLDs influences or contributes to NAFLD.

1.3.1.2 Current therapies to treat NAFLD

Although no pharmacological therapies are currently approved for the targeted treatment of NAFLD, several have shown promising effects. Part of the difficulty in treating NAFLD is its multifaceted nature, as it is associated with other metabolic diseases of abnormal lipid accumulation such as obesity and insulin resistance, but also presents with unique features within

hepatocytes including inflammation and oxidative stress which contribute to disease progression [181]. The current recommendation to treat NAFLD is weight loss through lifestyle changes [220]. However, multiple promising therapies targeting lipid metabolism and/or inflammation are in development. Therapies currently aimed towards NAFLD include PPAR and farnesoid X receptor (FXR) agonists, GLP-1 agonists, FGF-21 analogs [220, 221], as well as those targeting inflammatory pathways such as vitamin E [222]. The gut microbiota has also emerged as potential target to treat NAFLD [223]. Future breakthroughs in NAFLD research and success of therapies currently in clinical trials will help in the prevention and treatment of NAFLD and its associated metabolic disorders.

1.3.2 Intestinal dietary fat absorption, CLDs, and cardiovascular disease (CVD)

1.3.2.1 Cardiovascular disease

CVD is the leading cause of death in the United States [224], making it a major public health issue. A contributing factor to CVD is atherosclerosis, which develops from the deposition of cholesterol-containing remnant and oxidized lipoproteins into the arterial subendothelial space and activation of pro-inflammatory foam cells [225]. Plaques that develop with atherosclerosis can worsen over time and lead to an eventual blockage in blood flow, resulting in a heart attack and potentially death. Atherosclerosis develops in part due to a detrimental blood lipid profile termed "atherogenic dyslipidemia," which is defined as elevated blood TAG concentrations and postprandial lipemia, as well as abnormal lipoprotein profiles including reduced HDL, elevated small dense LDL, and elevated remnant lipoproteins [226]. On a molecular level, this pro-atherogenic lipid profile develops from abnormal regulation and activity of systemic lipid metabolism commonly present with insulin resistance, leading to excessive lipoprotein secretion and decreased lipoprotein clearance [226]. Therefore, it is necessary to understand the contributing factors to atherogenic dyslipidemia in order to prevent the development of CVD.

1.3.2.2 Postprandial lipemia

One of the features of atherogenic dyslipidemia is elevated postprandial lipemia, which is the rise in blood lipid concentrations after a lipid-containing meal. In fact, postprandial lipemia is an independent risk factor for CVD, as a greater blood TAG response after a meal is associated

with adverse cardiometabolic outcomes [227, 228]. This is relevant to the general population, as we spend most of the day in the postprandial state. The primary lipoproteins carrying dietary TAG are CMs secreted from the small intestine [143]. Postprandial blood TAG concentrations in healthy individuals generally reach a peak three to four hours after consumption of dietary fat, and TAG is subsequently cleared from circulation within three to five hours to return to baseline [229]. In contrast, in disease states, postprandial blood TAG reaches a greater peak concentration and remains high for a longer period of time [229]. This suggests a potential alteration in either enterocyte lipid metabolism and CM secretion or a defect in circulating lipoprotein clearance.

1.3.2.3 Dietary fat and its impact on health

Dietary fat makes up about 35% of calories consumed in a typical American diet [230]. Dietary fat is required for health, as it provides lipids necessary for bodily function including building blocks for cell membrane synthesis, signaling pathways, and cellular energy, and are of primary importance for infant development and growth. Dietary fat also facilitates the absorption of fat-soluble nutrients including vitamins A, D, E, and K [231], and provides the essential linoleic and α-linolenic FAs, which are required for essential metabolic pathways that maintain overall health and organ function [232]. Although dietary fat is required for health, it can also contribute to metabolic disease. The majority of dietary fat consumed is in the form of TAG, and the FA composition in dietary TAG can differentially influence health. For example, diets rich in saturated FA (and cholesterol) are more likely to contribute to the development of CVD, while diets rich in mono- and polyunsaturated FA are associated with a lower risk of CVD [233, 234]. Therefore, individual FA can have different effects on cellular and systemic metabolism. Dietary TAG can also contribute to metabolic disease due to overconsumption. The 2020-2025 Dietary Guidelines for Americans recommends consuming 27 g of mono- and polyunsaturated FA-containing oils per day on a 2,000 calorie diet [235]. Consumption of saturated fat should be limited to less than ten percent of calories per day and should be replaced by mono- and polyunsaturated FA-containing oils. However, the majority of Americans consume greater than the recommended amount of saturated fat [235]. A high fat diet can contribute to excess fat deposition and hypertriglyceridemia, which can lead to obesity, NAFLD, and CVD [236]. Therefore, over-consumption of dietary fat containing an unfavorable FA composition is a major contributor to the development of metabolic disease.

1.3.2.4 Dietary fat absorption in the small intestine

The small intestine is the major organ responsible for absorbing dietary fat. The efficiency of dietary fat absorption is exceptionally high at 95% [237], in part due to the physiological characteristics of the small intestine. In humans, the small intestine ranges from three to five meters in length and is divided into three anatomical regions: the proximal duodenum, the middle jejunum, and the distal ileum [238]. The duodenum is connected to the stomach and is the region shortest in length. The duodenum is primarily responsible for the digestion and emulsification of dietary fat by the action of pancreatic lipase and bile acids. The transition from the duodenum to the jejunum is demarcated by the ligament of Trietz [238]. The jejunum is the region second longest in length and is responsible for the majority of nutrient absorption due to its very large surface area conveyed by villi and microvilli [239]. The absorption of a low to moderate amount of dietary fat is complete by the end of the jejunum [240, 241]. The final and longest region is the ileum, which is responsible for the reabsorption of bile acids [242], nutrient sensing by enteroendocrine cells [243], and the absorption of dietary fat that escapes absorption in the upper intestine when large amounts of dietary fat are consumed [240, 241]. The ability of all three regions of the small intestine to absorb dietary fat is a significant factor contributing to the efficiency of this process.

1.3.2.4.1 Process of dietary fat absorption

The majority of dietary fat is digested in the duodenum primarily by pancreatic lipase, which is secreted from the pancreas into the intestinal lumen upon the presence of dietary fat [244]. Pancreatic lipase hydrolyzes dietary TAG to FA and *sn*-2 MAG, which are emulsified with bile acids into lipid micelles. Lipid micelles then cross the brush border membrane where the dietary fat digestion products enter enterocytes through passive diffusion and potentially protein-mediated transport [245]. Inside enterocytes, FAs are transported through the cell by fatty acid binding protein (FABP) 1 and/or 2 [246] and activated for their use in metabolic pathways by acyl-CoA synthetases (ACS) [247].

TAG and CM synthesis occur at the ER. TAG is synthesized by the MGAT pathway from *sn-2* MAG and FAs by the sequential action of MGAT2 and DGAT1 and/or 2 [29]. DGAT1 is imperative for TAG synthesis and dietary fat absorption in humans, as genetic deficiency of DGAT1 in humans results in severe fat malabsorption [248, 249]. CMs are synthesized by the

packaging of TAG onto lipid-poor APOB-48 particles (primordial CMs) by microsomal triglyceride transport protein (MTTP), forming pre-CMs [250]. The importance of both APOB and MTTP in the formation of CM and dietary fat absorption is exemplified in the genetic diseases hypobetalipoproteinemia and abetalipoproteinemia, which both result in the cellular accumulation of massive amounts of TAG due to defects in or absence of the APOB or MTTP gene, respectively, which prevent the normal synthesis and/or transport of CMs [251]. Pre-CMs are then packaged into pre-chylomicron transport vesicles (PCTV) for their transport from the ER to the Golgi. The budding of PCTVs from the ER is the rate-limiting step in the process of dietary fat absorption [250]. The PCTV is composed of multiple proteins including APOB-48, fatty acid translocase (CD36), vesicle-associated membrane protein 7 (VAMP7), and FABP1, as well as protein transport protein Sec24C (SEC24C) for Golgi targeting [252]. PCTV budding is initiated by a series of steps [253]. First, GTP-binding protein SAR1b (SAR1B) resides in the cytosol in a protein complex with FABP1, protein SEC13 homolog (SEC13), and small VCP/p97 interacting protein (SVIP). Next, SAR1B is phosphorylated by protein kinase C zeta (PKCζ), which releases FABP1 for association with the PCTV at the ER. FABP1 association stimulates PCTV budding from the ER. The PCTV is then transported to the Golgi where it attaches by SNARE proteins and empties its contents. Pre-CMs are modified in the Golgi by the addition of APOA-1 and glycosylation of APOB-48. Mature CMs then exit the Golgi in an undefined vesicle transport system and are shuttled to the basolateral sides of enterocytes where they are exocytosed into the lamina propria [250]. CMs then enter the central lacteal and are transported through the lymphatic system and eventually emptied into blood circulation through the thoracic duct [254].

In the presence of excess dietary fat, TAG not immediately used for CM synthesis and assembly is instead stored in CLDs. The signal that determines this alternative fate of dietary fat is unclear; however, it may depend on a certain saturation point reached in the CM synthesis pathway [155]. The process of CLD formation in enterocytes is expected to follow that of other cell types (see Section 1.2.3). CLDs in enterocytes are dynamic in nature and rapidly form in response to large amounts of dietary fat [255] and are eventually mobilized and used for CM secretion over time [154]. Consistently, CLDs that form in murine enterocytes after an olive oil gavage are mostly absent after twelve hours [155].

1.3.2.5 TAG storage pools in the small intestine

TAG secreted in enterocyte CM can originate from multiple different pools. First, TAG can originate from the resynthesis of incoming dietary FAs and immediate packaging onto CMs [143]. Second, CLDs present from a previous fatty meal can be broken down by lipolysis and the resulting FAs can be used for TAG and CM synthesis. Third, preformed CMs present in the secretory pathway within enterocytes or in the lamina propria may be mobilized and contribute to blood TAG concentrations. Lastly, CMs present in the lymphatics may also be mobilized [256]. Several physiological factors have been shown to stimulate an early peak in blood TAG during the postprandial lipemic response [154], suggesting they mobilize TAG stored in enterocytes from a previous meal. Therefore, chronic consumption of a high fat diet may result in continuous TAG storage in enterocytes in multiple pools that can potentially contribute to a greater or more sustained postprandial TAG response. The molecular mechanisms of TAG mobilization or the specific TAG storage pool mobilized by each physiological factor is an active area of research.

1.3.2.6 Factors influencing CM secretion and mobilization of stored TAG

1.3.2.6.1 Glucose

Glucose administered orally, enterally, and intravenously stimulates CM secretion from the small intestine, suggesting it influences enterocyte lipid metabolism. First, oral glucose stimulates CM secretion by mobilizing TAG stored in enterocyte CLDs [156, 157]. Consumption of a glucose drink five hours after a high-fat liquid meal results in a peak in plasma CM TAG approximately one hour later. This stimulation of CM secretion is attributable to the mobilization of CLDs in enterocytes, as CLDs were less numerous and smaller with glucose consumption [156, 157]. Although the same response was confirmed in two independent studies, the molecular mechanisms of glucose-mediated CLD mobilization have not been determined. However, proteomic analysis of intestinal biopsies in response to glucose identified several potential players, including syntaxin-binding protein 5 which may be involved in the docking of PCTVs to the Golgi [156]. Future studies are required to elucidate the role of potential molecular players in glucose-mediated CLD mobilization.

Consistent with ingested glucose, glucose present in the intestinal lumen also stimulates intestinal CM TAG secretion. An intraduodenal infusion of a lipid mixture with glucose results in

a higher plasma TAG concentration than infusion of a lipid mixture with saline [158]. This response coincided with a higher plasma triglyceride-rich lipoprotein (TRL) APOB-48 concentration, as both the production rate and catabolic rate of APOB-48 were higher with enteral glucose [158]. These results suggest that consumption of a large amount of carbohydrates or simple sugars may stimulate TAG mobilization and CM production. Whether the mechanism of this effect is similar to that of ingested glucose is not clear, however, elevated *de novo* lipogenesis from excess glucose in this scenario may also contribute to substrates available for CM synthesis and secretion [158, 257].

Hyperglycemia also increases intestinal CM secretion. For example, constant intravenous infusion of a glucose solution during the fed state results in a greater plasma CM TAG and APOB-48 concentration than in subjects receiving saline solution in part due to increased APOB-48 production [159]. Consistently, hyperinsulinemia also stimulates APOB-48 production and CM secretion [258]. Hyperglycemia and hyperinsulinemia are common features of insulin resistance and may therefore contribute to the abnormal blood lipid parameters present during this condition by stimulating intestinal CM secretion [8, 259-261]. Several mechanisms may contribute to this effect. First, excess blood glucose may be utilized by enterocytes for *de novo* FA synthesis, providing more substrate to be used for CM synthesis. Second, glucose may mobilize CLDs already present in enterocytes from a previous high-fat meal as described above. Third, insulin resistance is also associated with an elevated level of NEFAs in the circulation, which may also provide substrate for CM synthesis and stimulate CM secretion [262, 263]. Last, changes in the expression of genes or increased stability of proteins involved in lipid metabolism may enable increased production and secretion of CMs [8]. Therefore, insulin resistance contributes to elevated intestinal CM secretion, which contributes to atherogenic dyslipidemia and CVD risk.

1.3.2.6.2 Sequential meals

Sequential meal studies have demonstrated an early peak in plasma TAG containing lipids ingested with a previous meal upon consumption of a subsequent meal [160, 161, 264]. This "second meal effect" indicates that lipid stored in the small intestine from a previous meal is mobilized upon consumption of a second meal [265]. For example, consumption of a high fat lunch meal containing primarily 18:1 FAs stimulates an early CM TAG peak containing 18:2 FAs from a high fat breakfast [161]. Similar results were obtained using retinyl palmitate in a breakfast meal

[264]. This effect was dependent on the amount of fat in the breakfast meal, as consumption of a low-fat breakfast did not result in the same sharp peak in CM TAG seen with the high-fat breakfast after the lunch meal [161]. Altogether, these results suggest that TAG stored in either CLDs or another storage pool are quickly mobilized from enterocytes in response to an incoming mixed meal. In addition, these results also suggest that high-fat meals or chronic high-fat diets may provide more TAG storage in enterocytes that is mobilized in response to the next meal, contributing to elevated blood TAG concentrations and dyslipidemia associated with high-fat diets [160]. Although relevant to daily life, as we spend the majority of the day in the postprandial state and often eat meals with multiple components, the exact factor responsible for stimulating TAG mobilization upon consumption of a mixed meal is not clear. However, as explained in Section 1.3.2.6.1, glucose may be a contributing factor.

1.3.2.6.3 Sham fat feeding

Sham fat feeding elicits a plasma CM TAG response [160, 266], suggesting that oral taste receptors influence dietary fat absorption. For example, sham feeding of high-fat cream cheese stimulates a brief increase in CM TAG originating from an evening meal [160]. This effect was not observed with sham feeding of low-fat cream cheese. These results suggest that part of the cephalic phase response may be the mobilization of intestinal TAG stores to prime the intestine for incoming dietary fat through fat sensing in the mouth [160]. In fact, multiple FA receptors have been identified and are active in the mouth [267, 268]. However, the molecular and/or signaling connections between fat detection in the mouth and its subsequent effect on intestinal TAG secretion have not been determined.

1.3.2.6.4 Glucagon-like peptide-2 (GLP-2)

GLP-2 is an enteroendocrine hormone secreted from ileal L-cells in response to luminal nutrients [269] and has many roles in intestinal physiology and function [270]. For example, GLP-2 is known to stimulate intestinal growth and nutrient absorption and is therefore used as a treatment for intestinal disorders such as short bowel syndrome [270]. GLP-2 is also a potent stimulus for TAG mobilization from the small intestine [271]. For example, GLP-2 administration in human subjects during constant intraduodenal feeding results in a prompt yet temporary increase

in plasma TAG and TRL-APOB-48 concentrations [162]. Consistently, GLP-2 administration seven hours after consumption of a high-fat meal results in the same effect. A similar intestinal TAG response to GLP-2 administration was observed in mice and hamsters [272, 273], and rats [274], confirming a role for GLP-2 in intestinal TAG mobilization.

Although it is clear that GLP-2 influences CM secretion, the intestinal TAG pool mobilized and the mechanisms behind this effect are not clear. Data from several studies suggests GLP-2 mobilizes post-enterocyte CMs such as those within the lymphatics [256]. First, kinetic modeling [162] suggests that the observed rapid and large increase in APOB-48 secretion was due to the mobilization of unlabeled, pre-formed CMs; this pattern would be unreasonable if APOB-48 was newly synthesized. Pre-formed CM can exist within enterocytes in the secretory pathway, or outside enterocytes in the lamina propria or lymphatics. Consistently, a second study points to the mobilization of CMs within the lymphatics [274]. Comparison between the effects of GLP-2 and glucose on intestinal TAG mobilization in rats revealed differing mechanisms, as intraperitoneal GLP-2 stimulated lymph flow and did not increase CM size, while intraduodenal glucose resulted in increased lymph TAG concentration and larger CMs [274]. These results confirm previous findings that glucose mobilizes TAG within enterocyte CLDs for use in CM synthesis and secretion [156] and suggests GLP-2 likely mobilizes pre-formed CM residing in the lymphatic vasculature.

GLP-2 may stimulate post-enterocyte CM mobilization by several mechanisms. First, the GLP-2 receptor is not expressed in enterocytes [275] but is instead present on components in the intestine lamina propria, including enteric neurons, stromal cells, and myofibroblasts [276, 277], as well as on enteroendocrine cells [278]. This suggests that GLP-2 may exert its effects through the enteric nervous system by modulating intestinal vasodilation and increasing blood or lymph flow [271]. In fact, GLP-2 was shown to stimulate mesenteric blood flow in part by increasing nitric oxide synthase expression and activity in neonatal pigs [279], and nitric-oxide signaling was required for GLP-2-mediated stimulation of CM secretion in hamsters [273]. However, in human subjects, inhibiting nitric oxide synthase did not prevent the intestinal TAG response initiated by GLP-2 [280], suggesting a potential species difference in GLP-2 mechanism of action. Although the data points to an indirect action of GLP-2 on intestinal TAG mobilization, GLP-2 has also been shown to increase the glycosylation of the FA sensor CD36 in enterocytes of hamsters, and CD36 was required to mediate GLP-2's stimulatory effect on CM secretion in mice [272]. This suggests

that GLP-2 may also directly or indirectly influence enterocyte lipid metabolism which may contribute to its effects. Alternatively, GLP-2 may signal through another mechanism, for example through the intestinal insulin-like growth factor-1 receptor [281].

1.3.2.7 Current therapies to treat hyperlipidemia/intestinal CM secretion

Since intestinal CM secretion is a major contributor to blood TAG concentrations and risk of CVD, inhibiting dietary fat absorption and CM secretion is an attractive therapeutic target [8]. However, a major obstacle in inhibiting this process is the likely probability of fat malabsorption, which presents as severe gastrointestinal effects in humans. This makes the development of therapies targeting dietary fat absorption difficult and often unsuccessful.

The anti-obesity drug Orlistat, which inhibits gastric and pancreatic lipase and therefore dietary fat digestion in the intestinal lumen, can reduce the absorption of dietary fat by 30% and therefore promotes weight loss and improves CVD risk factors [282, 283]. However, it's widespread use is limited by its common gastrointestinal side effects [284]. Other therapies to reduce the absorption of dietary fat target enterocyte TAG synthesis, including DGAT1 inhibitors [8]. Loss of or inhibition of DGAT1 in mice confers protection against DIO [285] and results in a lower intestinal TAG secretion rate in response to an olive oil gavage with no apparent fat malabsorption [285-287]. These effects are specific to the intestine, as loss of DGAT1 specifically in the small intestine reduces the postprandial TAG response [287] and protects from atherosclerosis development [288]. In fact, mice expressing DGAT1 only in the small intestine are susceptible to DIO [289]. Although these results are promising in mice, inhibition of DGAT1 in humans leads to severe gastrointestinal effects and fat malabsorption [290, 291], likely due to the lack of DGAT2 in human enterocytes which may partly compensate for lack of DGAT1 in mice [29]. Consistently, mutations in *DGAT1* that decrease its function are associated with congenital diarrhea [248]. However, new compounds targeting DGAT1 are currently in development and show promising effects [8]. Another therapy that targets the intestine to reduce CM secretion is inhibition of MTTP, which is involved in the assembly of CM particles. This drug, called Lomitapide, is currently used as a treatment for familial hypercholesterolemia, a condition that generally leads to CVD [292]. Lomitapide treatment reduces circulating TAG and cholesterol levels by reducing the secretion of intestinal CM and liver lipoproteins into circulation [293].

Therapies designed to treat a variety of metabolic diseases have also been shown to reduce intestinal CM secretion, including GLP-1 receptor agonists, fibrates, statins, and the Type II diabetes drug Metformin [8]. How these therapies decrease CM secretion is unclear; however, reductions in intestinal TAG excursions by these treatments likely contributes to improved metabolic parameters observed with their use.

1.3.3 CLDs and cancer

1.3.3.1 Cancer incidence

Cancer is the second leading cause of death in the United States behind CVD, with an estimated number of 5,200 new cases diagnosed every day [294]. Therefore, understanding the contributing factors to cancer development is necessary in order to prevent the development and progression of this serious disease. The most common type of cancer depends on gender [294]. In men, prostate cancer accounts for 26% of new cases. In women, breast cancer accounts for 30% of new cases. The second and third most common types of cancers are lung and bronchus cancer (12-13%) followed by colon and rectum cancer (8%) for both men and women. Lung and bronchus cancer is responsible for the most cancer-related deaths in both men and women. Prostate cancer is the second-leading cause of cancer-related deaths in males, while breast cancer is the second-leading cause of cancer-related deaths in females [294].

Multiple factors can contribute to cancer development. First, lifestyle factors including dietary habits and level of physical activity can contribute to metabolic diseases such as obesity, which is a risk factor for cancer development [295]. In addition, smoking is a main contributor to lung cancer, which is the leading cause of cancer-related morbidity in the United States [296]. Next, environmental factors such as repeated and prolonged exposure to carcinogens also contribute to cancer development. These include radiation, air pollution, and certain chemicals [297]. Finally, genetic factors also contribute to cancer development, as certain people are predisposed to cancer due to inherited gene polymorphisms [298].

1.3.3.2 Disrupted cellular metabolism in cancer

A characteristic feature of cancer is aberrant cellular metabolism, which allows cancer cells to meet their elevated metabolic needs and survive in stressful conditions [299]. These metabolic

adaptations contribute to several features common among cancer types, termed the "hallmarks of cancer," including enhanced or perpetual activity of growth-related pathways and ignorance of anti-growth signals, unlimited replication ability, continuous angiogenesis, avoiding apoptosis, and tissue invasion and metastasis [300]. Several nutrient metabolic pathways are reprogrammed to contribute to these effects, including glucose and lipid metabolism. For example, elevated glucose uptake and aerobic glycolysis are features of the Warburg effect, which provides rapidly dividing cells with glycolytic intermediates for use as substrates in anabolic pathways [301]. Lipid metabolism is also abnormal, as cancer cells often have an elevated level of lipogenesis, FA uptake and catabolism, heightened cholesterol metabolism, and neutral lipid storage [302]. These changes can benefit cancer cells by altering PL membranes to make them more resistant to lipid peroxidation and more favorable for signaling, providing substrate for energy production or synthesis of cellular components in proliferating cells, or allow cancer cells to better communicate with the surrounding tumor microenvironment [302, 303]. Overall, adaptations in lipid metabolism prime cancer cells for elevated proliferative and migratory capability; therefore, lipids are a crucial factor perpetuating cancer cell survival and metastasis.

1.3.3.3 CLDs in cancer and their hypothesized roles

One adaptation in lipid metabolism adopted by cancer cells is the accumulation of TAG and CE in CLDs [173, 304]. In fact, the degree of CLD accumulation is often positively associated with cancer aggressiveness [96], which is exemplified in breast cancer cells [305, 306]. Inhibiting lipid storage is detrimental to cancer cells, suggesting CLDs play a crucial role in cancer. For example, inhibiting the rate-limiting TAG synthesis enzymes DGAT1 and/or DGAT2 diminishes CLD formation and decreases cancer cell proliferation, migration, and viability [307-310]. However, the exact role of CLDs in cancer is elusive. For example, it is unclear whether CLDs are a result of or contribute to disrupted cancer metabolism. Due to what we know about CLDs in physiological cell states, several hypotheses have been generated for the role of CLDs in cancer [304]. In fact, several of them align with the "hallmarks of cancer" proposed by Hanahan and Weinberg [173].

1.3.3.3.1 CLDs as a FA and cholesterol source

CLDs provide a reliable and sustained source of FA and cholesterol substrate for anabolic, energy-producing, and signaling pathways needed for cancer cell proliferation. Cancer cells often reside in hypoxic environments with fluctuating nutrient conditions due to lack of blood supply [299]. Therefore, storing lipid in CLDs during times of lipid excess is a metabolic adaptation to ensure a continuous supply of FA and/or cholesterol. Consistently, CLDs contribute to cell survival by providing substrate for energy production by FAO during times of starvation [304]. For example, induction of CLD formation in MDA-MB-231 metastatic breast cancer cells contributes to cell survival in serum-starved conditions over time due to the progressive degradation of CLDs [311]. Inhibiting FAO prevents this effect, confirming the use of FA stored in CLDs for energy production through FAO. Further, inhibiting the localization of lipolytic enzymes to the CLD surface and subsequent FAO in transformed *Drosophila* stem cells or human cancer stem cells results in reduced cell growth and tumor formation, suggesting a reliance on the lipolytic breakdown of CLDs for use in FAO to produce cellular energy for cell survival [312]. Lastly, ovarian cells co-incubated with adipocytes store FA released from adipocyte lipolysis in CLDs, which are then used for energy production through FAO to promote tumor growth [313]. Therefore, lipid stored in cancer cell CLDs provide substrate required for high energy demands of cancer cells in nutrient deplete conditions.

Similar to other metabolic pathways, cancer cells also often display disrupted cholesterol metabolism including elevated cholesterol synthesis and storage in CLDs [314]. Cholesterol contributes to cancer progression as it can disrupt or exacerbate cell signaling by altering membrane fluidity and lipid raft formation, or may perpetuate growth signals through the action of steroid hormones [303]. Cholesterol is vital to cancer cell metabolism and survival, as inhibiting cholesterol synthesis in certain types of cancer reduces cancer progression [303, 314]. Therefore, CLDs may provide the cholesterol stores necessary to maintain adequate membrane composition for elevated levels of membrane synthesis in order to facilitate the growth and signaling requirements of metabolically active cancer cells.

1.3.3.3.2 CLDs as a hub for signaling pathways

As described in Section 1.2.4.2.6, proteins involved in eicosanoid signaling localize to and are active on CLDs, suggesting CLDs serve as both substrate and a docking place for lipid-mediated signaling pathways that may stimulate cellular proliferation. The synthesis of one type of eicosanoid, prostaglandins, is initiated by the release of arachidonic acid from PL membranes by phospholipase A_2 (PLA_2) [315]. Next, COX enzymes act on arachidonic acid to form PGH_2. PGH_2 has multiple different fates depending on the prostaglandin synthase enzyme catalyzing the reaction, and can result in the formation of prostaglandins, thromboxanes, or prostacyclins [97]. Arachidonic acid may also be converted into another type of eicosanoid, leukotrienes, by lipoxygenases. These lipid signaling molecules bind to specific receptors to mediate both pro- and anti-inflammatory effects [98]. Eicosanoids have multiple roles in cancer, including stimulating cell proliferation, migration, survival, mediating communication between cancer cells and the tumor microenvironment, and promoting angiogenesis [316]. In fact, eicosanoids are often present at elevated levels in multiple types of cancer. CLDs have been identified as sites of eicosanoid synthesis, as they store arachidonic acid and house eicosanoid-synthesizing enzymes [97, 173]. CLD-associated eicosanoid synthesis contributes to cancer progression [100]. In colon cancer Caco-2 cells, for example, inhibiting either COX-2 or CLD formation reduces PGE_2 synthesis and cell proliferation [100]. These results suggest that CLDs may contribute to high levels of eicosanoids present in cancer cells and the subsequent effects of eicosanoid signaling on cancer cell metabolism.

1.3.3.3.3 CLDs as protection from cellular stress

Cancer cells endure a stressful environment, and CLDs allow cancer cells to adapt to changes in nutritive and metabolic conditions while maintaining a high proliferative capacity. CLDs form in response to physiological stressors, including ER stress [317, 318], lipotoxicity [187], oxidative stress [319, 320], and nutrient deprivation [321], suggesting CLDs are involved in the resolution of these issues [13]. For example, FA storage in CLDs protects from lipid peroxidation and generation of harmful ROS in *Drosophila* glial cells [320]. Cancer cells employ CLDs to mitigate these stressors that are commonly present in the cancer environment [96]. For example, CLDs protect cancer cells from cellular lipotoxicity by sequestering harmful FFA that

may be present in high concentrations due to elevated *de novo* FA synthesis, enhanced FA uptake, or autophagic breakdown of cellular organelles. In MDA-MB-231 metastatic breast cancer cells, CLD accumulation stimulated by secreted PLA$_2$ activity protects cells from lipotoxicity and oxidative stress induced by polyunsaturated FA [322]. Therefore, CLDs help mitigate potentially stressful conditions induced by fluctuating lipid levels by safely storing FA that can cause cell damage and regulating their release.

CLDs also protect cancer cells from ER stress-induced apoptosis by contributing to protein quality control. ER stress is often elevated in cancer cells due to amplified protein synthesis and the pressure of increased cell metabolic activity, leading to protein misfolding in the ER and ROS accumulation [323]. Other factors present in the tumor microenvironment also contribute to ER stress, including hypoxia and imbalanced nutrient flux. The accumulation of misfolded proteins in the ER activates the unfolded protein response (UPR), which is a mechanism to recover ER function and maintain cellular homeostasis and is utilized by cancer cells in multiple stages of cancer progression [323]. Uncontrolled ER stress can lead to apoptosis, suggesting cancer cells adapt to elevated metabolic burden on the ER in order to maintain cell survival. CLDs may help mitigate ER stress and the UPR by assisting with protein degradation. CLDs are thought to contribute to ERAD of proteins due to the localization of ERAD components on CLDs [65]. CLDs may facilitate ERAD by housing proteins destined for degradation, assist in their removal from the ER, or may be closely associated with regions of the ER involved in ERAD [65, 93]. Cancer cells often take advantage of the metabolic adaptations induced by ER stress and the UPR for survival in certain conditions [324]; therefore, CLD-assisted protein degradation may be part of this metabolic adaptation to maintain protein homeostasis and ER function required for cell survival.

1.3.3.4 Cancer treatments targeting lipid metabolism

Due to the integral role of lipids in promoting cancer progression, chemotherapeutic treatments targeting lipid metabolic pathways have been developed. These include therapies to limit FA synthesis (fatty acid synthase (FASN) or acetyl-CoA carboxylase (ACC) inhibitors), FA desaturation (stearoyl-CoA desaturase (SCD) inhibitors—preclinical), FAO (CPT1 inhibitors), FA uptake (CD36 inhibitors), cholesterol synthesis (statins), as well as suppress lipogenic gene transcription (SREBP and liver x receptor (LXR) inhibitors) and activate energy-sensing pathways

that deactivate lipogenesis (AMPK agonists) [10, 303]. However, many challenges exist in developing therapies targeting one aspect of lipid metabolism, as compensation by another avenue can bypass the effects of the treatment. For example, cancer cells may adapt to inhibition of FA synthesis by increasing FA uptake [10]. Therefore, targeting multiple aspects of lipid metabolism may be most effective. Another challenge is preventing detrimental side effects of systemic enzyme inhibition, as these enzymes both contribute to cancer progression in cancer cells themselves but also have physiological roles in normal tissues. Notably, no treatments specifically targeting CLD formation or metabolism have been developed as of yet. However, preventing CLD formation or maintenance by inhibiting TAG synthesis or the localization of PLINs to the CLD surface may serve as a promising chemotherapeutic target due to the involvement of CLDs in multiple central aspects of cancer metabolism.

1.4 Proteomic methods to study metabolic disease

1.4.1 Definition and introduction to proteomics

Proteomics is a field of research that encompasses the identification of proteins, their estimated quantitative levels, interacting partners, and modifications. Similar to other -omics applications, including genomics, lipidomics, and metabolomics [325], proteomic methods can be applied to better understand the molecular features of cell metabolism as proteins represent the functional consequence of gene expression [326]. Modern proteomic approaches employ the use of mass spectrometers for protein identification, and with the help of many technological and methodological advances [327] now have the ability to detect thousands of proteins in a complex mixture.

The major concept utilized for protein detection by mass spectrometry is peptide sequencing by tandem mass spectrometry (MS/MS) [328]. Briefly, proteins in a biological sample are isolated and digested into peptides by enzymes that cleave in specific regions of the amino acid protein sequence, such as trypsin. Next, peptides are introduced into the mass spectrometer gradually by elution from liquid chromatography columns. Peptides are then converted into gas and ionized by electrospray ionization (ESI). Peptides may also be ionized by a different method called matrix-assisted laser desorption/ionization (MALDI), a technique that uses a different method of peptide introduction into the mass [329]. Peptide ions travel through an electric field

within the mass spectrometer and the mass-to-charge ratio (m/z) and intensity for each peptide is recorded to create a mass spectrum. Selected peptide ions are then fragmented through collision-induced dissociation and the m/z of these fragment ions are recorded in a tandem mass spectrum. Information gathered from fragment ions in the tandem mass spectrum are then searched against protein databases using proteomics software and assigned to specific peptide sequences, which allows for the mapping of peptides to their proteins [328]. This technique of identifying proteins from their peptides is called "bottom-up" proteomics, as opposed to "top-down" proteomics, which analyzes intact proteins and is generally used to detect post-translational modifications [330]. Bottom-up proteomics by liquid-chromatography tandem mass spectrometry (LC-MS/MS) is a commonly employed proteomic technique in today's research and has enabled the detection of a multitude of proteins from a myriad of biological systems and therefore has provided a wealth of information in the overall understanding of molecular biology.

1.4.1.1 Types of proteomic studies

Proteins are highly diverse, and the application of multiple different methods is needed in order to understand protein cellular dynamics and complete function. For example, post-translational modifications (PTMs) such as phosphorylation can regulate enzyme activity and cellular signaling [331]. In addition, proteins can interact and form protein complexes that function to propagate cellular signals, catalyze metabolic reactions, or serve regulatory purposes [332]. Further, proteins can reside in specific subcellular compartments required for their proper function. Adding to this complexity of protein dynamics, many of these features are transient in nature, making it challenging to quantify all potential combinations and understand the whole picture as proteomic studies are generally performed in one snapshot in time. The development of innovative proteomic applications and methods along with increased instrument sensitivity for greater resolution and mass accuracy have only begun to uncover the complexities of biological proteomes [327].

1.4.1.1.1 Post-translational modifications (PTMs)

Determining PTMs of proteins can provide insight into protein regulation during physiological and pathophysiological states. Examples of PTMs include phosphorylation,

glycosylation, methylation, acetylation and ubiquitination, each controlling protein function or fate in different ways to contribute to the maintenance of cell metabolism [333]. Protein phosphorylation, which is the addition of a phosphate group most commonly to serine, threonine, or tyrosine residues in the amino acid sequence of a protein, plays an integral role in the regulation of cellular signaling and enzyme activity. Protein phosphorylation is regulated by the action of protein kinases and phosphatases [331]. Protein phosphorylation can activate and deactivate metabolic pathways in the cell; therefore, disrupted and/or abnormal protein phosphorylation can alter the activity of cellular pathways and contribute to dysregulated metabolism and development of metabolic disease. Another PTM is glycosylation, which is the addition of a carbohydrate moiety to proteins [334]. Glycoproteins function in many different aspects of cell biology including cell adhesion, self/non-self recognition, cell receptor activation, and endocytosis [335], and many diseases are associated with defects in protein glycosylation [334]. Methylation and acetylation is the addition of a methyl or acetyl group, respectively, to proteins. Histone methylation and acetylation plays a major role in the epigenetic regulation of gene expression [336]. Lastly, ubiquitination of proteins is commonly used to mark them for proteasomal degradation [337]. Overall, protein PTMs are important regulatory mechanisms that not only greatly diversify the cellular proteome but are necessary for normal cell function.

PTMs usually occur on a small subset of proteins present in a biological sample at one time; therefore, proteomic methods to detect PTM sites generally require the enrichment of modified peptides before analysis in the mass spectrometer [338]. Enrichment can be conducted through several techniques, including by use of antibodies, metabolic labeling, chemical derivatization, or affinity enrichment [338, 339]. For example, phosphoproteins are commonly enriched by ionic-based affinity methods such as PolyMAC [340] which allows for the selective association of phosphopeptides with metal ions and their subsequent analysis by mass spectrometry [339]. Enrichment methods are continuously improving, allowing for the characterization of a greater number of PTMs with high specificity.

1.4.1.1.2 Protein-protein interactions

Cellular proteins often do not act independently but exist in complexes with other proteins. These protein interactions are necessary for signal transduction, efficient reaction catalysis, or serve regulatory functions [332]; disruptions in these interactions may lead to metabolic

derangement. Therefore, identifying protein interacting partners can help in the understanding and targeting of cellular metabolic pathways for metabolic disease treatment. However, protein interactions may be unstable or temporary, making the identification of protein complexes *in situ* a challenge. Despite this obstacle, multiple proteomic methods exist for the determination of protein complexes, including affinity purification, surface-induced dissociation, size-exclusion chromatography [341], native proteomics [342], protein correlation profiling, and proximity labeling [327, 343, 344]. For example, high throughput affinity purification mass spectrometry applied to HEK293T cells identified over 50,000 protein interactions, some of which were associated with annotated diseases [345]. Therefore, identifying protein complexes can help in the understanding of cellular relationships and dynamics that may influence disease development.

1.4.1.1.3 Structural proteomics

Structural proteomics aims to define the three-dimensional structure of proteins [346]. Although appreciating protein function is important, knowing the structure is important for understanding how proteins interact, fold, and function, as well as for the development of structurally specific pharmacological agents targeting certain proteins that contribute to disease. Methods to determine protein structure include x-ray crystallography [346], nuclear-magnetic resonance (NMR)-spectroscopy [347, 348], or recently, cryo-electron microscopy [349]. Other techniques are used to determine conformational aspects of proteins [350]. Structural proteomics helps to connect structure with function and is therefore a developing field in protein research.

1.4.1.2 Proteomic methods and concepts

1.4.1.2.1 Targeted and untargeted proteomic methods

Two types of proteomic analyses are routinely performed: targeted methods, which aim to identify a specific protein or proteins in a sample, and untargeted/shotgun methods, which are exploratory analyses that aim to identify all proteins in a sample [351]. Untargeted proteomic analyses are generally employed to broadly characterize the proteome of cells, organisms, or tissues and are often used as hypothesis-generated experiments to identify proteins of interest for follow-up studies. Targeted methods are more sensitive than untargeted and are therefore commonly used to confirm information gathered in discovery approaches [351]. Targeted methods

of protein identification use a technique called multiple reaction monitoring (MRM), also known as selected reaction monitoring, which entails the selection of specific ions in the mass spectrometer for fragmentation [352]. MRM experiments are predesigned based on the fragmentation features of a particular peptide of interest [353] and can be used to determine changes in the relative levels of the protein between samples [352, 353]. MRM is in contrast to untargeted methods which do not preferentially specify particular proteins for identification. Both methods, either used independently or in conjunction with each other, provide valuable information that can be applied to understanding the relationship between cell proteomes or individual proteins and disease.

1.4.1.2.2 Methods of protein quantification

The two methods used to quantify the levels of proteins in a sample are relative quantification and absolute quantification. Relative quantification can be conducted using label-free methods or by labeling methods. Label-free methods do not require any extra steps in sample preparation and are conducted using the information gathered by the mass spectrometer for each protein. For example, the relative levels of a protein in a sample can be estimated by using the area under the peptide ion peak gathered from the first MS measurement or by spectral counting using information gathered by the second (MS/MS) measurement [354]. The peptide ion peak method is the preferred choice due to higher accuracy [355]. The peptide peak method has been adapted for use in the MaxQuant proteomic software platform [356], as well as other proteomic software [357] and has allowed for the relative label-free quantification of proteins in a wide variety of proteomic studies. Labeling methods, on the other hand, require the incorporation of isotopes into proteins during sample preparation so that identical peptides between groups are similarly detected in the mass spectrometer but uniquely recognized by their mass difference [357]. This concept is utilized in metabolic labeling methods such as stable isotope labeling of amino acids in cell culture (SILAC) [358], or chemical labeling by isotope-coded affinity tags (ICAT) [359]. Other labeling methods include chemical labeling by tandem mass tag (TMT) and isobaric tag for absolute and relative quantification (iTRAQ), and enzymatic ^{18}O labeling [357].

Absolute quantification employs the use of a spike-in internal protein standard of known concentration. For example, a labeled standard is added to the sample during one of several potential steps in sample preparation, and the protein's absolute amount is then based on the ion

intensity ratio between the protein and the standard [360]. Absolute quantification is commonly used in targeted MRM proteomic methods to accurately determine the amount of a specific protein in a sample [361].

1.4.2 Proteomics in the context of metabolic disease

Recent advancements in the field of proteomics have made it an emerging technique to study metabolic disease [325]. As proteins are the core constituents of metabolic pathways in the form of enzymes, transcription factors, and regulatory proteins, defining the proteome and protein PTMs in tissues and cells during disease states offers a molecular view of cellular components that may contribute to metabolic disruption. In addition, proteomic studies also serve as an effective starting place for the identification of new disease biomarkers [362]. Overall, the proteomic characterization of tissues and cells in various disease states has advanced our understanding of contributing factors to disease development, metabolic disruption and general whole cell metabolism. Therefore, proteomics serves as a promising method for the future of disease research.

1.4.2.1 Proteomics to identify disrupted metabolic pathways

Proteomic methods allow for the simultaneous analysis of multiple metabolic pathways at one time due to the large-scale untargeted identification of thousands of proteins that make up these pathways. Although the generation of large proteomic datasets provide a substantial amount of information, it is often difficult to interpret proteomic results in a biological context [325]. However, developments in proteomic analysis software have made it easy to annotate and map identified proteins to molecular functions and metabolic pathways in order to generate hypotheses as to how certain cellular pathways may be differentially active during disease states [363]. Examples of such software include The Database for Annotation, Visualization and Integrated Discovery (DAVID) [364, 365], Gene Ontology Enrichment Analysis and Visualization Tool (GOrilla) [366], STRING [367], Metascape [368], MetaboAnalyst [369], Cytoscape [370], Kyoto Encyclopedia of Genes and Genomes (KEGG) [371], PANTHER [372], and Qiagen Ingenuity Pathway Analysis [373]. Protein network mapping along with statistical analysis can generate associations between metabolic pathway deregulation and disease. For example, statistical analysis of results generated from a comparative shotgun proteomic study of healthy and disease state can

identify significantly up- or down-regulated proteins and indicate the activation or deactivation of their associated metabolic pathways [325]. Comparative proteomic analysis has been applied to the study of multiple metabolic disorders and diseases, including obesity [374], NAFLD [375], diabetes [376], and CVD [377, 378]. These studies have identified proteins and pathways involved in the pathogenesis of metabolic disease and are fundamental to the identification of disease biomarkers for disease diagnosis and treatment.

1.4.2.2 Proteomics to identify disease biomarkers and drug targets

One of the goals in metabolic disease research is to identify proteins that may indicate or contribute to a disease state in order to develop targeted therapies or use for disease detection, and proteomic analysis has been integral to identifying these biomarkers [379, 380]. Biomarkers can be used for several purposes, including disease diagnosis or prognosis, to indicate the degree of disease development, or to evaluate the efficacy of disease treatment [381]. Proteins serve as adequate disease biomarkers since dysregulated activity of specific proteins often contribute to the development of certain diseases. Protein biomarkers for many different diseases have been identified by proteomic methods, including cancer, neurological diseases, and Type 2 diabetes, by using biological sources such as blood, urine, saliva, cerebrospinal fluid, and tissues [362, 382, 383]. However, a challenge in proteomic biomarker research is identifying a functionally relevant candidate biomarker from large datasets generated from discovery studies that will be useful in clinical settings [379, 384]. Several important steps are required to determine the utility and applicability of a new potential biomarker, including qualification, verification, and validation [362, 379]. Therefore, although many candidate biomarkers have been discovered by proteomic analyses in recent years, most are not pursued in part due to the long and rigorous process necessary to establish them as clinically relevant biomarkers [379]. Despite these drawbacks, biomarker identification remains an important proteomic application and tool in metabolic disease research.

1.4.3 Proteomics to study CLDs in metabolic disease

The rapid increase in both CLD and proteomic research has resulted in an interest in CLD proteomes across cell types and disease states [59]. As discussed in Section 1.2.4, the proteins that associate with CLDs regulate both CLD and cellular metabolism. Therefore, identifying CLD-

associated proteins that are associated with metabolic disease provides a therapeutic avenue to prevent or treat these diseases by modulating cellular lipid storage. In fact, many CLD proteins are implicated in a wide spectrum of diseases including NAFLD (discussed in Section 1.3.1.1), CVD, Alzheimer's disease, diabetes, lipodystrophy, obesity, viruses, and cancer [14], which suggests that targeting CLDs and their proteins may serve as novel treatment strategies for multiple disorders of abnormal lipid accumulation.

1.4.3.1 Potential role of CLD proteins in metabolic disease

Although many CLD proteins are associated with disease, how exactly they contribute is generally unclear. Proteins may reside on CLDs and contribute to metabolic disease by several mechanisms. First, CLD-associated proteins may play a functional role at the CLD surface to contribute to lipid accumulation in metabolic disease. Examples of these types of CLD proteins are TAG synthesis (DGAT, MGAT, GPAT) and lipolysis (ATGL, HSL, MGL) enzymes as well as the PLIN family of proteins involved in CLD maintenance [14]. During metabolic disease, aberrant cellular signals may dysregulate these enzymes, i.e. hyperactivating TAG synthesis or inhibiting lipolysis, contributing to CLD growth and cellular lipid accumulation. On the other hand, signals to increase lipolysis can result in an elevated cellular concentration of FA and contribute to lipotoxicity or abnormal lipid signaling. Therefore, inhibiting TAG synthesis and either activating or inhibiting TAG lipolysis is a potential avenue to treat disorders of lipid accumulation and/or inflammation such as obesity. Interfering with the function of other proteins that play a functional role on CLDs including eicosanoid synthesis enzymes can modulate lipid signaling and may also potentially mitigate cellular inflammation and its associated pathologies. This avenue of treatment may prove efficacious in cancer, as increased eicosanoid concentrations and signaling is a feature of certain types of cancer [101].

CLD-associated proteins may also contribute to metabolic disease due to abnormal sequestration on the CLD surface, rendering them unable to perform their usual cellular function. One example is the association of transcription factors or histones with CLDs [89, 91]. Abnormal signaling during metabolic disease may retain transcription factors at the CLD surface preventing them from translocating to the nucleus to initiate gene expression. On the other hand, transcription factors may not be sequestered on CLDs in disease states as in normal conditions which may contribute to abnormal gene expression and metabolic dysregulation. To date, only one family of

transcription factors have been shown to be regulated by CLD association [91]. However, it is possible that the activity of other transcription factors are regulated by CLDs and have potential to be modulated to normalize gene expression in disease states. In addition to transcription factors, other cellular proteins identified in CLD proteomic studies may be mislocalized to CLDs from their normal cell location, potentially disrupting their function. Interestingly, many cellular proteins in murine liver relocalize to CLDs upon development of hepatosteatosis [385]. However, the functional consequence of this phenomenon is not clear.

1.4.3.2 Limitations of CLD proteomic studies

CLD proteins identified in proteomic studies must be validated at the CLD surface by imaging methods before studies to determine their potential role in CLD or cell metabolism should be considered. In many cases, the procedure to isolate CLDs from cells and tissues is not completely pure and results in the presence of other organellar proteins in the isolated CLD fraction and subsequent identification in proteomic studies. In fact, only a small subset of proteins in the CLD fraction isolated from human osteosarcoma U2OS cells or human hepatocellular carcinoma Huh7 cells were identified as high-confidence CLD-associated proteins by affinity labeling, and many commonly identified CLD proteins were determined to be artifacts of contamination [60]. Therefore, confirmation of proteins of interest identified in CLD proteomic studies must be a prerequisite to functional studies in order to correlate cause and effect with CLDs, CLD proteins, and metabolic disease. Further, although CLD proteomic studies have identified many proteins that have generated hypotheses as to how CLDs contribute to metabolic disease, lack of functional studies to determine the role of these proteins at the CLD surface greatly reduces the potential development of targeted therapeutics to treat disorders of CLD accumulation and disrupted lipid metabolism. Part of the difficulty in performing functional studies for identified CLD proteins is choosing a promising and fruitful protein out of a list of potentially hundreds. One technique may be to compare CLD proteomes across cell types, physiological conditions, and disease states in order to identify commonalities or differences in CLD proteins that may indicate a specific role for CLDs or certain CLD proteins in metabolic disease.
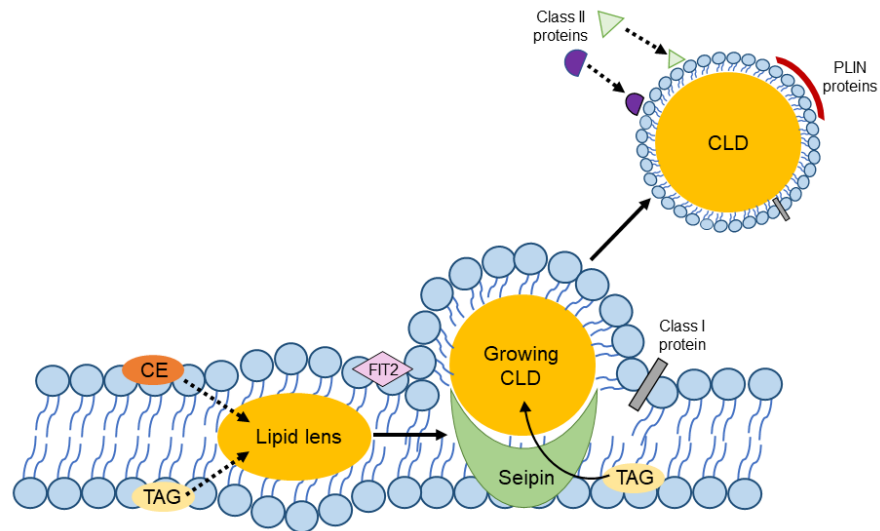
Figure 1-1. Cytoplasmic lipid droplet (CLD) formation at the endoplasmic reticulum (ER) membrane. Triacylglycerol (TAG) and cholesteryl ester (CE) synthesized at the ER membrane accumulates within the ER phospholipid bilayer to form a lipid lens. Upon stabilization of the nascent CLD by seipin (and its interacting partners), seipin facilitates the transfer of additional TAG to the growing CLD. The phospholipid composition of the ER is regulated by proteins such as FIT2 to promote CLD budding. Mature CLDs can bud from the ER membrane surrounded by a phospholipid monolayer, housing Class I proteins. CLDs can acquire Class II proteins from the cytosol. Perilipin (PLIN) proteins surround CLDs to protect from lipolysis and/or regulate CLD breakdown. See Section 1.2.3 for more details.

1.5 References

[1]   M. Eslam, A.J. Sanyal, J. George, MAFLD: A Consensus-Driven Proposed Nomenclature for Metabolic Associated Fatty Liver Disease, Gastroenterology 158(7) (2020) 1999-2014.e1.

[2]   M.G. Saklayen, The Global Epidemic of the Metabolic Syndrome, Curr Hypertens Rep 20(2) (2018) 12.

[3]   M.C. Petersen, G.I. Shulman, Mechanisms of Insulin Action and Insulin Resistance, Physiol Rev 98(4) (2018) 2133-2223.

[4]   J.X. Moore, N. Chaudhary, T. Akinyemiju, Metabolic Syndrome Prevalence by Race/Ethnicity and Sex in the United States, National Health and Nutrition Examination Survey, 1988-2012, Prev Chronic Dis 14 (2017) E24.

[5]   A. Engin, The Definition and Prevalence of Obesity and Metabolic Syndrome, Adv Exp Med Biol 960 (2017) 1-17.

[6]   P. Morigny, M. Houssier, E. Mouisel, D. Langin, Adipocyte lipolysis and insulin resistance, Biochimie 125 (2016) 259-66.

[7]   S.H. Choi, H.N. Ginsberg, Increased very low density lipoprotein (VLDL) secretion, hepatic steatosis, and insulin resistance, Trends Endocrinol Metab 22(9) (2011) 353-63.

[8]   P. Stahel, C. Xiao, A. Nahmias, G.F. Lewis, Role of the Gut in Diabetic Dyslipidemia, Front Endocrinol (Lausanne) 11 (2020) 116.

[9]   M.F. Linton, P.G. Yancey, S.S. Davies, W.G. Jerome, E.F. Linton, W.L. Song, A.C. Doran, K.C. Vickers, The Role of Lipids and Lipoproteins in Atherosclerosis, in: K.R. Feingold, B. Anawalt, A. Boyce, G. Chrousos, W.W. de Herder, K. Dungan, A. Grossman, J.M. Hershman, J. Hofland, G. Kaltsas, C. Koch, P. Kopp, M. Korbonits, R. McLachlan, J.E. Morley, M. New, J. Purnell, F. Singer, C.A. Stratakis, D.L. Trence, D.P. Wilson (Eds.), Endotext, MDText.com, Inc.Copyright © 2000-2021, MDText.com, Inc., South Dartmouth (MA), 2000.

[10]   L.M. Butler, Y. Perone, J. Dehairs, L.E. Lupien, V. de Laat, A. Talebi, M. Loda, W.B. Kinlaw, J.V. Swinnen, Lipids and cancer: Emerging roles in pathogenesis, diagnosis and therapeutic intervention, Adv Drug Deliv Rev 159 (2020) 245-293.

[11]   J.A. Olzmann, P. Carvalho, Dynamics and functions of lipid droplets, Nat Rev Mol Cell Biol 20(3) (2019) 137-155.

[12]   R.A. Coleman, The "discovery" of lipid droplets: A brief history of organelles hidden in plain sight, Biochim Biophys Acta Mol Cell Biol Lipids 1865(9) (2020) 158762.

[13]   F. Geltinger, L. Schartel, M. Wiederstein, J. Tevini, E. Aigner, T.K. Felder, M. Rinnerthaler, Friend or Foe: Lipid Droplets as Organelles for Protein and Lipid Storage in Cellular Stress Response, Aging and Disease, Molecules 25(21) (2020).

[14]   S. Xu, X. Zhang, P. Liu, Lipid droplet proteins and metabolic diseases, Biochim Biophys Acta Mol Basis Dis 1864(5 Pt B) (2018) 1968-1983.

[15]   C.L. Jackson, Lipid droplet biogenesis, Curr Opin Cell Biol 59 (2019) 88-96.

[16]   A. Jakobsson, R. Westerberg, A. Jacobsson, Fatty acid elongases in mammals: their regulation and roles in metabolism, Prog Lipid Res 45(3) (2006) 237-49.

[17]   C.M. Paton, J.M. Ntambi, Biochemical and physiological function of stearoyl-CoA desaturase, Am J Physiol Endocrinol Metab 297(1) (2009) E28-37.

[18]   I. Buhaescu, H. Izzedine, Mevalonate pathway: a review of clinical and therapeutical implications, Clin Biochem 40(9-10) (2007) 575-84.

[19]   S.Y. Lunt, M.G. Vander Heiden, Aerobic glycolysis: meeting the metabolic requirements of cell proliferation, Annu Rev Cell Dev Biol 27 (2011) 441-64.

[20]   P.O. Kwiterovich, Jr., The metabolic pathways of high-density lipoprotein, low-density lipoprotein, and triglycerides: a current review, Am J Cardiol 86(12a) (2000) 5l-10l.

[21]   M.S. Brown, J.L. Goldstein, Receptor-mediated endocytosis: insights from the lipoprotein receptor system, Proc Natl Acad Sci U S A 76(7) (1979) 3330-7.

[22]   R.E. Duncan, M. Ahmadian, K. Jaworski, E. Sarkadi-Nagy, H.S. Sul, Regulation of lipolysis in adipocytes, Annu Rev Nutr 27 (2007) 79-101.

[23]   C.L. Yen, S.J. Stone, S. Koliwad, C. Harris, R.V. Farese, Jr., Thematic review series: glycerolipids. DGAT enzymes and triacylglycerol biosynthesis, J Lipid Res 49(11) (2008) 2283-301.

[24]   H. Wang, M.V. Airola, K. Reue, How lipid droplets "TAG" along: Glycerolipid synthetic enzymes and lipid storage, Biochim Biophys Acta Mol Cell Biol Lipids 1862(10 Pt B) (2017) 1131-1145.

[25]   X. Sui, K. Wang, N.L. Gluchowski, S.D. Elliott, M. Liao, T.C. Walther, R.V. Farese, Jr., Structure and catalytic mechanism of a human triacylglycerol-synthesis enzyme, Nature 581(7808) (2020) 323-328.

[26]   L. Wang, H. Qian, Y. Nian, Y. Han, Z. Ren, H. Zhang, L. Hu, B.V.V. Prasad, A. Laganowsky, N. Yan, M. Zhou, Structure and mechanism of human diacylglycerol O-acyltransferase 1, Nature 581(7808) (2020) 329-332.

[27] P.J. McFie, S.L. Banman, S.J. Stone, Diacylglycerol acyltransferase-2 contains a c-terminal sequence that interacts with lipid droplets, Biochim Biophys Acta Mol Cell Biol Lipids 1863(9) (2018) 1068-1081.

[28] C.L. Yen, M. Monetti, B.J. Burri, R.V. Farese, Jr., The triacylglycerol synthesis enzyme DGAT1 also catalyzes the synthesis of diacylglycerols, waxes, and retinyl esters, J Lipid Res 46(7) (2005) 1502-11.

[29] C.L. Yen, D.W. Nelson, M.I. Yen, Intestinal triacylglycerol synthesis in fat absorption and systemic energy metabolism, J Lipid Res 56(3) (2015) 489-501.

[30] Y.H. Hung, A.L. Carreiro, K.K. Buhman, Dgat1 and Dgat2 regulate enterocyte triacylglycerol distribution and alter proteins associated with cytoplasmic lipid droplets in response to dietary fat, Biochim Biophys Acta 1862(6) (2017) 600-614.

[31] M.A. Rogers, J. Liu, B.L. Song, B.L. Li, C.C. Chang, T.Y. Chang, Acyl-CoA:cholesterol acyltransferases (ACATs/SOATs): Enzymes with multiple sterols as substrates and as activators, J Steroid Biochem Mol Biol 151 (2015) 102-7.

[32] W.J. Shen, S. Azhar, F.B. Kraemer, Lipid droplets and steroidogenic cells, Exp Cell Res 340(2) (2016) 209-14.

[33] A.R. Thiam, E. Ikonen, Lipid Droplet Nucleation, Trends Cell Biol 31(2) (2021) 108-118.

[34] M.F. Renne, Y.A. Klug, P. Carvalho, Lipid droplet biogenesis: A mystery "unmixing"?, Semin Cell Dev Biol 108 (2020) 14-23.

[35] M. Gao, X. Huang, B.L. Song, H. Yang, The biogenesis of lipid droplets: Lipids take center stage, Prog Lipid Res 75 (2019) 100989.

[36] V. Choudhary, G. Golani, A.S. Joshi, S. Cottier, R. Schneiter, W.A. Prinz, M.M. Kozlov, Architecture of Lipid Droplets in Endoplasmic Reticulum Is Determined by Phospholipid Intrinsic Curvature, Curr Biol 28(6) (2018) 915-926.e9.

[37] K. Ben M'barek, D. Ajjaji, A. Chorlay, S. Vanni, L. Foret, A.R. Thiam, ER Membrane Phospholipids and Surface Tension Control Cellular Lipid Droplet Formation, Dev Cell 41(6) (2017) 591-604.e7.

[38] V.J. Goh, J.S. Tan, B.C. Tan, C. Seow, W.Y. Ong, Y.C. Lim, L. Sun, S. Ghosh, D.L. Silver, Postnatal Deletion of Fat Storage-inducing Transmembrane Protein 2 (FIT2/FITM2) Causes Lethal Enteropathy, J Biol Chem 290(42) (2015) 25686-99.

[39] A. Chorlay, L. Monticelli, J. Veríssimo Ferreira, K. Ben M'barek, D. Ajjaji, S. Wang, E. Johnson, R. Beck, M. Omrane, M. Beller, P. Carvalho, A. Rachid Thiam, Membrane Asymmetry Imposes Directionality on Lipid Droplet Emergence from the ER, Dev Cell 50(1) (2019) 25-42.e7.

[40] V.T. Salo, S. Li, H. Vihinen, M. Holtta-Vuori, A. Szkalisity, P. Horvath, I. Belevich, J. Peranen, C. Thiele, P. Somerharju, H. Zhao, A. Santinho, A.R. Thiam, E. Jokitalo, E. Ikonen, Seipin Facilitates Triglyceride Flow to Lipid Droplet and Counteracts Droplet Ripening via Endoplasmic Reticulum Contact, Dev Cell 50(4) (2019) 478-493.e9.

[41] H. Wang, M. Becuwe, B.E. Housden, C. Chitraju, A.J. Porras, M.M. Graham, X.N. Liu, A.R. Thiam, D.B. Savage, A.K. Agarwal, A. Garg, M.J. Olarte, Q. Lin, F. Frohlich, H.K. Hannibal-Bach, S. Upadhyayula, N. Perrimon, T. Kirchhausen, C.S. Ejsing, T.C. Walther, R.V. Farese, Seipin is required for converting nascent to mature lipid droplets, Elife 5 (2016) e16582.

[42] X. Sui, H. Arlt, K.P. Brock, Z.W. Lai, F. DiMaio, D.S. Marks, M. Liao, R.V. Farese, Jr., T.C. Walther, Cryo-electron microscopy structure of the lipid droplet-formation protein seipin, J Cell Biol 217(12) (2018) 4080-4091.

[43] A. Santinho, V.T. Salo, A. Chorlay, S. Li, X. Zhou, M. Omrane, E. Ikonen, A.R. Thiam, Membrane Curvature Catalyzes Lipid Droplet Assembly, Curr Biol 30(13) (2020) 2481-2494.e6.

[44] V.T. Salo, M. Hölttä-Vuori, E. Ikonen, Seipin-Mediated Contacts as Gatekeepers of Lipid Flux at the Endoplasmic Reticulum–Lipid Droplet Nexus, Contact 3 (2020) 1-16.

[45] M. Bohnert, New friends for seipin - Implications of seipin partner proteins in the life cycle of lipid droplets, Semin Cell Dev Biol 108 (2020) 24-32.

[46] V.T. Salo, E. Ikonen, Moving out but keeping in touch: contacts between endoplasmic reticulum and lipid droplets, Curr Opin Cell Biol 57 (2019) 64-70.

[47] N.T. Nettebrock, M. Bohnert, Born this way - Biogenesis of lipid droplets from specialized ER subdomains, Biochim Biophys Acta Mol Cell Biol Lipids (2019).

[48] J. Magre, M. Delepine, E. Khallouf, T. Gedde-Dahl, Jr., L. Van Maldergem, E. Sobel, J. Papp, M. Meier, A. Megarbane, A. Bachy, A. Verloes, F.H. d'Abronzo, E. Seemanova, R. Assan, N. Baudic, C. Bourut, P. Czernichow, F. Huet, F. Grigorescu, M. de Kerdanet, D. Lacombe, P. Labrune, M. Lanza, H. Loret, F. Matsuda, J. Navarro, A. Nivelon-Chevalier, M. Polak, J.J. Robert, P. Tric, N. Tubiana-Rufi, C. Vigouroux, J. Weissenbach, S. Savasta, J.A. Maassen, O. Trygstad, P. Bogalho, P. Freitas, J.L. Medina, F. Bonnicci, B.I. Joffe, G. Loyson, V.R. Panz, F.J. Raal, S. O'Rahilly, T. Stephenson, C.R. Kahn, M. Lathrop, J. Capeau, Identification of the gene altered in Berardinelli-Seip congenital lipodystrophy on chromosome 11q13, Nat Genet 28(4) (2001) 365-70.

[49] F. Wilfling, H. Wang, J.T. Haas, N. Krahmer, T.J. Gould, A. Uchida, J.X. Cheng, M. Graham, R. Christiano, F. Frohlich, X. Liu, K.K. Buhman, R.A. Coleman, J. Bewersdorf, R.V. Farese, Jr., T.C. Walther, Triacylglycerol synthesis enzymes mediate lipid droplet growth by relocalizing from the ER to lipid droplets, Dev Cell 24(4) (2013) 384-99.

[50]   F. Wilfling, A.R. Thiam, M.J. Olarte, J. Wang, R. Beck, T.J. Gould, E.S. Allgeyer, F. Pincet, J. Bewersdorf, R.V. Farese, Jr., T.C. Walther, Arf1/COPI machinery acts directly on lipid droplets and enables their connection to the ER for protein targeting, Elife 3 (2014) e01607.

[51]   S. Zhang, Y. Wang, L. Cui, Y. Deng, S. Xu, J. Yu, S. Cichello, G. Serrero, Y. Ying, P. Liu, Morphologically and Functionally Distinct Lipid Droplet Subpopulations, Sci Rep 6 (2016) 29539.

[52]   F.J. Chen, Y. Yin, B.T. Chua, P. Li, CIDE family proteins control lipid homeostasis and the development of metabolic diseases, Traffic 21(1) (2020) 94-105.

[53]   G. Gao, F.J. Chen, L. Zhou, L. Su, D. Xu, L. Xu, P. Li, Control of lipid droplet fusion and growth by CIDE family proteins, Biochim Biophys Acta Mol Cell Biol Lipids 1862(10 Pt B) (2017) 1197-1204.

[54]   R.B. Cornell, Membrane lipid compositional sensing by the inducible amphipathic helix of CCT, Biochim Biophys Acta 1861(8 Pt B) (2016) 847-861.

[55]   N. Krahmer, Y. Guo, F. Wilfling, M. Hilger, S. Lingrell, K. Heger, H.W. Newman, M. Schmidt-Supprian, D.E. Vance, M. Mann, R.V. Farese, Jr., T.C. Walther, Phosphatidylcholine synthesis for lipid droplet expansion is mediated by localized activation of CTP:phosphocholine cytidylyltransferase, Cell Metab 14(4) (2011) 504-15.

[56]   A.J. Aitchison, D.J. Arsenault, N.D. Ridgway, Nuclear-localized CTP:phosphocholine cytidylyltransferase alpha regulates phosphatidylcholine synthesis required for lipid droplet biogenesis, Mol Biol Cell 26(16) (2015) 2927-38.

[57]   Y. Guo, T.C. Walther, M. Rao, N. Stuurman, G. Goshima, K. Terayama, J.S. Wong, R.D. Vale, P. Walter, R.V. Farese, Functional genomic screen reveals genes involved in lipid-droplet formation and utilization, Nature 453(7195) (2008) 657-61.

[58]   A.R. Thiam, M. Beller, The why, when and how of lipid droplet diversity, J Cell Sci 130(2) (2017) 315-324.

[59]   C. Zhang, P. Liu, The New Face of the Lipid Droplet: Lipid Droplet Proteins, Proteomics 19(10) (2019) e1700223.

[60]   K. Bersuker, C.W.H. Peterson, M. To, S.J. Sahl, V. Savikhin, E.A. Grossman, D.K. Nomura, J.A. Olzmann, A Proximity Labeling Strategy Provides Insights into the Composition and Dynamics of Lipid Droplet Proteomes, Dev Cell 44(1) (2018) 97-112.e7.

[61]   N. Aviram, M. Schuldiner, Targeting and translocation of proteins to the endoplasmic reticulum at a glance, J Cell Sci 130(24) (2017) 4079-4085.

[62]   M.A. Roberts, J.A. Olzmann, Protein Quality Control and Lipid Droplet Metabolism, Annu Rev Cell Dev Biol 36 (2020) 115-139.

[63]   R. Dhiman, S. Caesar, A.R. Thiam, B. Schrul, Mechanisms of protein targeting to lipid droplets: A unified cell biological and biophysical perspective, Semin Cell Dev Biol 108 (2020) 4-13.

[64]   A. Ruggiano, G. Mora, L. Buxo, P. Carvalho, Spatial control of lipid droplet proteins by the ERAD ubiquitin ligase Doa10, Embo J 35(15) (2016) 1644-55.

[65]   K. Bersuker, J.A. Olzmann, Establishing the lipid droplet proteome: Mechanisms of lipid droplet protein targeting and degradation, Biochim Biophys Acta Mol Cell Biol Lipids 1862(10 Pt B) (2017) 1166-1177.

[66]   A. Chorlay, A.R. Thiam, Neutral lipids regulate amphipathic helix affinity for model lipid droplets, J Cell Biol 219(4) (2020) e201907099.

[67]   C. Prevost, M.E. Sharp, N. Kory, Q. Lin, G.A. Voth, R.V. Farese, Jr., T.C. Walther, Mechanism and Determinants of Amphipathic Helix-Containing Protein Targeting to Lipid Droplets, Dev Cell 44(1) (2018) 73-86.e4.

[68]   N. Kory, A.R. Thiam, R.V. Farese, Jr., T.C. Walther, Protein Crowding Is a Determinant of Lipid Droplet Protein Composition, Dev Cell 34(3) (2015) 351-63.

[69]   M. Schuldiner, M. Bohnert, A different kind of love - lipid droplet contact sites, Biochim Biophys Acta 1862(10 Pt B) (2017) 1188-1196.

[70]   C. Sztalryd, D.L. Brasaemle, The perilipin family of lipid droplet proteins: Gatekeepers of intracellular lipolysis, Biochim Biophys Acta Mol Cell Biol Lipids 1862(10 Pt B) (2017) 1221-1232.

[71]   E.R. Rowe, M.L. Mimmack, A.D. Barbosa, A. Haider, I. Isaac, M.M. Ouberai, A.R. Thiam, S. Patel, V. Saudek, S. Siniossoglou, D.B. Savage, Conserved Amphipathic Helices Mediate Lipid Droplet Targeting of Perilipins 1-3, J Biol Chem 291(13) (2016) 6664-78.

[72]   D. Ajjaji, K. Ben M'barek, M.L. Mimmack, C. England, H. Herscovitz, L. Dong, R.G. Kay, S. Patel, V. Saudek, D.M. Small, D.B. Savage, A.R. Thiam, Dual binding motifs underpin the hierarchical association of perilipins1-3 with lipid droplets, Mol Biol Cell 30(5) (2019) 703-716.

[73]   A.S. Greenberg, J.J. Egan, S.A. Wek, N.B. Garty, E.J. Blanchette-Mackie, C. Londos, Perilipin, a major hormonally regulated adipocyte-specific phosphoprotein associated with the periphery of lipid storage droplets, J Biol Chem 266(17) (1991) 11341-6.

[74] J.G. Granneman, H.P. Moore, R. Krishnamoorthy, M. Rathod, Perilipin controls lipolysis by regulating the interactions of AB-hydrolase containing 5 (Abhd5) and adipose triglyceride lipase (Atgl), J Biol Chem 284(50) (2009) 34538-44.

[75] D.L. Brasaemle, B. Rubin, I.A. Harten, J. Gruia-Gray, A.R. Kimmel, C. Londos, Perilipin A increases triacylglycerol storage by decreasing the rate of triacylglycerol hydrolysis, J Biol Chem 275(49) (2000) 38486-93.

[76] L.L. Listenberger, A.G. Ostermeyer-Fay, E.B. Goldberg, W.J. Brown, D.A. Brown, Adipocyte differentiation-related protein reduces the lipid droplet association of adipose triglyceride lipase and slows triacylglycerol turnover, J Lipid Res 48(12) (2007) 2751-61.

[77] N.E. Wolins, B.K. Quaynor, J.R. Skinner, M.J. Schoenfish, A. Tzekov, P.E. Bickel, S3-12, Adipophilin, and TIP47 package lipid in adipocytes, J Biol Chem 280(19) (2005) 19146-55.

[78] B. Lee, J. Zhu, N.E. Wolins, J.X. Cheng, K.K. Buhman, Differential association of adipophilin and TIP47 proteins with cytoplasmic lipid droplets in mouse enterocytes during dietary fat absorption, Biochim Biophys Acta 1791(12) (2009) 1173-80.

[79] W. Chen, B. Chang, X. Wu, L. Li, M. Sleeman, L. Chan, Inactivation of Plin4 downregulates Plin5 and reduces cardiac lipid accumulation in mice, Am J Physiol Endocrinol Metab 304(7) (2013) E770-9.

[80] A. Čopič, S. Antoine-Bally, M. Giménez-Andrés, C. La Torre Garay, B. Antonny, M.M. Manni, S. Pagnotta, J. Guihot, C.L. Jackson, A giant amphipathic helix from a perilipin that is adapted for coating lipid droplets, Nat Commun 9(1) (2018) 1332.

[81] H. Wang, U. Sreenivasan, H. Hu, A. Saladino, B.M. Polster, L.M. Lund, D.W. Gong, W.C. Stanley, C. Sztalryd, Perilipin 5, a lipid droplet-associated protein, provides physical and metabolic linkage to mitochondria, J Lipid Res 52(12) (2011) 2159-68.

[82] S.N. Keenan, W. DeNardo, J. Lou, R.B. Schittenhelm, M.K. Montgomery, J.G. Granneman, E. Hinde, M.J. Watt, Perilipin 5 S155 phosphorylation by PKA is required for the control of hepatic lipid metabolism and glycemic control, J Lipid Res 62 (2021) 100016.

[83] C.P. Najt, S.A. Khan, T.D. Heden, B.A. Witthuhn, M. Perez, J.L. Heier, L.E. Mead, M.P. Franklin, K.K. Karanja, M.J. Graham, M.T. Mashek, D.A. Bernlohr, L. Parker, L.S. Chow, D.G. Mashek, Lipid Droplet-Derived Monounsaturated Fatty Acids Traffic via PLIN5 to Allosterically Activate SIRT1, Mol Cell 77(4) (2020) 810-824.e8.

[84] A.M. Valm, S. Cohen, W.R. Legant, J. Melunis, U. Hershberg, E. Wait, A.R. Cohen, M.W. Davidson, E. Betzig, J. Lippincott-Schwartz, Applying systems-level spectral imaging and analysis to reveal the organelle interactome, Nature 546(7656) (2017) 162-167.

[85]   A.R. Thiam, I. Dugail, Lipid droplet-membrane contact sites - from protein binding to function, J Cell Sci 132(12) (2019) jcs230169.

[86]   A. Gemmink, S. Daemen, H.J.H. Kuijpers, G. Schaart, H. Duimel, C. Lopez-Iglesias, M. van Zandvoort, K. Knoops, M.K.C. Hesselink, Super-resolution microscopy localizes perilipin 5 at lipid droplet-mitochondria interaction sites and at lipid droplets juxtaposing to perilipin 2, Biochim Biophys Acta Mol Cell Biol Lipids 1863(11) (2018) 1423-1432.

[87]   M. Varghese, V.A. Kimler, F.R. Ghazi, G.K. Rathore, G.A. Perkins, M.H. Ellisman, J.G. Granneman, Adipocyte lipolysis affects Perilipin 5 and cristae organization at the cardiac lipid droplet-mitochondrial interface, Sci Rep 9(1) (2019) 4734.

[88]   I.Y. Benador, M. Veliova, K. Mahdaviani, A. Petcherski, J.D. Wikstrom, E.A. Assali, R. Acin-Perez, M. Shum, M.F. Oliveira, S. Cinti, C. Sztalryd, W.D. Barshop, J.A. Wohlschlegel, B.E. Corkey, M. Liesa, O.S. Shirihai, Mitochondria Bound to Lipid Droplets Have Unique Bioenergetics, Composition, and Dynamics that Support Lipid Droplet Expansion, Cell Metab 27(4) (2018) 869-885.e6.

[89]   Z. Li, K. Thiel, P.J. Thul, M. Beller, R.P. Kuhnlein, M.A. Welte, Lipid droplets control the maternal histone supply of Drosophila embryos, Curr Biol 22(22) (2012) 2104-13.

[90]   S. Cermelli, Y. Guo, S.P. Gross, M.A. Welte, The lipid-droplet proteome reveals that droplets are a protein-storage depot, Curr Biol 16(18) (2006) 1783-95.

[91]   N. Mejhert, L. Kuruvilla, K.R. Gabriel, S.D. Elliott, M.A. Guie, H. Wang, Z.W. Lai, E.A. Lane, R. Christiano, N.N. Danial, R.V. Farese, Jr., T.C. Walther, Partitioning of MLX-Family Transcription Factors to Lipid Droplets Regulates Metabolic Gene Expression, Mol Cell 77(6) (2020) 1251-1264.e9.

[92]   E.J. Klemm, E. Spooner, H.L. Ploegh, Dual role of ancient ubiquitous protein 1 (AUP1) in lipid droplet accumulation and endoplasmic reticulum (ER) protein quality control, J Biol Chem 286(43) (2011) 37602-14.

[93]   H.L. Ploegh, A lipid-based model for the creation of an escape hatch from the endoplasmic reticulum, Nature 448(7152) (2007) 435-8.

[94]   M. Suzuki, T. Otsuka, Y. Ohsaki, J. Cheng, T. Taniguchi, H. Hashimoto, H. Taniguchi, T. Fujimoto, Derlin-1 and UBXD8 are engaged in dislocation and degradation of lipidated ApoB-100 at lipid droplets, Mol Biol Cell 23(5) (2012) 800-10.

[95]   Y. Ohsaki, J. Cheng, A. Fujita, T. Tokumoto, T. Fujimoto, Cytoplasmic lipid droplets are sites of convergence of proteasomal and autophagic degradation of apolipoprotein B, Mol Biol Cell 17(6) (2006) 2674-83.

[96]   P. Shyu, Jr., X.F.A. Wong, K. Crasta, G. Thibault, Dropping in on lipid droplets: insights into cellular stress and cancer, Biosci Rep 38(5) (2018) BSR20180764.

[97] P.T. Bozza, I. Bakker-Abreu, R.A. Navarro-Xavier, C. Bandeira-Melo, Lipid body function in eicosanoid synthesis: an update, Prostaglandins Leukot Essent Fatty Acids 85(5) (2011) 205-13.

[98] E.A. Dennis, P.C. Norris, Eicosanoid storm in infection and inflammation, Nat Rev Immunol 15(8) (2015) 511-23.

[99] L.S. Moreira, B. Piva, L.B. Gentile, F.P. Mesquita-Santos, H. D'Avila, C.M. Maya-Monteiro, P.T. Bozza, C. Bandeira-Melo, B.L. Diaz, Cytosolic phospholipase A2-driven PGE2 synthesis within unsaturated fatty acids-induced lipid bodies of epithelial cells, Biochim Biophys Acta 1791(3) (2009) 156-65.

[100] M.T. Accioly, P. Pacheco, C.M. Maya-Monteiro, N. Carrossini, B.K. Robbs, S.S. Oliveira, C. Kaufmann, J.A. Morgado-Diaz, P.T. Bozza, J.P. Viola, Lipid bodies are reservoirs of cyclooxygenase-2 and sites of prostaglandin-E2 synthesis in colon cancer cells, Cancer Res 68(6) (2008) 1732-40.

[101] E. Jarc, T. Petan, A twist of FATe: Lipid droplets and inflammatory lipid mediators, Biochimie 169 (2020) 69-87.

[102] M. Bosch, M. Sánchez-Álvarez, A. Fajardo, R. Kapetanovic, B. Steiner, F. Dutra, L. Moreira, J.A. López, R. Campo, M. Marí, F. Morales-Paytuví, O. Tort, A. Gubern, R.M. Templin, J.E.B. Curson, N. Martel, C. Català, F. Lozano, F. Tebar, C. Enrich, J. Vázquez, M.A. Del Pozo, M.J. Sweet, P.T. Bozza, S.P. Gross, R.G. Parton, A. Pol, Mammalian lipid droplets are innate immune hubs integrating cell metabolism and host defense, Science 370(6514) (2020) eaay8085.

[103] P. Anand, S. Cermelli, Z. Li, A. Kassan, M. Bosch, R. Sigua, L. Huang, A.J. Ouellette, A. Pol, M.A. Welte, S.P. Gross, A novel role for lipid droplets in the organismal antibacterial response, Elife 1 (2012) e00003.

[104] R. Zechner, F. Madeo, D. Kratky, Cytosolic lipolysis and lipophagy: two sides of the same coin, Nat Rev Mol Cell Biol 18(11) (2017) 671-684.

[105] T.S. Nielsen, N. Jessen, J.O. Jørgensen, N. Møller, S. Lund, Dissecting adipose tissue lipolysis: molecular regulation and implications for metabolic disease, J Mol Endocrinol 52(3) (2014) R199-222.

[106] A. Lass, R. Zimmermann, G. Haemmerle, M. Riederer, G. Schoiswohl, M. Schweiger, P. Kienesberger, J.G. Strauss, G. Gorkiewicz, R. Zechner, Adipose triglyceride lipase-mediated lipolysis of cellular fat stores is activated by CGI-58 and defective in Chanarin-Dorfman Syndrome, Cell Metab 3(5) (2006) 309-19.

[107] E. Cakmak, G. Bagci, Chanarin-Dorfman Syndrome: A comprehensive review, Liver Int 00 (2021) 1-10.

[108] C. Lefèvre, F. Jobard, F. Caux, B. Bouadjar, A. Karaduman, R. Heilig, H. Lakhdar, A. Wollenberg, J.L. Verret, J. Weissenbach, M. Ozgüc, M. Lathrop, J.F. Prud'homme, J. Fischer, Mutations in CGI-58, the gene encoding a new protein of the esterase/lipase/thioesterase subfamily, in Chanarin-Dorfman syndrome, Am J Hum Genet 69(5) (2001) 1002-12.

[109] J.J. Egan, A.S. Greenberg, M.K. Chang, S.A. Wek, M.C. Moos, Jr., C. Londos, Mechanism of hormone-stimulated lipolysis in adipocytes: translocation of hormone-sensitive lipase to the lipid storage droplet, Proc Natl Acad Sci U S A 89(18) (1992) 8537-41.

[110] C.J. Fowler, Monoacylglycerol lipase - a target for drug development?, Br J Pharmacol 166(5) (2012) 1568-85.

[111] N. Martinez-Lopez, R. Singh, Autophagy and Lipid Droplets in the Liver, Annu Rev Nutr 35 (2015) 215-37.

[112] R.J. Schulze, A. Sathyanarayan, D.G. Mashek, Breaking fat: The regulation and mechanisms of lipophagy, Biochim Biophys Acta Mol Cell Biol Lipids 1862(10 Pt B) (2017) 1178-1187.

[113] R. Singh, S. Kaushik, Y. Wang, Y. Xiang, I. Novak, M. Komatsu, K. Tanaka, A.M. Cuervo, M.J. Czaja, Autophagy regulates lipid metabolism, Nature 458(7242) (2009) 1131-5.

[114] R.J. Schulze, E.W. Krueger, S.G. Weller, K.M. Johnson, C.A. Casey, M.B. Schott, M.A. McNiven, Direct lysosome-based autophagy of lipid droplets in hepatocytes, Proc Natl Acad Sci U S A 117(51) (2020) 32443-32452.

[115] Y.H. Hung, K.K. Buhman, DGAT1 deficiency disrupts lysosome function in enterocytes during dietary fat absorption, Biochim Biophys Acta Mol Cell Biol Lipids 1864(4) (2019) 587-595.

[116] V. Valayannopoulos, E. Mengel, A. Brassier, G. Grabowski, Lysosomal acid lipase deficiency: Expanding differential diagnosis, Mol Genet Metab 120(1-2) (2017) 62-66.

[117] D.W. Shin, Lipophagy: Molecular Mechanisms and Implications in Metabolic Disorders, Mol Cells 43(8) (2020) 686-693.

[118] M.B. Schott, S.G. Weller, R.J. Schulze, E.W. Krueger, K. Drizyte-Miller, C.A. Casey, M.A. McNiven, Lipid droplet size directs lipolysis and lipophagy catabolism in hepatocytes, J Cell Biol 218(10) (2019) 3320-3335.

[119] A. Sathyanarayan, M.T. Mashek, D.G. Mashek, ATGL Promotes Autophagy/Lipophagy via SIRT1 to Control Hepatic Lipid Droplet Catabolism, Cell Rep 19(1) (2017) 1-9.

[120] E.O. Balasse, F. Fery, Ketone body production and disposal: effects of fasting, diabetes, and exercise, Diabetes Metab Rev 5(3) (1989) 247-70.

[121] S.M. Houten, S. Violante, F.V. Ventura, R.J. Wanders, The Biochemistry and Physiology of Mitochondrial Fatty Acid beta-Oxidation and Its Genetic Disorders, Annu Rev Physiol 78 (2016) 23-44.

[122] M. Rakhshandehroo, B. Knoch, M. Muller, S. Kersten, Peroxisome proliferator-activated receptor alpha target genes, PPAR Res 2010 (2010) 612089.

[123] K.T. Ong, M.T. Mashek, S.Y. Bu, A.S. Greenberg, D.G. Mashek, Adipose triglyceride lipase is a major hepatic lipase that regulates triacylglycerol turnover and fatty acid signaling and partitioning, Hepatology 53(1) (2011) 116-26.

[124] G. Haemmerle, T. Moustafa, G. Woelkart, S. Buttner, A. Schmidt, T. van de Weijer, M. Hesselink, D. Jaeger, P.C. Kienesberger, K. Zierler, R. Schreiber, T. Eichmann, D. Kolb, P. Kotzbeck, M. Schweiger, M. Kumari, S. Eder, G. Schoiswohl, N. Wongsiriroj, N.M. Pollak, F.P. Radner, K. Preiss-Landl, T. Kolbe, T. Rulicke, B. Pieske, M. Trauner, A. Lass, R. Zimmermann, G. Hoefler, S. Cinti, E.E. Kershaw, P. Schrauwen, F. Madeo, B. Mayer, R. Zechner, ATGL-mediated fat catabolism regulates cardiac mitochondrial function via PPAR-alpha and PGC-1, Nat Med 17(9) (2011) 1076-85.

[125] S. Obrowsky, P.G. Chandak, J.V. Patankar, S. Povoden, S. Schlager, E.E. Kershaw, J.G. Bogner-Strauss, G. Hoefler, S. Levak-Frank, D. Kratky, Adipose triglyceride lipase is a TG hydrolase of the small intestine and regulates intestinal PPARalpha signaling, J Lipid Res 54(2) (2013) 425-35.

[126] P.C. Schulze, K. Drosatos, I.J. Goldberg, Lipid Use and Misuse by the Heart, Circ Res 118(11) (2016) 1736-51.

[127] L.J. van Loon, B.H. Goodpaster, Increased intramuscular lipid storage in the insulin-resistant and endurance-trained state, Pflugers Arch 451(5) (2006) 606-16.

[128] C.S. Shaw, D.A. Jones, A.J. Wagenmakers, Network distribution of mitochondria and lipid droplets in human muscle fibres, Histochem Cell Biol 129(1) (2008) 65-72.

[129] Z. Guo, B. Burguera, M.D. Jensen, Kinetics of intramuscular triglyceride fatty acids in exercising humans, J Appl Physiol (1985) 89(5) (2000) 2057-64.

[130] L.J. van Loon, R. Koopman, J.H. Stegen, A.J. Wagenmakers, H.A. Keizer, W.H. Saris, Intramyocellular lipids form an important substrate source during moderate intensity exercise in endurance-trained males in a fasted state, J Physiol 553(Pt 2) (2003) 611-25.

[131] H.E. Koh, J. Nielsen, B. Saltin, H.C. Holmberg, N. Ortenblad, Pronounced limb and fibre type differences in subcellular lipid droplet content and distribution in elite skiers before and after exhaustive exercise, J Physiol 595(17) (2017) 5781-5795.

[132] P.C. Turnbull, A.B. Longo, S.V. Ramos, B.D. Roy, W.E. Ward, S.J. Peters, Increases in skeletal muscle ATGL and its inhibitor G0S2 following 8 weeks of endurance training in metabolically different rat skeletal muscles, Am J Physiol Regul Integr Comp Physiol 310(2) (2016) R125-33.

[133] T.J. Alsted, L. Nybo, M. Schweiger, C. Fledelius, P. Jacobsen, R. Zimmermann, R. Zechner, B. Kiens, Adipose triglyceride lipase in human skeletal muscle is upregulated by exercise training, Am J Physiol Endocrinol Metab 296(3) (2009) E445-53.

[134] A. Gemmink, S. Daemen, B. Brouwers, J. Hoeks, G. Schaart, K. Knoops, P. Schrauwen, M.K.C. Hesselink, Decoration of myocellular lipid droplets with perilipins as a marker for in vivo lipid droplet dynamics: A super-resolution microscopy study in trained athletes and insulin resistant individuals, Biochim Biophys Acta Mol Cell Biol Lipids 1866(2) (2021) 158852.

[135] R. Zechner, R. Zimmermann, T.O. Eichmann, S.D. Kohlwein, G. Haemmerle, A. Lass, F. Madeo, FAT SIGNALS--lipases and lipolysis in lipid metabolism and signaling, Cell Metab 15(3) (2012) 279-91.

[136] T. Coll, R. Rodrïguez-Calvo, E. Barroso, L. Serrano, E. Eyre, X. Palomer, M. Vázquez-Carrera, Peroxisome proliferator-activated receptor (PPAR) beta/delta: a new potential therapeutic target for the treatment of metabolic syndrome, Curr Mol Pharmacol 2(1) (2009) 46-55.

[137] S. Tyagi, P. Gupta, A.S. Saini, C. Kaushal, S. Sharma, The peroxisome proliferator-activated receptor: A family of nuclear receptors role in various diseases, J Adv Pharm Technol Res 2(4) (2011) 236-40.

[138] S. Kersten, B. Desvergne, W. Wahli, Roles of PPARs in health and disease, Nature 405(6785) (2000) 421-4.

[139] R.C. Meex, A.J. Hoy, R.M. Mason, S.D. Martin, S.L. McGee, C.R. Bruce, M.J. Watt, ATGL-mediated triglyceride turnover and the regulation of mitochondrial capacity in skeletal muscle, Am J Physiol Endocrinol Metab 308(11) (2015) E960-70.

[140] G.F. Gibbons, K. Islam, R.J. Pease, Mobilisation of triacylglycerol stores, Biochim Biophys Acta 1483(1) (2000) 37-57.

[141] A.M. Dvorak, H.F. Dvorak, S.P. Peters, E.S. Shulman, D.W. MacGlashan, Jr., K. Pyne, V.S. Harvey, S.J. Galli, L.M. Lichtenstein, Lipid bodies: cytoplasmic organelles important to arachidonate metabolism in macrophages and mast cells, J Immunol 131(6) (1983) 2965-76.

[142] A. Dichlberger, S. Schlager, J. Lappalainen, R. Käkelä, K. Hattula, S.J. Butcher, W.J. Schneider, P.T. Kovanen, Lipid body formation during maturation of human mast cells, J Lipid Res 52(12) (2011) 2198-208.

[143] T. D'Aquila, Y.H. Hung, A. Carreiro, K.K. Buhman, Recent discoveries on absorption of dietary fat: Presence, synthesis, and metabolism of cytoplasmic lipid droplets within enterocytes, Biochim Biophys Acta 1861(8 Pt A) (2016) 730-47.

[144] G.F. Gibbons, D. Wiggins, Intracellular triacylglycerol lipase: its role in the assembly of hepatic very-low-density lipoprotein (VLDL), Adv Enzyme Regul 35 (1995) 179-98.

[145] D. Wiggins, G.F. Gibbons, The lipolysis/esterification cycle of hepatic triacylglycerol. Its role in the secretion of very-low-density lipoprotein and its response to hormones and sulphonylureas, Biochem J 284 (Pt 2) (1992) 457-62.

[146] A.D. Quiroga, R. Lehner, Pharmacological intervention of liver triacylglycerol lipolysis: The good, the bad and the ugly, Biochem Pharmacol 155 (2018) 233-241.

[147] R. Lehner, D.E. Vance, Cloning and expression of a cDNA encoding a hepatic microsomal lipase that mobilizes stored triacylglycerol, Biochem J 343 Pt 1(Pt 1) (1999) 1-10.

[148] E. Wei, M. Alam, F. Sun, L.B. Agellon, D.E. Vance, R. Lehner, Apolipoprotein B and triacylglycerol secretion in human triacylglycerol hydrolase transgenic mice, J Lipid Res 48(12) (2007) 2597-606.

[149] H. Wang, E. Wei, A.D. Quiroga, X. Sun, N. Touret, R. Lehner, Altered lipid droplet dynamics in hepatocytes lacking triacylglycerol hydrolase expression, Mol Biol Cell 21(12) (2010) 1991-2000.

[150] D. Gilham, S. Ho, M. Rasouli, P. Martres, D.E. Vance, R. Lehner, Inhibitors of hepatic microsomal triacylglycerol hydrolase decrease very low density lipoprotein secretion, Faseb J 17(12) (2003) 1685-7.

[151] E. Wei, Y. Ben Ali, J. Lyon, H. Wang, R. Nelson, V.W. Dolinsky, J.R. Dyck, G. Mitchell, G.S. Korbutt, R. Lehner, Loss of TGH/Ces3 in mice decreases blood lipids, improves glucose tolerance, and increases energy expenditure, Cell Metab 11(3) (2010) 183-93.

[152] J. Lian, E. Wei, S.P. Wang, A.D. Quiroga, L. Li, A. Di Pardo, J. van der Veen, S. Sipione, G.A. Mitchell, R. Lehner, Liver specific inactivation of carboxylesterase 3/triacylglycerol hydrolase decreases blood lipids without causing severe steatosis in mice, Hepatology 56(6) (2012) 2154-62.

[153] J. Lian, E. Wei, J. Groenendyk, S.K. Das, M. Hermansson, L. Li, R. Watts, A. Thiesen, G.Y. Oudit, M. Michalak, R. Lehner, Ces3/TGH Deficiency Attenuates Steatohepatitis, Sci Rep 6 (2016) 25747.

[154] C. Xiao, P. Stahel, A.L. Carreiro, K.K. Buhman, G.F. Lewis, Recent Advances in Triacylglycerol Mobilization by the Gut, Trends Endocrinol Metab 29(3) (2018) 151-163.

[155] J. Zhu, B. Lee, K.K. Buhman, J.X. Cheng, A dynamic, cytoplasmic triacylglycerol pool in enterocytes revealed by ex vivo and in vivo coherent anti-Stokes Raman scattering imaging, J Lipid Res 50(6) (2009) 1080-9.

[156] C. Xiao, P. Stahel, A.L. Carreiro, Y.H. Hung, S. Dash, I. Bookman, K.K. Buhman, G.F. Lewis, Oral Glucose Mobilizes Triglyceride Stores From the Human Intestine, Cell Mol Gastroenterol Hepatol 7(2) (2019) 313-337.

[157] M.D. Robertson, M. Parkes, B.F. Warren, D.J. Ferguson, K.G. Jackson, D.P. Jewell, K.N. Frayn, Mobilisation of enterocyte fat stores by oral glucose in humans, Gut 52(6) (2003) 834-9.

[158] C. Xiao, S. Dash, C. Morgantini, G.F. Lewis, Novel role of enteral monosaccharides in intestinal lipoprotein production in healthy humans, Arterioscler Thromb Vasc Biol 33(5) (2013) 1056-62.

[159] C. Xiao, S. Dash, C. Morgantini, G.F. Lewis, Intravenous Glucose Acutely Stimulates Intestinal Lipoprotein Secretion in Healthy Humans, Arterioscler Thromb Vasc Biol 36(7) (2016) 1457-63.

[160] R.N. Chavez-Jauregui, R.D. Mattes, E.J. Parks, Dynamics of fat absorption and effect of sham feeding on postprandial lipema, Gastroenterology 139(5) (2010) 1538-48.

[161] B.A. Fielding, J. Callow, R.M. Owen, J.S. Samra, D.R. Matthews, K.N. Frayn, Postprandial lipemia: the origin of an early peak studied by specific dietary fatty acid intake during sequential meals, Am J Clin Nutr 63(1) (1996) 36-41.

[162] S. Dash, C. Xiao, C. Morgantini, P.W. Connelly, B.W. Patterson, G.F. Lewis, Glucagon-like peptide-2 regulates release of chylomicrons from the intestine, Gastroenterology 147(6) (2014) 1275-1284.e4.

[163] M. Korbelius, N. Vujic, V. Sachdev, S. Obrowsky, S. Rainer, B. Gottschalk, W.F. Graier, D. Kratky, ATGL/CGI-58-Dependent Hydrolysis of a Lipid Storage Pool in Murine Enterocytes, Cell Rep 28(7) (2019) 1923-1934.e4.

[164] S. Obrowsky, P.G. Chandak, J.V. Patankar, T. Pfeifer, S. Povoden, R. Schreiber, G. Haemmerle, S. Levak-Frank, D. Kratky, Cholesteryl ester accumulation and accelerated cholesterol absorption in intestine-specific hormone sensitive lipase-null mice, Biochim Biophys Acta 1821(11) (2012) 1406-14.

[165] P. Xie, F. Guo, Y. Ma, H. Zhu, F. Wang, B. Xue, H. Shi, J. Yang, L. Yu, Intestinal Cgi-58 deficiency reduces postprandial lipid absorption, PLoS One 9(3) (2014) e91652.

[166] J.D. Douglass, Y.X. Zhou, A. Wu, J.A. Zadroga, A.M. Gajda, A.I. Lackey, W. Lang, K.M. Chevalier, S.W. Sutton, S.P. Zhang, C.M. Flores, M.A. Connelly, J. Storch, Global deletion of MGL in mice delays lipid absorption and alters energy homeostasis and diet-induced obesity, J Lipid Res 56(6) (2015) 1153-71.

[167] J. Lian, R. Nelson, R. Lehner, Carboxylesterases in lipid metabolism: from mouse to human, Protein Cell 9(2) (2018) 178-195.

[168] M. Schittmayer, N. Vujic, B. Darnhofer, M. Korbelius, S. Honeder, D. Kratky, R. Birner-Gruenberger, Spatially resolved activity-based proteomic profiles of the murine small intestinal lipases, Mol Cell Proteomics 19(12) (2020) 2104-2115.

[169] A.D. Quiroga, J. Lian, R. Lehner, Carboxylesterase1/Esterase-x regulates chylomicron production in mice, PLoS One 7(11) (2012) e49515.

[170] L.K. Maresch, P. Benedikt, U. Feiler, S. Eder, K.A. Zierler, U. Taschler, S. Kolleritsch, T.O. Eichmann, G. Schoiswohl, C. Leopold, B.I. Wieser, C. Lackner, T. Rülicke, J. van Klinken, D. Kratky, T. Moustafa, G. Hoefler, G. Haemmerle, Intestine-Specific Overexpression of Carboxylesterase 2c Protects Mice From Diet-Induced Liver Steatosis and Obesity, Hepatol Commun 3(2) (2019) 227-245.

[171] S.A. Khaldoun, M.A. Emond-Boisjoly, D. Chateau, V. Carrière, M. Lacasa, M. Rousset, S. Demignot, E. Morel, Autophagosomes contribute to intracellular lipid distribution in enterocytes, Mol Biol Cell 25(1) (2014) 118-32.

[172] Y. Kawano, D.E. Cohen, Mechanisms of hepatic triglyceride accumulation in non-alcoholic fatty liver disease, J Gastroenterol 48(4) (2013) 434-41.

[173] A.L.S. Cruz, E.A. Barreto, N.P.B. Fazolini, J.P.B. Viola, P.T. Bozza, Lipid droplets: platforms with multiple functions in cancer hallmarks, Cell Death Dis 11(2) (2020) 105.

[174] S.C. Bergheanu, M.C. Bodde, J.W. Jukema, Pathophysiology and treatment of atherosclerosis : Current view and future perspective on lipoprotein modification treatment, Neth Heart J 25(4) (2017) 231-242.

[175] S.M. Abd El-Kader, E.M. El-Den Ashmawy, Non-alcoholic fatty liver disease: The diagnosis and management, World J Hepatol 7(6) (2015) 846-58.

[176] M. Shaker, A. Tabbaa, M. Albeldawi, N. Alkhouri, Liver transplantation for nonalcoholic fatty liver disease: new challenges and new opportunities, World J Gastroenterol 20(18) (2014) 5320-30.

[177] Z.M. Younossi, A.B. Koenig, D. Abdelatif, Y. Fazel, L. Henry, M. Wymer, Global epidemiology of nonalcoholic fatty liver disease-Meta-analytic assessment of prevalence, incidence, and outcomes, Hepatology 64(1) (2016) 73-84.

[178] H. El Hadi, A. Di Vincenzo, R. Vettor, M. Rossato, Cardio-Metabolic Disorders in Non-Alcoholic Fatty Liver Disease, Int J Mol Sci 20(9) (2019) 2215.

[179] B. Cariou, C.D. Byrne, R. Loomba, A.J. Sanyal, Nonalcoholic fatty liver disease as a metabolic disease in humans: A literature review, Diabetes Obes Metab (2021) 1-15.

[180] K.L. Donnelly, C.I. Smith, S.J. Schwarzenberg, J. Jessurun, M.D. Boldt, E.J. Parks, Sources of fatty acids stored in liver and secreted via lipoproteins in patients with nonalcoholic fatty liver disease, J Clin Invest 115(5) (2005) 1343-51.

[181] E. Buzzetti, M. Pinzani, E.A. Tsochatzis, The multiple-hit pathogenesis of non-alcoholic fatty liver disease (NAFLD), Metabolism 65(8) (2016) 1038-48.

[182] D.G. Mashek, Hepatic lipid droplets: A balancing act between energy storage and metabolic dysfunction in NAFLD, Mol Metab (2020) 101115.

[183] W. Motomura, M. Inoue, T. Ohtake, N. Takahashi, M. Nagamine, S. Tanno, Y. Kohgo, T. Okumura, Up-regulation of ADRP in fatty liver in human and liver steatosis in mice fed with high fat diet, Biochem Biophys Res Commun 340(4) (2006) 1111-8.

[184] B. Magnusson, L. Asp, P. Bostrom, M. Ruiz, P. Stillemark-Billton, D. Linden, J. Boren, S.O. Olofsson, Adipocyte differentiation-related protein promotes fatty acid storage in cytosolic triglycerides and inhibits secretion of very low-density lipoproteins, Arterioscler Thromb Vasc Biol 26(7) (2006) 1566-71.

[185] M. Imamura, T. Inoguchi, S. Ikuyama, S. Taniguchi, K. Kobayashi, N. Nakashima, H. Nawata, ADRP stimulates lipid accumulation and lipid droplet formation in murine fibroblasts, Am J Physiol Endocrinol Metab 283(4) (2002) E775-83.

[186] T.H. Tsai, E. Chen, L. Li, P. Saha, H.J. Lee, L.S. Huang, G.S. Shelness, L. Chan, B.H. Chang, The constitutive lipid droplet protein PLIN2 regulates autophagy in liver, Autophagy 13(7) (2017) 1130-1144.

[187] L.L. Listenberger, X. Han, S.E. Lewis, S. Cases, R.V. Farese, Jr., D.S. Ory, J.E. Schaffer, Triglyceride accumulation protects against fatty acid-induced lipotoxicity, Proc Natl Acad Sci U S A 100(6) (2003) 3077-82.

[188] J.L. McManaman, E.S. Bales, D.J. Orlicky, M. Jackman, P.S. MacLean, S. Cain, A.E. Crunk, A. Mansur, C.E. Graham, T.A. Bowman, A.S. Greenberg, Perilipin-2-null mice are protected against diet-induced obesity, adipose inflammation, and fatty liver disease, J Lipid Res 54(5) (2013) 1346-59.

[189] A.E. Libby, E. Bales, D.J. Orlicky, J.L. McManaman, Perilipin-2 Deletion Impairs Hepatic Lipid Accumulation by Interfering with Sterol Regulatory Element-binding Protein (SREBP) Activation and Altering the Hepatic Lipidome, J Biol Chem 291(46) (2016) 24231-24246.

[190] C.P. Najt, S. Senthivinayagam, M.B. Aljazi, K.A. Fader, S.D. Olenic, J.R. Brock, T.A. Lydic, A.D. Jones, B.P. Atshaves, Liver-specific loss of Perilipin 2 alleviates diet-induced hepatic steatosis, inflammation, and fibrosis, Am J Physiol Gastrointest Liver Physiol 310(9) (2016) G726-38.

[191] D.J. Orlicky, A.E. Libby, E.S. Bales, R.H. McMahan, J. Monks, F.G. La Rosa, J.L. McManaman, Perilipin-2 promotes obesity and progressive fatty liver disease in mice through mechanistically distinct hepatocyte and extra-hepatocyte actions, J Physiol 597(6) (2019) 1565-1584.

[192] B.H. Chang, L. Li, A. Paul, S. Taniguchi, V. Nannegari, W.C. Heird, L. Chan, Protection against fatty liver but normal adipogenesis in mice lacking adipose differentiation-related protein, Mol Cell Biol 26(3) (2006) 1063-76.

[193] W. Xu, L. Wu, M. Yu, F.J. Chen, M. Arshad, X. Xia, H. Ren, J. Yu, L. Xu, D. Xu, J.Z. Li, P. Li, L. Zhou, Differential Roles of Cell Death-inducing DNA Fragmentation Factor-alpha-like Effector (CIDE) Proteins in Promoting Lipid Droplet Fusion and Growth in Subpopulations of Hepatocytes, J Biol Chem 291(9) (2016) 4282-93.

[194] A. Sans, S. Bonnafous, D. Rousseau, S. Patouraux, C.M. Canivet, P.S. Leclere, J. Tran-Van-Nhieu, C. Luci, B. Bailly-Maitre, X. Xu, A.H. Lee, K. Minehira, R. Anty, A. Tran, A. Iannelli, P. Gual, The Differential Expression of Cide Family Members is Associated with Nafld Progression from Steatosis to Steatohepatitis, Sci Rep 9(1) (2019) 7501.

[195] K. Matsusue, T. Kusakabe, T. Noguchi, S. Takiguchi, T. Suzuki, S. Yamano, F.J. Gonzalez, Hepatic steatosis in leptin-deficient mice is promoted by the PPARgamma target gene Fsp27, Cell Metab 7(4) (2008) 302-11.

[196] L. Zhou, L. Xu, J. Ye, D. Li, W. Wang, X. Li, L. Wu, H. Wang, F. Guan, P. Li, Cidea promotes hepatic steatosis by sensing dietary fatty acids, Hepatology 56(1) (2012) 95-107.

[197] J.Z. Li, J. Ye, B. Xue, J. Qi, J. Zhang, Z. Zhou, Q. Li, Z. Wen, P. Li, Cideb regulates diet-induced obesity, liver steatosis, and insulin sensitivity by controlling lipogenesis and fatty acid oxidation, Diabetes 56(10) (2007) 2523-32.

[198] L. Su, L. Zhou, F.J. Chen, H. Wang, H. Qian, Y. Sheng, Y. Zhu, H. Yu, X. Gong, L. Cai, X. Yang, L. Xu, T.J. Zhao, J.Z. Li, X.W. Chen, P. Li, Cideb controls sterol-regulated ER export of SREBP/SCAP by promoting cargo loading at ER exit sites, Embo J 38(8) (2019) e100156.

[199] R.A. DeBose-Boyd, J. Ye, SREBPs in Lipid Metabolism, Insulin Signaling, and Beyond, Trends Biochem Sci 43(5) (2018) 358-368.

[200] J. Ye, J.Z. Li, Y. Liu, X. Li, T. Yang, X. Ma, Q. Li, Z. Yao, P. Li, Cideb, an ER- and lipid droplet-associated protein, mediates VLDL lipidation and maturation by interacting with apolipoprotein B, Cell Metab 9(2) (2009) 177-90.

[201] X. Li, J. Ye, L. Zhou, W. Gu, E.A. Fisher, P. Li, Opposing roles of cell death-inducing DFF45-like effector B and perilipin 2 in controlling hepatic VLDL lipidation, J Lipid Res 53(9) (2012) 1877-89.

[202] S. Tiwari, S. Siddiqi, S.A. Siddiqi, CideB protein is required for the biogenesis of very low density lipoprotein (VLDL) transport vesicle, J Biol Chem 288(7) (2013) 5157-65.

[203] S. Romeo, I. Huang-Doran, M.G. Baroni, A. Kotronen, Unravelling the pathogenesis of fatty liver disease: patatin-like phospholipase domain-containing 3 protein, Curr Opin Lipidol 21(3) (2010) 247-52.

[204] S. Romeo, J. Kozlitina, C. Xing, A. Pertsemlidis, D. Cox, L.A. Pennacchio, E. Boerwinkle, J.C. Cohen, H.H. Hobbs, Genetic variation in PNPLA3 confers susceptibility to nonalcoholic fatty liver disease, Nat Genet 40(12) (2008) 1461-5.

[205] M. Graff, K.E. North, N. Franceschini, A.P. Reiner, M. Feitosa, J.J. Carr, P. Gordon-Larsen, M.K. Wojczynski, I.B. Borecki, PNPLA3 gene-by-visceral adipose tissue volume interaction and the pathogenesis of fatty liver disease: the NHLBI family heart study, Int J Obes (Lond) 37(3) (2013) 432-8.

[206] C. Pirazzi, M. Adiels, M.A. Burza, R.M. Mancina, M. Levin, M. Ståhlman, M.R. Taskinen, M. Orho-Melander, J. Perman, A. Pujia, L. Andersson, C. Maglio, T. Montalcini, O. Wiklund, J. Borén, S. Romeo, Patatin-like phospholipase domain-containing 3 (PNPLA3) I148M (rs738409) affects hepatic VLDL secretion in humans and in vitro, J Hepatol 57(6) (2012) 1276-82.

[207] S. He, C. McPhaul, J.Z. Li, R. Garuti, L. Kinch, N.V. Grishin, J.C. Cohen, H.H. Hobbs, A sequence variation (I148M) in PNPLA3 associated with nonalcoholic fatty liver disease disrupts triglyceride hydrolysis, J Biol Chem 285(9) (2010) 6706-15.

[208] M. Kumari, G. Schoiswohl, C. Chitraju, M. Paar, I. Cornaciu, A.Y. Rangrez, N. Wongsiriroj, H.M. Nagy, P.T. Ivanova, S.A. Scott, O. Knittelfelder, G.N. Rechberger, R. Birner-Gruenberger, S. Eder, H.A. Brown, G. Haemmerle, M. Oberer, A. Lass, E.E. Kershaw, R. Zimmermann, R. Zechner, Adiponutrin functions as a nutritionally regulated lysophosphatidic acid acyltransferase, Cell Metab 15(5) (2012) 691-702.

[209] E. Smagris, S. BasuRay, J. Li, Y. Huang, K.M. Lai, J. Gromada, J.C. Cohen, H.H. Hobbs, Pnpla3I148M knockin mice accumulate PNPLA3 on lipid droplets and develop hepatic steatosis, Hepatology 61(1) (2015) 108-18.

[210] M. Hoekstra, Z. Li, J.K. Kruijt, M. Van Eck, T.J. Van Berkel, J. Kuiper, The expression level of non-alcoholic fatty liver disease-related gene PNPLA3 in hepatocytes is highly influenced by hepatic lipid status, J Hepatol 52(2) (2010) 244-51.

[211] X. Zhang, Y. Wang, P. Liu, Omic studies reveal the pathogenic lipid droplet proteins in non-alcoholic fatty liver disease, Protein Cell 8(1) (2017) 4-13.

[212] P. Pingitore, C. Pirazzi, R.M. Mancina, B.M. Motta, C. Indiveri, A. Pujia, T. Montalcini, K. Hedfalk, S. Romeo, Recombinant PNPLA3 protein shows triglyceride hydrolase activity and its I148M mutation results in loss of function, Biochim Biophys Acta 1841(4) (2014) 574-80.

[213] Y. Ma, O.V. Belyaeva, P.M. Brown, K. Fujita, K. Valles, S. Karki, Y.S. de Boer, C. Koh, Y. Chen, X. Du, S.K. Handelman, V. Chen, E.K. Speliotes, C. Nestlerode, E. Thomas, D.E. Kleiner, J.M. Zmuda, A.J. Sanyal, N.Y. Kedishvili, T.J. Liang, Y. Rotman, 17-Beta Hydroxysteroid Dehydrogenase 13 Is a Hepatic Retinol Dehydrogenase Associated With Histological Features of Nonalcoholic Fatty Liver Disease, Hepatology 69(4) (2019) 1504-1519.

[214] W. Su, Y. Wang, X. Jia, W. Wu, L. Li, X. Tian, S. Li, C. Wang, H. Xu, J. Cao, Q. Han, S. Xu, Y. Chen, Y. Zhong, X. Zhang, P. Liu, J. Gustafsson, Y. Guan, Comparative proteomic study reveals 17β-HSD13 as a pathogenic protein in nonalcoholic fatty liver disease, Proc Natl Acad Sci U S A 111(31) (2014) 11437-42.

[215] N.S. Abul-Husn, X. Cheng, A.H. Li, Y. Xin, C. Schurmann, P. Stevis, Y. Liu, J. Kozlitina, S. Stender, G.C. Wood, A.N. Stepanchick, M.D. Still, S. McCarthy, C. O'Dushlaine, J.S. Packer, S. Balasubramanian, N. Gosalia, D. Esopi, S.Y. Kim, S. Mukherjee, A.E. Lopez, E.D. Fuller, J. Penn, X. Chu, J.Z. Luo, U.L. Mirshahi, D.J. Carey, C.D. Still, M.D. Feldman, A. Small, S.M. Damrauer, D.J. Rader, B. Zambrowicz, W. Olson, A.J. Murphy, I.B. Borecki, A.R. Shuldiner, J.G. Reid, J.D. Overton, G.D. Yancopoulos, H.H. Hobbs, J.C. Cohen, O. Gottesman, T.M. Teslovich, A. Baras, T. Mirshahi, J. Gromada, F.E. Dewey, A Protein-Truncating HSD17B13 Variant and Protection from Chronic Liver Disease, N Engl J Med 378(12) (2018) 1096-1106.

[216] C.J. Pirola, M. Garaycoechea, D. Flichman, M. Arrese, J. San Martino, C. Gazzi, G.O. Castaño, S. Sookoian, Splice variant rs72613567 prevents worst histologic outcomes in patients with nonalcoholic fatty liver disease, J Lipid Res 60(1) (2019) 176-185.

[217] S. Marchais-Oberwinkler, C. Henn, G. Möller, T. Klein, M. Negri, A. Oster, A. Spadaro, R. Werth, M. Wetzel, K. Xu, M. Frotscher, R.W. Hartmann, J. Adamski, 17β-Hydroxysteroid dehydrogenases (17β-HSDs) as therapeutic targets: protein structures, functions, and recent progress in inhibitor development, J Steroid Biochem Mol Biol 125(1-2) (2011) 66-82.

[218] M. Adam, H. Heikelä, C. Sobolewski, D. Portius, J. Mäki-Jouppila, A. Mehmood, P. Adhikari, I. Esposito, L.L. Elo, F.P. Zhang, S.T. Ruohonen, L. Strauss, M. Foti, M. Poutanen, Hydroxysteroid (17β) dehydrogenase 13 deficiency triggers hepatic steatosis and inflammation in mice, Faseb J 32(6) (2018) 3434-3447.

[219] B.C. Das, P. Thapa, R. Karki, S. Das, S. Mahapatra, T.C. Liu, I. Torregroza, D.P. Wallace, S. Kambhampati, P. Van Veldhuizen, A. Verma, S.K. Ray, T. Evans, Retinoic acid signaling pathways in development and diseases, Bioorg Med Chem 22(2) (2014) 673-83.

[220] A. Fougerat, A. Montagner, N. Loiseau, H. Guillou, W. Wahli, Peroxisome Proliferator-Activated Receptors and Their Novel Ligands as Candidates for the Treatment of Non-Alcoholic Fatty Liver Disease, Cells 9(7) (2020) 1638.

[221] Y. Yang, Y. Zhao, W. Li, Y. Wu, X. Wang, Y. Wang, T. Liu, T. Ye, Y. Xie, Z. Cheng, J. He, P. Bai, Y. Zhang, L. Ouyang, Emerging targets and potential therapeutic agents in non-alcoholic fatty liver disease treatment, Eur J Med Chem 197 (2020) 112311.

[222] H. Wang, W. Mehal, L.E. Nagy, Y. Rotman, Immunological mechanisms and therapeutic targets of fatty liver diseases, Cell Mol Immunol 18(1) (2021) 73-91.

[223] K.T. Suk, D.J. Kim, Gut microbiota: novel therapeutic target for nonalcoholic fatty liver disease, Expert Rev Gastroenterol Hepatol 13(3) (2019) 193-204.

[224] S.S. Virani, A. Alonso, E.J. Benjamin, M.S. Bittencourt, C.W. Callaway, A.P. Carson, A.M. Chamberlain, A.R. Chang, S. Cheng, F.N. Delling, L. Djousse, M.S.V. Elkind, J.F. Ferguson, M. Fornage, S.S. Khan, B.M. Kissela, K.L. Knutson, T.W. Kwan, D.T. Lackland, T.T. Lewis, J.H. Lichtman, C.T. Longenecker, M.S. Loop, P.L. Lutsey, S.S. Martin, K. Matsushita, A.E. Moran, M.E. Mussolino, A.M. Perak, W.D. Rosamond, G.A. Roth, U.K.A. Sampson, G.M. Satou, E.B. Schroeder, S.H. Shah, C.M. Shay, N.L. Spartano, A. Stokes, D.L. Tirschwell, L.B. VanWagner, C.W. Tsao, Heart Disease and Stroke Statistics-2020 Update: A Report From the American Heart Association, Circulation 141(9) (2020) e139-e596.

[225] B.J. Arsenault, R. Bourgeois, P. Mathieu, Do Oxidized Lipoproteins Cause Atherosclerotic Cardiovascular Diseases?, Can J Cardiol 33(12) (2017) 1513-1516.

[226] P. Stahel, C. Xiao, R.A. Hegele, G.F. Lewis, The Atherogenic Dyslipidemia Complex and Novel Approaches to Cardiovascular Disease Prevention in Diabetes, Can J Cardiol 34(5) (2018) 595-604.

[227] B.G. Nordestgaard, M. Benn, P. Schnohr, A. Tybjaerg-Hansen, Nonfasting triglycerides and risk of myocardial infarction, ischemic heart disease, and death in men and women, Jama 298(3) (2007) 299-308.

[228] S. Bansal, J.E. Buring, N. Rifai, S. Mora, F.M. Sacks, P.M. Ridker, Fasting compared with nonfasting triglycerides and risk of cardiovascular events in women, Jama 298(3) (2007) 309-16.

[229] A. Pirillo, G.D. Norata, A.L. Catapano, Postprandial lipemia as a cardiometabolic risk factor, Curr Med Res Opin 30(8) (2014) 1489-503.

[230] National Center for Health Statistics. Diet/Nutrition., 2020.

[231] P. Borel, C. Desmarchelier, Bioavailability of Fat-Soluble Vitamins and Phytochemicals in Humans: Effects of Genetic Variation, Annu Rev Nutr 38 (2018) 69-96.

[232] N. Kaur, V. Chugh, A.K. Gupta, Essential fatty acids as functional components of foods-a review, J Food Sci Technol 51(10) (2014) 2289-303.

[233] S. Brandhorst, V.D. Longo, Dietary Restrictions and Nutrition in the Prevention and Treatment of Cardiovascular Disease, Circ Res 124(6) (2019) 952-965.

[234] F.M. Sacks, A.H. Lichtenstein, J.H.Y. Wu, L.J. Appel, M.A. Creager, P.M. Kris-Etherton, M. Miller, E.B. Rimm, L.L. Rudel, J.G. Robinson, N.J. Stone, L.V. Van Horn, Dietary Fats and Cardiovascular Disease: A Presidential Advisory From the American Heart Association, Circulation 136(3) (2017) e1-e23.

[235] U.S. Department of Agriculture and U.S. Department of Health and Human Services. Dietary Guidelines for Americans, 2020-2025. 9th Edition, 2020.

[236] J.A. Wali, N. Jarzebska, D. Raubenheimer, S.J. Simpson, R.N. Rodionov, J.F. O'Sullivan, Cardio-Metabolic Effects of High-Fat Diets and Their Underlying Mechanisms-A Narrative Review, Nutrients 12(5) (2020) 1505.

[237] H. Kasper, Faecal fat excretion, diarrhea, and subjective complaints with highly dosed oral fat intake, Digestion 3(6) (1970) 321-30.

[238] J.T. Collins, A. Nguyen, M. Badireddy, Anatomy, Abdomen and Pelvis, Small Intestine, StatPearls, StatPearls Publishing. Copyright © 2020, StatPearls Publishing LLC., Treasure Island (FL), 2020.

[239] H.F. Helander, L. Fändriks, Surface area of the digestive tract - revisited, Scand J Gastroenterol 49(6) (2014) 681-9.

[240] C.C. Booth, A.E. Read, E. Jones, Studies on the site of fat absorption: 1. The sites of absorption of increasing doses of I-labelled triolein in the rat, Gut 2(1) (1961) 23-31.

[241] C.C. Booth, D. Alldis, A.E. Read, Studies on the site of fat absorption: 2 Fat balances after resection of varying amounts of the small intestine in man, Gut 2(2) (1961) 168-74.

[242] P.A. Dawson, S.J. Karpen, Intestinal transport and metabolism of bile acids, J Lipid Res 56(6) (2015) 1085-99.

[243] S. Moran-Ramos, A.R. Tovar, N. Torres, Diet: friend or foe of enteroendocrine cells--how it interacts with enteroendocrine cells, Adv Nutr 3(1) (2012) 8-20.

[244] P. Tso, Gastrointestinal digestion and absorption of lipid, Adv Lipid Res 21 (1985) 143-86.

[245] V. Cifarelli, N.A. Abumrad, Intestinal CD36 and Other Key Proteins of Lipid Utilization: Role in Absorption and Gut Homeostasis, Compr Physiol 8(2) (2018) 493-507.

[246] H. Xu, A. Diolintzi, J. Storch, Fatty acid-binding proteins: functional understanding and diagnostic implications, Curr Opin Clin Nutr Metab Care 22(6) (2019) 407-412.

[247] J.M. Ellis, C.E. Bowman, M.J. Wolfgang, Metabolic and tissue-specific regulation of acyl-CoA metabolism, PLoS One 10(3) (2015) e0116587.

[248] N.L. Gluchowski, C. Chitraju, J.A. Picoraro, N. Mejhert, S. Pinto, W. Xin, D.S. Kamin, H.S. Winter, W.K. Chung, T.C. Walther, R.V. Farese, Jr., Identification and characterization of a novel DGAT1 missense mutation associated with congenital diarrhea, J Lipid Res 58(6) (2017) 1230-1237.

[249] J.M. van Rijn, R.C. Ardy, Z. Kuloğlu, B. Härter, D.Y. van Haaften-Visser, H.P.J. van der Doef, M. van Hoesel, A. Kansu, A.H.M. van Vugt, M. Thian, F.T.M. Kokke, A. Krolo, M.K. Başaran, N.G. Kaya, A. Aksu, B. Dalgıç, F. Ozcay, Z. Baris, R. Kain, E.C.A. Stigter, K.D. Lichtenbelt, M.P.G. Massink, K.J. Duran, J. Verheij, D. Lugtenberg, P.G.J. Nikkels, H.G.F. Brouwer, H.J. Verkade, R. Scheenstra, B. Spee, E.E.S. Nieuwenhuis, P.J. Coffer, A.R. Janecke, G. van Haaften, R.H.J. Houwen, T. Müller, S. Middendorp, K. Boztug, Intestinal Failure and Aberrant Lipid Metabolism in Patients With DGAT1 Deficiency, Gastroenterology 155(1) (2018) 130-143.e15.

[250] C.M. Mansbach, 2nd, S. Siddiqi, Control of chylomicron export from the intestine, Am J Physiol Gastrointest Liver Physiol 310(9) (2016) G659-68.

[251] E. Levy, Insights from human congenital disorders of intestinal lipid metabolism, J Lipid Res 56(5) (2015) 945-62.

[252] S. Siddiqi, U. Saleem, N.A. Abumrad, N.O. Davidson, J. Storch, S.A. Siddiqi, C.M. Mansbach, 2nd, A novel multiprotein complex is required to generate the prechylomicron transport vesicle from intestinal ER, J Lipid Res 51(7) (2010) 1918-28.

[253] S. Siddiqi, C.M. Mansbach, 2nd, Phosphorylation of Sar1b protein releases liver fatty acid-binding protein from multiprotein complex in intestinal cytosol enabling it to bind to endoplasmic reticulum (ER) and bud the pre-chylomicron transport vesicle, J Biol Chem 287(13) (2012) 10178-88.

[254] J.B. Dixon, Lymphatic lipid transport: sewer or subway?, Trends Endocrinol Metab 21(8) (2010) 480-7.

[255] Z. Soayfane, F. Tercé, M. Cantiello, H. Robenek, M. Nauze, V. Bézirard, S. Allart, B. Payré, F. Capilla, C. Cartier, C. Peres, T. Al Saati, V. Théodorou, D.W. Nelson, C.E. Yen, X. Collet, C. Coméra, Exposure to dietary lipid leads to rapid production of cytosolic lipid droplets near the brush border membrane, Nutr Metab (Lond) 13 (2016) 48.

[256] C. Xiao, P. Stahel, A. Nahmias, G.F. Lewis, Emerging Role of Lymphatics in the Regulation of Intestinal Lipid Mobilization, Front Physiol 10 (2020) 1604.

[257] P. Stahel, C. Xiao, G.F. Lewis, Control of intestinal lipoprotein secretion by dietary carbohydrates, Curr Opin Lipidol 29(1) (2018) 24-29.

[258] H. Duez, B. Lamarche, K.D. Uffelman, R. Valero, J.S. Cohn, G.F. Lewis, Hyperinsulinemia is associated with increased production rate of intestinal apolipoprotein B-48-containing lipoproteins in humans, Arterioscler Thromb Vasc Biol 26(6) (2006) 1357-63.

[259] K. Adeli, G.F. Lewis, Intestinal lipoprotein overproduction in insulin-resistant states, Curr Opin Lipidol 19(3) (2008) 221-8.

[260] L.M. Federico, M. Naples, D. Taylor, K. Adeli, Intestinal insulin resistance and aberrant production of apolipoprotein B48 lipoproteins in an animal model of insulin resistance and metabolic dyslipidemia: evidence for activation of protein tyrosine phosphatase-1B, extracellular signal-related kinase, and sterol regulatory element-binding protein-1c in the fructose-fed hamster intestine, Diabetes 55(5) (2006) 1316-26.

[261] A. Leon-Acuña, J.F. Alcala-Diaz, J. Delgado-Lista, J.D. Torres-Peña, J. Lopez-Moreno, A. Camargo, A. Garcia-Rios, C. Marin, F. Gomez-Delgado, J. Caballero, B. Van-Ommen, M.M. Malagon, P. Perez-Martinez, J. Lopez-Miranda, Hepatic insulin resistance both in prediabetic and diabetic patients determines postprandial lipoprotein metabolism: from the CORDIOPREV study, Cardiovasc Diabetol 15 (2016) 68.

[262] H. Duez, B. Lamarche, R. Valero, M. Pavlic, S. Proctor, C. Xiao, L. Szeto, B.W. Patterson, G.F. Lewis, Both intestinal and hepatic lipoprotein production are stimulated by an acute elevation of plasma free fatty acids in humans, Circulation 117(18) (2008) 2369-76.

[263] G.F. Lewis, M. Naples, K. Uffelman, N. Leung, L. Szeto, K. Adeli, Intestinal lipoprotein production is stimulated by an acute elevation of plasma free fatty acids in the fasting state: studies in insulin-resistant and insulin-sensitized Syrian golden hamsters, Endocrinology 145(11) (2004) 5006-12.

[264] K.D. Silva, J.W. Wright, C.M. Williams, J.A. Lovegrove, Meal ingestion provokes entry of lipoproteins containing fat from the previous meal: possible metabolic implications, Eur J Nutr 44(6) (2005) 377-83.

[265] J.E. Lambert, E.J. Parks, Postprandial metabolism of meal triglyceride in humans, Biochim Biophys Acta 1821(5) (2012) 721-6.

[266] R.D. Mattes, Oral fat exposure increases the first phase triacylglycerol concentration due to release of stored lipid in humans, J Nutr 132(12) (2002) 3656-62.

[267] T.A. Gilbertson, D.T. Fontenot, L. Liu, H. Zhang, W.T. Monroe, Fatty acid modulation of K+ channels in taste receptor cells: gustatory cues for dietary fat, Am J Physiol 272(4 Pt 1) (1997) C1203-10.

[268] R.D. Mattes, Frontiers in Neuroscience. Fat Taste in Humans: Is It a Primary?, in: J.P. Montmayeur, J. le Coutre (Eds.), Fat Detection: Taste, Texture, and Post Ingestive Effects, CRC Press/Taylor & Francis. Copyright © 2010, Taylor & Francis Group, LLC., Boca Raton (FL), 2010.

[269] Q. Xiao, R.P. Boushey, D.J. Drucker, P.L. Brubaker, Secretion of the intestinotropic hormone glucagon-like peptide 2 is differentially regulated by nutrients in humans, Gastroenterology 117(1) (1999) 99-105.

[270] D.G. Burrin, Y. Petersen, B. Stoll, P. Sangild, Glucagon-like peptide 2: a nutrient-responsive gut growth factor, J Nutr 131(3) (2001) 709-12.

[271] C. Xiao, P. Stahel, G.F. Lewis, Regulation of Chylomicron Secretion: Focus on Post-Assembly Mechanisms, Cell Mol Gastroenterol Hepatol 7(3) (2019) 487-501.

[272] J. Hsieh, C. Longuet, A. Maida, J. Bahrami, E. Xu, C.L. Baker, P.L. Brubaker, D.J. Drucker, K. Adeli, Glucagon-like peptide-2 increases intestinal lipid absorption and chylomicron production via CD36, Gastroenterology 137(3) (2009) 997-1005, 1005.e1-4.

[273] J. Hsieh, K.E. Trajcevski, S.L. Farr, C.L. Baker, E.J. Lake, J. Taher, J. Iqbal, M.M. Hussain, K. Adeli, Glucagon-Like Peptide 2 (GLP-2) Stimulates Postprandial Chylomicron Production and Postabsorptive Release of Intestinal Triglyceride Storage Pools via Induction of Nitric Oxide Signaling in Male Hamsters and Mice, Endocrinology 156(10) (2015) 3538-47.

[274] P. Stahel, C. Xiao, X. Davis, P. Tso, G.F. Lewis, Glucose and GLP-2 (Glucagon-Like Peptide-2) Mobilize Intestinal Triglyceride by Distinct Mechanisms, Arterioscler Thromb Vasc Biol 39(8) (2019) 1565-1573.

[275] J. Pedersen, N.B. Pedersen, S.W. Brix, K.V. Grunddal, M.M. Rosenkilde, B. Hartmann, C. Ørskov, S.S. Poulsen, J.J. Holst, The glucagon-like peptide 2 receptor is expressed in enteric neurons and not in the epithelium of the intestine, Peptides 67 (2015) 20-8.

[276] B. Yusta, D. Matthews, J.A. Koehler, G. Pujadas, K.D. Kaur, D.J. Drucker, Localization of Glucagon-Like Peptide-2 Receptor Expression in the Mouse, Endocrinology 160(8) (2019) 1950-1963.

[277] C. Ørskov, B. Hartmann, S.S. Poulsen, J. Thulesen, K.J. Hare, J.J. Holst, GLP-2 stimulates colonic growth via KGF, released by subepithelial myofibroblasts with GLP-2 receptors, Regul Pept 124(1-3) (2005) 105-12.

[278] B. Yusta, L. Huang, D. Munroe, G. Wolff, R. Fantaske, S. Sharma, L. Demchyshyn, S.L. Asa, D.J. Drucker, Enteroendocrine localization of GLP-2 receptor expression in humans and rodents, Gastroenterology 119(3) (2000) 744-55.

[279] X. Guan, H.E. Karpen, J. Stephens, J.T. Bukowski, S. Niu, G. Zhang, B. Stoll, M.J. Finegold, J.J. Holst, D. Hadsell, B.L. Nichols, D.G. Burrin, GLP-2 receptor localizes to enteric neurons and endocrine cells expressing vasoactive peptides and mediates increased blood flow, Gastroenterology 130(1) (2006) 150-64.

[280] C. Xiao, P. Stahel, C. Morgantini, A. Nahmias, S. Dash, G.F. Lewis, Glucagon-like peptide-2 mobilizes lipids from the intestine by a systemic nitric oxide-independent mechanism, Diabetes Obes Metab 21(11) (2019) 2535-2541.

[281] M.A. Markovic, A. Srikrishnaraj, D. Tsang, P.L. Brubaker, Requirement for the intestinal epithelial insulin-like growth factor-1 receptor in the intestinal responses to glucagon-like peptide-2 and dietary fat, Faseb J 34(5) (2020) 6628-6640.

[282] J. Hauptman, Orlistat: selective inhibition of caloric absorption can affect long-term body weight, Endocrine 13(2) (2000) 201-6.

[283] A. Sahebkar, L.E. Simental-Mendia, Z. Reiner, P.T. Kovanen, M. Simental-Mendia, V. Bianconi, M. Pirro, Effect of orlistat on plasma lipids and body weight: A systematic review and meta-analysis of 33 randomized controlled trials, Pharmacol Res 122 (2017) 53-65.

[284] B.S. Drew, A.F. Dixon, J.B. Dixon, Obesity management: update on orlistat, Vasc Health Risk Manag 3(6) (2007) 817-21.

[285] S.J. Smith, S. Cases, D.R. Jensen, H.C. Chen, E. Sande, B. Tow, D.A. Sanan, J. Raber, R.H. Eckel, R.V. Farese, Jr., Obesity resistance and multiple mechanisms of triglyceride synthesis in mice lacking Dgat, Nat Genet 25(1) (2000) 87-90.

[286] K.K. Buhman, S.J. Smith, S.J. Stone, J.J. Repa, J.S. Wong, F.F. Knapp, Jr., B.J. Burri, R.L. Hamilton, N.A. Abumrad, R.V. Farese, Jr., DGAT1 is not essential for intestinal triacylglycerol absorption or chylomicron synthesis, J Biol Chem 277(28) (2002) 25474-9.

[287] G.P. Ables, K.J. Yang, S. Vogel, A. Hernandez-Ono, S. Yu, J.J. Yuen, S. Birtles, L.K. Buckett, A.V. Turnbull, I.J. Goldberg, W.S. Blaner, L.S. Huang, H.N. Ginsberg, Intestinal DGAT1 deficiency reduces postprandial triglyceride and retinyl ester excursions by inhibiting chylomicron secretion and delaying gastric emptying, J Lipid Res 53(11) (2012) 2364-79.

[288] N. Vujić, M. Korbelius, V. Sachdev, S. Rainer, A. Zimmer, A. Huber, B. Radović, D. Kratky, Intestine-specific DGAT1 deficiency improves atherosclerosis in apolipoprotein E knockout mice by reducing systemic cholesterol burden, Atherosclerosis 310 (2020) 26-36.

[289] B. Lee, A.M. Fast, J. Zhu, J.X. Cheng, K.K. Buhman, Intestine-specific expression of acyl CoA:diacylglycerol acyltransferase 1 reverses resistance to diet-induced hepatic steatosis and obesity in Dgat1-/- mice, J Lipid Res 51(7) (2010) 1770-80.

[290] H. Denison, C. Nilsson, M. Kujacic, L. Lofgren, C. Karlsson, M. Knutsson, J.W. Eriksson, Proof of mechanism for the DGAT1 inhibitor AZD7687: results from a first-time-in-human single-dose study, Diabetes Obes Metab 15(2) (2013) 136-43.

[291] H. Denison, C. Nilsson, L. Löfgren, A. Himmelmann, G. Mårtensson, M. Knutsson, A. Al-Shurbaji, H. Tornqvist, J.W. Eriksson, Diacylglycerol acyltransferase 1 inhibition with AZD7687 alters lipid handling and hormone secretion in the gut with intolerable side effects: a randomized clinical trial, Diabetes Obes Metab 16(4) (2014) 334-43.

[292] R. Alonso, A. Cuevas, P. Mata, Lomitapide: a review of its clinical use, efficacy, and tolerability, Core Evid 14 (2019) 19-30.

[293] J. Roeters van Lennep, M. Averna, R. Alonso, Treating homozygous familial hypercholesterolemia in a real-world setting: Experiences with lomitapide, J Clin Lipidol 9(4) (2015) 607-17.

[294] R.L. Siegel, K.D. Miller, H.E. Fuchs, A. Jemal, Cancer Statistics, 2021, CA Cancer J Clin 71(1) (2021) 7-33.

[295] G. Argyrakopoulou, M. Dalamaga, N. Spyrou, A. Kokkinos, Gender Differences in Obesity-Related Cancers, Curr Obes Rep (2021).

[296] F. Siddiqui, A.H. Siddiqui, Lung Cancer, StatPearls, StatPearls Publishing. Copyright © 2020, StatPearls Publishing LLC., Treasure Island (FL), 2020.

[297] N. Parsa, Environmental factors inducing human cancers, Iran J Public Health 41(11) (2012) 1-9.

[298] M.M. Pomerantz, M.L. Freedman, The genetics of cancer risk, Cancer J 17(6) (2011) 416-22.

[299] R.J. DeBerardinis, N.S. Chandel, Fundamentals of cancer metabolism, Sci Adv 2(5) (2016) e1600200.

[300] D. Hanahan, R.A. Weinberg, The hallmarks of cancer, Cell 100(1) (2000) 57-70.

[301] M.V. Liberti, J.W. Locasale, The Warburg Effect: How Does it Benefit Cancer Cells?, Trends Biochem Sci 41(3) (2016) 211-218.

[302] S. Beloribi-Djefaflia, S. Vasseur, F. Guillaumond, Lipid metabolic reprogramming in cancer cells, Oncogenesis 5(1) (2016) e189.

[303] M.T. Snaebjornsson, S. Janaki-Raman, A. Schulze, Greasing the Wheels of the Cancer Machine: The Role of Lipid Metabolism in Cancer, Cell Metab 31(1) (2020) 62-76.

[304] T. Petan, E. Jarc, M. Jusovic, Lipid Droplets in Cancer: Guardians of Fat in a Stressful World, Molecules 23(8) (2018) 1941.

[305] C. Nieva, M. Marro, N. Santana-Codina, S. Rao, D. Petrov, A. Sierra, The lipid phenotype of breast cancer cells characterized by Raman microspectroscopy: towards a stratification of malignancy, PLoS One 7(10) (2012) e46456.

[306] H. Abramczyk, J. Surmacki, M. Kopec, A.K. Olejnik, K. Lubecka-Pietruszewska, K. Fabianowska-Majewska, The role of lipid droplets and adipocytes in cancer. Raman imaging of cell cultures: MCF10A, MCF7, and MDA-MB-231 compared to adipocytes in cancerous human breast tissue, Analyst 140(7) (2015) 2224-35.

[307] F. Nardi, O.E. Franco, P. Fitchev, A. Morales, R.E. Vickman, S.W. Hayward, S.E. Crawford, DGAT1 Inhibitor Suppresses Prostate Tumor Growth and Migration by Regulating Intracellular Lipids and Non-Centrosomal MTOC Protein GM130, Sci Rep 9(1) (2019) 3035.

[308] D. Ackerman, S. Tumanov, B. Qiu, E. Michalopoulou, M. Spata, A. Azzam, H. Xie, M.C. Simon, J.J. Kamphorst, Triglycerides Promote Lipid Homeostasis during Hypoxic Stress by Balancing Fatty Acid Saturation, Cell Rep 24(10) (2018) 2596-2605.e5.

[309] X. Cheng, F. Geng, M. Pan, X. Wu, Y. Zhong, C. Wang, Z. Tian, C. Cheng, R. Zhang, V. Puduvalli, C. Horbinski, X. Mo, X. Han, A. Chakravarti, D. Guo, Targeting DGAT1 Ameliorates Glioblastoma by Increasing Fat Catabolism and Oxidative Stress, Cell Metab 32(2) (2020) 229-242.e8.

[310] M.J. Hernández-Corbacho, L.M. Obeid, A novel role for DGATs in cancer, Adv Biol Regul 72 (2019) 89-101.

[311] A. Pucer, V. Brglez, C. Payré, J. Pungerčar, G. Lambeau, T. Petan, Group X secreted phospholipase A(2) induces lipid droplet formation and prolongs breast cancer cell survival, Mol Cancer 12(1) (2013) 111.

[312] S.R. Singh, X. Zeng, J. Zhao, Y. Liu, G. Hou, H. Liu, S.X. Hou, The lipolysis pathway sustains normal and transformed stem cells in adult Drosophila, Nature 538(7623) (2016) 109-113.

[313] K.M. Nieman, H.A. Kenny, C.V. Penicka, A. Ladanyi, R. Buell-Gutbrod, M.R. Zillhardt, I.L. Romero, M.S. Carey, G.B. Mills, G.S. Hotamisligil, S.D. Yamada, M.E. Peter, K. Gwin, E. Lengyel, Adipocytes promote ovarian cancer metastasis and provide energy for rapid tumor growth, Nat Med 17(11) (2011) 1498-503.

[314] A. Chimento, I. Casaburi, P. Avena, F. Trotta, A. De Luca, V. Rago, V. Pezzi, R. Sirianni, Cholesterol and Its Metabolites in Tumor Growth: Therapeutic Potential of Statins in Cancer Treatment, Front Endocrinol (Lausanne) 9 (2018) 807.

[315] S. Chell, A. Kaidi, A.C. Williams, C. Paraskeva, Mediators of PGE2 synthesis and signalling downstream of COX-2 represent potential targets for the prevention/treatment of colorectal cancer, Biochim Biophys Acta 1766(1) (2006) 104-19.

[316] D. Wang, R.N. Dubois, Eicosanoids and cancer, Nat Rev Cancer 10(3) (2010) 181-93.

[317] J.S. Lee, R. Mendez, H.H. Heng, Z.Q. Yang, K. Zhang, Pharmacological ER stress promotes hepatic lipogenesis and lipid droplet formation, Am J Transl Res 4(1) (2012) 102-13.

[318] W. Fei, H. Wang, X. Fu, C. Bielby, H. Yang, Conditions of endoplasmic reticulum stress stimulate lipid droplet formation in Saccharomyces cerevisiae, Biochem J 424(1) (2009) 61-7.

[319] S.J. Lee, J. Zhang, A.M. Choi, H.P. Kim, Mitochondrial dysfunction induces formation of lipid droplets as a generalized response to stress, Oxid Med Cell Longev 2013 (2013) 327167.

[320] A.P. Bailey, G. Koster, C. Guillermier, E.M. Hirst, J.I. MacRae, C.P. Lechene, A.D. Postle, A.P. Gould, Antioxidant Role for Lipid Droplets in a Stem Cell Niche of Drosophila, Cell 163(2) (2015) 340-53.

[321] T.B. Nguyen, S.M. Louie, J.R. Daniele, Q. Tran, A. Dillin, R. Zoncu, D.K. Nomura, J.A. Olzmann, DGAT1-Dependent Lipid Droplet Biogenesis Protects Mitochondrial Function during Starvation-Induced Autophagy, Dev Cell 42(1) (2017) 9-21.e5.

[322] E. Jarc, A. Kump, P. Malavašič, T.O. Eichmann, R. Zimmermann, T. Petan, Lipid droplets induced by secreted phospholipase A(2) and unsaturated fatty acids protect breast cancer cells from nutrient and lipotoxic stress, Biochim Biophys Acta Mol Cell Biol Lipids 1863(3) (2018) 247-265.

[323] X. Chen, J.R. Cubillos-Ruiz, Endoplasmic reticulum stress signals in the tumour and its microenvironment, Nat Rev Cancer 21(2) (2021) 71-88.

[324] H.J. Clarke, J.E. Chambers, E. Liniker, S.J. Marciniak, Endoplasmic reticulum stress in malignancy, Cancer Cell 25(5) (2014) 563-73.

[325] Y. Hasin, M. Seldin, A. Lusis, Multi-omics approaches to disease, Genome Biol 18(1) (2017) 83.

[326] A. Pandey, M. Mann, Proteomics to study genes and genomes, Nature 405(6788) (2000) 837-46.

[327] J.R. Yates, 3rd, Recent technical advances in proteomics, F1000Res 8 (2019) F1000 Faculty Rev-351.

[328] H. Steen, M. Mann, The ABC's (and XYZ's) of peptide sequencing, Nat Rev Mol Cell Biol 5(9) (2004) 699-711.

[329] A. Croxatto, G. Prod'hom, G. Greub, Applications of MALDI-TOF mass spectrometry in clinical diagnostic microbiology, FEMS Microbiol Rev 36(2) (2012) 380-407.

[330] A.D. Catherman, O.S. Skinner, N.L. Kelleher, Top Down proteomics: facts and perspectives, Biochem Biophys Res Commun 445(4) (2014) 683-93.

[331] F. Ardito, M. Giuliani, D. Perrone, G. Troiano, L. Lo Muzio, The crucial role of protein phosphorylation in cell signaling and its use as targeted therapy (Review), Int J Mol Med 40(2) (2017) 271-280.

[332] J.A. Marsh, S.A. Teichmann, Structure, dynamics, assembly, and evolution of protein complexes, Annu Rev Biochem 84 (2015) 551-75.

[333] A. Doerr, In pursuit of PTMs, Nat Methods 12(20) (2015).

[334] C. Reily, T.J. Stewart, M.B. Renfrow, J. Novak, Glycosylation in health and disease, Nat Rev Nephrol 15(6) (2019) 346-366.

[335] K. Ohtsubo, J.D. Marth, Glycosylation in cellular mechanisms of health and disease, Cell 126(5) (2006) 855-67.

[336] N. Javaid, S. Choi, Acetylation- and Methylation-Related Epigenetic Proteins in the Context of Their Targets, Genes (Basel) 8(8) (2017) 196.

[337] S.H. Lecker, A.L. Goldberg, W.E. Mitch, Protein degradation by the ubiquitin-proteasome pathway in normal and disease states, J Am Soc Nephrol 17(7) (2006) 1807-19.

[338] L. Pieroni, F. Iavarone, A. Olianas, V. Greco, C. Desiderio, C. Martelli, B. Manconi, M.T. Sanna, I. Messana, M. Castagnola, T. Cabras, Enrichments of post-translational modifications in proteomic studies, J Sep Sci 43(1) (2020) 313-336.

[339] Y. Zhao, O.N. Jensen, Modification-specific proteomics: strategies for characterization of post-translational modifications using enrichment techniques, Proteomics 9(20) (2009) 4632-41.

[340] A.B. Iliuk, V.A. Martin, B.M. Alicie, R.L. Geahlen, W.A. Tao, In-depth analyses of kinase-dependent tyrosine phosphoproteomes based on metal ion-functionalized soluble nanopolymers, Mol Cell Proteomics 9(10) (2010) 2162-72.

[341] A.R. Kristensen, J. Gsponer, L.J. Foster, A high-throughput approach for measuring temporal changes in the interactome, Nat Methods 9(9) (2012) 907-9.

[342] O.S. Skinner, N.A. Haverland, L. Fornelli, R.D. Melani, L.H.F. Do Vale, H.S. Seckler, P.F. Doubleday, L.F. Schachner, K. Srzentić, N.L. Kelleher, P.D. Compton, Top-down characterization of endogenous protein complexes with native proteomics, Nat Chem Biol 14(1) (2018) 36-41.

[343] J. Snider, M. Kotlyar, P. Saraon, Z. Yao, I. Jurisica, I. Stagljar, Fundamentals of protein interaction network mapping, Mol Syst Biol 11(12) (2015) 848.

[344] Y. Xu, X. Fan, Y. Hu, In vivo interactome profiling by enzyme-catalyzed proximity labeling, Cell Biosci 11(1) (2021) 27.

[345] E.L. Huttlin, R.J. Bruckner, J.A. Paulo, J.R. Cannon, L. Ting, K. Baltier, G. Colby, F. Gebreab, M.P. Gygi, H. Parzen, J. Szpyt, S. Tam, G. Zarraga, L. Pontano-Vaites, S. Swarup, A.E. White, D.K. Schweppe, R. Rad, B.K. Erickson, R.A. Obar, K.G. Guruharsha, K. Li, S. Artavanis-Tsakonas, S.P. Gygi, J.W. Harper, Architecture of the human interactome defines protein communities and disease networks, Nature 545(7655) (2017) 505-509.

[346] B.A. Manjasetty, K. Büssow, S. Panjikar, A.P. Turnbull, Current methods in structural proteomics and its applications in biological sciences, 3 Biotech, © The Author(s) 2011.2012, pp. 89-113.

[347] S.J. Opella, F.M. Marassi, Structure determination of membrane proteins by NMR spectroscopy, Chem Rev 104(8) (2004) 3587-606.

[348] I. Sengupta, P.S. Nadaud, C.P. Jaroniec, Protein structure determination with paramagnetic solid-state NMR spectroscopy, Acc Chem Res 46(9) (2013) 2117-26.

[349] C.M. Ho, X. Li, M. Lai, T.C. Terwilliger, J.R. Beck, J. Wohlschlegel, D.E. Goldberg, A.W.P. Fitzpatrick, Z.H. Zhou, Bottom-up structural proteomics: cryoEM of protein complexes enriched from the cellular milieu, Nat Methods 17(1) (2020) 79-85.

[350] U. Kaur, H. Meng, F. Lui, R. Ma, R.N. Ogburn, J.H.R. Johnson, M.C. Fitzgerald, L.M. Jones, Proteome-Wide Structural Biology: An Emerging Field for the Structural Analysis of Proteins on the Proteomic Scale, J Proteome Res 17(11) (2018) 3614-3627.

[351] C.A. Sobsey, S. Ibrahim, V.R. Richard, V. Gaspar, G. Mitsa, V. Lacasse, R.P. Zahedi, G. Batist, C.H. Borchers, Targeted and Untargeted Proteomics Approaches in Biomarker Development, Proteomics 20(9) (2020) e1900029.

[352] M.A. Gillette, S.A. Carr, Quantitative analysis of peptides and proteins in biomedicine by targeted mass spectrometry, Nat Methods 10(1) (2013) 28-34.

[353] P. Picotti, R. Aebersold, Selected reaction monitoring-based proteomics: workflows, potential, pitfalls and future directions, Nat Methods 9(6) (2012) 555-66.

[354] W. Zhu, J.W. Smith, C.M. Huang, Mass spectrometry-based label-free quantitative proteomics, J Biomed Biotechnol 2010 (2010) 840518.

[355] P. Mallick, B. Kuster, Proteomics: a pragmatic perspective, Nat Biotechnol 28(7) (2010) 695-709.

[356] J. Cox, M.Y. Hein, C.A. Luber, I. Paron, N. Nagaraj, M. Mann, Accurate proteome-wide label-free quantification by delayed normalization and maximal peptide ratio extraction, termed MaxLFQ, Mol Cell Proteomics 13(9) (2014) 2513-26.

[357] S. Anand, M. Samuel, C.S. Ang, S. Keerthikumar, S. Mathivanan, Label-Based and Label-Free Strategies for Protein Quantitation, Methods Mol Biol 1549 (2017) 31-43.

[358] S.E. Ong, B. Blagoev, I. Kratchmarova, D.B. Kristensen, H. Steen, A. Pandey, M. Mann, Stable isotope labeling by amino acids in cell culture, SILAC, as a simple and accurate approach to expression proteomics, Mol Cell Proteomics 1(5) (2002) 376-86.

[359] S.P. Gygi, B. Rist, S.A. Gerber, F. Turecek, M.H. Gelb, R. Aebersold, Quantitative analysis of complex protein mixtures using isotope-coded affinity tags, Nat Biotechnol 17(10) (1999) 994-9.

[360] K. Kito, T. Ito, Mass spectrometry-based approaches toward absolute quantitative proteomics, Curr Genomics 9(4) (2008) 263-74.

[361] D.S. Kirkpatrick, S.A. Gerber, S.P. Gygi, The absolute quantification strategy: a general procedure for the quantification of proteins and post-translational modifications, Methods 35(3) (2005) 265-73.

[362] N. Amiri-Dashatan, M. Koushki, H.A. Abbaszadeh, M. Rostami-Nejad, M. Rezaei-Tavirani, Proteomics Applications in Health: Biomarker and Drug Discovery and Food Industry, Iran J Pharm Res 17(4) (2018) 1523-1536.

[363] A. Schmidt, I. Forne, A. Imhof, Bioinformatic analysis of proteomics data, BMC Syst Biol 8 Suppl 2(Suppl 2) (2014) S3.

[364] W. Huang da, B.T. Sherman, R.A. Lempicki, Systematic and integrative analysis of large gene lists using DAVID bioinformatics resources, Nat Protoc 4(1) (2009) 44-57.

[365] W. Huang da, B.T. Sherman, R.A. Lempicki, Bioinformatics enrichment tools: paths toward the comprehensive functional analysis of large gene lists, Nucleic Acids Res 37(1) (2009) 1-13.

[366] E. Eden, R. Navon, I. Steinfeld, D. Lipson, Z. Yakhini, GOrilla: a tool for discovery and visualization of enriched GO terms in ranked gene lists, BMC Bioinformatics 10 (2009) 48.

[367] D. Szklarczyk, A.L. Gable, D. Lyon, A. Junge, S. Wyder, J. Huerta-Cepas, M. Simonovic, N.T. Doncheva, J.H. Morris, P. Bork, L.J. Jensen, C.V. Mering, STRING v11: protein-protein association networks with increased coverage, supporting functional discovery in genome-wide experimental datasets, Nucleic Acids Res 47(D1) (2019) D607-d613.

[368] Y. Zhou, B. Zhou, L. Pache, M. Chang, A.H. Khodabakhshi, O. Tanaseichuk, C. Benner, S.K. Chanda, Metascape provides a biologist-oriented resource for the analysis of systems-level datasets, Nat Commun 10(1) (2019) 1523.

[369] J. Chong, O. Soufan, C. Li, I. Caraus, S. Li, G. Bourque, D.S. Wishart, J. Xia, MetaboAnalyst 4.0: towards more transparent and integrative metabolomics analysis, Nucleic Acids Res 46(W1) (2018) W486-w494.

[370] P. Shannon, A. Markiel, O. Ozier, N.S. Baliga, J.T. Wang, D. Ramage, N. Amin, B. Schwikowski, T. Ideker, Cytoscape: a software environment for integrated models of biomolecular interaction networks, Genome Res 13(11) (2003) 2498-504.

[371] M. Kanehisa, M. Furumichi, Y. Sato, M. Ishiguro-Watanabe, M. Tanabe, KEGG: integrating viruses and cellular organisms, Nucleic Acids Res 49(D1) (2021) D545-d551.

[372] H. Mi, D. Ebert, A. Muruganujan, C. Mills, L.P. Albou, T. Mushayamaha, P.D. Thomas, PANTHER version 16: a revised family classification, tree-based classification tool, enhancer regions and extensive API, Nucleic Acids Res 49(D1) (2021) D394-d403.

[373] A. Krämer, J. Green, J. Pollard, Jr., S. Tugendreich, Causal analysis approaches in Ingenuity Pathway Analysis, Bioinformatics 30(4) (2014) 523-30.

[374] A. Masood, H. Benabdelkamel, A.A. Alfadda, Obesity Proteomics: An Update on the Strategies and Tools Employed in the Study of Human Obesity, High Throughput 7(3) (2018) 27.

[375] J.W. Lim, J. Dillon, M. Miller, Proteomic and genomic studies of non-alcoholic fatty liver disease--clues in the pathogenesis, World J Gastroenterol 20(26) (2014) 8325-40.

[376] T. Sundsten, H. Ortsäter, Proteomics in diabetes research, Mol Cell Endocrinol 297(1-2) (2009) 93-103.

[377] M. Lynch, J. Barallobre-Barreiro, M. Jahangiri, M. Mayr, Vascular proteomics in metabolic and cardiovascular diseases, J Intern Med 280(4) (2016) 325-38.

[378] P. Leon-Mimila, J. Wang, A. Huertas-Vazquez, Relevance of Multi-Omics Studies in Cardiovascular Diseases, Front Cardiovasc Med 6 (2019) 91.

[379] N. Rifai, M.A. Gillette, S.A. Carr, Protein biomarker discovery and validation: the long and uncertain path to clinical utility, Nat Biotechnol 24(8) (2006) 971-83.

[380] M. Schirle, M. Bantscheff, B. Kuster, Mass spectrometry-based proteomics in preclinical drug discovery, Chem Biol 19(1) (2012) 72-84.

[381] Biomarkers and surrogate endpoints: preferred definitions and conceptual framework, Clin Pharmacol Ther 69(3) (2001) 89-95.

[382] N. Bergman, J. Bergquist, Recent developments in proteomic methods and disease biomarkers, Analyst 139(16) (2014) 3836-51.

[383] A. Tessitore, A. Gaggiano, G. Cicciarelli, D. Verzella, D. Capece, M. Fischietti, F. Zazzeroni, E. Alesse, Serum biomarkers identification by mass spectrometry in high-mortality tumors, Int J Proteomics 2013 (2013) 125858.

[384] J.W. Lee, V. Devanarayan, Y.C. Barrett, R. Weiner, J. Allinson, S. Fountain, S. Keller, I. Weinryb, M. Green, L. Duan, J.A. Rogers, R. Millham, P.J. O'Brien, J. Sailstad, M. Khan, C. Ray, J.A. Wagner, Fit-for-purpose method development and validation for successful biomarker measurement, Pharm Res 23(2) (2006) 312-28.

[385] N. Krahmer, B. Najafi, F. Schueder, F. Quagliarini, M. Steger, S. Seitz, R. Kasper, F. Salinas, J. Cox, N.H. Uhlenhaut, T.C. Walther, R. Jungmann, A. Zeigerer, G.H.H. Borner, M. Mann, Organellar Proteomics and Phospho-Proteomics Reveal Subcellular Reorganization in Diet-Induced Hepatic Steatosis, Dev Cell 47(2) (2018) 205-221.e7.

CHAPTER 2 PROTEOMIC CHARACTERIZATION OF CYTOPLASMIC LIPID DROPLETS IN HUMAN METASTATIC BREAST CANCER CELLS

2.1 Abstract

One of the characteristic features of metastatic breast cancer is increased cellular storage of neutral lipid in cytoplasmic lipid droplets (CLDs). CLD accumulation is associated with increased cancer aggressiveness, suggesting CLDs contribute to metastasis. However, how CLDs contribute to metastasis is not clear. CLDs are composed of a neutral lipid core, a phospholipid monolayer, and associated proteins. Proteins that associate with CLDs regulate both cellular and CLD metabolism; however, the proteome of CLDs in metastatic breast cancer and how these proteins may contribute to breast cancer progression is unknown. Therefore, the purpose of this study was to identify the proteome and assess the characteristics of CLDs in the MCF10CA1a human metastatic breast cancer cell line. Utilizing shotgun proteomics, we identified over 1500 proteins involved in a variety of cellular processes in the isolated CLD fraction. Interestingly, unlike other cell lines such as adipocytes or enterocytes, the most enriched protein categories were involved in cellular processes outside of lipid metabolism. For example, cell-cell adhesion was the most enriched category of proteins identified, and many of these proteins have been implicated in breast cancer metastasis. In addition, we characterized CLD size and area in MCF10CA1a cells using transmission electron microscopy. Our results provide a hypothesis-generating list of potential players in breast cancer progression and offers a new perspective on the role of CLDs in cancer.

2.2 Introduction

Breast cancer is the leading type of cancer among women in the United States and is predicted to account for 30% of new cancer cases in 2021 [1]. Although breast cancer survival rates are relatively high if the cancer remains localized, life expectancy dramatically decreases

once the cancer metastasizes to distant organs such as bone and lung [2]. Therefore, understanding the characteristic features of metastatic breast cancer cells is critical in order to develop strategies to prevent the progression of breast cancer.

Metastatic breast cancer cells often exhibit altered lipid metabolism, which is an adaptation that allows cells to survive in nutrient-depleted conditions [3]. One of these alterations includes the accumulation of neutral lipid in cytoplasmic lipid droplets (CLDs). The degree of CLD accumulation associates with breast cancer aggressiveness [4-6]; however, the mechanisms behind this relationship are incompletely understood. CLDs are composed of a neutral lipid core of triacylglycerol (TAG) and/or cholesteryl esters surrounded by a phospholipid monolayer and associated proteins [7]. The role of CLDs differs depending on cell type, for example serving as the body's TAG storage pool in adipocytes [8], acting as a local energy source for skeletal and cardiomyocytes [9, 10], and mediating the process of dietary fat absorption in enterocytes [11]. Although multiple hypotheses exist for how CLDs contribute to cancer progression, including protection from cellular stress or serving as a storage pool for fatty acids that can be used for cellular energy, biosynthetic processes, or signaling [6, 12, 13], the exact role of CLDs in metastatic breast cancer cells has not been determined.

Proteins that associate with CLDs serve a variety of functions, but their role in metastasis in unknown. A common function of CLD proteins is to mediate TAG synthesis and lipolysis, reflecting the main purpose of CLDs in storing neutral lipid and maintaining cellular lipid homeostasis [14]. However, recent functional studies of CLD proteins demonstrate novel cellular roles for CLDs by regulating cellular protein location, degradation, and functional activity. For example, histone proteins and transcription factors sequester at the CLD as a mechanism to regulate gene expression [15-17]. In addition, some CLD proteins are destined for degradation [18] such as apolipoprotein B-100, a component of very-low-density lipoproteins, which translocates from the endoplasmic reticulum (ER) to the CLD for degradation in hepatocytes [19, 20]. Finally, CLD proteins may also have specific functions on the CLD, for example mediating inflammatory signaling pathways [21-23]. Despite the identification of proteins involved in a variety of roles in CLD proteomic studies, the functional significance of the majority of CLD proteins has yet to be uncovered. Further, the functional significance of CLD proteins in metastatic breast cancer cells and whether they reflect unique roles for CLDs in cancer is unknown.

The purpose of this study was to identify the proteome of CLDs in metastatic breast cancer cells to generate hypotheses about how CLDs promote breast cancer progression and contribute to altered lipid metabolism and/or other cell functions. To do this, we performed untargeted shotgun proteomic analysis and utilized transmission electron microscopy (TEM) to identify the proteome and characteristics of CLDs from the human metastatic breast cancer cell line, MCF10CA1a.

2.3 Materials and Methods

2.3.1 Cell culture

The MCF10CA1a human metastatic mammary cell line was utilized for these studies. Cells were cultured in Dulbecco's Modified Eagle Medium: Nutrient Mixture F-12 (DMEM/F12, 1:1), supplemented with 5% horse serum, 100 units/ml penicillin, and 100 µg /mL streptomycin in a humidified environment at 37°C with 5% CO_2. Cells were harvested at 70-80% confluence for each experiment.

2.3.2 CLD isolation

Cells from eight 150 mm dishes were pooled and considered one sample. Four samples were prepared for CLD isolation as follows. Cells were rinsed with phosphate buffered saline (PBS, pH 7.4, 137 mM NaCl, 2.7 mM KCl, 8 mM Na_2HPO_4, and 2 mM KH_2PO_4) scraped and pelleted by centrifugation. CLDs were isolated from pelleted cells using a previously established sucrose gradient ultracentrifugation protocol [24, 25]. Briefly, cells were lysed in ice cold sucrose lysis buffer (175 mM sucrose, 10 mM HEPES and 1 mM EDTA pH 7.4) and disrupted by passing through a 23 gauge, 1 inch needle. An aliquot was taken representing the whole cell lysate (WCL) to be used for later applications. The remaining lysate was transferred into a 13.2 mL Open-Top Thinwall UltraClear tube (Beckman Coulter, #344059) and ice-cold lysis buffer was layered on top of the lysate. Samples were centrifuged at 100,000 x g at 4°C for one hour. After centrifugation, the white floating fraction (FF) from each sample was aspirated using a pipette. The remaining soluble and pellet fractions were removed in 1 mL increments. Samples were stored at -80°C until analysis.

2.3.3 Triacylglycerol and protein concentration

TAG concentrations of each fraction were measured using the Wako L-Type Triglyceride M kit (FUJIFILM Wako Diagnostics U.S.A.). Protein concentrations of each fraction were measured using the Pierce^{TM} BCA Protein Assay Kit (Thermo Fisher Scientific).

2.3.4 Validation of CLD isolation by Western blotting

An aliquot of each isolated fraction (CLD fraction through pellet fraction) and the WCL was delipidated with 2:1 chloroform:methanol, then proteins were precipitated with ice-cold acetone. The precipitated proteins were pelleted by centrifugation, then dried and resuspended in Laemmli loading buffer. Samples were subjected to SDS-PAGE using a 12% Tris-glycine gel (Bio-Rad #4561046). Samples were loaded into the gel by volume: 10 uL each of the FF through fraction 10, 5 uL of the pellet fraction and 5 uL of the WCL. See Figure 2-8 for representative Ponceau stain demonstrating differences in protein levels between fractions. The membrane was probed with one of the following primary antibodies at a 1:1,000 concentration (PLIN3, Sigma-Aldrich HPA006427; GAPDH, Cell Signaling Technologies #14C10; CANX, Santa Cruz Biotechnology SC-11397). After washing, a fluorescent secondary antibody was added at a concentration of 1:10,000 (LI-COR IRDye donkey anti-rabbit 680RD, 926-68073). Membranes were imaged using the LI-COR Odyssey CLx Imaging System (LI-COR Biosciences).

2.3.5 Transmission electron microscopy

Cells were prepared as previously described [26]. One 60 mm dish of MCF10CA1a cells and one 60 mm dish of MCF10CA-ras were prepared for TEM. Cells were fixed in 2.5% glutaraldehyde in 0.1 M sodium cacodylate buffer, rinsed, and embedded in agarose. Small pieces of cell pellet were post-fixed in 1% osmium tetroxide containing 0.8% potassium ferricyanide and stained in 1% uranyl acetate. They were then dehydrated with a graded series of ethanol, transferred into acetonitrile, and embedded in EMbed-812 resin. Thin sections were cut on a Reichert-Jung Ultracut E ultramicrotome and post-stained with 4% uranyl acetate and lead citrate. Images were acquired on a FEI Tecnai T12 electron microscope equipped with a tungsten source and operating at 80kV.

2.3.6 CLD size analysis

Acquired TEM images were analyzed using ImageJ [27]. 50 cells were counted and used for CLD analysis. CLD diameter was assessed using ImageJ.

2.3.7 Immunocytochemistry

MCF10CA1a cells were cultured in a #1.5H-N high performance glass bottom 12 well plate (Cellvis) and processed for immunofluorescence microscopy. The cells were fixed in 4% paraformaldehyde, permeabilized with 0.1% Triton X-100, and blocked with BlockAid (Invitrogen, B10710). Cells were probed with antibodies for Plin3, SQLE, and NSDHL (Sigma, HPA006427; SantaCruz Biotechnologies, sc-271651; Atlas Antibodies, HPA000571, respectively). Proteins were detected using secondary AlexaFluor antibodies (Life Technologies, A-21070 and A-21052), and cells were counterstained for neutral lipids using 1 μg/ml 4,4-difluoro-1,3,5,7,8-pentamethyl-4-bora-3a,4a-diaza-s-indacene (BODIPY 493/503; Life Technologies, Grand Island, NY, United States), and for nuclei using 300 nM 4',6-Diamidino-2-Phenylindole, Dihydrochloride (DAPI; Invitrogen, D1306). Samples were imaged using a Nikon A1R-MP inverted confocal microscope (Nikon Instruments Inc., Melville, NY, United States). Images were acquired using the Plan Apo λ 100x Oil objective, 76.63 µm pinhole size, and DAPI, FITC, and Cy5 lasers. All image processing was conducted using Nikon NIS-Elements AR acquisition and analysis software. A Landweber 2D deconvolution algorithm was implemented, with point scan confocal modality, clear noise, and 12, 12, 12 iterations.

2.3.8 CLD protein isolation and in-solution digestion

An aliquot of each CLD fraction containing 50 μg protein was prepared for proteomic analysis. The CLD fractions were delipidated and precipitated as above. The dried protein pellets were reduced and solubilized using 10 mM dithiothreitol/8 M urea, then alkylated using iodoethanol. Samples were dried using a vacuum centrifuge. Proteins were digested with 4 μg Trypsin/Lys-C Mix, Mass Spec Grade (Promega) per sample using a barocycler at 50°C, 20 kpsi, 60 cycles (Barocycler NEP2320, Pressure Biosciences, INC). Peptides were cleaned with MacroSpin C18 spin columns (The Nest Group, Inc) and dried using a vacuum centrifuge. Dried

peptides were resuspended in 3% acetonitrile/0.1% formic acid in preparation for mass spectrometry.

2.3.9 Liquid chromatography/tandem mass spectrometry (LC-MS/MS)

Samples were analyzed as previously described [28]. Samples were analyzed by reverse-phase LC-ESI-MS/MS system using the Dionex UltiMate 3000 RSLC nano System coupled to the Orbitrap Fusion Lumos Mass Spectrometer (Thermo Fisher Scientific). Peptides were loaded onto a trap column (300 mm ID ´ 5 mm) packed with 5 mm 100 Å PepMap C18 medium, then separated on a reverse phase column (50-cm long × 75 µm ID) packed with 2 µm 100 Å PepMap C18 silica (Thermo Fisher Scientific). The column temperature was maintained at 50°C. All MS measurements were performed in positive ion mode using a 120 minute LC gradient and standard data-dependent mode. MS data were acquired with a Top20 data-dependent MS/MS scan method.

2.3.10 LC-MS/MS data analysis

LC-MS/MS data were analyzed using MaxQuant software version 1.6.3.4 [29-31]. Data was searched against the UniProtKB *Homo sapiens* reference proteome (www.uniprot.org). Trypsin/P and Lys-C were selected with a maximum of 2 missed cleavages. Oxidation of methionine was set as a variable modification, iodoethanol set as a fixed modification. First search peptide mass tolerance was set to 20 ppm, main search peptide mass tolerance was set to 10 ppm. False discovery rate was set to 1%. Match between runs was selected and Label-free quantification (LFQ) was used.

2.3.11 Proteomic data analysis

Reverse identifications and contaminants were removed from the dataset. LFQ values were subjected to Log2 transformation. A protein was considered identified if it was present in at least three out of four samples. Uniprot accession numbers in the Majority Protein IDs column were used to categorize proteins into Gene Ontology Biological Process (GO_BP) terms using The Database for Annotation, Visualization and Integrated Discovery (DAVID) v6.8 [32, 33]. Functional relationships between proteins were visualized using STRING version 11 [34]. Raw

LC-MS/MS data is available on the Mass Spectrometry Interactive Virtual Environment (MassIVE) data repository at ftp://massive.ucsd.edu/MSV000086731/.

2.4 Results

2.4.1 Characterization of CLDs in MCF10CA1a cells

To characterize CLDs in the metastatic breast cancer MCF10CA1a cell line, we visualized cells by TEM. A representative MCF10CA1a cell containing CLDs is shown in Figure 2-1A. CLDs present within the cell are highlighted (Figure 2-1B). To determine the distribution of CLDs across cells, we assessed the number and diameter of CLDs per cell (Table 2-1 and Figure 2-2). Ninety percent of cells counted contained CLDs, and the number of CLDs per cell ranged from 0-41. CLD diameter also varied across cells. CLD diameter ranged from 0.17-1.38 µm (Figure 2-2), with an average CLD diameter of 0.58 µm. As expected, only 10% of non-metastatic MCF10A-*ras* cells of the same cell series analyzed contained CLDs (data not shown). A representative MCF10A-*ras* cell without CLDs is shown in Figure 2-9. Due to the absence of CLDs in most MCF10A-*ras* cells, we were unable to isolate CLDs from MCF10A-ras cells and therefore only assessed the proteome of CLDs from MCF10CA1a cells.

2.4.2 CLD isolation from MCF10CA1a cells

To confirm successful isolation of CLDs from MCF10CA1a cells, we determined the TAG to protein ratio of each isolated fraction after sucrose density gradient ultracentrifugation (Figure 2-3A). A high TAG to protein ratio in the floating fraction (FF) indicates the presence of CLDs. In addition, we determined the purity of our isolation based on the presence of specific cell component markers in each isolated fraction (Figure 2-3B). Perilipin (PLIN) 3, a bona-fide CLD-associated protein and marker of CLDs [35], is present in the FF. PLIN3 resides in the cytosol but associates with CLDs when CLDs are present [36], which is consistent with its identification in the soluble fractions. The localization of PLIN3 to CLDs was confirmed by immunocytochemistry (Figure 2-4). Glyceraldehyde 3-phosphate dehydrogenase (GAPDH), a cytosolic marker, is present in the FF and soluble fractions but absent in the pellet fraction (Figure 2-3B). GAPDH is identified in CLD proteomic studies of certain cell types [37, 38], and the identification of GAPDH in the FF suggests GAPDH is a CLD-associated protein in MCF10CA1a cells. Calnexin (CANX),

a marker of ER, is present in only the pellet fraction (Figure 2-3B), as expected based on published CLD isolation protocols [24]. Isolated fractions were loaded by volume and therefore contain different amounts of protein; see representative Ponceau stain in Figure 2-8 for the relative amount of protein in each fraction.

2.4.3 Proteomic characterization of CLDs in MCF10CA1a cells

To determine the proteome of CLDs in MCF10CA1a cells, we performed untargeted shotgun proteomic analysis of the isolated CLD fraction using LC-MS/MS. We identified 1534 proteins that are involved in a wide array of cellular functions (Figure 2-5A). Many of the proteins identified have functions in DNA and RNA metabolic processes (19%) and protein metabolism (18%). To determine whether a specific category of proteins was overrepresented in our dataset, we sorted proteins by Gene Ontology Biological Process (GO_BP) enrichment (Figure 2-5B). Cell-cell adhesion was the most enriched category of proteins identified, followed by translational initiation, and cotranslational protein targeting to membrane (Figure 2-5B). Surprisingly, proteins involved in lipid metabolism comprise only 3% of the proteins identified (Figure 2-5A), and lipid metabolic terms are not represented within the top 50 most enriched GO_BP categories. Low abundance of lipid metabolism proteins is in contrast to other CLD proteomic studies, where they are frequently enriched [14]. We analyzed the 41 proteins identified as associated with lipid metabolism (Figure 2-6). Most of these proteins are involved in cholesterol synthesis, including hydroxymethylglutaryl-CoA synthase, cytoplasmic (HMGCS1), squalene monooxygenase (SQLE), and sterol-4-alpha-carboxylate 3-dehydrogenase, decarboxylating (NSDHL). The localization of SQLE and NSDHL to CLDs was confirmed by immunocytochemistry (Figure 2-7). Both SQLE and NSDHL are shown to concentrate around CLDs. Other identified proteins have basic roles in CLD metabolism, including lipolysis (patatin-like phospholipase domain-containing protein 2/adipose triglyceride lipase (PNPLA2/ATGL), 1-acylglycerol-3-phosphate O-acyltransferase ABHD5 (ABHD5)), phospholipid synthesis (choline-phosphate cytidylyltransferase A (PCYT1A)), TAG synthesis (glycerol-3-phosphate acyltransferase 4 (GPAT4)), and the Plins (PLIN3 and PLIN4).

2.4.4 Proteins involved in cell-cell adhesion are implicated in breast cancer progression

We further analyzed the proteins belonging to the cell-cell adhesion category, as this was the most enriched GO_BP term of proteins identified (Figure 2-5B). To determine how CLDs and their proteins contribute to breast cancer metastasis, we chose proteins in the cell-cell adhesion category that also had GO_BP terms in cell migration and signaling. Proteins with these criteria are listed in Table 2-2. Many of these proteins have been shown to promote breast cancer progression, and the references for each are included in Table 2-2.

2.5 Discussion

To determine mechanisms by which CLDs contribute to breast cancer metastasis, we examined the characteristics and proteome of CLDs in the human metastatic breast cancer cell line, MCF10CA1a, using TEM and LC-MS/MS. We found that the majority of MCF10CA1a cells analyzed contain multiple CLDs that associate with a variety of proteins. To our knowledge, this is the first report of the proteome of CLDs in metastatic breast cancer. We identified 1534 proteins in the isolated CLD fraction representing a wide array of cellular functions. Many of the proteins identified are implicated in breast cancer metastasis. Our results provide a hypothesis-generating list of potential players contributing to cancer progression and provide a new perspective on the role of CLDs in metastatic breast cancer.

Our results are consistent with previous work demonstrating that neutral lipid accumulation in breast cancer cells correlates with metastatic potential [4, 5]. MCF10CA1a cells are the most metastatic in the MCF10A series of breast cancer progression [39] and contain twelve times more TAG than the non-metastatic MCF10A-*ras* cell line from which they were derived [40]. Consistently, while most MCF10CA1a cells analyzed contained at least one CLD (Table 2-1), almost no CLDs were present in non-metastatic MCF10A-ras cells (Figure 2-9). These results support our use of the MCF10CA1a cell line as a model of mammary metastasis to investigate the CLD proteome.

CLD size is often used to estimate the amount of cellular neutral lipid storage and the metabolic state of the cell. For example, cells that store large amounts of TAG, such as adipocytes [41] and enterocytes [42], have large CLDs (ranging up to 100 µm), whereas other cell types tend to have smaller CLDs. Consistent with the size of CLDs in cell types that do not store large

amounts of TAG, including skeletal myocytes [43], hepatocytes [44], and Chinese Hamster Ovary (CHO) cells [45], the diameter of CLDs in the MCF10CA1a cells averaged 0.58 µm (Table 2-1). Further, the distribution of CLDs of various sizes in MCF10CA1a cells (Figure 2-2) may reflect different pools of CLDs that have potentially distinct functions [37, 46]. For example, specific pools of CLDs in brown adipose tissue are differentially involved in fatty acid oxidation or TAG synthesis [47]. It is possible that unique pools of CLDs with different functions may exist in MCF10CA1a cells; however, this requires further investigation.

The proteome of CLDs identified in MCF10CA1a cells has similarities and differences compared to that of other cell types. Many of the proteins identified are consistent with the general categories of proteins commonly found on CLDs. These include proteins involved in lipid and CLD metabolism, translation, protein folding and degradation, cytoskeleton, and histones [14]. Several of the proteins identified involved in lipid metabolism have been validated as CLD-associated proteins and also have functional roles at the CLD surface, including PLIN3 in CLD maintenance [48], GPAT4 [49] and PCYT1A [50, 51] in CLD expansion and size, ATGL in CLD lipolysis [52], and NSDHL in cholesterol synthesis [53, 54]. The identification of lipid metabolism proteins on CLDs in MCF10CA1a cells suggests CLDs across cell types may share similar lipid metabolic machinery and core CLD proteins.

A key difference between the proteome of CLDs in MCF10CA1a cells and that of other cell types is the representation of proteins in the commonly identified categories. For example, lipid metabolism was not a highly enriched protein category in MCF10CA1a cells as it is in other cells types [14]. Further, many of the proteins we identified in the lipid metabolism category are involved in cholesterol metabolism, suggesting CLDs in MCF10CA1a cells may store cholesterol [55, 56]. Consistently, cholesteryl ester accumulation and altered cholesterol metabolism is a common feature of cancer [57, 58]. We found that two enzymes involved in cholesterol synthesis, NSDHL and SQLE, concentrate in areas around CLDs in MCF10CA1a cells (Figure 2-7).

The identification of NSDHL with CLDs in breast cancer cells is consistent with previous observations of its functional association with CLDs and role in metastasis. NSDHL modifies lanosterol before its synthesis into cholesterol [59], and has been shown to localize to CLDs upon oleate loading in CHO cells [53] and in COS-7 cells [54]. In fact, oleate loading and CLD formation in CHO cells decreased the synthesis of C-27 sterols, which includes cholesterol, and increased the synthesis of precursor sterols, including lanosterol [53]. These results suggest the

localization of NSDHL to CLDs may be a mechanism to regulate cholesterol synthesis. NSDHL has also been shown to promote breast cancer progression. NSDHL is present at higher protein levels in metastatic compared to non-metastatic breast cancer cell lines [60], and knockdown of NSDHL in metastatic BT-20 and MDA-MB-231 cells reduced cell viability, colony formation, and cell migration [60]. However, whether these effects are due to lack of NSDHL itself or lack of cholesterol synthesis due to NSDHL inhibition is unclear. Thus, the localization of NSDHL to CLDs in MCF10CA1a cells shown in this study suggests that it may promote breast cancer progression by regulating cholesterol synthesis. Future studies are required to determine the role of NSDHL on CLDs in MCF10CA1a cells and its contribution to metastasis.

The identification of SQLE with CLDs in breast cancer cells is also consistent with previous observations of its functional association with CLDs and role in metastasis. SQLE catalyzes the epoxidation of squalene and is considered the second rate-limiting step in cholesterol synthesis [61]. SQLE localizes to CLDs in yeast cells [62] and has been shown to regulate CLD dynamics. For example, inhibition of SQLE results in CLD clustering and squalene accumulation in yeast [63], and CLD accumulation in MCF7 breast cancer cells [64]. SQLE may regulate CLD dynamics by interacting with microprotein CASIMO1 [64]. CASIMO1 in MCF7 cells was shown to regulate the expression of SQLE as well as CLD formation. How CASIMO1 and/or SQLE influences CLDs is not clear; however, it may involve changes in the cytoskeleton. Interestingly, SQLE has been identified as an oncogene in breast cancer cells [65], suggesting it plays a role in breast cancer metabolism. Consistently, inhibiting SQLE in MCF7 breast cancer cells reduces cell proliferation and ERK phosphorylation/activation [64], which is a key factor involved in initiating cell proliferation and migration in cancer cells [66]. ERK phosphorylation and activation has previously been shown to be regulated by SQLE in other cell types including hepatocellular carcinoma cells [67] and lung squamous cell carcinoma cells [68]. In fact, SQLE-mediated cholesterol synthesis preserves breast cancer stem cell stemness through PI3K/AKT signaling, another proliferative survival pathway, upon stabilization of SQLE mRNA by long non-coding RNA 030 and poly(rC) binding protein 2 [69]. Therefore, the metabolites produced by the action of SQLE may activate cell signaling pathways necessary for cancer cell proliferation. Overall, these results suggest that the localization of enzymes involved in cholesterol synthesis to CLDs in MCF10CA1a cells may be a metabolic adaptation by cancer cells that stimulates cell proliferation. Future studies are required to determine the role of SQLE on CLDs in MCF10CA1a cells.

Instead of lipid metabolism proteins representing the majority of the CLD proteome, proteins with roles in cell-cell adhesion, translation, and mRNA metabolism were the most prevalent in the CLD fraction of MCF10CA1a cells, suggesting these proteins may have a novel functional role on CLDs in cancer. The most enriched category of proteins identified were those involved in cell-cell adhesion. This is particularly interesting, since loss of cell adhesion is a critical first step in the metastatic cascade [70]. Many of the proteins identified in this category have been implicated in breast cancer metastasis (Table 2-2), suggesting CLDs may play a novel role in this process. For example, CLDs may serve as a hub for signaling pathways and cytoskeletal remodeling proteins that are needed to facilitate the epithelial-mesenchymal transition (EMT). However, CLD proteins may either play an active role at the CLD surface or may be mislocalized from their typical cell location, which could interrupt their function and contribute to metastasis. Future studies are required to determine the role of signaling and cytoskeletal proteins identified in Table 2-2 on CLDs in MCF10CA1a cells.

Another category of proteins identified in the isolated CLD fraction of MCF10CA1a cells is RNA binding proteins and translational proteins. Some of these proteins are also implicated in cell motility and breast cancer metastasis [71, 72], suggesting their localization on CLDs contributes to metastatic potential. For example, downregulation of the RNA-binding protein ZBP1 in metastatic breast cancer cells increased cell migration by altering the expression of mRNAs involved in cell-cell adhesion, cytoskeleton, and cell proliferation [73]. In addition, overexpression of the 60S ribosomal subunit RPL15 in circulating tumor cells isolated from patients with metastatic breast cancer increased the translation of ribosomal proteins and proteins involved in cell proliferation, and when injected into mice resulted in increased metastasis and tumor formation [74]. Interestingly, RNA localizes to CLDs in human mast cells [75] and ribosomes localize to CLDs in human monocyte U937 cells and leukocytes [76]. It is possible that CLDs in MCF10CA1a cells house RNA-binding and translational proteins in order to facilitate localized gene expression and protein translation to promote cell migration. This hypothesis requires testing in future experiments.

Validation of proteins identified in the CLD fraction by methods such as immunocytochemistry is needed to conclude that a protein associates with CLDs. It is possible that some proteins identified localize near, but may not directly associate with, CLDs. CLDs interact with multiple cellular organelles [77] and proteins associated with an interacting organelle

may be isolated with the CLD fraction. Since we have not validated all the proteins in our analysis for cellular location via another mechanism, only hypotheses about their localization and function in cancer progression can be made. Despite this limitation, our analysis has generated a novel list of proteins that can be studied in more detail in future experiments.

In summary, we characterized CLDs and the CLD proteome isolated from the human metastatic breast cancer cell line, MCF10CA1a. The identification of an interesting variety of proteins in the isolated CLD fraction reflects both similarities with CLDs in other cell types, as well as differences that may support a novel role of CLDs in cancer. It is possible that proteins associated with CLDs in metastatic cancer cells may play a role in permitting the advantageous metabolic plasticity that supports cancer progression. It would be interesting to assess the similarities and differences of CLD proteomes in other metastatic breast cancer cell lines which may further our understanding of cancer progression and identify factors that can be targeted to prevent metastasis. In conclusion, this study provides a new perspective on the role of CLDs in breast cancer metastasis.

2.6 Acknowledgments

Table 2-1. Number and diameter of CLDs within MCF10CA1a cells. 50 cells were counted and used for the analysis. CLD diameter was measured using ImageJ. Distribution of CLD diameters is shown in Figure 2-2.

% of cells containing CLDs	# CLDs per cell	Average # CLDs per cell	CLD diameter range (μm)	Average CLD diameter (μm)
90	0-41	12	0.17-1.38	0.58

Table 2-2. Proteins in cell-cell adhesion are associated with breast cancer metastasis. List of proteins within the Gene Ontology Biological Process (GO_BP) category "cell-cell adhesion" that also have GO_BP terms of signaling and/or cell migration.

Protein name	Gene	General function	Proposed role in breast cancer metastasis	References
IQ motif containing GTPase activating protein 1	IQGAP1	Scaffold protein; signaling and cytoskeleton dynamics	Promotes cell proliferation, migration, tumor growth	[78-82]
Serine/threonine kinase 24	STK24	MAPK signaling	Promotes cell proliferation, tumor growth	[83]
S100 calcium binding protein P	S100P	Calcium signaling	Promotes cell proliferation, migration, motility	[84-86]
Fascin actin-bundling protein 1	FSCN1	Actin-binding protein; cell adhesion, motility, migration	Promotes metastasis through NFκB and STAT3 signaling	[87-92]
GIPC PDZ domain containing family member 1	GIPC1	Scaffold protein; signaling	Involved in cell cycle, apoptosis, motility	[93, 94]
Profilin 1	PFN1	Actin-binding protein; cytoskeletal dynamics	Suppresses cell migration and cell cycle	[95-98]
Tumor-associated calcium signal transducer 2	TACSTD2	Calcium signaling	Promotes cell growth, migration, proliferation through AKT signaling	[99, 100]
Syndecan binding protein	SDCBP	Adaptor protein; signaling and cytoskeletal dynamics	Promotes cell proliferation, growth, motility, cell cycle	[101-104]
RAB1A, member RAS oncogene family	RAB1A	Vesicle trafficking from ER to Golgi	Involved in cell proliferation, migration, EMT; involved in mTORC1 signaling	[105, 106]
STE20 like kinase	SLK	Apoptosis, cytoskeletal dynamics	Promotes cell migration	[107]
Coronin 1B	CORO1B	Actin-binding protein; cell motility	Involved in cell cycle progression	[108]
Heat shock protein family A (Hsp70) member 5	HSPA5	Protein folding	Promotes cell motility and proliferation	[109-111]
Microtubule associated protein RP/EB family member 1	MAPRE1	Microtubule dynamics	Promotes cell proliferation and tumor growth	[112]
Radixin	RDX	Binds actin	Involved in cell motility; interacts with ERBB2 receptors	[113, 114]
Signal transducer and activator of transcription 1	STAT1	Transcription factor; responds to cytokines and growth factors	Either promotes or inhibits tumor growth	[115-118]
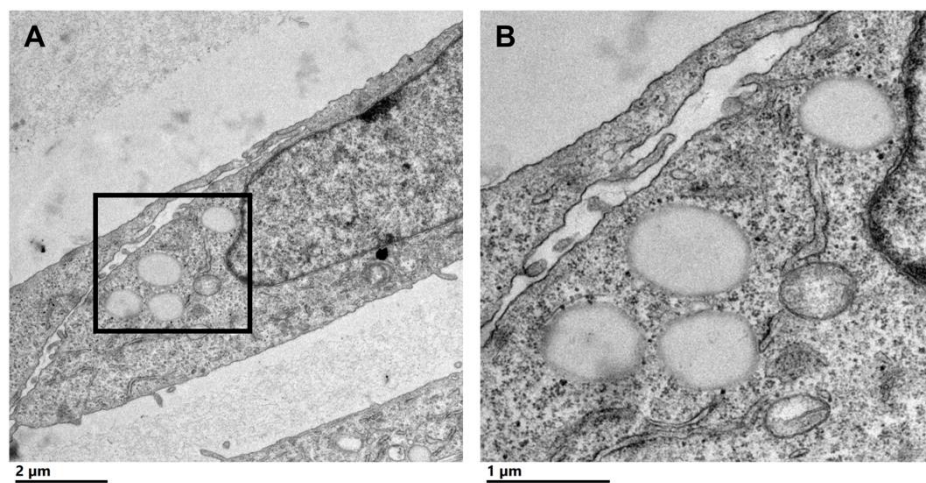
Figure 2-1. Cytoplasmic lipid droplets (CLDs) are present in MCF10CA1a cells. (A) Representative transmission electron microscopy (TEM) image of a MCF10CA1a cell containing CLDs (boxed region), scale bar 2 μm. (B) Magnified image of the CLDs present in A, scale bar 1 μm.
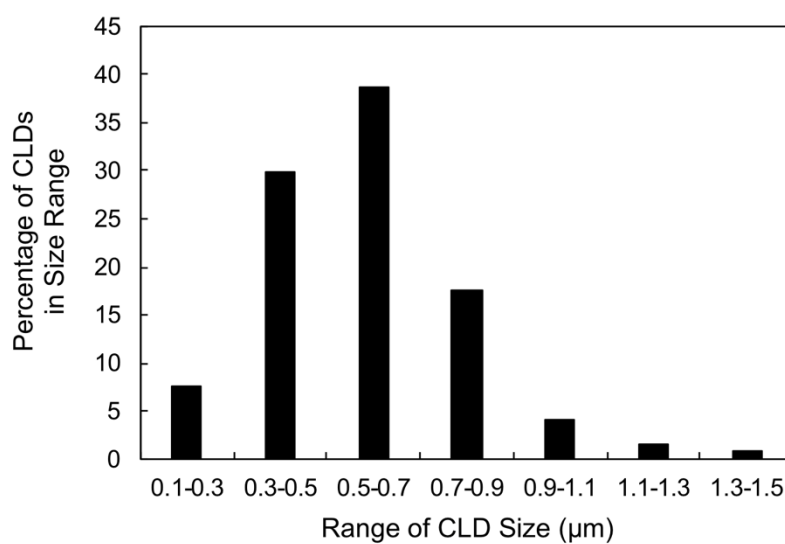
Figure 2-2. Cytoplasmic lipid droplet (CLD) size distribution. Percentage of CLDs analyzed in Table 2-1 within the indicated size range. 50 cells were counted and used for the analysis. CLD diameter was measured using ImageJ.
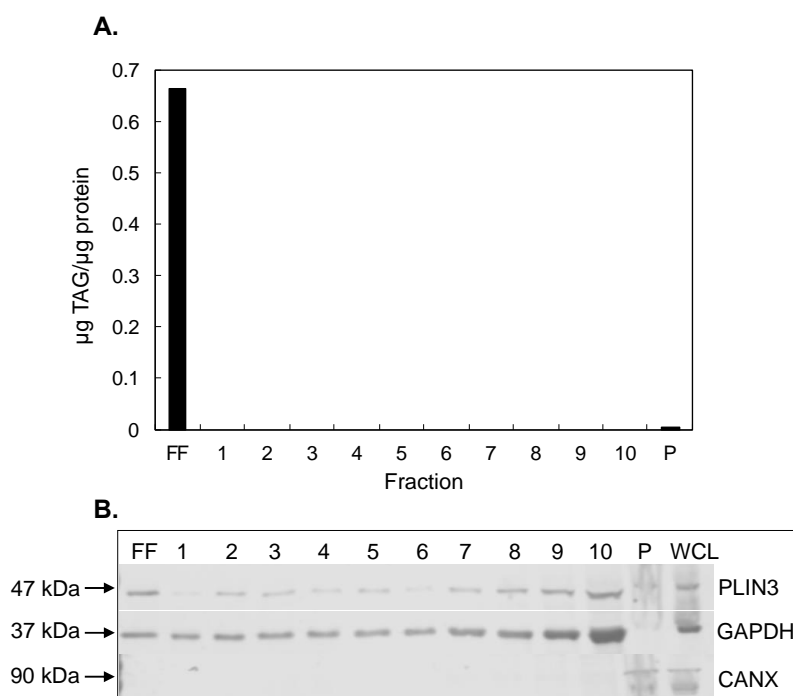
Figure 2-3. Validation of cytoplasmic lipid droplet (CLD) isolation. (A) Triacylglycerol (TAG) to protein ratio of each isolated fraction. CLDs were isolated from MCF10CA1a cells using sucrose density gradient ultracentrifugation. Fractions were removed sequentially from the top of the gradient to the bottom. Floating fraction (FF): isolated CLDs, 1-10: soluble fractions, P: pellet. (B) Western blot of isolated fractions and whole cell lysate (WCL). Fractions were loaded by volume: 10 µL FF-10, 5 µL P and WCL. Membrane was probed for markers of CLDs (PLIN3), cytosol (GAPDH), and endoplasmic reticulum (CANX). Approximate molecular weight markers for each protein are listed. See Figure 2-8 for a representative Ponceau stain reflecting the relative levels of protein in each fraction.
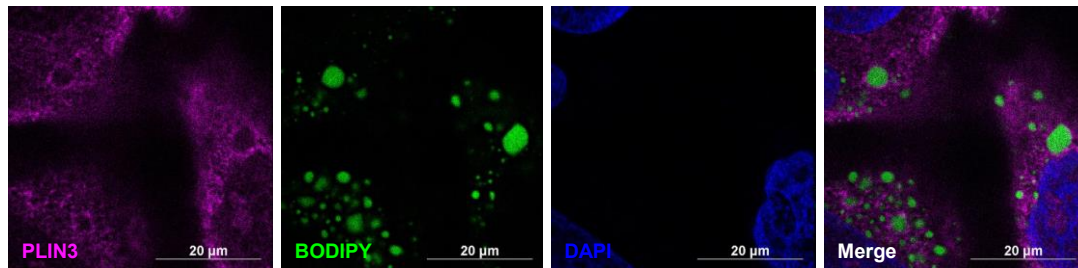
Figure 2-4. PLIN3 surrounds cytoplasmic lipid droplets (CLDs) in MCF10CA1a cells. Representative immunofluorescence images of MCF10CA1a cells. Cells were stained with AlexaFluor 633 to visualize PLIN3, BODIPY to visualize CLDs, and DAPI to visualize nuclei. Signals from all three channels were merged for the final image.

A

- DNA/RNA
- Protein metabolism
- Other
- Translation
- Cytoskeleton
- Cellular transport
- Signaling, including Ca binding and signaling
- Redox
- Cell cycle and apoptosis
- Lipid metabolism
- Transcription
- Carbohydrate metabolism
- Cell-cell adhesion
- Organelle structure, function, and autophagy
- ATP synthesis/energy homeostasis

B

GO:0098609~cell-cell adhesion
GO:0006413~translational initiation
GO:0006614~cotranslational protein targeting to membrane
GO:0000184~nuclear-transcribed mRNA catabolic process
GO:0019083~viral transcription
GO:0000398~mRNA splicing, via spliceosome
GO:0006364~rRNA processing
GO:0043488~regulation of mRNA stability
GO:0006412~translation
GO:0038061~NIK/NF-kappaB signaling

$-\log_{10}(P)$

Figure 2-5. General functions of identified proteins and Gene Ontology (GO) term enrichment. (A) Identified proteins grouped into general categories. Data shown as a percent of total proteins identified. Categories with the highest to lowest percent of proteins listed from top to bottom and are read clockwise around the pie chart. (B) Chart of the top 10 most enriched Gene Ontology Biological Process (GO_BP) terms. Most to least enriched term listed from top to bottom. Data shown as -log10 (p-value). Enrichment scores/p-values calculated in DAVID.
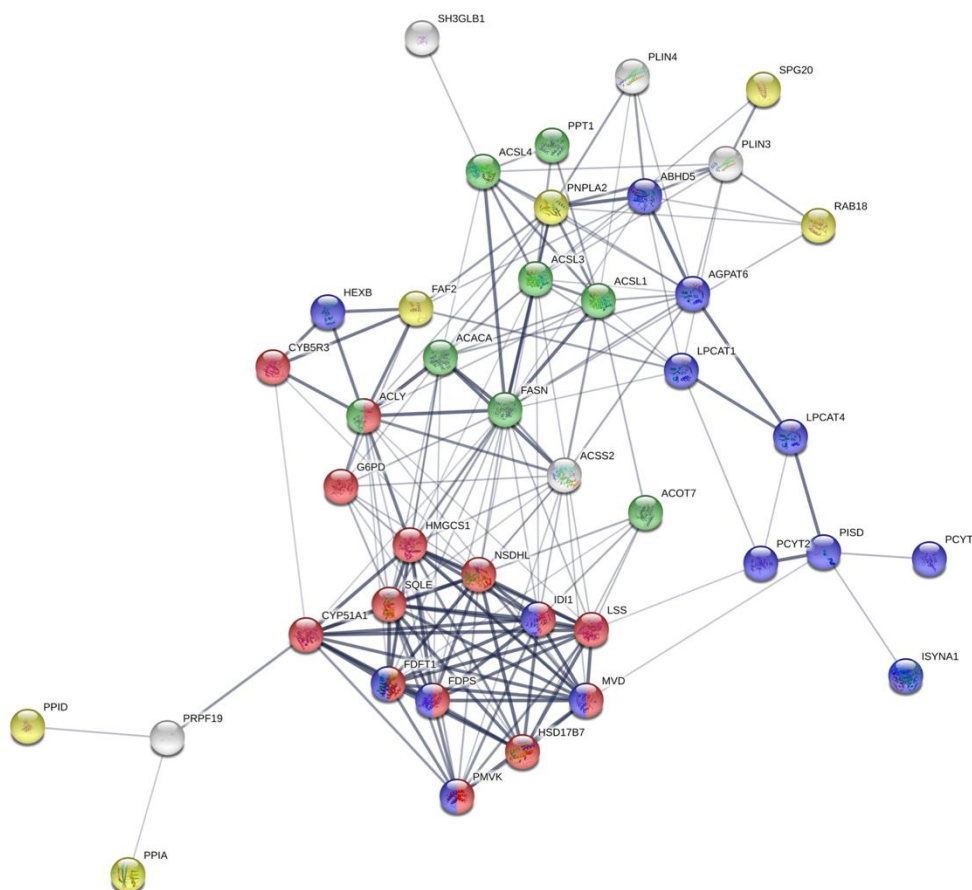
Figure 2-6. STRING analysis of identified proteins involved in lipid metabolism. Proteins with known functions in lipid metabolism and those associated with lipid-related Gene Ontology Biological Process (GO_BP) terms. Red: cholesterol biosynthetic process; green: fatty-acyl-CoA metabolic process; purple: phospholipid metabolic process; yellow: lipid droplet organization.
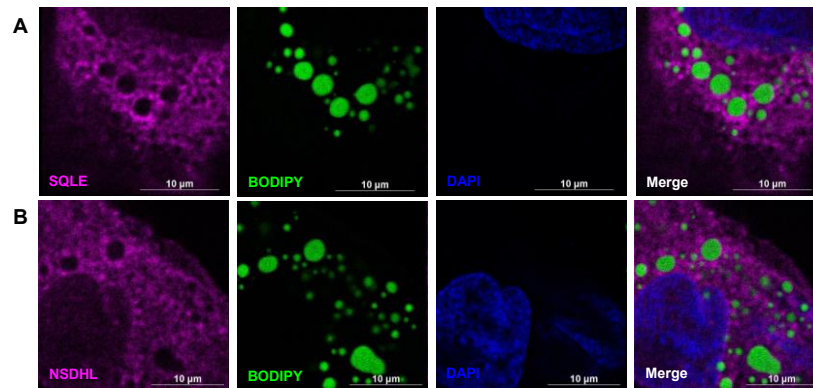
Figure 2-7. SQLE and NSDHL localize to cytoplasmic lipid droplets (CLDs) in MCF10CA1a cells. Representative immunofluorescence images of MCF10CA1a cells. Cells were stained with AlexaFluor 633 to visualize SQLE (A) and NSDHL (B), BODIPY to visualize CLDs, and DAPI to visualize nuclei. Signals from all three channels were merged for the final image in A and B.
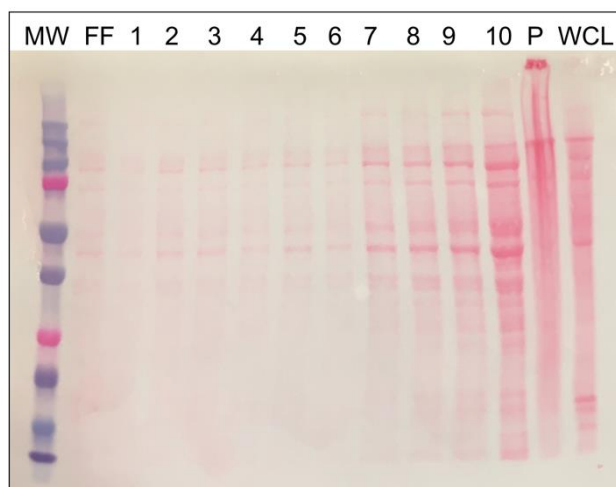
Figure 2-8. Representative Ponceau stain for Western blots. Fractions were loaded by volume: 10 µL floating fraction (FF)-10, 5 µL pellet (P) and whole cell lysate (WCL). Membrane demonstrates the relative amount of protein per lane.
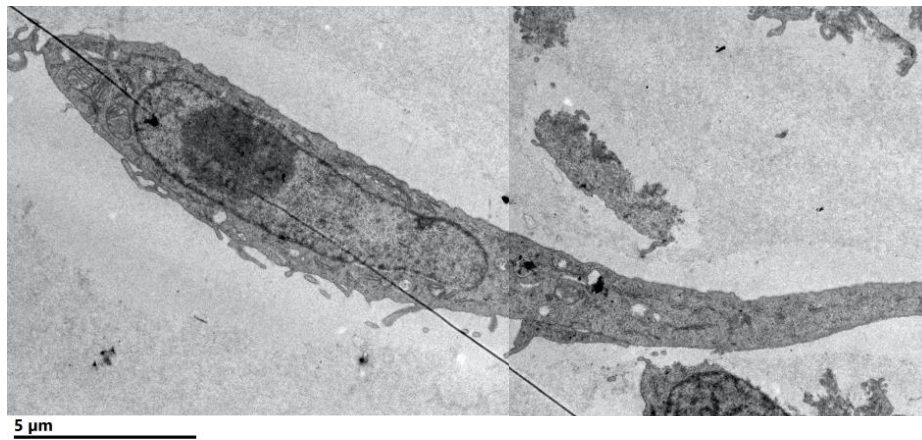
Figure 2-9. Cytoplasmic lipid droplets (CLDs) are not present in non-metastatic MCF10A-*ras* cells. Representative transmission electron microscopy (TEM) image of a MCF10A-*ras* cell. Scale bar 5 μm.

2.7 References

[1]   R.L. Siegel, K.D. Miller, H.E. Fuchs, A. Jemal, Cancer Statistics, 2021, CA Cancer J Clin 71(1) (2021) 7-33.

[2]   X. Jin, P. Mu, Targeting Breast Cancer Metastasis, Breast Cancer (Auckl) 9(Suppl 1) (2015) 23-34.

[3]   S. Beloribi-Djefaflia, S. Vasseur, F. Guillaumond, Lipid metabolic reprogramming in cancer cells, Oncogenesis 5 (2016) e189.

[4]   C. Nieva, M. Marro, N. Santana-Codina, S. Rao, D. Petrov, A. Sierra, The lipid phenotype of breast cancer cells characterized by Raman microspectroscopy: towards a stratification of malignancy, PLoS One 7(10) (2012) e46456.

[5]   H. Abramczyk, J. Surmacki, M. Kopec, A.K. Olejnik, K. Lubecka-Pietruszewska, K. Fabianowska-Majewska, The role of lipid droplets and adipocytes in cancer. Raman imaging of cell cultures: MCF10A, MCF7, and MDA-MB-231 compared to adipocytes in cancerous human breast tissue, Analyst 140(7) (2015) 2224-35.

[6]   P. Shyu, Jr., X.F.A. Wong, K. Crasta, G. Thibault, Dropping in on lipid droplets: insights into cellular stress and cancer, Biosci Rep 38(5) (2018) BSR20180764.

[7]   T.C. Walther, J. Chung, R.V. Farese, Jr., Lipid Droplet Biogenesis, Annu Rev Cell Dev Biol 33 (2017) 491-510.

[8]   Y. Qi, L. Sun, H. Yang, Lipid droplet growth and adipocyte development: mechanistically distinct processes connected by phospholipids, Biochim Biophys Acta Mol Cell Biol Lipids 1862(10 Pt B) (2017) 1273-1283.

[9]   M. Bosma, Lipid droplet dynamics in skeletal muscle, Exp Cell Res 340(2) (2016) 180-6.

[10]   I.J. Goldberg, K. Reue, N.A. Abumrad, P.E. Bickel, S. Cohen, E.A. Fisher, Z.S. Galis, J.G. Granneman, E.D. Lewandowski, R. Murphy, M. Olive, J.E. Schaffer, L. Schwartz-Longacre, G.I. Shulman, T.C. Walther, J. Chen, Deciphering the Role of Lipid Droplets in Cardiovascular Disease: A Report From the 2017 National Heart, Lung, and Blood Institute Workshop, Circulation 138(3) (2018) 305-315.

[11]   T. D'Aquila, Y.H. Hung, A. Carreiro, K.K. Buhman, Recent discoveries on absorption of dietary fat: Presence, synthesis, and metabolism of cytoplasmic lipid droplets within enterocytes, Biochim Biophys Acta 1861(8 Pt A) (2016) 730-47.

[12]   A.L.S. Cruz, E.A. Barreto, N.P.B. Fazolini, J.P.B. Viola, P.T. Bozza, Lipid droplets: platforms with multiple functions in cancer hallmarks, Cell Death Dis 11(2) (2020) 105.

[13]   T. Petan, E. Jarc, M. Jusovic, Lipid Droplets in Cancer: Guardians of Fat in a Stressful World, Molecules 23(8) (2018) 1941.

[14] C. Zhang, P. Liu, The New Face of the Lipid Droplet: Lipid Droplet Proteins, Proteomics 19(10) (2019) e1700223.

[15] N. Mejhert, L. Kuruvilla, K.R. Gabriel, S.D. Elliott, M.A. Guie, H. Wang, Z.W. Lai, E.A. Lane, R. Christiano, N.N. Danial, R.V. Farese, Jr., T.C. Walther, Partitioning of MLX-Family Transcription Factors to Lipid Droplets Regulates Metabolic Gene Expression, Mol Cell 77(6) (2020) 1251-1264.e9.

[16] M.R. Johnson, R.A. Stephenson, S. Ghaemmaghami, M.A. Welte, Developmentally regulated H2Av buffering via dynamic sequestration to lipid droplets in Drosophila embryos, Elife 7 (2018) e36021.

[17] Z. Li, K. Thiel, P.J. Thul, M. Beller, R.P. Kuhnlein, M.A. Welte, Lipid droplets control the maternal histone supply of Drosophila embryos, Curr Biol 22(22) (2012) 2104-13.

[18] K. Bersuker, J.A. Olzmann, Establishing the lipid droplet proteome: Mechanisms of lipid droplet protein targeting and degradation, Biochim Biophys Acta Mol Cell Biol Lipids 1862(10 Pt B) (2017) 1166-1177.

[19] Y. Ohsaki, J. Cheng, A. Fujita, T. Tokumoto, T. Fujimoto, Cytoplasmic lipid droplets are sites of convergence of proteasomal and autophagic degradation of apolipoprotein B, Mol Biol Cell 17(6) (2006) 2674-83.

[20] M. Suzuki, T. Otsuka, Y. Ohsaki, J. Cheng, T. Taniguchi, H. Hashimoto, H. Taniguchi, T. Fujimoto, Derlin-1 and UBXD8 are engaged in dislocation and degradation of lipidated ApoB-100 at lipid droplets, Mol Biol Cell 23(5) (2012) 800-10.

[21] E. Jarc, T. Petan, A twist of FATe: Lipid droplets and inflammatory lipid mediators, Biochimie 169 (2020) 69-87.

[22] M.T. Accioly, P. Pacheco, C.M. Maya-Monteiro, N. Carrossini, B.K. Robbs, S.S. Oliveira, C. Kaufmann, J.A. Morgado-Diaz, P.T. Bozza, J.P. Viola, Lipid bodies are reservoirs of cyclooxygenase-2 and sites of prostaglandin-E2 synthesis in colon cancer cells, Cancer Res 68(6) (2008) 1732-40.

[23] A.R. Silva, P. Pacheco, A. Vieira-de-Abreu, C.M. Maya-Monteiro, B. D'Alegria, K.G. Magalhaes, E.F. de Assis, C. Bandeira-Melo, H.C. Castro-Faria-Neto, P.T. Bozza, Lipid bodies in oxidized LDL-induced foam cells are leukotriene-synthesizing organelles: a MCP-1/CCL2 regulated phenomenon, Biochim Biophys Acta 1791(11) (2009) 1066-75.

[24] D.L. Brasaemle, N.E. Wolins, Isolation of Lipid Droplets from Cells by Density Gradient Centrifugation, Curr Protoc Cell Biol 72 (2016) 3.15.1-3.15.13.

[25] L.A. Harris, T.M. Shew, J.R. Skinner, N.E. Wolins, A single centrifugation method for isolating fat droplets from cells and tissues, J Lipid Res 53(5) (2012) 1021-5.

[26] K.J. Wijesinghe, L. McVeigh, M.L. Husby, N. Bhattarai, J. Ma, B.S. Gerstman, P.P. Chapagain, R.V. Stahelin, Mutation of Hydrophobic Residues in the C-Terminal Domain of the Marburg Virus Matrix Protein VP40 Disrupts Trafficking to the Plasma Membrane, Viruses 12(4) (2020) 482.

[27] C.A. Schneider, W.S. Rasband, K.W. Eliceiri, NIH Image to ImageJ: 25 years of image analysis, Nat Methods 9(7) (2012) 671-5.

[28] A.J. Barabas, U.K. Aryal, B.N. Gaskill, Proteome characterization of used nesting material and potential protein sources from group housed male mice, Mus musculus, Sci Rep 9(1) (2019) 17524.

[29] J. Cox, M.Y. Hein, C.A. Luber, I. Paron, N. Nagaraj, M. Mann, Accurate proteome-wide label-free quantification by delayed normalization and maximal peptide ratio extraction, termed MaxLFQ, Mol Cell Proteomics 13(9) (2014) 2513-26.

[30] J. Cox, N. Neuhauser, A. Michalski, R.A. Scheltema, J.V. Olsen, M. Mann, Andromeda: a peptide search engine integrated into the MaxQuant environment, J Proteome Res 10(4) (2011) 1794-805.

[31] J. Cox, M. Mann, MaxQuant enables high peptide identification rates, individualized p.p.b.-range mass accuracies and proteome-wide protein quantification, Nat Biotechnol 26(12) (2008) 1367-72.

[32] W. Huang da, B.T. Sherman, R.A. Lempicki, Systematic and integrative analysis of large gene lists using DAVID bioinformatics resources, Nat Protoc 4(1) (2009) 44-57.

[33] W. Huang da, B.T. Sherman, R.A. Lempicki, Bioinformatics enrichment tools: paths toward the comprehensive functional analysis of large gene lists, Nucleic Acids Res 37(1) (2009) 1-13.

[34] D. Szklarczyk, A.L. Gable, D. Lyon, A. Junge, S. Wyder, J. Huerta-Cepas, M. Simonovic, N.T. Doncheva, J.H. Morris, P. Bork, L.J. Jensen, C.V. Mering, STRING v11: protein-protein association networks with increased coverage, supporting functional discovery in genome-wide experimental datasets, Nucleic Acids Res 47(D1) (2019) D607-d613.

[35] A.R. Kimmel, C. Sztalryd, The Perilipins: Major Cytosolic Lipid Droplet-Associated Proteins and Their Roles in Cellular Lipid Storage, Mobilization, and Systemic Homeostasis, Annu Rev Nutr 36 (2016) 471-509.

[36] B. Lee, J. Zhu, N.E. Wolins, J.X. Cheng, K.K. Buhman, Differential association of adipophilin and TIP47 proteins with cytoplasmic lipid droplets in mouse enterocytes during dietary fat absorption, Biochim Biophys Acta 1791(12) (2009) 1173-80.

[37]   S. Zhang, Y. Wang, L. Cui, Y. Deng, S. Xu, J. Yu, S. Cichello, G. Serrero, Y. Ying, P. Liu, Morphologically and Functionally Distinct Lipid Droplet Subpopulations, Sci Rep 6 (2016) 29539.

[38]   Y. Fujimoto, H. Itabe, J. Sakai, M. Makita, J. Noda, M. Mori, Y. Higashi, S. Kojima, T. Takano, Identification of major proteins in the lipid droplet-enriched fraction isolated from the human hepatocyte cell line HuH7, Biochim Biophys Acta 1644(1) (2004) 47-59.

[39]   S.J. Santner, P.J. Dawson, L. Tait, H.D. Soule, J. Eliason, A.N. Mohamed, S.R. Wolman, G.H. Heppner, F.R. Miller, Malignant MCF10CA1 cell lines derived from premalignant human breast epithelial MCF10AT cells, Breast Cancer Res Treat 65(2) (2001) 101-10.

[40]   T. Wilmanski, K. Buhman, S.S. Donkin, J.R. Burgess, D. Teegarden, 1alpha,25-dihydroxyvitamin D inhibits de novo fatty acid synthesis and lipid accumulation in metastatic breast cancer cells through down-regulation of pyruvate carboxylase, J Nutr Biochem 40 (2017) 194-200.

[41]   M. Suzuki, Y. Shinohara, Y. Ohsaki, T. Fujimoto, Lipid droplets: size matters, J Electron Microsc (Tokyo) 60 Suppl 1 (2011) S101-16.

[42]   T. D'Aquila, A.S. Zembroski, K.K. Buhman, Diet Induced Obesity Alters Intestinal Cytoplasmic Lipid Droplet Morphology and Proteome in the Postprandial Response to Dietary Fat, Front Physiol 10 (2019) 180.

[43]   S. Daemen, N. van Polanen, M.K.C. Hesselink, The effect of diet and exercise on lipid droplet dynamics in human muscle tissue, J Exp Biol 221(Pt Suppl 1) (2018) jeb167015.

[44]   M.B. Schott, S.G. Weller, R.J. Schulze, E.W. Krueger, K. Drizyte-Miller, C.A. Casey, M.A. McNiven, Lipid droplet size directs lipolysis and lipophagy catabolism in hepatocytes, J Cell Biol 218(10) (2019) 3320-3335.

[45]   Ding, S. Zhang, L. Yang, H. Na, P. Zhang, H. Zhang, Y. Wang, Y. Chen, J. Yu, C. Huo, S. Xu, M. Garaiova, Y. Cong, P. Liu, Isolating lipid droplets from multiple species, Nat Protoc 8(1) (2013) 43-51.

[46]   A.R. Thiam, M. Beller, The why, when and how of lipid droplet diversity, J Cell Sci 130(2) (2017) 315-324.

[47]   I.Y. Benador, M. Veliova, K. Mahdaviani, A. Petcherski, J.D. Wikstrom, E.A. Assali, R. Acin-Perez, M. Shum, M.F. Oliveira, S. Cinti, C. Sztalryd, W.D. Barshop, J.A. Wohlschlegel, B.E. Corkey, M. Liesa, O.S. Shirihai, Mitochondria Bound to Lipid Droplets Have Unique Bioenergetics, Composition, and Dynamics that Support Lipid Droplet Expansion, Cell Metab 27(4) (2018) 869-885.e6.

[48]   C. Sztalryd, D.L. Brasaemle, The perilipin family of lipid droplet proteins: Gatekeepers of intracellular lipolysis, Biochim Biophys Acta Mol Cell Biol Lipids 1862(10 Pt B) (2017) 1221-1232.

[49]   F. Wilfling, H. Wang, J.T. Haas, N. Krahmer, T.J. Gould, A. Uchida, J.-X. Cheng, M. Graham, R. Christiano, F. Froehlich, X. Liu, K.K. Buhman, R.A. Coleman, J. Bewersdorf, R.V. Farese, Jr., T.C. Walther, Triacylglycerol Synthesis Enzymes Mediate Lipid Droplet Growth by Relocalizing from the ER to Lipid Droplets, Developmental Cell 24(4) (2013) 384-399.

[50]   N. Krahmer, Y. Guo, F. Wilfling, M. Hilger, S. Lingrell, K. Heger, H.W. Newman, M. Schmidt-Supprian, D.E. Vance, M. Mann, R.V. Farese, Jr., T.C. Walther, Phosphatidylcholine synthesis for lipid droplet expansion is mediated by localized activation of CTP:phosphocholine cytidylyltransferase, Cell Metab 14(4) (2011) 504-15.

[51]   Y. Guo, T.C. Walther, M. Rao, N. Stuurman, G. Goshima, K. Terayama, J.S. Wong, R.D. Vale, P. Walter, R.V. Farese, Functional genomic screen reveals genes involved in lipid-droplet formation and utilization, Nature 453(7195) (2008) 657-61.

[52]   E. Smirnova, E.B. Goldberg, K.S. Makarova, L. Lin, W.J. Brown, C.L. Jackson, ATGL has a key role in lipid droplet/adiposome degradation in mammalian cells, EMBO Rep 7(1) (2006) 106-13.

[53]   M. Ohashi, N. Mizushima, Y. Kabeya, T. Yoshimori, Localization of mammalian NAD(P)H steroid dehydrogenase-like protein on lipid droplets, J Biol Chem 278(38) (2003) 36819-29.

[54]   H. Caldas, G.E. Herman, NSDHL, an enzyme involved in cholesterol biosynthesis, traffics through the Golgi and accumulates on ER membranes and on the surface of lipid droplets, Hum Mol Genet 12(22) (2003) 2981-91.

[55]   C.J. Antalis, T. Arnold, T. Rasool, B. Lee, K.K. Buhman, R.A. Siddiqui, High ACAT1 expression in estrogen receptor negative basal-like breast cancer cells is associated with LDL-induced proliferation, Breast Cancer Res Treat 122(3) (2010) 661-70.

[56]   C.J. Antalis, A. Uchida, K.K. Buhman, R.A. Siddiqui, Migration of MDA-MB-231 breast cancer cells depends on the availability of exogenous lipids and cholesterol esterification, Clin Exp Metastasis 28(8) (2011) 733-41.

[57]   A. Chimento, I. Casaburi, P. Avena, F. Trotta, A. De Luca, V. Rago, V. Pezzi, R. Sirianni, Cholesterol and Its Metabolites in Tumor Growth: Therapeutic Potential of Statins in Cancer Treatment, Front Endocrinol (Lausanne) 9 (2018) 807.

[58]   B. Huang, B.-l. Song, C. Xu, Cholesterol metabolism in cancer: mechanisms and therapeutic opportunities, Nature Metabolism 2(2) (2020) 132-141.

[59]   L.J. Sharpe, A.J. Brown, Controlling cholesterol synthesis beyond 3-hydroxy-3-methylglutaryl-CoA reductase (HMGCR), J Biol Chem 288(26) (2013) 18707-15.

[60]   S.H. Yoon, H.S. Kim, R.N. Kim, S.Y. Jung, B.S. Hong, E.J. Kang, H.B. Lee, H.G. Moon, D.Y. Noh, W. Han, NAD(P)-dependent steroid dehydrogenase-like is involved in breast cancer cell growth and metastasis, BMC Cancer 20(1) (2020) 375.

[61]   S. Feltrin, F. Ravera, N. Traversone, L. Ferrando, D. Bedognetti, A. Ballestrero, G. Zoppoli, Sterol synthesis pathway inhibition as a target for cancer treatment, Cancer Lett 493 (2020) 19-30.

[62]   R. Leber, K. Landl, E. Zinser, H. Ahorn, A. Spök, S.D. Kohlwein, F. Turnowsky, G. Daum, Dual localization of squalene epoxidase, Erg1p, in yeast reflects a relationship between the endoplasmic reticulum and lipid particles, Mol Biol Cell 9(2) (1998) 375-86.

[63]   M.T. Ta, T.S. Kapterian, W. Fei, X. Du, A.J. Brown, I.W. Dawes, H. Yang, Accumulation of squalene is associated with the clustering of lipid droplets, Febs J 279(22) (2012) 4231-44.

[64]   M. Polycarpou-Schwarz, M. Groß, P. Mestdagh, J. Schott, S.E. Grund, C. Hildenbrand, J. Rom, S. Aulmann, H.P. Sinn, J. Vandesompele, S. Diederichs, The cancer-associated microprotein CASIMO1 controls cell proliferation and interacts with squalene epoxidase modulating lipid droplet formation, Oncogene 37(34) (2018) 4750-4768.

[65]   D.N. Brown, I. Caffa, G. Cirmena, D. Piras, A. Garuti, M. Gallo, S. Alberti, A. Nencioni, A. Ballestrero, G. Zoppoli, Squalene epoxidase is a bona fide oncogene by amplification with clinical relevance in breast cancer, Sci Rep 6 (2016) 19435.

[66]   Y.J. Guo, W.W. Pan, S.B. Liu, Z.F. Shen, Y. Xu, L.L. Hu, ERK/MAPK signalling pathway and tumorigenesis, Exp Ther Med 19(3) (2020) 1997-2007.

[67]   Z. Sui, J. Zhou, Z. Cheng, P. Lu, Squalene epoxidase (SQLE) promotes the growth and migration of the hepatocellular carcinoma cells, Tumour Biol 36(8) (2015) 6173-9.

[68]   H. Ge, Y. Zhao, X. Shi, Z. Tan, X. Chi, M. He, G. Jiang, L. Ji, H. Li, Squalene epoxidase promotes the proliferation and metastasis of lung squamous cell carcinoma cells though extracellular signal-regulated kinase signaling, Thorac Cancer 10(3) (2019) 428-436.

[69]   Y. Qin, Y. Hou, S. Liu, P. Zhu, X. Wan, M. Zhao, M. Peng, H. Zeng, Q. Li, T. Jin, X. Cui, M. Liu, A Novel Long Non-Coding RNA lnc030 Maintains Breast Cancer Stem Cell Stemness by Stabilizing SQLE mRNA and Increasing Cholesterol Synthesis, Adv Sci (Weinh) 8(2) (2020) 2002232.

[70]   S. Valastyan, R.A. Weinberg, Tumor metastasis: molecular insights and evolving paradigms, Cell 147(2) (2011) 275-92.

[71]   L. Wurth, Versatility of RNA-Binding Proteins in Cancer, Comp Funct Genomics 2012 (2012) 178525.

[72]   S. Mohibi, X. Chen, J. Zhang, Cancer the'RBP'eutics-RNA-binding proteins as therapeutic targets for cancer, Pharmacol Ther 203 (2019) 107390.

[73]   W. Gu, F. Pan, R.H. Singer, Blocking beta-catenin binding to the ZBP1 promoter represses ZBP1 expression, leading to increased proliferation and migration of metastatic breast-cancer cells, J Cell Sci 122(Pt 11) (2009) 1895-905.

[74]   R.Y. Ebright, S. Lee, B.S. Wittner, K.L. Niederhoffer, B.T. Nicholson, A. Bardia, S. Truesdell, D.F. Wiley, B. Wesley, S. Li, A. Mai, N. Aceto, N. Vincent-Jordan, A. Szabolcs, B. Chirn, J. Kreuzer, V. Comaills, M. Kalinich, W. Haas, D.T. Ting, M. Toner, S. Vasudevan, D.A. Haber, S. Maheswaran, D.S. Micalizzi, Deregulation of ribosomal protein expression and translation promotes breast cancer metastasis, Science 367(6485) (2020) 1468-1473.

[75]   A.M. Dvorak, E.S. Morgan, P.F. Weller, RNA is closely associated with human mast cell lipid bodies, Histol Histopathol 18(3) (2003) 943-68.

[76]   H.C. Wan, R.C. Melo, Z. Jin, A.M. Dvorak, P.F. Weller, Roles and origins of leukocyte lipid bodies: proteomic and ultrastructural studies, Faseb J 21(1) (2007) 167-78.

[77]   M. Schuldiner, M. Bohnert, A different kind of love - lipid droplet contact sites, Biochim Biophys Acta 1862(10 Pt B) (2017) 1188-1196.

[78]   M. Alemayehu, M. Dragan, C. Pape, I. Siddiqui, D.B. Sacks, G.M. Di Guglielmo, A.V. Babwah, M. Bhattacharya, beta-Arrestin2 regulates lysophosphatidic acid-induced human breast tumor cell migration and invasion via Rap1 and IQGAP1, PLoS One 8(2) (2013) e56174.

[79]   C.D. White, Z. Li, D.A. Dillon, D.B. Sacks, IQGAP1 protein binds human epidermal growth factor receptor 2 (HER2) and modulates trastuzumab resistance, J Biol Chem 286(34) (2011) 29734-47.

[80]   L. Jadeski, J.M. Mataraza, H.W. Jeong, Z. Li, D.B. Sacks, IQGAP1 stimulates proliferation and enhances tumorigenesis of human breast epithelial cells, J Biol Chem 283(2) (2008) 1008-17.

[81]   G. Sun, Y. Liu, K. Wang, Z. Xu, miR-506 regulates breast cancer cell metastasis by targeting IQGAP1, Int J Oncol 47(5) (2015) 1963-70.

[82]   D.E. Casteel, S. Turner, R. Schwappacher, H. Rangaswami, J. Su-Yuo, S. Zhuang, G.R. Boss, R.B. Pilz, Rho isoform-specific interaction with IQGAP1 promotes breast cancer cell proliferation and migration, J Biol Chem 287(45) (2012) 38367-78.

[83]   C.Y. Cho, K.T. Lee, W.C. Chen, C.Y. Wang, Y.S. Chang, H.L. Huang, H.P. Hsu, M.C. Yen, M.Z. Lai, M.D. Lai, MST3 promotes proliferation and tumorigenicity through the VAV2/Rac1 signal axis in breast cancer, Oncotarget 7(12) (2016) 14586-604.

[84]   C.J. Clarke, S.R. Gross, T.M. Ismail, P.S. Rudland, M. Al-Medhtiy, M. Santangeli, R. Barraclough, Activation of tissue plasminogen activator by metastasis-inducing S100P protein, Biochem J 474(19) (2017) 3227-3240.

[85]   C. Zhou, Q. Zhong, L.V. Rhodes, I. Townley, M.R. Bratton, Q. Zhang, E.C. Martin, S. Elliott, B.M. Collins-Burow, M.E. Burow, G. Wang, Proteomic analysis of acquired tamoxifen resistance in MCF-7 cells reveals expression signatures associated with enhanced migration, Breast Cancer Res 14(2) (2012) R45.

[86]   K. Kikuchi, K.M. McNamara, Y. Miki, E. Iwabuchi, A. Kanai, M. Miyashita, T. Ishida, H. Sasano, S100P and Ezrin promote trans-endothelial migration of triple negative breast cancer cells, Cell Oncol (Dordr) 42(1) (2019) 67-80.

[87]   C.Q. Wang, Y. Li, B.F. Huang, Y.M. Zhao, H. Yuan, D. Guo, C.M. Su, G.N. Hu, Q. Wang, T. Long, Y. Wang, C.H. Tang, X. Li, EGFR conjunct FSCN1 as a Novel Therapeutic Strategy in Triple-Negative Breast Cancer, Sci Rep 7(1) (2017) 15654.

[88]   C.Q. Wang, C.H. Tang, Y. Wang, L. Jin, Q. Wang, X. Li, G.N. Hu, B.F. Huang, Y.M. Zhao, C.M. Su, FSCN1 gene polymorphisms: biomarkers for the development and progression of breast cancer, Sci Rep 7(1) (2017) 15887.

[89]   S. Acharya, J. Yao, P. Li, C. Zhang, F.J. Lowery, Q. Zhang, H. Guo, J. Qu, F. Yang, Wistuba, II, H. Piwnica-Worms, A.A. Sahin, D. Yu, Sphingosine Kinase 1 Signaling Promotes Metastasis of Triple-Negative Breast Cancer, Cancer Res 79(16) (2019) 4211-4226.

[90]   M. Snyder, X.Y. Huang, J.J. Zhang, Signal transducers and activators of transcription 3 (STAT3) directly regulates cytokine-induced fascin expression and is required for breast cancer cell migration, J Biol Chem 286(45) (2011) 38886-93.

[91]   M. Al-Alwan, S. Olabi, H. Ghebeh, E. Barhoush, A. Tulbah, T. Al-Tweigeri, D. Ajarim, C. Adra, Fascin is a key regulator of breast cancer invasion that acts via the modification of metastasis-associated molecules, PLoS One 6(11) (2011) e27339.

[92]   H. Zhao, X. Kang, X. Xia, L. Wo, X. Gu, Y. Hu, X. Xie, H. Chang, L. Lou, X. Shen, miR-145 suppresses breast cancer cell migration by targeting FSCN-1 and inhibiting epithelial-mesenchymal transition, Am J Transl Res 8(7) (2016) 3106-14.

[93]   D. Wu, A. Haruta, Q. Wei, GIPC1 interacts with MyoGEF and promotes MDA-MB-231 breast cancer cell invasion, J Biol Chem 285(37) (2010) 28643-50.

[94] T.W. Chittenden, J. Pak, R. Rubio, H. Cheng, K. Holton, N. Prendergast, V. Glinskii, Y. Cai, A. Culhane, S. Bentink, M. Schwede, J.C. Mar, E.A. Howe, M. Aryee, R. Sultana, A.A. Lanahan, J.M. Taylor, C. Holmes, W.C. Hahn, J.J. Zhao, J.D. Iglehart, J. Quackenbush, Therapeutic implications of GIPC1 silencing in cancer, PLoS One 5(12) (2010) e15581.

[95] C. Jiang, W. Veon, H. Li, K.R. Hallows, P. Roy, Epithelial morphological reversion drives Profilin-1-induced elevation of p27(kip1) in mesenchymal triple-negative human breast cancer cells through AMP-activated protein kinase activation, Cell Cycle 14(18) (2015) 2914-23.

[96] S. Chakraborty, C. Jiang, D. Gau, M. Oddo, Z. Ding, L. Vollmer, M. Joy, W. Schiemann, D.B. Stolz, A. Vogt, S. Ghosh, P. Roy, Profilin-1 deficiency leads to SMAD3 upregulation and impaired 3D outgrowth of breast cancer cells, Br J Cancer 119(9) (2018) 1106-1117.

[97] Z. Ding, M. Joy, R. Bhargava, M. Gunsaulus, N. Lakshman, M. Miron-Mendoza, M. Petroll, J. Condeelis, A. Wells, P. Roy, Profilin-1 downregulation has contrasting effects on early vs late steps of breast cancer metastasis, Oncogene 33(16) (2014) 2065-74.

[98] L. Zou, M. Jaramillo, D. Whaley, A. Wells, V. Panchapakesa, T. Das, P. Roy, Profilin-1 is a negative regulator of mammary carcinoma aggressiveness, Br J Cancer 97(10) (2007) 1361-71.

[99] H. Lin, H. Zhang, J. Wang, M. Lu, F. Zheng, C. Wang, X. Tang, N. Xu, R. Chen, D. Zhang, P. Zhao, J. Zhu, Y. Mao, Z. Feng, A novel human Fab antibody for Trop2 inhibits breast cancer growth in vitro and in vivo, Int J Cancer 134(5) (2014) 1239-49.

[100] E. Guerra, M. Trerotola, R. Tripaldi, A.L. Aloisi, P. Simeone, A. Sacchetti, V. Relli, A. D'Amore, R. La Sorda, R. Lattanzio, M. Piantelli, S. Alberti, Trop-2 Induces Tumor Growth Through AKT and Determines Sensitivity to AKT Inhibitors, Clin Cancer Res 22(16) (2016) 4197-205.

[101] T. Pu, M. Shen, S. Li, L. Yang, H. Gao, L. Xiao, X. Zhong, H. Zheng, Y. Liu, F. Ye, H. Bu, Repression of miR-135b-5p promotes metastasis of early-stage breast cancer by regulating downstream target SDCBP, Lab Invest 99(9) (2019) 1296-1308.

[102] J. Zhang, X. Qian, F. Liu, X. Guo, F. Gu, L. Fu, Silencing of syndecan-binding protein enhances the inhibitory effect of tamoxifen and increases cellular sensitivity to estrogen, Cancer Biol Med 15(1) (2018) 29-38.

[103] X.L. Qian, Y.Q. Li, B. Yu, F. Gu, F.F. Liu, W.D. Li, X.M. Zhang, L. Fu, Syndecan binding protein (SDCBP) is overexpressed in estrogen receptor negative breast cancers, and is a potential promoter for tumor proliferation, PLoS One 8(3) (2013) e60046.

[104] J. Liu, Y. Yang, H. Wang, B. Wang, K. Zhao, W. Jiang, W. Bai, J. Yin, Syntenin1/MDA-9 (SDCBP) induces immune evasion in triple-negative breast cancer by upregulating PD-L1, Breast Cancer Res Treat 171(2) (2018) 345-357.

[105] H. Xu, M. Qian, B. Zhao, C. Wu, N. Maskey, H. Song, D. Li, J. Song, K. Hua, L. Fang, Inhibition of RAB1A suppresses epithelial-mesenchymal transition and proliferation of triple-negative breast cancer cells, Oncol Rep 37(3) (2017) 1619-1626.

[106] W. Zhang, J. Xu, K. Wang, X. Tang, J. He, miR1393p suppresses the invasion and migration properties of breast cancer cells by targeting RAB1A, Oncol Rep 42(5) (2019) 1699-1708.

[107] K. Roovers, S. Wagner, C.J. Storbeck, P. O'Reilly, V. Lo, J.J. Northey, J. Chmielecki, W.J. Muller, P.M. Siegel, L.A. Sabourin, The Ste20-like kinase SLK is required for ErbB2-driven breast cancer cell motility, Oncogene 28(31) (2009) 2839-48.

[108] N. Molinie, S.N. Rubtsova, A. Fokin, S.P. Visweshwaran, N. Rocques, A. Polesskaya, A. Schnitzler, S. Vacher, E.V. Denisov, L.A. Tashireva, V.M. Perelmuter, N.V. Cherdyntseva, I. Bieche, A.M. Gautreau, Cortical branched actin determines cell cycle progression, Cell Res 29(6) (2019) 432-445.

[109] Y.W. Chang, H.A. Chen, C.F. Tseng, C.C. Hong, J.T. Ma, M.C. Hung, C.H. Wu, M.T. Huang, J.L. Su, De-acetylation and degradation of HSPA5 is critical for E1A metastasis suppression in breast cancer cells, Oncotarget 5(21) (2014) 10558-70.

[110] Y.W. Chang, C.F. Tseng, M.Y. Wang, W.C. Chang, C.C. Lee, L.T. Chen, M.C. Hung, J.L. Su, Deacetylation of HSPA5 by HDAC6 leads to GP78-mediated HSPA5 ubiquitination at K447 and suppresses metastasis of breast cancer, Oncogene 35(12) (2016) 1517-28.

[111] K.L. Cook, R. Clarke, Heat shock 70 kDa protein 5/glucose-regulated protein 78 "AMP"ing up autophagy, Autophagy 8(12) (2012) 1827-9.

[112] X. Dong, F. Liu, L. Sun, M. Liu, D. Li, D. Su, Z. Zhu, J.T. Dong, L. Fu, J. Zhou, Oncogenic function of microtubule end-binding protein 1 in breast cancer, J Pathol 220(3) (2010) 361-9.

[113] X. Hu, J. Guo, L. Zheng, C. Li, T.M. Zheng, J.L. Tanyi, S. Liang, C. Benedetto, M. Mitidieri, D. Katsaros, X. Zhao, Y. Zhang, Q. Huang, L. Zhang, The heterochronic microRNA let-7 inhibits cell motility by regulating the genes in the actin cytoskeleton pathway in breast cancer, Mol Cancer Res 11(3) (2013) 240-50.

[114] N. Asp, A. Kvalvaag, K. Sandvig, S. Pust, Regulation of ErbB2 localization and function in breast cancer cells by ERM proteins, Oncotarget 7(18) (2016) 25443-60.

[115] P. Huang, R. Liao, X. Chen, X. Wu, X. Li, Y. Wang, Q. Cao, C. Dong, Nuclear translocation of PLSCR1 activates STAT1 signaling in basal-like breast cancer, Theranostics 10(10) (2020) 4644-4658.

[116] S. Varikuti, S. Oghumu, M. Elbaz, G. Volpedo, D.K. Ahirwar, P.C. Alarcon, R.H. Sperling, E. Moretti, M.S. Pioso, J. Kimble, M.W. Nasser, R.K. Ganju, C. Terrazas, A.R. Satoskar, STAT1 gene deficient mice develop accelerated breast cancer growth and metastasis which is reduced by IL-17 blockade, Oncoimmunology 6(11) (2017) e1361088.

[117] S.R. Chan, W. Vermi, J. Luo, L. Lucini, C. Rickert, A.M. Fowler, S. Lonardi, C. Arthur, L.J. Young, D.E. Levy, M.J. Welch, R.D. Cardiff, R.D. Schreiber, STAT1-deficient mice spontaneously develop estrogen receptor alpha-positive luminal mammary carcinomas, Breast Cancer Res 14(1) (2012) R16.

[118] L.M. Hix, J. Karavitis, M.W. Khan, Y.H. Shi, K. Khazaie, M. Zhang, Tumor STAT1 transcription factor activity enhances breast tumor growth and immune suppression mediated by myeloid-derived suppressor cells, J Biol Chem 288(17) (2013) 11676-88.

CHAPTER 3 CHARACTERIZATION OF CYTOPLASMIC LIPID DROPLETS IN EACH REGION OF THE SMALL INTESTINE OF LEAN AND DIET-INDUCED OBESE MICE IN THE RESPONSE TO DIETARY FAT

3.1 Abstract

The absorptive cells of the small intestine, enterocytes, contribute to postprandial blood lipid levels by secreting dietary triacylglycerol in chylomicrons. The rate and amount of dietary triacylglycerol absorbed varies along the length of the small intestine. Excess dietary triacylglycerol not immediately secreted in chylomicrons can be temporarily stored in cytoplasmic lipid droplets (CLDs) and repackaged in chylomicrons at later times. The characteristics of CLDs, including their size, number per cell, and associated proteins, may influence CLD metabolism and reflect differences in lipid processing or storage in each intestinal region. However, it is unknown whether the characteristics or proteome of CLDs differ in enterocytes of each intestine region in the response to dietary fat. Furthermore, it is unclear if obesity influences the characteristics or proteome of CLDs in each intestine region. To address this, we utilized transmission electron microscopy and shotgun LC-MS/MS analysis to assess the characteristics and proteome of CLDs in the proximal, middle, and distal regions of the small intestine of lean and diet-induced obese (DIO) mice two hours after an oil gavage. We identified differences in lipid storage along the length of the small intestine and between lean and DIO mice, as well as distinct CLD proteomes reflecting potentially unique roles of CLDs in each region. This study reveals differences in lipid processing along the length of the small intestine in response to dietary fat in lean and DIO mice and reflects distinct features of the proximal, middle, distal region of the small intestine.

3.2 Introduction

Postprandial lipemia is an independent risk factor for cardiovascular disease, the leading cause of death of both men and women in the United States [1]. Therefore, understanding the

mechanisms of dietary fat absorption that contribute to postprandial lipemia is critical in the prevention and treatment of cardiovascular disease. Dietary fat is efficiently absorbed by enterocytes in the small intestine through the process of chylomicron (CM) synthesis and secretion [2, 3]. This process begins with the breakdown of dietary triacylglycerol (TAG) in the intestinal lumen to fatty acids and monoacylglycerol, which are taken up by enterocytes and resynthesized into TAG at the endoplasmic reticulum (ER). Resynthesized TAG is packaged on apolipoprotein (apo) B-48 by microsomal triglyceride transport protein (MTTP), forming pre-CMs that are shuttled to the Golgi in pre-chylomicron transport vesicles for modification. Modified CMs exit enterocytes at the basolateral side and enter the villus lacteal for transport to the thoracic duct for entry into the circulation.

Chylomicron synthesis and secretion occurs along the entire length of the small intestine, although to different extents. The small intestine can be divided into three regions: duodenum (proximal), jejunum (middle), and ileum (distal) [4], and each have distinct roles during the process of dietary fat absorption. For example, dietary fat is digested primarily in the duodenum. The duodenum is exposed to stomach contents and maintains a high concentration of pancreatic lipase and bile acids required for dietary fat breakdown and emulsification due to secretions from the pancreas and liver, respectively [5]. Next, the majority of dietary fat absorption occurs in the jejunum, which is reflected in its more efficient rate of absorption and greater lymphatic TAG output compared to the ileum [6-9]. Lastly, the ileum maintains the bile acid pool by reabsorbing bile acids for their transport back to the liver through enterohepatic circulation [10], and is also home to specific enteroendocrine cells that secrete hormones involved in regulating satiety, gastric emptying, and insulin secretion in response to nutrients [11]. The ileum also contributes to dietary fat absorption. For example, although almost all of a low to moderate quantity of dietary fat is absorbed by the jejunum, the ileum serves as a safety net for dietary lipid that exceeds the chylomicron synthesis and secretion capacity of the more proximal intestine regions upon consumption of larger quantities of dietary fat [12, 13]. Therefore, the three regions of the small intestine serve unique yet codependent functions that all contribute to the extraordinary efficacy of intestinal fat absorption. However, whether each intestine region responds to and processes dietary fat differently is not clear.

Understanding how enterocytes in the ileum of the small intestine process dietary fat is of special interest, as certain conditions that expose the distal intestine to greater amounts of dietary

135

fat have different physiological outcomes. For example, the ileum plays a more active and consistent role in dietary fat absorption with the consumption of chronic fat high diets, which are generally associated with poor metabolic outcomes. In addition, the absorption of dietary fat shifts to the ileum in patients that have undergone certain types of bariatric surgery in which the more proximal regions of the small intestine are bypassed. However, bariatric surgery is associated with beneficial health outcomes [14]. Whether differences in lipid processing and storage in each intestine region may account for or contribute to these differences is not clear.

Though resynthesized dietary TAG in enterocytes is primarily used for CM synthesis and secretion, TAG can also be stored in cytoplasmic lipid droplets (CLDs) [2]. CLDs are composed of a neutral lipid core surrounded by a phospholipid monolayer and protein coat [15]. CLDs form in enterocytes in the presence of large quantities of dietary TAG not immediately packaged into CMs [16], although the exact threshold required to stimulate CLD formation is not yet clear. CLDs can reside in enterocytes up to 12 hours in mice [16] and 18 hours in humans [17, 18], and can be mobilized for CM synthesis and secretion by physiological factors such as glucose and contribute to blood lipid concentrations hours after consumption of a high fat meal [19]. Therefore, CLDs in enterocytes are an important factor in understanding the small intestine's contribution to blood lipid concentrations and prevention of cardiovascular disease. CLDs have been identified in enterocytes along the length of the small intestine in mice in the response to dietary fat [16]; however, the characteristics of CLDs in each region and whether these characteristics differ in each region has not been defined.

The proteins that associate with CLDs are thought to regulate their metabolism [20] and therefore may influence the utilization of CLDs for CM synthesis and secretion in enterocytes. In fact, several studies have identified the proteome of CLDs in mouse enterocytes of the jejunum [21-23] and of CLDs in the human Caco-2 cell model of enterocytes [24, 25], which have revealed many candidate proteins involved in lipid metabolism that may regulate this balance. However, whether the proteome of CLDs differs in the proximal, middle, and distal regions of the small intestine is unknown; further, whether CLDs in each intestine region are differentially utilized is not clear.

Obesity has been shown to influence both the absorption of dietary fat and the characteristics of CLDs [22, 26, 27]. First, both diet-induced obese (DIO) and genetically-induced obese mice display reduced intestinal TAG secretion, larger CMs, and lipid accumulation in

enterocytes [26, 27]. Second, CLDs in the jejunum of DIO mice are significantly larger and display an altered proteome compared to CLDs in the jejunum of lean mice [22], which may contribute to their defect in CM secretion. However, whether CLDs in enterocytes of the proximal and distal regions of the small intestine of DIO mice are also larger than those of lean mice has not been determined. Further, whether obesity influences the proteome of CLDs in each intestine region compared to lean mice has also not been determined.

Therefore, to determine whether lipid processing and storage or CLD metabolism differs in each region of the small intestine in response to dietary fat, and to determine the influence of obesity on these factors, we assessed and compared the characteristics and proteome of CLDs in the proximal, middle, and distal regions of the small intestine in lean and DIO mice two hours after an olive oil gavage using transmission electron microscopy (TEM) and LC-MS/MS analysis.

3.3 Methods

3.3.1 Mice care and generation of DIO mouse model

All animal experiments were conducted in accordance with the National Institute of Health Guide for the Care and Use of Laboratory Animals and approved by the Purdue Animal Care and Use committee. C57BL/6 male mice were housed in a temperature and humidity-controlled facility with a 12-hour light/dark cycle and *ad libitum* access to food and water. Mice were maintained on a chow diet (PicoLab 5053, Lab Diets, Richmond, IN, USA) consisting of 62.1% calories from carbohydrate, 24.7% from protein, and 13.2% from fat from weaning to five weeks of age. At five weeks of age, mice were randomly distributed into a "DIO" or "lean" group and fed either a high-fat diet (60% calories from fat, D12492) or a low-fat matched diet (10% calories from fat, D12450J) (Research Diets, Inc; New Brunswick, NJ, USA), respectively, for 12 additional weeks. Mice fed the chronic high-fat diet for this time period develop obesity, glucose intolerance, and hepatosteatosis [28].

3.3.2 Transmission electron microscopy (TEM)

3.3.2.1 Sample collection, preparation, and imaging

Cardiac perfusion, fixation, and preparation of samples for imaging by TEM was completed as previously described [21, 22]. Briefly, three lean and three DIO mice were fasted for

four hours at the beginning of the light cycle, then administered 200 μL olive oil by oral gavage. Two hours later, mice were anesthetized by inhaled isoflurane, and via cardiac infusion perfused with 1.5% glutaraldehyde in 0.1 M sodium cacodylate. The small intestine was divided into three equal length sections (proximal, middle, distal) and samples from each section were isolated and used for further processing. Samples were stained with osmium tetroxide, dehydrated with ethanol, and embedded in resin. Ultrathin sections were cut via ultramicrotomy and stained with lead citrate and uranyl acetate. Sample grids were imaged using a FEI Tecnai T12 electron microscope equipped with a tungsten source and operating at 80 kV. Individual images used to construct entire villi were merged together using the "auto-blend layers" function in Adobe Photoshop 2020.

3.3.2.2 TEM CLD analysis

Acquired TEM images were used to assess CLD characteristics. Images from intact enterocytes representing the middle region of at least two villi per region per mouse were used for the analysis, resulting in the inclusion on average of 75-98 enterocytes per region per mouse for lean and DIO mice. CLD diameter was measured using ImageJ [29] and CLD area was estimated from the measured diameters using the formula πr^2. A two-way mixed model ANOVA was used to determine significant effects of obesity, region, or their interaction on the measured CLD characteristics. Obesity, region, and their interaction were considered fixed effects, while mouse was considered a random effect. Significant differences in CLD diameter distributions were determined by Kolmogorov-Smirnov test. Significance considered $p < 0.05$. Statistical analysis was performed using SAS version 9.4.

3.3.3 Enterocyte and CLD isolation

Enterocytes and their CLDs were isolated as described [21, 22]. Briefly, five lean and five DIO mice were fasted for four hours at the beginning of the light cycle. Mice were administered 200 μL olive oil by oral gavage and euthanized two hours later. The small intestine of each mouse was divided into three equal length sections (proximal, middle, distal) and tissue from each section was washed with tissue buffer, then placed in warmed isolation buffer for 15 minutes. Samples were briefly vortexed and the supernatant containing isolated enterocytes was removed and saved. The isolation was repeated and supernatants combined. CLDs were collected from isolated

enterocytes by sucrose gradient ultracentrifugation. Enterocytes were lysed in ice-cold sucrose lysis buffer and disrupted by passing through a 27-gauge 1-inch needle. The resulting cell lysate was transferred to the bottom of an ultracentrifuge tube (344059, Beckman Coulter) and layered with sucrose-free lysis buffer. Samples were centrifuged for two hours at 20,000 x g, 4°C in a SW 41 Ti rotor (Beckman Coulter). After centrifugation, tubes were frozen then sliced into approximately one centimeter-sized fractions. The top-most fraction includes isolated CLDs. This CLD isolation procedure has been previously validated [21].

3.3.4 In-solution digestion and LC-MS/MS

CLD fractions were prepared for proteomic analysis as described [21, 22]. Briefly, the isolated CLD fractions were delipidated using 2:1 chloroform methanol and proteins precipitated using ice-cold acetone. Proteins were denatured and reduced using 8 M urea and 10 mM dithiothreitol. Samples were digested with trypsin (Sigma-Aldrich, St. Louis MO, USA) and the reaction quenched with trifluoroacetic acid. Peptides were separated on a nanoLC system (1100 Series LC, Agilent Technologies, Santa Clara, CA, USA). Peptides were loaded onto an Agilent 300SB-C18 enrichment column and switched to the nano-flow path after five minutes. Peptides were separated with a reversed phase ZORBAX 300SB-C18 column coupled to the LTQ-Orbitrap LX (Thermo Fisher Scientific, Waltham MA, USA) operated in the data-dependent positive acquisition mode. Each full MS scan was followed by six MS/MS scans where the six most abundant molecular ions were selected for fragmentation by collision-induced dissociation using a normalized collision energy of 35%.

3.3.5 LC-MS/MS analysis

LC-MS/MS data were analyzed using Maxquant version 1.6.3.4. [30-32] against the Uniprot *Mus musculus* protein database. The following parameters were used: 10 ppm precursor mass tolerance, 20 ppm fragment mass tolerance, enzyme specificity for trypsin with two missed cleavages, minimum peptide length of six amino acids, fixed modification of iodoethanol to cysteine, variable modifications of oxidation of methionine and acetylation of the N-terminal. The false discovery rate for peptides and proteins was set to 0.01. Match between runs was selected. Reverse hits, contaminant proteins, and proteins with only one MS/MS count were removed from

the dataset. Label-free quantification (LFQ) intensity values were transformed by log2. A protein was considered identified if it was detected in at least three out of five biological replicates (three out of three biological replicates for lean distal samples). Of the proteins considered identified in the isolated CLD fraction of all three regions of the intestine in both lean and DIO mice, a two-way mixed model ANOVA was used to determine whether obesity, region, or their interaction influence the relative levels of identified proteins. Obesity, region, and their interaction were considered fixed effects, while mouse was considered a random effect. Statistical significance considered $p < 0.05$. Statistical analysis was performed using SAS version 9.4. Functional annotation analysis was performed using Metascape with default settings [33].

3.3.6 Immunofluorescence microscopy

Three lean and three DIO mice were fasted for four hours at the beginning of the light cycle. Mice were given 200 μL olive oil by oral gavage and euthanized two hours later. The small intestine of each mouse was divided into three equal length sections (proximal, middle, distal) and a small section of tissue from each of the three intestinal regions was placed in optimal cutting temperature compound and frozen in cooled 2-methyl butane. Tissue in frozen blocks was sectioned with thickness of 10 μm and placed onto microscope slides. Samples were fixed with paraformaldehyde, permeabilized with saponin, and blocked with BSA. Sections were incubated with antibodies to Plin3 (a gift from Dr. Perry Bickel at the University of Texas Southwestern, Dallas, TX, USA) or Fabp6 (Abcam, ab91184) at a concentration of 1:1000. Sections were also incubated with BODIPY to label CLDs, DAPI to label nuclei, and AlexaFluor 568 (Invitrogen, A11011) or 633 (Invitrogen, A21071) secondary antibodies at a concentration of 1:1000 to label Plin3 or Fabp6. Samples were imaged with a Zeiss LSM 880 Upright Confocal microscope using a 63x oil objective (Zeiss International). The following laser lines were used to excite DAPI, BODIPY, and AlexaFluor 568 or 633, respectively: 405, 488, and 561 or 633. Post-acquisition image analysis was conducted using Zen blue software (Zeiss International). Brightness and contrast were adjusted by histogram stretch. For colocalization analysis, the threshold to remove background pixels was set by hand.

3.4 Results

3.4.1 CLD characteristics differ in each region of the small intestine in lean and DIO mice

To visualize CLDs in the proximal, middle, and distal regions of the small intestine of lean and DIO mice in response to dietary fat, we used TEM. Representative electron micrographs of villi and enterocytes in each region of the small intestine of a lean and DIO mouse two hours after an olive oil gavage are shown in Figure 3-1. Images of the distal region of the small intestine were variable in whether CLDs were present or not, making it challenging to select a single representative image. The images of the distal region of the small intestine in Figure 3-1C and 3-1F show CLDs and are representative of when CLDs are present; however, only two out of three lean and one out of three DIO mice had CLDs present in the distal region.

To investigate differences in CLD characteristics in the proximal, middle, and distal regions of the small intestine in lean and DIO mice, we assessed the percent of cells containing CLDs, the number of CLDs per cell, CLD diameter, and CLD area per cell (an estimate of TAG storage) in each intestine region of lean and DIO mice (Figure 3-2). There was a significant effect of intestine region on the percent of cells with CLDs (Figure 3-2A) and CLD area per cell (Figure 3-2C). However, the percent of cells with CLDs in the distal intestine was highly variable (Figure 3-2A) and differences between individual regions assessed in post-hoc analysis were not significant (p=0.0502 proximal vs. distal; p=0.0536 middle vs. distal). In contrast, CLD area per cell was significantly different between all regions (Figure 3-2C). The middle region contained the greatest CLD area per cell, while the distal region had the least. Regardless of intestine region, however, CLD area per cell was significantly greater in DIO mice. There was a significant interaction effect of intestine region and obesity on the number of CLDs per cell (Figure 3-2B) and CLD diameter (Figure 3-2D); an interaction effect for CLD area per cell was trending (p=0.051) (Figure 3-2C). The number of CLDs per cell was significantly different between each region of both lean and DIO mice, with the middle region having the greatest number of CLDs per cell. However, in lean mice, the proximal region had the least number of CLDs per cell while in DIO mice the distal region had the least number of CLDs per cell. The number of CLDs per cell was greater in DIO compared to lean mice only in the proximal region. Of those cells containing CLDs, CLD diameter was significantly different between each intestine region in lean mice, as CLD diameter decreased from proximal to distal regions (Figure 3-2D). In DIO mice, CLD diameter was not statistically different between regions, although a difference in CLD diameter between the

proximal and distal regions of DIO mice was trending (p=0.0535). CLD diameter was greater in DIO compared to lean mice in the middle and distal regions, while CLD diameter in the proximal region was greater in lean mice. The diameter distribution of CLDs was significantly different between indicated regions in lean and DIO mice, and between lean and DIO mice for each region (Figure 3-2E).

3.4.2 The proteome of CLDs exhibits similarities and differences in each region of the small intestine in lean and DIO mice

To investigate differences in the potential role of CLDs or their metabolism in each intestine region, we performed LC-MS/MS on the proteins present in the CLD fraction isolated from each region of the small intestine of lean and DIO mice. We identified a total number of 563 proteins, of which 40 were unique to lean and 57 were unique to DIO. To determine unique features of CLDs by intestine region, we analyzed the 304 proteins identified in the CLD fraction that were present in the same region in both lean and DIO mice (Figure 3-3A). Of these, 223 proteins were present in all three regions, 39 proteins were unique to the proximal region, two proteins were unique to the middle region, and three proteins were unique to the distal region. The proximal and middle regions shared 34 proteins, the proximal and distal shared two proteins, and the middle and distal regions shared one protein. Among the 223 proteins identified in all three regions of both lean and DIO mice, we identified the bona-fide CLD-associated protein, Plin3. The cellular localization of Plin3 on CLDs in the proximal, middle, and distal regions was confirmed by immunofluorescence microscopy (Figure 3-4).

To identify and sort proteins by metabolic function, we used functional annotation and network analysis of the 223 proteins identified in the CLD fraction of all three regions in both lean and DIO mice (Figure 3-3B, C). The most enriched Gene Ontology Biological Process (GO_BP) term of proteins identified in all three regions was drug metabolism (Figure 3-3B), which was related to other enriched GO_BP terms including antibiotic metabolism and mitochondrial ATP synthesis by network analysis (Figure 3-3C). These three GO_BP terms include proteins with a wide range of functions, including those involved in ATP synthesis and glycolysis. The second most enriched GO_BP term was lipid catabolism, which was related to other enriched GO_BP terms including steroid and hormone metabolism, regulation of lipid localization, and low-density lipoprotein clearance by network analysis (Figure 3-3C). These five GO_BP terms include

apolipoproteins (Apoa1, Apoa4, Apoc3, Apob), proteins involved in fatty acid oxidation (FAO) (Acadvl, Acox1, Hsd17b4, Acaa2, Ehhadh, Hadha, Etfb, Acaa1a), lipolysis (Lipe), TAG synthesis (Dgat1, Acsl5), chylomicron synthesis (Mttp), CLD maintenance (Plin2, Plin3), carboxylesterase (Ces) enzymes (Ces2a, Ces2c, Ces2e) and others (Scp2, Por, Aldh3a2, Rab7, Sgpl1, Slc27a4, Cyp4f14). The third most enriched term was nucleosome assembly, which includes histone proteins (Hist1h1d, Hist1h1e, Hist1h4a, Hist1h2bp, Hist1h2aa, Hist1h1b, Hist1h1a, H2afv). Other related enriched terms include protein folding and stabilization, viral genome replication, and response to interleukin-7; protein to plasma membrane, actin filament process, response to indole-3-methanol.

To determine whether intestine region, obesity, or their interaction influences the relative levels of CLD proteins, we performed a two-way mixed model ANOVA on the LFQ values of the 223 proteins identified in the CLD fraction of all three regions of the intestine in both lean and DIO mice. Intestine region had a significant effect on 90 proteins, diet had a significant effect on two proteins, both intestine region and diet had a significant effect on nine proteins, and there was a significant interaction between intestine region and diet for 31 proteins. We focused on proteins involved in lipid metabolism, as patterns in their relative levels along the length of the intestine may indicate differences in CLD metabolism in each region in lean and DIO mice. Proteins involved in lipid metabolism whose relative levels were significantly influenced by intestine region, obesity, or their interaction are shown in Table 3-1. Several proteins involved in lipid metabolism were present at significantly higher levels in the proximal compared to the middle and distal regions, including Acadvl, Acsl5, Ces2c, Dgat1 (lean mice), Ehhadh, and Mttp. In contrast, Apoa1 was present at significantly higher levels in the distal region compared to the proximal and middle regions. Acadvl was also present at significantly higher levels in DIO compared to lean mice independent of intestine region. Some proteins showed an interaction effect of intestine region and obesity, including ApoB and Hsd17b11. Both were present at the lowest levels in the middle region compared to proximal and distal regions in both lean and DIO mice, but this only reached significance in lean mice.

3.4.3 Fabp6 localizes to CLDs present in the distal region of the small intestine

To generate hypotheses as to how CLDs or their proteins serve unique functions in each intestine region, we next analyzed the proteins identified only in one region but present in both

lean and DIO mice (Figure 3-3A). Of the 39 proteins identified only in the proximal region, several were involved in lipid metabolism including Iap, Acsl1, Abhd6, and Slc27a2. The two proteins identified only in the middle region include Ddx5 and Arfgap3. The three proteins identified only in the distal intestine include Fabp6, Slc51b, Psma1. Because of the unique role of Fabp6 in bile acid transport, the identification of Fabp6 in the CLD fraction from only the distal region suggests CLDs may influence bile acid transport and/or metabolism. To confirm the localization of Fabp6 to CLDs in the distal region of the intestine, we performed immunofluorescence microscopy (Figure 3-5). Fabp6 adopts a net-like pattern on CLDs (Figure 3-5A, B). Upon colocalization analysis, the Mander's colocalization coefficient was 0.91043, indicating a high degree of overlap between Fabp6 and CLDs. Therefore, Fabp6 localizes to CLDs in the distal region of the small intestine.

3.5 Discussion

To determine whether lipid processing and storage or CLD metabolism differs in each region of the small intestine in response to dietary fat and to determine the influence of obesity on these factors, we assessed the characteristics and proteome of CLDs in the proximal, middle, and distal regions of the small intestine in lean and DIO mice two hours after an olive oil gavage. We found that TAG storage was greatest in the middle region of the intestine in both lean and DIO mice, while TAG storage was greater in enterocytes of DIO mice overall. We also identified CLD proteins that were common among intestine regions as well as region-specific CLD proteins that may differentially influence CLD or cell metabolism. Lastly, we found that Fabp6 localizes to CLDs in the distal region, which generates hypotheses as to the role of CLDs in bile acid transport or metabolism. Our results demonstrate differences in TAG storage in each region of the small intestine in lean and DIO mice and have uncovered potentially novel roles for CLDs in each region in the response to dietary fat.

Our results support early studies describing regional differences in the processing and absorption of dietary fat along the length of the small intestine. For example, multiple studies have shown that lymphatic TAG output from the distal region is lower than that of the proximal region after intestinal lipid infusion [6, 7, 9]. Other studies have demonstrated that the distal intestine is slower to process lipid [34], accumulates more lipid than the proximal regions after intestinal lipid infusion [6-9], and secretes larger CMs with an altered apolipoprotein composition compared to

those of the proximal region [7, 8]. These results suggest fundamental differences in the processing of dietary fat and efficiency of CM secretion between the proximal and distal regions during times of lipid surplus. Our results contribute to this information, as we observed differences in TAG storage in each region in response to dietary fat due to differences in CLD characteristics in each region (Figure 3-2). TAG storage was greatest in the proximal and middle regions compared to the distal, which is consistent with their greater and more rapid ability to respond to dietary fat. As most dietary fat is absorbed by the proximal 130 cm of the intestine in humans [35], a greater TAG storage pool in the middle region serves as a readily available pool of substrates needed for CM synthesis and secretion, therefore allowing more effective fat absorption. To note, the presence of CLDs, and therefore the storage of TAG, in the distal region was variable. Differences in gastric emptying rates [12] and variations in the total length of the small intestine in each mouse may increase the amount of time needed for the same amount of dietary lipid to reach, be processed, and stored by the distal intestine.

Consistent with previous studies, our results demonstrate that CLDs form in distal enterocytes [16, 36]. This is significant for several reasons. First, our results indicate that enough dietary fat reaches the distal intestine to stimulate CLD formation. Products of dietary fat digestion reaching the distal region activate the ileal brake response, which decreases gastric emptying, slows intestinal transit, and increases satiety, potentially due in part to the secretion of enteroendocrine hormones such as glucagon-like peptide-1 (GLP-1) and peptide YY (PYY) [37]. Conditions that push the absorption of dietary fat to lower parts of the small intestine, such as inhibition of TAG synthesis [38, 39] or bariatric surgery [40], result in greater GLP-1 and PYY responses. However, whether the presence of CLDs in distal enterocytes contributes to a greater enteroendocrine cell response is not clear. Second, CLDs in the distal intestine may also be mobilized by physiological factors such as glucose and contribute to a greater blood TAG response [19]. As the distal region has a slower rate of TAG turnover [6], lipid stored in distal enterocytes may remain there for a longer period of time and contribute to blood lipid levels many hours after CLDs have been mobilized from the proximal regions [8]. Therefore, lipid stored in the distal intestine may be another contributing factor to the negative health consequences associated with chronic high fat diets.

The third reason why CLDs in distal enterocytes is significant is because they may regulate or interfere with bile acid homeostasis. Bile acids are important not only for the digestion and

absorption of dietary fat in the intestinal lumen, but they are also important signaling molecules that regulate gene expression and nutrient metabolism in multiple organs [41]. The intracellular transport of bile acids in ileal enterocytes during enterohepatic circulation is facilitated by Fabp6 [42]. Fabp6 has also been shown to associate with and stimulate farnesoid x receptor (FXR) [43, 44], a transcription factor that regulates the expression of genes involved in bile acid metabolism, including Ostα/β and Fgf15/19 in enterocytes [41]. Due to the localization of Fabp6 on CLDs (Figure 3-5), we hypothesize that when CLDs are present in the distal region of the intestine, CLDs serve as a docking place for Fabp6-bile acid complexes or may instead interfere with intracellular bile acid trafficking by Fabp6. Therefore, it is possible that the formation of CLDs in the distal intestine upon consumption of large quantities of dietary fat may interfere with or enhance intestinal bile acid signaling or reabsorption, which can influence systemic bile acid homeostasis and either contribute to or prevent metabolic disease [45]. Interestingly, we also identified another protein involved in bile acid export from distal enterocytes, Ostβ/Slc51b, in the CLD fraction from only the distal region. Future studies are required to determine the influence or role of CLDs in distal enterocytes on bile acid homeostasis.

Consistent with previous studies that investigated the enterocyte CLD proteome [21-25], we identified CLD proteins with potential core roles in CLD metabolism. For example, we identified and confirmed the localization of the bona-fide CLD-associated protein Plin3 in the proximal, middle, and distal region of the intestine (Figure 3-4). Although unsurprising, this observation confirms both our CLD isolation procedure as well as our proteomic method. In addition, we identified several Ces enzymes in the CLD fraction of all three regions of the intestine that have recently been shown to have intestine region-specific expression and activity in mice [46]. Ces enzymes are potential candidates responsible for the lipolytic breakdown and mobilization of CLDs [47], and multiple Ces enzymes have been shown to regulate dietary fat absorption and enterocyte lipid metabolism [48, 49]. The identification of three of the most abundant and active Ces enzymes in the murine intestine (Ces2a, Ces2c, Ces2e) [46] in the CLD fraction of all three regions in both lean and DIO mice suggests they may indeed serve this role. However, validation of these proteins at the CLD is prerequisite to functional studies. Lastly, we identified Pcyt1a in the CLD fraction of all regions with highest relative levels in the proximal compared to distal region (Table 3-1). Pcyt1a has been identified as a critical regulator of cellular phosphatidylcholine levels in Caco2 cells and mouse enterocytes, and regulates CLD size, CM

secretion [50] and is also necessary for cellular adaptation to a high-fat diet [51]. This suggests it plays a central role on CLDs in each intestine region. However, to our knowledge, the localization of Pcyt1a to CLDs in mouse enterocytes has not been confirmed.

In contrast to other murine enterocyte CLD proteomic studies in which only one intestine region was analyzed [21-23], our study identified proteins in the CLD fraction from each region of the small intestine, allowing us to make hypotheses as to the potential differences in CLD metabolism that contribute to differences in dietary fat processing in each region. For example, proteins involved in FAO were identified in all three regions but were present at higher levels in the proximal compared to distal region (Table 3-1). Recently, it was demonstrated that intestinal crypts in the proximal region of the intestine have a greater reliance on FAO than those of the distal intestine, consistent with a gradient pattern in the expression of FAO genes from the proximal to distal intestine [52]. These regional differences in metabolism influenced epithelial cell renewal and intestinal morphology. Although the study did not investigate enterocytes, it is possible that enterocytes along the length of the intestine also differ in their requirement for FAO and may differentially utilize CLDs for this purpose.

Another example is the identification of intestinal alkaline phosphatase (Iap) in the CLD fraction of only the proximal region. This observation, along with the large diameter of CLDs in the proximal region of lean mice (Figure 3-2), suggests CLDs in the proximal region may serve as long-term storage [53]. Iap has been implicated in the process of dietary fat absorption, as lack of Iap in mice reduces the accumulation of lipid in enterocytes over time by increasing the rate at which dietary fat is absorbed [54, 55]. In fact, Iap supplementation in mice fed a high fat diet prevents the development of conditions associated with the metabolic syndrome [56], and low fecal levels of IAP are associated with ischemic heart disease in humans [57]. It is possible that the association of Iap with CLDs in the proximal region slows their use for CM synthesis and secretion [55, 58], and may therefore contribute to the regulation of blood lipid concentrations. However, the mechanisms supporting this hypothesis have not been determined.

Our results expand on previous studies that demonstrate a larger size and altered proteome of CLDs in jejunal enterocytes of DIO mice [22]. Consistently, we found that TAG storage in every intestine region of DIO mice was greater than that of lean mice. Obesity often arises due to the chronic consumption of a high fat diet, which exposes enterocytes along the entire length of the intestine to a large quantity of dietary fat. Each region of the small intestine adapts to the

substrates available and can increase absorption with increased doses of fat [12, 13]. Our results suggest TAG storage in each region of DIO mice can also be augmented with a chronic high fat diet. It is possible that large amounts of TAG stored in enterocytes of DIO mice is less efficiently mobilized and utilized, which may contribute to defective or prolonged CM secretion after a dietary fat load [26, 27]. An interesting observation is that CLD diameter was the same in each region in DIO mice, which is in contrast to the distinct differences in CLD diameter in each region of lean mice (Figure 3-2). Whether regional differences in CLD size, or lack thereof, serves a metabolic purpose is not clear.

We identified proteins in the CLD fraction of DIO mice that differed from those of lean mice. For example, 57 proteins were identified in the CLD fraction of only DIO mice, including the nuclear lamina protein Lmna, which was identified in the CLD fraction of every region. Mutations in Lmna are associated with various forms of lipodystrophy and metabolic dysfunction [59, 60], which are often due to altered storage capacity of adipocytes in part by disrupted activity of transcription factors such as SREBP1 [61]. Lmna may therefore be a candidate protein influencing CLD or lipid metabolism in enterocytes of DIO mice. However, whether the association of Lmna with CLDs influences its ability to regulate cellular metabolism is not clear. In addition, several proteins were present at different relative levels in the CLD fraction of DIO compared to lean mice. For example, Acadvl, which catalyzes the first step in FAO, was present at higher relative levels in the CLD fraction of DIO mice independent of region (Table 3-1). The identification of proteins involved in FAO in the CLD fraction may indicate an association of CLDs with mitochondria; therefore, higher relative levels of Acadvl may reflect an attempt to increase CLD catabolism to compensate for lipid accumulation in enterocytes of obese mice [26].

In conclusion, we investigated the characteristics and proteome of CLDs in the proximal, middle, and distal regions of the small intestine in lean and DIO mice two hours after an olive oil gavage to determine differences in lipid processing, storage, or CLD metabolism in each region in response to dietary fat and to determine the influence of obesity on these factors. Our findings uncover the dynamics of dietary fat absorption along the length of the small intestine on an enterocyte level and have revealed potentially unique roles of CLDs in each intestine region. As many previous studies have investigated the lipid processing abilities of each intestine region under non-physiological conditions, i.e. a constant lipid infusion directly into each intestine region, our study is significant as it is applicable to the physiological response to the consumption of a lipid

meal. A limitation of our study is that our results are mainly descriptive and hypothesis generating. The cellular localization of proteins we identified in the isolated CLD fraction must be confirmed before functional studies can be conducted. However, the data we generated in this study can be applied to future studies to determine the fate and/or metabolism of CLDs in each intestine region as well as the functional significance of CLD proteins in enterocytes. Understanding how CLDs in enterocytes along the length of the intestine contribute to or influence the process of dietary fat absorption will help in the prevention and treatment of hypertriglyceridemia and CVD.

3.6 Acknowledgments

Figure 3-1. Representative TEM images of villi and enterocytes from each region of the small intestine of lean and DIO mice in response to dietary fat. Mice were fasted for four hours, administered a 200 µL olive oil oral gavage, two hours later samples were collected after perfusion fixation. (A-C) Villi and enterocytes from the proximal (A), middle (B), distal (C) intestine of a lean mouse. Boxed regions on villi are magnified in the image directly below each villus. (D-F) Enterocytes from the proximal (D), middle (E), distal (F) intestine of a DIO mouse. Scale bar for images of villi is 20 µm and scale bar for images of enterocytes is 10 µm. Individual images used to construct entire villi were merged together using Photoshop. Images in A-C and D-F are from mice that had CLDs present in the distal region. Two out three lean and one out of three DIO mice had CLDs present in the distal region; therefore, images of the distal region shown here are representative of when CLDs are present in this region.
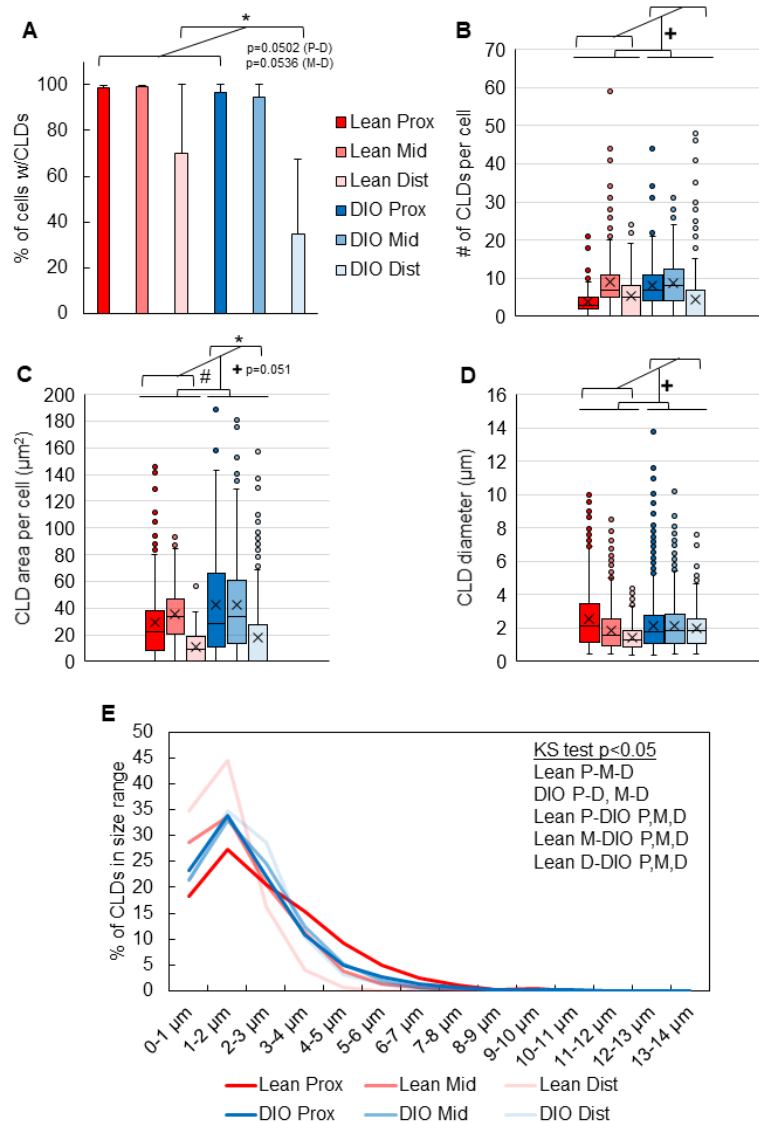
Figure 3-2. Quantitative CLD analysis of each region of the small intestine in lean and DIO mice reveal differences in CLD characteristics. (A) Percent of cells per region containing CLDs in lean and DIO mice. n=3 mice per group. (B) Number of CLDs per cell of all cells analyzed. (C) Total CLD area per cell of all cells analyzed. (D) CLD diameter of those cells containing CLDs. (E) Distribution of CLD diameter of those cells containing CLDs. Significant differences in the distribution of CLD diameter between each region and between lean and DIO mice were determined by Kolmogorov-Smirnov test. Significant differences between each region in lean and DIO mice are indicated. P, proximal, M, middle, D, distal. A two-way mixed model ANOVA was used to determine whether there was a significant effect of region, diet, or their interaction on CLD characteristics. Significant effect of region (*), diet (#), or their interaction (+) is indicated on each graph. Significance considered $p < 0.05$.

151
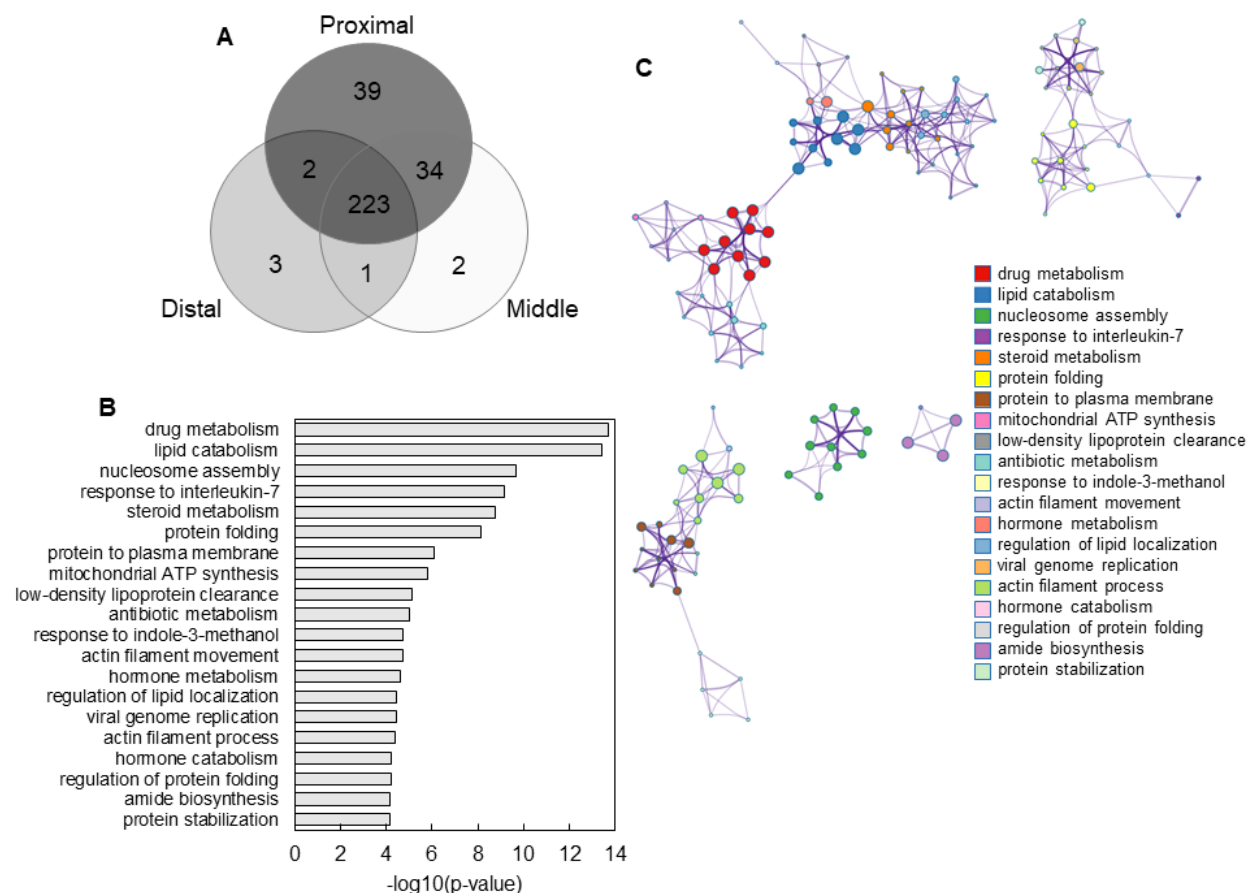
Figure 3-3. Regional distribution of proteins identified in the isolated CLD fraction from each region of the small intestine of both lean and DIO mice. (A) Venn diagram of the number of proteins identified in the same regions in both lean and DIO mice. (B) Top 20 most enriched GO_BP terms of the 223 proteins identified in the isolated CLD fraction from all three regions of the small intestine in both lean and DIO mice. (C) Network display of enriched terms in B. Each circle in a cluster is one term, and the size of the circle is determined by the number of proteins within that term. The color of circles in a cluster is determined based on the representative enriched term for that cluster, listed in the key. Related clusters are connected by a line, with the thickness of the line indicating the strength of the relationship. Enrichment analysis and network image calculated in Metascape. n=5 mice per group for proximal, middle; n=5 mice for DIO distal, n=3 mice for lean distal.
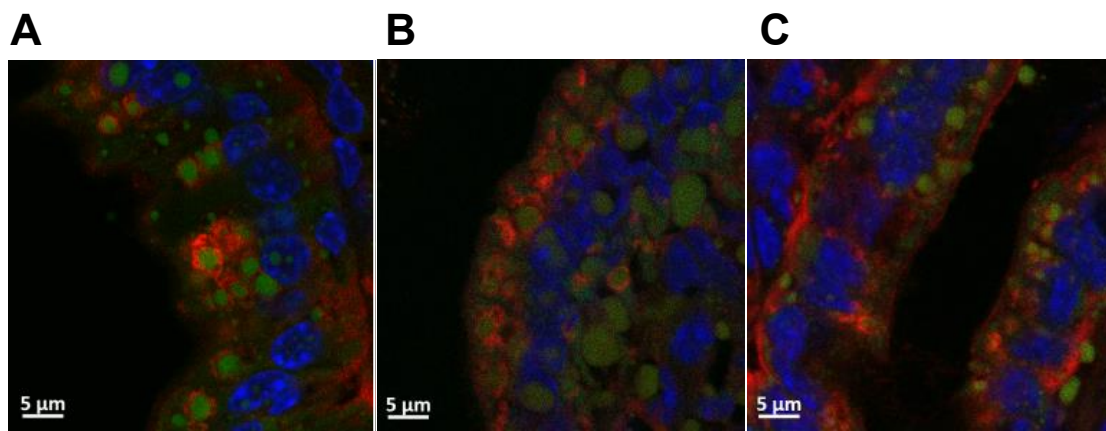
Figure 3-4. Plin3 surrounds CLDs in all three regions of the small intestine in response to dietary fat. Representative immunofluorescence images of enterocytes from the proximal (A), middle (B), and distal (C) regions of the small intestine of lean mice two hours after an olive oil gavage. Intestine sections were stained with BODIPY 493/503 to visualize CLDs (green), AlexaFluor 568 or 633 to visualize Plin3 (red), and DAPI to visualize nuclei (blue). Signals from individual channels were merged for the final image. n=3 mice.
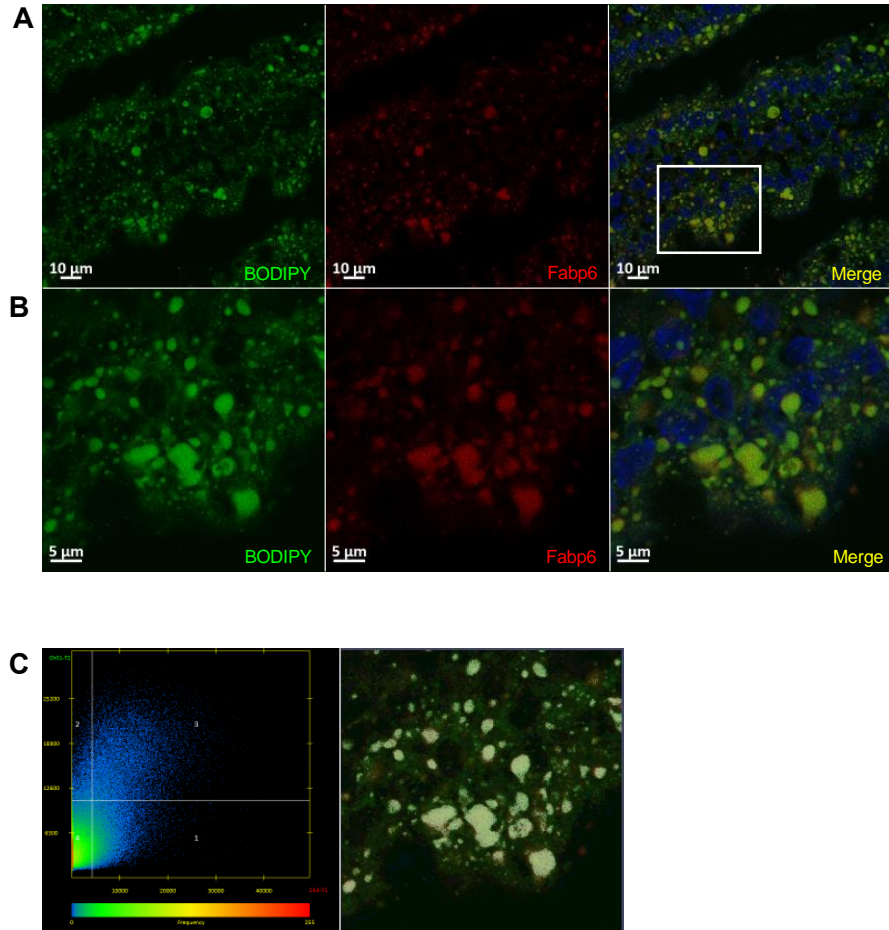
Figure 3-5. Fabp6 localizes to CLDs present in the distal region of the small intestine. Representative immunofluorescence images of a villus (A, across) and enterocytes boxed in A (B, across) from the distal region of the small intestine of a lean mouse. Intestine sections were stained with BODIPY 493/503 to visualize CLDs (green), AlexaFluor 633 to assess the localization of Fabp6 (red), and DAPI to visualize nuclei (blue). Signals from individual channels were merged in the last column of both A and B. (C) Scatterplot of colocalized green and red pixels in the merged image of B (left), which are labeled in white overlay (right). Pixels in Quadrant 3 of the scatterplot are those that are colocalized. n=3 mice.

Table 3-1. Intestine region and obesity influence the relative levels of CLD proteins involved in lipid metabolism in the response to dietary fat. A two-way mixed model ANOVA was performed on the relative levels (LFQ) of proteins identified in the isolated CLD fraction from all three regions of the small intestine in both lean and DIO mice. Proteins involved in lipid metabolism that demonstrate a significant effect of region, obesity, region and obesity, or an interaction between region and obesity on their relative levels are listed. In the case of multiple comparisons, significant results of post-hoc Tukey test are listed. Significant differences between regions are indicated by letters for each region: P, proximal; M, middle; D, distal. LS Means estimates of the LFQ for each protein in each region in lean and DIO mice is included for reference. n=5 lean proximal, middle; DIO proximal, middle distal; n=3 lean distal.

Uniprot ID	Protein	Signif. effect	P-value	Post-hoc Tukey	LS Means Estimate of LFQ										
					Lean	DIO	Prox	Mid	Dist	Lean Prox	Lean Mid	Lean Dist	DIO Prox	DIO Mid	DIO Dist
Q8BWT1	Acaa2	region	0.003	P-D, M-D	20.57	21.49	21.98	21.54	19.56	20.99	21.20	19.53	22.97	21.89	19.60
P50544	Acadvl	region; diet	0.0033; 0.0049	P-D, P-M; DIO>lean	20.15	21.06	21.19	20.51	20.11	20.76	20.11	19.58	21.63	20.91	20.65
Q8JZR0	Acsl5	region	<.0001	P-D, P-M	23.96	24.14	25.01	23.51	23.61	25.16	23.22	23.49	24.87	23.81	23.73
Q00623	Apoa1	region	<.0001	P-D, P-M, M-D	24.91	24.19	23.84	24.55	25.26	24.01	24.85	25.89	23.67	24.26	24.63
P06728	Apoa4	region	0.0004	P-D, M-D	25.45	25.93	25.98	26.27	24.82	25.93	25.91	24.51	26.02	26.62	25.14
E9Q1Y3	Apob	interact.	0.0346	Lean P-M, M-D	22.48	22.02	22.51	21.54	22.70	23.13	21.32	23.00	21.88	21.76	22.41
A0A0R4J1N3	Apoc3	region	0.0012	P-D, P-M	20.43	20.10	19.19	20.86	20.75	19.35	21.00	20.94	19.02	20.72	20.56
Q91WG0	Ces2c	region	0.0083	P-D, P-M	22.21	22.88	23.44	22.05	22.14	23.31	21.19	22.13	23.57	22.91	22.15
Q8BK48	Ces2e	region	0.002	P-M	24.67	24.52	24.97	24.28	24.54	25.15	24.20	24.68	24.79	24.37	24.41
Q9Z2A7	Dgat1	interact.	0.0316	Lean P-M, P-D; Lean P-DIO D	21.98	21.57	22.35	21.76	21.23	22.92	21.86	21.17	21.77	21.66	21.29
Q9DBM2	Ehhadh	region	<.0001	P-D, P-M	21.56	21.05	22.41	21.05	20.46	22.41	21.23	21.03	22.41	20.86	19.89
Q8BFZ9	Erlin2	interact.	0.0276	Lean M-D; lean M-DIO P, M	20.42	19.66	20.13	20.24	19.75	20.63	20.87	19.74	19.62	19.60	19.76
Q8BMS1	Hadha	region	0.004	P-D	21.14	21.69	22.40	21.31	20.54	21.74	20.90	20.80	23.06	21.71	20.29
Q9EQ06	Hsd17b11	interact.	0.0167	Lean P-M, M-D; Lean M-DIO P,D	22.74	23.69	23.98	22.14	23.53	24.02	21.01	23.18	23.94	23.26	23.88
P51660	Hsd17b4	region	0.0034	P-M	22.21	22.55	22.88	21.94	22.32	22.62	21.58	22.42	23.13	22.30	22.23
O08601	Mttp	region	<.0001	P-D, P-M	25.11	25.40	25.97	24.87	24.93	26.09	24.56	24.70	25.85	25.17	25.17
P49586	Pcyt1a	region	0.0223	P-D	20.41	19.71	20.35	20.11	19.73	20.85	20.36	20.03	19.86	19.85	19.43
P32020	Scp2	region	0.0317	M-D	20.89	21.00	20.87	21.46	20.50	20.92	21.56	20.19	20.83	21.35	20.81
Q91VE0	Slc27a4	region	0.0164	P-M	21.51	21.59	21.91	21.09	21.66	22.02	20.82	21.71	21.79	21.37	21.61

3.7 References

[1]   B.G. Nordestgaard, M. Benn, P. Schnohr, A. Tybjaerg-Hansen, Nonfasting triglycerides and risk of myocardial infarction, ischemic heart disease, and death in men and women, Jama 298(3) (2007) 299-308.

[2]   T. D'Aquila, Y.H. Hung, A. Carreiro, K.K. Buhman, Recent discoveries on absorption of dietary fat: Presence, synthesis, and metabolism of cytoplasmic lipid droplets within enterocytes, Biochim Biophys Acta 1861(8 Pt A) (2016) 730-47.

[3]   C.M. Mansbach, 2nd, S. Siddiqi, Control of chylomicron export from the intestine, Am J Physiol Gastrointest Liver Physiol 310(9) (2016) G659-68.

[4]   J.T. Collins, A. Nguyen, M. Badireddy, Anatomy, Abdomen and Pelvis, Small Intestine, StatPearls, StatPearls Publishing. Copyright © 2020, StatPearls Publishing LLC., Treasure Island (FL), 2020.

[5]   J. Iqbal, M.M. Hussain, Intestinal lipid absorption, Am J Physiol Endocrinol Metab 296(6) (2009) E1183-94.

[6]   A.L. Wu, S.B. Clark, P.R. Holt, Transmucosal triglyceride transport rates in proximal and distal rat intestine in vivo, J Lipid Res 16(4) (1975) 251-7.

[7]   A.L. Wu, S.B. Clark, P.R. Holt, Composition of lymph chylomicrons from proximal or distal rat small intestine, Am J Clin Nutr 33(3) (1980) 582-9.

[8]   S.M. Sabesin, P.R. Holt, Intestinal lipid absorption: evidence for an intrinsic defect of chylomicron secretion by normal rat distal intestine, Lipids 10(12) (1975) 840-6.

[9]   S.B. Clark, B. Lawergren, J.V. Martin, Regional intestinal absorptive capacities for triolein: an alternative to markers, Am J Physiol 225(3) (1973) 574-85.

[10]   P.A. Dawson, S.J. Karpen, Intestinal transport and metabolism of bile acids, J Lipid Res 56(6) (2015) 1085-99.

[11]   S. Moran-Ramos, A.R. Tovar, N. Torres, Diet: friend or foe of enteroendocrine cells--how it interacts with enteroendocrine cells, Adv Nutr 3(1) (2012) 8-20.

[12]   C.C. Booth, A.E. Read, E. Jones, Studies on the site of fat absorption: 1. The sites of absorption of increasing doses of I-labelled triolein in the rat, Gut 2(1) (1961) 23-31.

[13]   C.C. Booth, D. Alldis, A.E. Read, Studies on the site of fat absorption: 2 Fat balances after resection of varying amounts of the small intestine in man, Gut 2(2) (1961) 168-74.

[14]   Z.N. Hanipah, P.R. Schauer, Bariatric Surgery as a Long-Term Treatment for Type 2 Diabetes/Metabolic Syndrome, Annu Rev Med 71 (2020) 1-15.

[15]   J.A. Olzmann, P. Carvalho, Dynamics and functions of lipid droplets, Nat Rev Mol Cell Biol 20(3) (2019) 137-155.

[16]   J. Zhu, B. Lee, K.K. Buhman, J.X. Cheng, A dynamic, cytoplasmic triacylglycerol pool in enterocytes revealed by ex vivo and in vivo coherent anti-Stokes Raman scattering imaging, J Lipid Res 50(6) (2009) 1080-9.

[17]   C. Xiao, P. Stahel, A.L. Carreiro, Y.H. Hung, S. Dash, I. Bookman, K.K. Buhman, G.F. Lewis, Oral Glucose Mobilizes Triglyceride Stores From the Human Intestine, Cell Mol Gastroenterol Hepatol 7(2) (2019) 313-337.

[18]   R.N. Chavez-Jauregui, R.D. Mattes, E.J. Parks, Dynamics of fat absorption and effect of sham feeding on postprandial lipema, Gastroenterology 139(5) (2010) 1538-48.

[19]   C. Xiao, P. Stahel, A.L. Carreiro, K.K. Buhman, G.F. Lewis, Recent Advances in Triacylglycerol Mobilization by the Gut, Trends Endocrinol Metab 29(3) (2018) 151-163.

[20]   C. Zhang, P. Liu, The New Face of the Lipid Droplet: Lipid Droplet Proteins, Proteomics 19(10) (2019) e1700223.

[21]   T. D'Aquila, D. Sirohi, J.M. Grabowski, V.E. Hedrick, L.N. Paul, A.S. Greenberg, R.J. Kuhn, K.K. Buhman, Characterization of the proteome of cytoplasmic lipid droplets in mouse enterocytes after a dietary fat challenge, PLoS One 10(5) (2015) e0126823.

[22]   T. D'Aquila, A.S. Zembroski, K.K. Buhman, Diet Induced Obesity Alters Intestinal Cytoplasmic Lipid Droplet Morphology and Proteome in the Postprandial Response to Dietary Fat, Front Physiol 10 (2019) 180.

[23]   Y.H. Hung, A.L. Carreiro, K.K. Buhman, Dgat1 and Dgat2 regulate enterocyte triacylglycerol distribution and alter proteins associated with cytoplasmic lipid droplets in response to dietary fat, Biochim Biophys Acta 1862(6) (2017) 600-614.

[24]   F. Beilstein, J. Bouchoux, M. Rousset, S. Demignot, Proteomic Analysis of Lipid Droplets from Caco-2/TC7 Enterocytes Identifies Novel Modulators of Lipid Secretion, Plos One 8(1) (2013) 17.

[25]   J. Bouchoux, F. Beilstein, T. Pauquai, I.C. Guerrera, D. Chateau, N. Ly, M. Alqub, C. Klein, J. Chambaz, M. Rousset, J.M. Lacorte, E. Morel, S. Demignot, The proteome of cytosolic lipid droplets isolated from differentiated Caco-2/TC7 enterocytes reveals cell-specific characteristics, Biology of the Cell 103(11) (2011) 499-517.

[26]   J.D. Douglass, N. Malik, S.H. Chon, K. Wells, Y.X. Zhou, A.S. Choi, L.B. Joseph, J. Storch, Intestinal Mucosal Triacylglycerol Accumulation Secondary to Decreased Lipid Secretion in Obese and High Fat Fed Mice, Front Physiol 3 (2012) 25.

[27]   A. Uchida, M.C. Whitsitt, T. Eustaquio, M.N. Slipchenko, J.F. Leary, J.X. Cheng, K.K. Buhman, Reduced triglyceride secretion in response to an acute dietary fat challenge in obese compared to lean mice, Front Physiol 3 (2012) 26.

[28]   A.S. Zembroski, K.K. Buhman, U.K. Aryal, Proteome and phosphoproteome characterization of liver in the postprandial state from diet-induced obese and lean mice, J Proteomics 232 (2021) 104072.

[29]   C.A. Schneider, W.S. Rasband, K.W. Eliceiri, NIH Image to ImageJ: 25 years of image analysis, Nat Methods 9(7) (2012) 671-5.

[30]   J. Cox, M. Mann, MaxQuant enables high peptide identification rates, individualized p.p.b.-range mass accuracies and proteome-wide protein quantification, Nat Biotechnol 26(12) (2008) 1367-72.

[31]   J. Cox, N. Neuhauser, A. Michalski, R.A. Scheltema, J.V. Olsen, M. Mann, Andromeda: a peptide search engine integrated into the MaxQuant environment, J Proteome Res 10(4) (2011) 1794-805.

[32]   J. Cox, M.Y. Hein, C.A. Luber, I. Paron, N. Nagaraj, M. Mann, Accurate proteome-wide label-free quantification by delayed normalization and maximal peptide ratio extraction, termed MaxLFQ, Mol Cell Proteomics 13(9) (2014) 2513-26.

[33]   Y. Zhou, B. Zhou, L. Pache, M. Chang, A.H. Khodabakhshi, O. Tanaseichuk, C. Benner, S.K. Chanda, Metascape provides a biologist-oriented resource for the analysis of systems-level datasets, Nat Commun 10(1) (2019) 1523.

[34]   R.A. Jersild, Jr., R.T. Clayton, A comparison of the morphology of lipid absorption in the jejunum and ileum of the adult rat, Am J Anat 131(4) (1971) 481-503.

[35]   D.F. Newton, C.M. Mansbach, 2nd, beta-Sitosterol as a nonabsorbable marker of dietary lipid absorption in man, Clin Chim Acta 89(2) (1978) 331-9.

[36]   R.L. Snipes, Morphological appearance of fat in the epithelial cells of different portions of the intestines in mice, Experientia 33(10) (1977) 1335-6.

[37]   H.S. Shin, J.R. Ingram, A.T. McGill, S.D. Poppitt, Lipids, CHOs, proteins: can all macronutrients put a 'brake' on eating?, Physiol Behav 120 (2013) 114-23.

[38]   J. Liu, D.G. McLaren, D. Chen, Y. Kan, S.J. Stout, X. Shen, B.A. Murphy, G. Forrest, B. Karanam, L. Sonatore, S. He, T.P. Roddy, S. Pinto, Potential mechanism of enhanced postprandial glucagon-like peptide-1 release following treatment with a diacylglycerol acyltransferase 1 inhibitor, Pharmacol Res Perspect 3(6) (2015) e00193.

[39]   B.S. Maciejewski, T.B. Manion, C.M. Steppan, Pharmacological inhibition of diacylglycerol acyltransferase-1 and insights into postprandial gut peptide secretion, World J Gastrointest Pathophysiol 8(4) (2017) 161-175.

[40]   C.R. Hutch, D. Sandoval, The Role of GLP-1 in the Metabolic Success of Bariatric Surgery, Endocrinology 158(12) (2017) 4139-4151.

[41]   T. Li, J.Y. Chiang, Bile acid signaling in metabolic disease and drug therapy, Pharmacol Rev 66(4) (2014) 948-83.

[42]   D. Praslickova, E.C. Torchia, M.G. Sugiyama, E.J. Magrane, B.L. Zwicker, L. Kolodzieyski, L.B. Agellon, The ileal lipid binding protein is required for efficient absorption and transport of bile acids in the distal portion of the murine small intestine, PLoS One 7(12) (2012) e50810.

[43]   M. Nakahara, N. Furuya, K. Takagaki, T. Sugaya, K. Hirota, A. Fukamizu, T. Kanda, H. Fujii, R. Sato, Ileal bile acid-binding protein, functionally associated with the farnesoid X receptor or the ileal bile acid transporter, regulates bile acid activity in the small intestine, J Biol Chem 280(51) (2005) 42283-9.

[44]   C. Fang, F.V. Filipp, J.W. Smith, Unusual binding of ursodeoxycholic acid to ileal bile acid binding protein: role in activation of FXRα, J Lipid Res 53(4) (2012) 664-73.

[45]   A.L. Ticho, P. Malhotra, P.K. Dudeja, R.K. Gill, W.A. Alrefai, Intestinal Absorption of Bile Acids in Health and Disease, Compr Physiol 10(1) (2019) 21-56.

[46]   M. Schittmayer, N. Vujic, B. Darnhofer, M. Korbelius, S. Honeder, D. Kratky, R. Birner-Gruenberger, Spatially resolved activity-based proteomic profiles of the murine small intestinal lipases, Mol Cell Proteomics 19(12) (2020) 2104-2115.

[47]   J. Lian, R. Nelson, R. Lehner, Carboxylesterases in lipid metabolism: from mouse to human, Protein Cell 9(2) (2018) 178-195.

[48]   A.D. Quiroga, J. Lian, R. Lehner, Carboxylesterase1/Esterase-x regulates chylomicron production in mice, PLoS One 7(11) (2012) e49515.

[49]   L.K. Maresch, P. Benedikt, U. Feiler, S. Eder, K.A. Zierler, U. Taschler, S. Kolleritsch, T.O. Eichmann, G. Schoiswohl, C. Leopold, B.I. Wieser, C. Lackner, T. Rülicke, J. van Klinken, D. Kratky, T. Moustafa, G. Hoefler, G. Haemmerle, Intestine-Specific Overexpression of Carboxylesterase 2c Protects Mice From Diet-Induced Liver Steatosis and Obesity, Hepatol Commun 3(2) (2019) 227-245.

[50]   J. Lee, N.D. Ridgway, Phosphatidylcholine synthesis regulates triglyceride storage and chylomicron secretion by Caco2 cells, J Lipid Res 59(10) (2018) 1940-1950.

[51]   J.P. Kennelly, J.N. van der Veen, R.C. Nelson, K.A. Leonard, R. Havinga, J. Buteau, F. Kuipers, R.L. Jacobs, Intestinal de novo phosphatidylcholine synthesis is required for dietary lipid absorption and metabolic homeostasis, J Lipid Res 59(9) (2018) 1695-1708.

[52]   R.R. Stine, A.P. Sakers, T. TeSlaa, M. Kissig, Z.E. Stine, C.W. Kwon, L. Cheng, H.W. Lim, K.H. Kaestner, J.D. Rabinowitz, P. Seale, PRDM16 Maintains Homeostasis of the Intestinal Epithelium by Controlling Region-Specific Metabolism, Cell Stem Cell 25(6) (2019) 830-845.e8.

[53]   A.R. Thiam, M. Beller, The why, when and how of lipid droplet diversity, J Cell Sci 130(2) (2017) 315-324.

[54]   T. Nakano, I. Inoue, I. Koyama, K. Kanazawa, K. Nakamura, S. Narisawa, K. Tanaka, M. Akita, T. Masuyama, M. Seo, S. Hokari, S. Katayama, D.H. Alpers, J.L. Millán, T. Komoda, Disruption of the murine intestinal alkaline phosphatase gene Akp3 impairs lipid transcytosis and induces visceral fat accumulation and hepatic steatosis, Am J Physiol Gastrointest Liver Physiol 292(5) (2007) G1439-49.

[55]   S. Narisawa, L. Huang, A. Iwasaki, H. Hasegawa, D.H. Alpers, J.L. Millán, Accelerated fat absorption in intestinal alkaline phosphatase knockout mice, Mol Cell Biol 23(21) (2003) 7525-30.

[56]   K. Kaliannan, S.R. Hamarneh, K.P. Economopoulos, S. Nasrin Alam, O. Moaven, P. Patel, N.S. Malo, M. Ray, S.M. Abtahi, N. Muhammad, A. Raychowdhury, A. Teshager, M.M. Mohamed, A.K. Moss, R. Ahmed, S. Hakimian, S. Narisawa, J.L. Millán, E. Hohmann, H.S. Warren, A.K. Bhan, M.S. Malo, R.A. Hodin, Intestinal alkaline phosphatase prevents metabolic syndrome in mice, Proc Natl Acad Sci U S A 110(17) (2013) 7003-8.

[57]   J. Malo, M.J. Alam, M. Shahnaz, K. Kaliannan, G. Chandra, T. Aziz, T. Sarker, M. Bala, R. Paul, C.K. Saha, P.K. Karmakar, M.S. Malo, Intestinal Alkaline Phosphatase Deficiency Is Associated with Ischemic Heart Disease, Dis Markers 2019 (2019) 8473565.

[58]   A. Mahmood, F. Yamagishi, R. Eliakim, K. DeSchryver-Kecskemeti, T.L. Gramlich, D.H. Alpers, A possible role for rat intestinal surfactant-like particles in transepithelial triacylglycerol transport, J Clin Invest 93(1) (1994) 70-80.

[59]   G. Bidault, C. Vatier, J. Capeau, C. Vigouroux, V. Béréziat, LMNA-linked lipodystrophies: from altered fat distribution to cellular alterations, Biochem Soc Trans 39(6) (2011) 1752-7.

[60]   C. Vigouroux, A.C. Guénantin, C. Vatier, E. Capel, C. Le Dour, P. Afonso, G. Bidault, V. Béréziat, O. Lascols, J. Capeau, N. Briand, I. Jéru, Lipodystrophic syndromes due to LMNA mutations: recent developments on biomolecular aspects, pathophysiological hypotheses and therapeutic perspectives, Nucleus 9(1) (2018) 235-248.

[61]   N. Vadrot, I. Duband-Goulet, E. Cabet, W. Attanda, A. Barateau, P. Vicart, F. Gerbal, N. Briand, C. Vigouroux, A.R. Oldenburg, E.G. Lund, P. Collas, B. Buendia, The p.R482W substitution in A-type lamins deregulates SREBP1 activity in Dunnigan-type familial partial lipodystrophy, Hum Mol Genet 24(7) (2015) 2096-109.

CHAPTER 4 MOLECULAR MECHANISMS OF GLUCAGON-LIKE PEPTIDE-2 MOBILIZATION OF INTESTINAL TRIACYLGLYCEROL STORES

4.1 Abstract

Hypertriglyceridemia is a risk factor for cardiovascular disease, the number one cause of death in the United States. A contributing factor to blood triacylglycerol (TAG) concentrations is chylomicron secretion from the small intestine. The majority of chylomicrons are secreted after the consumption of a lipid-rich meal, however, they can also be mobilized from the small intestine hours after the postprandial state by certain factors such as the enteroendocrine hormone glucagon-like peptide-2 (GLP-2). Upon administration, GLP-2 promptly stimulates a brief increase in blood TAG concentrations hours after a meal by mobilizing TAG stored in the small intestine. However, the intestinal TAG storage pool mobilized by GLP-2 or the molecular mechanisms of this response are unclear. To investigate the molecular mechanisms of GLP-2-mediated intestinal TAG mobilization, we performed transmission electron microscopy and untargeted comparative proteome analysis of duodenal biopsies from subjects receiving GLP-2 or placebo five hours after a lipid-rich meal. We identified no change in the presence or diameter of cytoplasmic lipid droplets in enterocytes of subjects in the GLP-2 group, confirming previous studies suggesting GLP-2 mobilizes TAG stores residing beyond enterocytes. Further, we identified several proteins present at significantly different levels in biopsies from subjects receiving GLP-2 compared to those receiving placebo that may contribute to the intestinal response to GLP-2. Overall, this study helps define the intestinal TAG pool mobilized by GLP-2 and potential players involved. Understanding the molecular mechanisms of GLP-2-mediated TAG mobilization will contribute to the understanding of how dietary fat absorption is regulated and can be targeted for the prevention or treatment of cardiovascular disease.

4.2 Introduction

Hypertriglyceridemia is a feature of the atherogenic dyslipidemia complex, which comprises several abnormal blood lipid parameters often present in conditions of dysregulated metabolism such as obesity and Type II diabetes that contribute to the development of cardiovascular disease (CVD) [1]. Therefore, it is necessary to understand the contributing factors to hypertriglyceridemia in order to prevent CVD and its associated conditions. One contributing factor to blood triacylglycerol (TAG) concentrations is the secretion of chylomicrons (CMs) containing dietary fat from the small intestine [2]. The process of CM synthesis and secretion begins with the uptake of dietary fat digestion products (fatty acids and monoacylglycerol) into enterocytes, their resynthesis into TAG at the endoplasmic reticulum (ER) membrane, and packaging onto an apolipoproteinB (apoB)-48 molecule by microsomal triglyceride transport protein (MTTP). After their transport to and modification in the Golgi, CMs are secreted from the basolateral sides enterocytes into the lamina propria where they are taken up into the central lacteal and lymphatic system for eventual release into circulation. An alternative fate of resynthesized TAG in enterocytes is storage in cytoplasmic lipid droplets (CLDs), which are broken down and used for CM secretion at later times [3]. Identifying factors that regulate the absorption of dietary fat and TAG secretion from the small intestine is therefore critical to mitigate hypertriglyceridemia and CVD.

Several factors have been shown to stimulate the release of TAG from the small intestine, including glucose [4-6], sham fat feeding [7], and consumption of a meal [8, 9]. The mechanisms behind these effects are mostly unclear, however, consumption of glucose was shown stimulate intestinal TAG secretion five hours after consumption of a lipid meal in part by mobilizing intracellular CLDs [6]. Another factor implicated in intestinal TAG mobilization is glucagon-like hormone-2 (GLP-2), an enteroendocrine hormone secreted from the distal region of the small intestine in response to nutrients [10]. GLP-2 administration seven hours after consumption of a high-fat meal in human subjects stimulates a significant yet brief increase in plasma TAG originating from the small intestine [11]. This effect is hypothesized to be due to the mobilization of pre-formed CMs in post-enterocyte lipid pools [12, 13]. Post-enterocyte lipid pools include CMs within the lamina propria and lymphatics. This hypothesis is supported by results comparing the effect of GLP-2 on intestinal TAG mobilization to that of enteral glucose [14]. GLP-2 administration after an intraduodenal lipid bolus in rats stimulated intestinal TAG secretion by

increasing lymph flow but not lymph TAG concentration or CM size, suggesting no contribution from CLDs for CM assembly [14]. However, the exact TAG pool mobilized by GLP-2, and the molecular mechanisms involved in this response, have not been determined.

Additional support for GLP-2-mediated mobilization of pre-formed CMs already secreted from enterocytes is the localization of the GLP-2 receptor. Expression of the GLP-2 receptor is notably absent from enterocytes themselves but is instead expressed on sub-epithelial cell types such as stromal cells and myofibroblasts, as well as enteric neurons [15-17]. These observations suggest that GLP-2 may act to mobilize intestinal TAG by an indirect mechanism.

To better define the intestinal TAG pool mobilized by GLP-2 and the potential molecular contributors to this process, we assessed the presence and size of CLDs as well as the tissue proteome of duodenal biopsies from subjects receiving GLP-2 or placebo five hours after a lipid-rich meal. Our results support a role for GLP-2 in mobilizing post-enterocyte TAG storage pools and identified several candidate proteins contributing to the response.

4.3 Methods

4.3.1 Plasma sampling study

4.3.1.1 Subjects

Eight healthy males (49 ± 4.7 years, 26 ± 0.9 kg/m^2 body mass index, 0.84 ± 0.1 mM fasting TAG) were recruited to the study through newspaper advertisements. All subjects had no known medical conditions and were not taking any medications. All subjects gave written, informed consent. The study was approved by the Research Ethics Board at the University Health Network.

4.3.1.2 Study protocol

Subjects participated in two study visits in which they received either GLP-2 during one visit and placebo during the other, in random order, 4 to 6 weeks apart. Following an overnight fast, subjects arrived at the Metabolic Test Centre at the Toronto General Hospital. Subjects ingested a 100-ml high-fat liquid formula containing 50 g of fat (5.3g saturated fat, 14.3g unsaturated fat, 30.4g monounsaturated fat), 0 g protein and 0.1 g carbohydrate (Calogen; Nutricia

Advanced Medical Nutrition). Five hours later they received either a subcutaneous injection of GLP-2 (0.05mg/kg Teduglutide; Shire Canada) or placebo (Figure 4-1). Blood samples were collected at regular intervals into vacutainer tubes containing EDTA and tetrahydrolipstatin, a lipase inhibitor (Roche Canada). Plasma was stored at -20°C until further analyses.

4.3.1.3 Sample analysis

TRL were isolated from plasma and CM- and VLDL-sized particles were further isolated from the TRL fraction, as previously described [18]. TRL fractions (1 mL) were transferred to a 6-mL centrifuge tube on ice and carefully overlaid with 1.006 g/mL density sodium bromide solution. Tubes were centrifuged at 13,500 rpm for 30 minutes at 12°C using a Ti50.4 rotor. Following clear separation, the top 0.5 mL was collected as CM by tube slicing, whereas the bottom fraction was collected as VLDL-sized lipoproteins. TG in plasma and lipoprotein fractions were measured with a commercial assay kit (Wako Diagnostics).

4.3.1.4 Statistical analysis

Data are presented as means ± SE. Time-courses were analyzed by PROC MIXED procedure using SAS (version 9.4, SAS Institute, Inc, Cary, NC) with time as a repeated measure, where time, treatment and treatment x time were considered fixed effects. First-order autoregressive covariance structure was assumed, and least square means were separated by the PDIFF option of SAS.

4.3.2 Duodenal biopsy study

4.3.2.1 Subjects

Twenty-three healthy subjects who were undergoing gastroduodenoscopy to address gastrointestinal symptoms were recruited to the study. One subject withdrew consent and another was excluded due to a diagnosis of Celiac disease. Biopsies from a total of 21 subjects were analyzed in the study (Subject characteristics, Table 4-1). The study protocol was approved by the Research Ethics Board at Advarra, Inc (Columbia, MD). All subjects gave written, informed consent. A screening visit to acquire pertinent medical history and collect blood and urine samples occurred 1-4 weeks prior to the gastroduodenoscopy. Subjects were referred to

gastroduodenoscopy due to dyspepsia, epigastric/abdominal discomfort or gastroesophageal reflux disease. All subjects included in the analysis were demonstrated by endoscopy and duodenal biopsy to have no gastrointestinal pathology.

4.3.2.2 Study protocol

Subjects were randomized to receive either GLP-2 or placebo after giving informed consent. Six hours prior to the gastroduodenoscopy, subjects consumed a 100-ml high-fat liquid meal containing 50 g of fat (5.3g saturated fat, 14.3g unsaturated fat, 30.4g monounsaturated fat), 0 g protein and 0.1 g carbohydrate (Calogen; Nutricia Advanced Medical Nutrition). Five hours later, one hour prior to undergoing endoscopy, subjects received a subcutaneous injection of either GLP-2 (0.05mg/kg Teduglutide; Shire Canada) or placebo (Figure 4-3). Duodenal biopsy samples were collected under general anesthesia, snap-frozen and stored at -80°C for proteomic analysis, or preserved in 2.5% glutaraldehyde in 0.1 M sodium cacodylate (pH 7.4) and stored at 4°C for transmission electron microscopy analysis.

4.3.2.3 In-solution digestion and liquid chromatography-tandem mass spectrometry (LC-MS/MS)

Intestine biopsy samples were washed once with Milli-Q Ultrapure water, then twice with 100mM ammonium bicarbonate until supernatant was clear. Samples were transferred into 2 mL reinforced tubes containing ceramic beads (Precellys CK28-R Hard Tissue Homogenizing Kit) and homogenized in 100mM ammonium bicarbonate using the Precellys 24 homogenizer (Bertin Technologies): 6500 rpm, 3 cycles of 20 seconds each. Protein concentration of homogenates was determined by BCA assay (Pierce^{TM} BCA Protein Assay Kit, Thermo Fisher Scientific #23225). An aliquot containing 100 ug protein was used for proteomic preparation. Proteins were precipitated overnight using ice-cold acetone, then pelleted at 15,000 x g for 10 minutes at 4°C. Acetone was removed and samples dried using a vacuum centrifuge. Dried protein pellets were reduced and solubilized with dithiothreitol and urea, then alkylated using iodoethanol. Samples were digested with Trypsin/Lys-C Mix, Mass Spec Grade (Promega) at a ratio of 1:25 enzyme to protein using a barocycler (Pressure Biosciences Inc, Barocycler NEP2320) at 50°C, 20 kpsi, 60 cycles. After digestion, samples were spun down at 1500 x g for 2 minutes, then cleaned using MacroSpin^{TM} C18 reversed phase spin columns (The Nest Group, Inc.). Cleaned peptides were

dried using a vacuum centrifuge. Peptides were resuspended in 3% ACN/0.1% formic acid before loading into the mass spectrometer.

4.3.2.3.1 LC-MS/MS

LC-MS/MS data were collected using a Dionex UltiMate 3000 RSLC Nano System coupled with Orbitrap Fusion Lumos Tribrid Mass Spectrometer (Thermo Fisher Scientific, Waltham, MA, USA). Peptide separation was accomplished using a trap column (300 mm ID × 5 mm) packed with 5 mm 100 Å PepMap C18 medium coupled to a 50-cm long × 75 µm inner diameter analytical column packed with 2 µm 100 Å PepMap C18 silica (Thermo Fisher Scientific). The column temperature was maintained at 50°C. Mobile-phase solvent A was a purified water and 0.1% formic acid and mobile-phase solvent B was 80% acetonitrile and 0.1% formic acid. 3µl (~1µg) of desalted clean peptides were loaded to the trap column in a loading buffer (3% acetonitrile, 0.1% formic acid) at a flow rate of 5 mL/min for 5 min and separated by reverse phase on the analytical column at a flow rate of 200 nL/min using a 120-min LC gradient as described previously [19, 20]. LC-MS/MS data were acquired in the Orbitrap mass analyzer using an HCD fragmentation. Full scan MS data were collected from 350 to 1600 m/z at a resolution of 120,000 at 200 m/z with automatic gain control target at 4×105, maximum injection time set at 50 ms, dynamic exclusion 30 s and intensity threshold 5.0×104. MS data were acquired in Data Dependent Acquisition mode with cycle time of 5 s/scan. The MS/MS scans were acquired at a resolution of 15,000 at m/z 200 with an ion-target value of 1×105 and a maximum injection of 60 milliseconds.

4.3.2.3.2 LC-MS/MS data analysis

Mass spectral data was searched using MaxQuant version 1.6.3.4 [21, 22] against the UniprotKB *Homo sapiens* database (www.uniprot.org). Trypsin/P and LysC were selected, with 2 missed cleavages allowed. Variable modifications were set as oxidation and acetylation, and fixed modification was set as iodoethanol. The first and main search peptide tolerance was set to 20 and 12, respectively. Minimum peptide length was set to 6 amino acids. A false discovery rate of 1% was used. Match between runs and was selected and label free quantification (LFQ) was used for relative quantification. A routine script was used for statistical analysis and to remove contaminant

167

proteins, $\log_2$ transform the LFQ values, and input missing values for those proteins with at least 3 LFQ values in one treatment group and none in the other using half of the highest LFQ value. A protein was considered identified if it was present in at least 3 samples in at least one group. A protein was considered identified in only one group if it was present in at least 3 samples of one group and none of the other. Of the proteins that were identified in at least 3 samples in both groups or in at least 3 samples in one group and none in the other, a t-test was performed to determine statistical differences between groups (statistical significance considered p<0.05). Functional annotation enrichment using Gene Ontology Biological Process and Kyoto Encyclopedia of Genes and Genomes (KEGG) pathways was performed using Metascape [23]. STRING v11 [24] was used to generate Figure 4-7B.

4.3.2.4 Transmission electron microscopy (TEM)

Biopsy samples were prepared as previously described [25]. Samples were post-fixed in 1% osmium tetroxide containing 0.8% potassium ferricyanide, and en bloc stained in 1% uranyl acetate. They were then dehydrated with a graded series of ethanols, transferred into acetonitrile and embedded in EMbed-812 resin. Thin sections were cut on a Reichert-Jung Ultracut E ultramicrotome and stained with 4% uranyl acetate and lead citrate. Images were acquired on a FEI Tecnai T12 electron microscope equipped with a tungsten source and operating at 80 kV. 30-55 intact enterocytes located in the middle region of the villi from at least two villi per sample were counted and used for analysis. In cells containing CLDs, CLD diameter was measured using ImageJ software [26], and CLD area was estimated by the formula: πr^2 using the measured diameters. Percent of enterocytes containing CLDs, average CLD diameter, number and total CLD area per enterocyte were compared using a two-tailed t-test. Data are presented as means ± SEM. Significance considered p<0.05.

4.4 Results

4.4.1 Plasma analysis

To characterize the physiological response to GLP-2, subjects consumed a high-fat liquid meal and five hours later were administered GLP-2 or placebo (Figure 4-1). Blood was collected in fifteen- or 30-minute intervals for three hours after GLP-2 administration. Plasma TAG

concentrations peaked about four hours after consumption of the high fat meal in both groups and began to decline at five hours (Figure 4-2A). Upon administration of GLP-2 or placebo at five hours, plasma TAG rose to a sharp peak in the GLP-2 group within 30 minutes, while it continued to decline in the placebo group (Figure 4-2A,B). This response was due to a significant 2.5-fold increase in TAG from the CM fraction of isolated triglyceride-rich lipoproteins (TRL) (Figure 4-2C,D). TAG in the VLDL fraction of isolated TRL was also significantly increased with GLP-2 administration (Figure 4-2E); however, this effect was less dramatic.

4.4.2 Transmission electron microscopy

To better define the intestinal TAG pool mobilized in response to GLP-2, we performed TEM analysis on enterocytes within intestinal tissue taken from duodenal biopsies. Subjects consumed a high-fat liquid meal and were administered GLP-2 or placebo five hours later (Figure 4-3). One hour after GLP-2 or placebo administration, duodenal biopsies were taken. Enterocytes within biopsies in both groups were analyzed for the presence CLDs. A representative electron micrograph depicting enterocytes and a CLD within an enterocyte is shown in Figure 4-4A. GLP-2 administration did not significantly alter the percent of enterocytes containing CLDs (Figure 4-4B), average number of CLDs per enterocyte (Figure 4-4C), average CLD diameter (Figure 4-4D), or average CLD area per enterocyte (Figure 4-4E).

4.4.3 Proteomic analysis

To identify potential molecular mediators of intestinal TAG mobilization by GLP-2, we performed global shotgun comparative proteome analysis of duodenal biopsies from subjects receiving GLP-2 or placebo (Figure 4-3). We identified a total of 2524 proteins, 38 of which were identified only in the placebo group and 14 only in the GLP-2 group (Figure 4-5). Of the 2472 proteins identified in both groups, 237 proteins were present at significantly lower levels in the GLP-2 group and 329 proteins were present at significantly higher levels in the GLP-2 group (Figure 4-5).

To determine the metabolic and functional identity of proteins present at significantly higher or lower levels in biopsies of subjects receiving GLP-2 compared to those receiving placebo, we performed functional annotation analysis (Figure 4-6). The most enriched term of proteins

present at lower levels in biopsies of subjects receiving GLP-2 compared to those receiving placebo was precursor metabolites and energy, followed by carboxylic acid biosynthesis and cofactor metabolism (Figure 4-6A lower panel). These three enriched terms were shown to be greatly related by network analysis (Figure 4-6A upper panel). Proteins within these terms include those involved in the mitochondrial electron transport chain, fatty acid metabolism, and glycolysis/gluconeogenesis. Interestingly, Golgi vesicle transport was another enriched term of proteins present at significantly lower biopsies of subjects receiving GLP-2 (Figure 4-6A upper panel). The most enriched term of proteins present at higher levels in biopsies of subjects receiving GLP-2 compared to those receiving placebo was RNA splicing followed by regulated exocytosis and actin filament process (Figure 4-6B). By network analysis, RNA splicing was shown to be related to other enriched terms including ribonucleoprotein complex, translation, and protein localization (Figure 4-6B upper panel). Another cluster of related terms include those with actin filament process, which was related to the enriched terms of cellular component organization, actomyosin structure organization, muscle system process, DNA conformation change, and response to ER stress (Figure 4-6B upper panel).

To determine whether changes in lipid metabolism may contribute to the intestinal response to GLP-2, we analyzed the 252 proteins identified in both groups involved in lipid metabolism (Figure 4-7A). Of these 252 proteins, 31 of them were present at significantly different levels between biopsies of subjects receiving GLP-2 compared to those receiving placebo (Figure 4-7B and Table 4-2). Significantly different lipid metabolism proteins have roles in TAG metabolism, fatty acid synthesis and oxidation, and CM assembly (Figure 4-7B).

4.5 Discussion

To define the intestinal TAG pool mobilized by GLP-2 and identify candidate proteins involved in this response, we examined duodenal biopsies from subjects receiving GLP-2 or placebo five hours after a lipid-rich meal by TEM and LC-MS/MS analysis. We determined no significant differences in the presence or average diameter of CLDs in enterocytes of subjects receiving GLP-2 compared to those receiving placebo, supporting a role for GLP-2 in mobilizing post-enterocyte TAG pools. Support for this mechanism of GLP-2 mediated TAG mobilization are the observed changes in the relative levels of proteins involved in lipid metabolism identified in intestine biopsies of subjects receiving GLP-2 compared to those receiving placebo. Overall, these

results better characterize the intestinal response and hypothesized mechanisms of GLP-2 mediated TAG mobilization.

The ability of GLP-2 to rapidly and dramatically stimulate an increase in plasma TAG concentrations hours after consumption of dietary fat confirms a role for the small intestine in lipid storage. It has previously been shown that the small intestine can store dietary lipid for a significant amount of time, for example up to 18 hours in humans [7] and 12 hours in mice [27]. Although it is assumed that the majority of TAG is stored in CLDs within enterocytes in order to provide fatty acids for CM synthesis upon demand, data on the intestinal TAG response to GLP-2 by us and others suggests that other pools of stored TAG exists in the intestine. These other pools, including pre-formed CMs in the lamina propria or within the lymphatics, are thought to be mobilized by GLP-2 to contribute to blood TAG concentrations [12].

Several pieces of data support this hypothesis. First, the plasma TAG response to GLP-2 is abrupt and occurs in a short time frame before CLD lipolysis, TAG synthesis, CM assembly and secretion could occur. Indeed, this scenario was predicted by mathematical modeling [11]. Second, GLP-2 administration after duodenal lipid bolus in rats increases lymph flow but not lymph TAG concentrations or TAG:apoB-48 ratio, an estimate of CM size [14]. This is opposed to glucose, which initially temporarily decreased lymph flow, but increased lymph TAG concentration and TAG:apoB-48 ratio [14]. As glucose is thought to mobilize TAG stored in enterocyte CLDs [6], and stimulates a different lymphatic response [14], this study supports an alternative mechanism of TAG mobilization GLP-2. Third, CLD analysis of enterocytes from duodenal biopsies of subjects administered GLP-2 or placebo conducted in this study determined no significant difference between the presence or average diameter of CLDs in enterocytes of the GLP-2 group (Figure 4-4). These results are in contrast to the mechanisms of oral glucose on intestinal TAG mobilization, as enterocyte CLDs were less numerous and had a greater amount of smaller CLDs in enterocytes of subjects receiving glucose compared to placebo [6]. Altogether, these results point to the mobilization of TAG stored beyond the enterocyte by GLP-2, such as those in the lymphatics.

Another piece of data supporting the mobilization of intestinal lipid stored beyond enterocytes is a study performed by Gary Lewis's group that is in conjunction with the data presented in this chapter (unpublished results). To investigate whether GLP-2 acts by intracellular mechanisms to influence CM secretion, they collapsed the Golgi by intraduodenal infusion of

Brefeldin A in rats before administration of a lipid bolus. Brefeldin A treatment did not interfere with GLP-2-mediated lymphatic TAG output, TAG concentration, or CM size (unpublished results). These results further confirm that GLP-2 stimulates the mobilization of pre-formed CMs residing in post-enterocyte storage pools.

The mobilization of TAG in post-enterocyte storage pools such as within the lymphatics may occur by several mechanisms. The localization of the GLP-2 receptor on myofibroblasts, enteric neurons, and stromal cells [15-17] suggests GLP-2 may activate lymphatic contractions and stimulate the movement of CMs through the lymph and into circulation [14]. The signaling mechanisms and mediators behind this hypothesis have not been investigated as of yet. However, vascular endothelial growth factor (VEGF) may potentially be involved in this response, as VEGF is secreted from myofibroblast CCD18Co cells in response to GLP-2 [28] and VEGF-3 is necessary to maintain lymphatic vessel integrity in the small intestine as well as dietary fat absorption [29]. Another potential mechanism may be stimulation of blood flow through activation of nitric oxide signaling by GLP-2. In hamsters, inhibiting nitric oxide synthase prevented the stimulatory effect of GLP-2 on TAG and apoB-48 secretion after oil gavage [30]. Further, GLP-2 increased nitric oxide synthase expression and mesenteric blood flow in neonatal pigs [31]. However, inhibiting nitric oxide synthase in humans did not affect intestinal TAG secretion stimulated by GLP-2 despite reduced mesenteric blood flow [32], suggesting potential species differences in the mechanism of action of GLP-2. Therefore, the mechanisms behind GLP-2-mediated intestinal TAG mobilization remain outstanding.

In this study, we identified potential protein mediators or contributors to the intestinal response to GLP-2 by comparative shotgun proteomic analysis of intestine biopsies from subjects receiving GLP-2 compared to those receiving placebo (Figures 4-5, 4-6, 4-7). Interestingly, one of the most enriched functional annotation terms of proteins present at significantly lower levels in the GLP-2 group was fatty acid derivative metabolism, suggesting changes in lipid metabolism may contribute to the intestinal response to GLP-2. For example, several proteins involved in TAG and CM synthesis were present at significantly lower levels in GLP-2 samples compared to placebo, including long-chain-fatty-acid-CoA ligase 5 (ACSL5), diacylglycerol O-acyltransferase 1 (DGAT1), and microsomal triglyceride transport protein (MTTP) (Table 4-2). ACSL5 activates fatty acids for TAG synthesis and has been shown to localize to enterocyte CLDs [33]. Loss of ACSL5 in mice results in a reduced intestinal TAG secretion rate in response to an oil gavage [34],

172

suggesting it may regulate dietary fat absorption. DGAT1 is the major TAG synthesis enzyme in human enterocytes [35] and therefore plays a critical role in providing substrate for CM assembly. CM assembly is catalyzed by MTTP [36]. Altogether, the lower relative levels of these proteins in the GLP-2 group is consistent with a role of GLP-2 in stimulating pre-formed CMs. We also found the putative lipolytic enzymes CES1 and CES2 to be present at significantly lower levels in GLP-2 samples. CES1 has been shown to promote VLDL assembly and secretion in the liver [37-40]. In the intestine, overexpression of Ces2c in mice increased CM size in part by elevated TAG lipolysis and release of FA for TAG synthesis and CM assembly [41]. Therefore, lower relative levels of CES1 and CES2 in GLP-2 samples is consistent with the hypothesis that GLP-2 does not mobilize intracellular TAG stores.

Lower levels of proteins involved in CM assembly in biopsies of subjects receiving GLP-2 compared to those receiving placebo suggests CM transport is also downregulated in response to GLP-2. Consistently, another enriched term of proteins present at lower levels in biopsies of subjects receiving GLP-2 compared to those receiving placebo was Golgi vesicle transport, which includes SAR1B, SEC13, SEC24C involved in pre-CM transport vesicle (PCTV) transport. Newly synthesized CMs must be transported from the ER to the Golgi for modification in PCTV [2]. PCTV budding from the ER is the rate-limiting step in the process of dietary fat absorption. PCTV budding is mediated by the action of SAR1B. SAR1B resides in the cytosol in a complex composed of FABP1, Sec13, and SVIP [2]. Phosphorylation of SAR1B by PKCζ releases FABP1 which translocates to the ER to bind and activate the PCTV for budding [42]. Deficiency of SAR1B causes CM retention disease in humans, which results in massive TAG accumulation in enterocytes and severe fat malabsorption [43]. SEC24 and SEC13 are members of the COPII complex that transports proteins from the ER to the Golgi [44] but are also necessary for the delivery and fusion of PCTV with the Golgi [45, 46]. Other proteins involved in ER to Golgi vesicle transport identified in our analysis present at lower relative levels in the GLP-2 group including ARF1, ARF4, COP proteins (COPA, COPB2, COPG1), DYNC1H1, and VCP suggests a general downregulation of ER to Golgi intracellular transport in response to GLP-2. Overall, the lower relative levels of these proteins in response to GLP-2 supports the mobilization of TAG stored beyond enterocytes.

Proteins involved in lipid metabolism present at significantly higher levels in biopsies of subjects receiving GLP-2 compared to those receiving placebo include several apolipoproteins

such as APOA1, APOA2, and APOD. All three proteins are components of high-density lipoprotein (HDL) particles, which catalyze reverse cholesterol transport to maintain cellular and tissue cholesterol homeostasis [47]. The major HDL protein is APOA1, which activates lecithin-cholesterol acyltransferase (LCAT) for transfer of cholesterol from tissues to HDL and storage as cholesteryl esters [48]. APOA2 is less abundant on HDL than APOA1 and has multiple potential functions on HDL [49]. APOD interacts with both APOA2 and LCAT [48] but may also have other functions binding partners outside of HDL and cholesterol homeostasis [50]. Whether GLP-2 influences reverse cholesterol transport in the intestine is unknown. Further, APOA1 is required for CM maturation in the Golgi [2]. The functional significance of these proteins in the intestinal response to GLP-2 awaits further investigation.

There are several limitations to this study. First, changes in the relative levels of proteins that occur in response to GLP-2, including those involved in CM synthesis and transport, does not necessarily correlate to changes in activity or cellular effects. As with most exploratory proteomic analyses, we are only able to hypothesize the functional significance of changes in protein levels and cannot make mechanistic conclusions. Further studies are required to confirm whether changes in these proteins contribute to the intestinal response to GLP-2. Next, since the intestine biopsies contain multiple cell types in addition to enterocytes, follow-up studies are required to determine whether the changes observed in relative protein levels in biopsies of subjects receiving GLP-2 compared to those receiving placebo occur in enterocytes. However, as many of the proteins we discussed are involved in CM synthesis, and CM synthesis occurs in enterocytes, we hypothesize that the observed changes are relevant to enterocytes. Lastly, although we observed no significant changes in CLD presence or size in enterocytes in response to GLP-2, it is possible that GLP-2 may mobilize mature CMs within enterocytes that have been secreted from the Golgi in secretory vesicles. This scenario was not analyzed in the TEM analysis conducted in this study; however, the difficulty inherent in visually quantifying this effect by TEM necessitates alternative studies.

Overall, although both the TEM and proteomic results are mainly descriptive, this study helps to define the intestinal TAG pool mobilized by GLP-2 and identified potential proteins involved in this response that can be investigated in future studies. Understanding the molecular mechanisms of GLP-2-mediated TAG mobilization will provide additional insight as to how the process of dietary fat absorption is regulated, where TAG originating from the intestine can be

stored, and how intestinal TAG mobilization may be targeted in order to reduce hypertriglyceridemia and CVD.

4.6 Acknowledgments

Table 4-1. Demographic and fasting biochemical characteristics during screening of study participants enrolled for gastroduodenoscopy. Data are means ± standard error.

Characteristics	
Sex (M/F)	11/10
Age (y)	30.9 ± 0.3
BMI (kg/m^2)	25.6 ± 0.2
Fasting Plasma Analyses	
Glucose (mM)	4.8 ± 0.02
Triglyceride (mM)	4.4 ± 0.03
HDL-c (mM)	1.3 ± 0.01
LDL-c (mM)	2.5 ± 0.03
Complete blood count Hg (g/L)	140 ± 0.5
TSH (mU/L)	1.4 ± 0.02
AST (U/L)	20 ± 0.3
ALT (U/L)	19 ± 0.3
ALP (U/L)	64 ± 0.8
Creatinine (uM)	76 ± 0.5
Abbreviations: ALP: alkaline phosphatase; ALT: alanine aminotransferase; AST: aspartate aminotransferase; BMI: body mass index; HDL-c: high-density lipoprotein cholesterol; Hg: hemoglobin; LDL-c: low-density lipoprotein cholesterol; TSH: thyroid stimulation hormone	

Table 4-2. Lipid-related proteins present at significantly higher or lower relative levels in biopsies of subjects receiving GLP-2 compared to those receiving placebo.

Protein ID	Protein names	Protein function	Fold Change	P-value
P33261	Cytochrome P450 2C19 [a]	FA Transport/Metabolism	-5.2953	7.3E-16
P22570	NADPH:adrenodoxin oxidoreductase; mitochondrial [a]	Steroid Metabolism	-5.0581	1.4E-08
Q6P1M0	Long-chain fatty acid transport protein 4	FA Transport/Metabolism	-0.8886	0.01747
P32189	Glycerol kinase	TG Synthesis	-0.7552	0.00565
A0A3B3ITW3	ATP-binding cassette sub-family D member 3	FA Transport/Metabolism	-0.7373	0.00998
P22760	Arylacetamide deacetylase	FA Transport/Metabolism	-0.7319	0.04147
P37059	Estradiol 17-beta-dehydrogenase 2	Steroid Metabolism	-0.6901	0.01589
Q15067	Peroxisomal acyl-coenzyme A oxidase 1	FA Transport/Metabolism	-0.6681	0.00832
O75907	Diacylglycerol O-acyltransferase 1	TG Synthesis	-0.6464	0.0048
P50416	Carnitine O-palmitoyltransferase 1; liver isoform	FA Transport/Metabolism	-0.5774	0.00488
Q9ULC5	Long-chain-fatty-acid-CoA ligase 5	FA Transport/Metabolism	-0.5548	0.02128
Q9NR19	Acetyl-coenzyme A synthetase; cytoplasmic	FA Transport/Metabolism	-0.4805	0.00592
P55157	Microsomal triglyceride transfer protein large subunit	CM production	-0.4789	0.0205
Q9NUB1	Acetyl-coenzyme A synthetase 2-like; mitochondrial	FA Transport/Metabolism	-0.4762	0.01015
P07099	Epoxide hydrolase 1	FA Transport/Metabolism	-0.4658	0.02284
A0A0A0MT32	Lysosomal acid lipase/cholesteryl ester hydrolase	Lysosomal Lipid/Cholesterol Catabolism	-0.4517	0.00826
P49327	Fatty acid synthase	TG Synthesis	-0.4448	0.02643
O15173	Membrane-associated progesterone receptor component 2	Steroid Metabolism	-0.4443	0.01953
O43772	Mitochondrial carnitine/acylcarnitine carrier protein	FA Transport/Metabolism	-0.3959	0.02429
P53396	ATP-citrate synthase	Lipid Metabolism	-0.3674	0.00963
P23141	Liver carboxylesterase 1	Cholesterol metabolism	-0.3594	0.04748
Q6UWP2	Dehydrogenase/reductase SDR family member 11	Steroid Metabolism	-0.3374	0.02416
P14324	Farnesyl pyrophosphate synthase	Cholesterol Synthesis	-0.3032	0.008
P09960	Leukotriene A-4 hydrolase	Eicosanoid Metabolism	-0.267	0.04949
P49748	Very long-chain specific acyl-CoA dehydrogenase; mitochondrial	FA Transport/Metabolism	-0.2606	0.01483
O95674	Phosphatidate cytidylyltransferase 2	Phospholipid metabolism	0.1615	0.03402
A0A1B0GTP7	Acid ceramidase	Ceramide metabolism	0.4771	0.00738
Q01469	Fatty acid-binding protein 5	FA Transport/Metabolism	0.4823	0.01096
C9JF17	Apolipoprotein D	Apolipoprotein	0.6665	0.00472
V9GYM3	Apolipoprotein A-II	Apolipoprotein	0.6884	0.00867
P02647	Apolipoprotein A-I	Chylomicron Production	0.8282	0.00663

Proteins identified in at least 3 samples in both groups, or at least 3 samples in 1 group and 0 samples in the other group were compared. Proteins listed here were present at significantly different levels (P<0.05, by T-Test). Proteins are listed from smallest to largest fold change in response to GLP-2 relative to placebo. Negative fold change represents down-regulation by GLP-2.
[a]Only identified in response to placebo
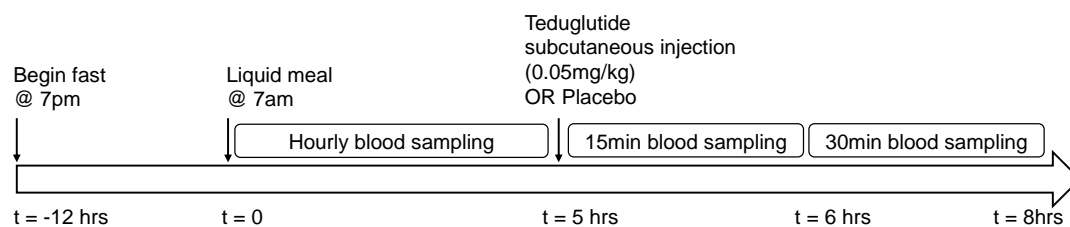
Figure 4-1. Study protocol for physiological data.
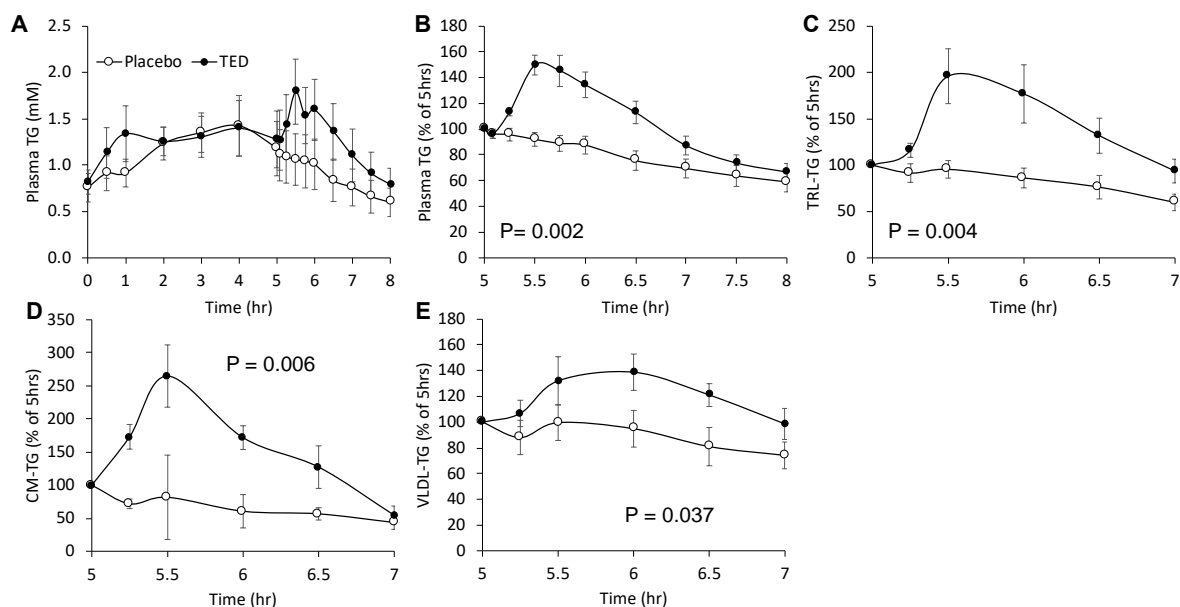
Figure 4-2. Physiological response to GLP-2. (A) Plasma triglycerides (TG) throughout the study. (B) Plasma TG as a percent of time of treatment (5 hrs). (C-E) TG concentrations in total TRL, CM-sized, and VLDL-sized TRL 2 hours after expressed as percentage of time of treatment (5hrs). TED, Teduglutide (GLP-2 analog).

Begin fast
@ 7pm

Liquid meal
@ 7am

Teduglutide
subcutaneous injection
(0.05mg/kg)
OR Placebo

Duodenal
biopsy

t = -12hrs   t = 0   t = 5 hrs   t = 6 hrs
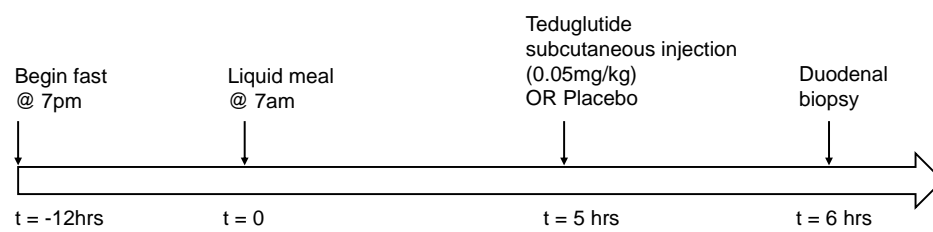
Figure 4-3. Study protocol for biopsy sampling.
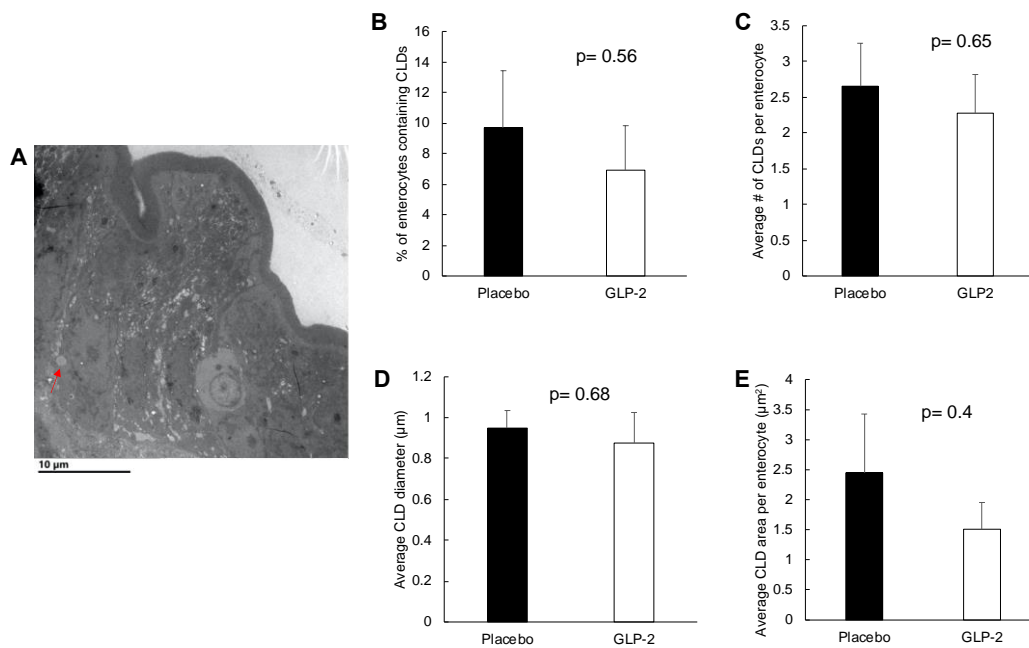
Figure 4-4. Transmission electron microscopy (TEM) CLD analysis. (A) Representative electron micrograph of enterocytes five hours a high-fat liquid meal and one hour after placebo. Arrow indicates a CLD within an enterocyte. (B) Percent of enterocytes containing CLDs. (C) Average number of CLDs per enterocyte. (D) Average CLD diameter. (E) Average CLD area per enterocyte.
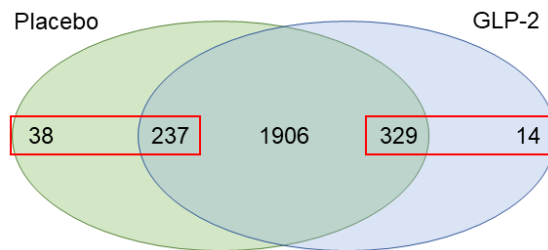
Figure 4-5. Distribution of proteins identified in biopsies of subjects receiving placebo or GLP-2. A total of 2524 proteins were identified of which 2472 were present in at least 3 samples per group. Proteins were considered identified in only one condition if they were identified in at least 3 samples in one group and none in the other. 38 proteins were identified only in the placebo group, 14 proteins were identified only in the GLP-2 group. Of the 2472 proteins identified in both groups, 237 of them were present at significantly lower levels in the GLP-2 group (higher in placebo) and 329 of them were present at significantly higher levels in GLP-2 the group. Red boxes indicated those proteins unique to or present at higher levels in that group.
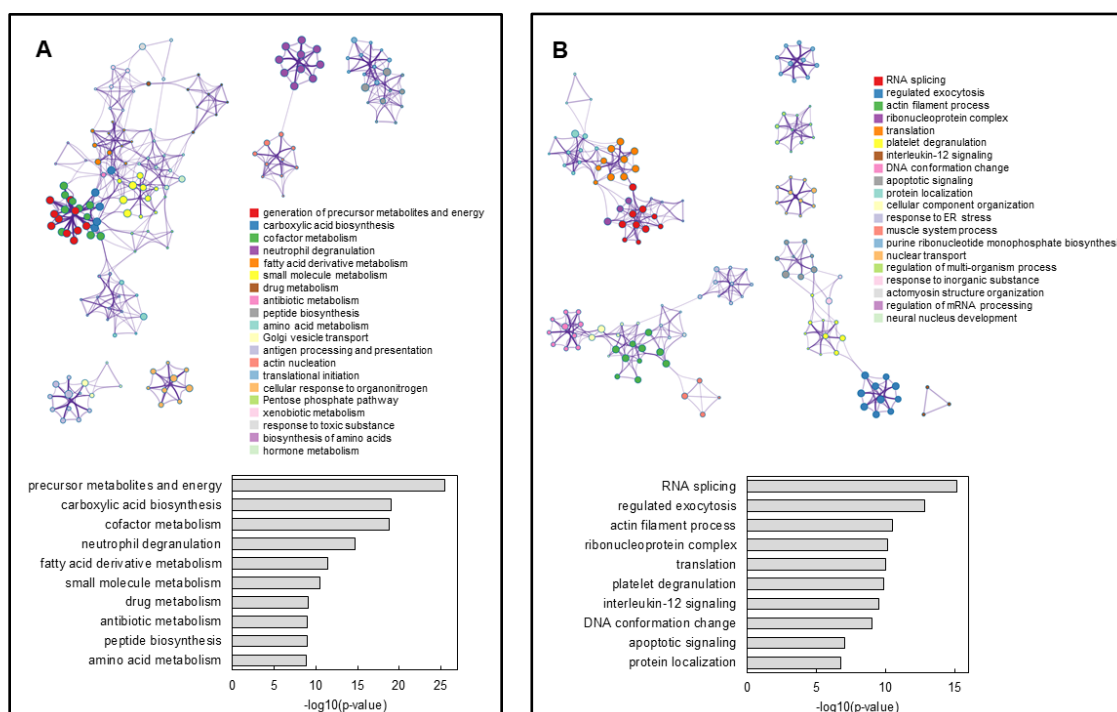
Figure 4-6. Functional annotation analysis of proteins present at significantly lower or higher levels in biopsies of subjects receiving GLP-2 compared to those receiving placebo. (A) Proteins present at lower relative levels in biopsies of subjects receiving GLP-2 compared to those receiving placebo. (B) Proteins present at higher relative levels in biopsies of subjects receiving GLP-2 compared to those receiving placebo. Upper panel in both is a network analysis of the top 20 most enriched functional annotation terms (GO_BP and KEGG pathways). Enriched terms are color coded in the key. Related terms are connected by a line. Lower panel in both is the top 10 most enriched functional annotation terms. Enrichment values shown as -log10(p-value).

183

A

B
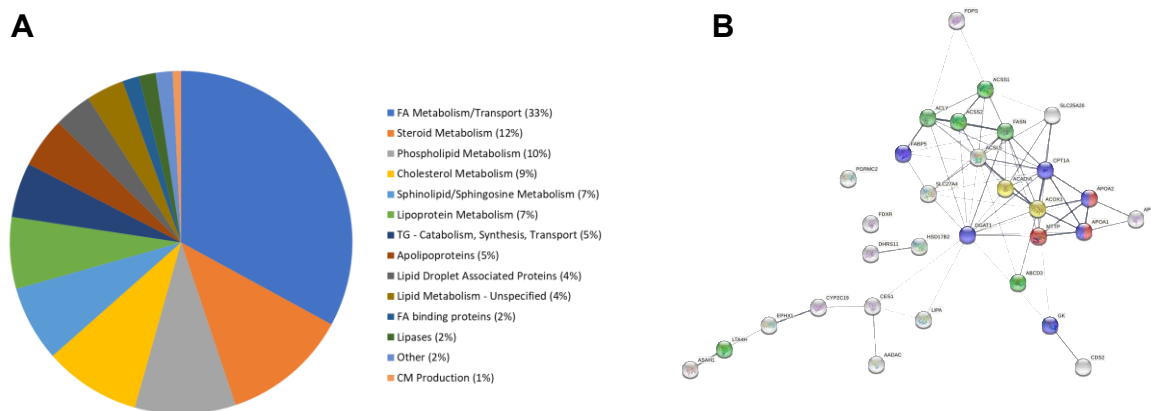
Figure 4-7. Identified proteins involved in lipid metabolism. (A) All 252 lipid-related proteins identified categorized by general function. (B) 31 proteins involved in lipid metabolism present at significantly higher or lower levels in biopsies of subjects receiving GLP-2 compared to placebo. Colored circles represent different functional categories. Blue: triacylglycerol metabolism; Green: fatty acid biosynthesis; Yellow: fatty acid oxidation; Red: chylomicron assembly.

4.7 References

[1]   P. Stahel, C. Xiao, R.A. Hegele, G.F. Lewis, The Atherogenic Dyslipidemia Complex and Novel Approaches to Cardiovascular Disease Prevention in Diabetes, Can J Cardiol 34(5) (2018) 595-604.

[2]   C.M. Mansbach, 2nd, S. Siddiqi, Control of chylomicron export from the intestine, Am J Physiol Gastrointest Liver Physiol 310(9) (2016) G659-68.

[3]   T. D'Aquila, Y.H. Hung, A. Carreiro, K.K. Buhman, Recent discoveries on absorption of dietary fat: Presence, synthesis, and metabolism of cytoplasmic lipid droplets within enterocytes, Biochim Biophys Acta 1861(8 Pt A) (2016) 730-47.

[4]   C. Xiao, S. Dash, C. Morgantini, G.F. Lewis, Novel role of enteral monosaccharides in intestinal lipoprotein production in healthy humans, Arterioscler Thromb Vasc Biol 33(5) (2013) 1056-62.

[5]   C. Xiao, S. Dash, C. Morgantini, G.F. Lewis, Intravenous Glucose Acutely Stimulates Intestinal Lipoprotein Secretion in Healthy Humans, Arterioscler Thromb Vasc Biol 36(7) (2016) 1457-63.

[6]   C. Xiao, P. Stahel, A.L. Carreiro, Y.H. Hung, S. Dash, I. Bookman, K.K. Buhman, G.F. Lewis, Oral Glucose Mobilizes Triglyceride Stores From the Human Intestine, Cell Mol Gastroenterol Hepatol 7(2) (2019) 313-337.

[7]   R.N. Chavez-Jauregui, R.D. Mattes, E.J. Parks, Dynamics of fat absorption and effect of sham feeding on postprandial lipema, Gastroenterology 139(5) (2010) 1538-48.

[8]   B.A. Fielding, J. Callow, R.M. Owen, J.S. Samra, D.R. Matthews, K.N. Frayn, Postprandial lipemia: the origin of an early peak studied by specific dietary fatty acid intake during sequential meals, Am J Clin Nutr 63(1) (1996) 36-41.

[9]   K.D. Silva, J.W. Wright, C.M. Williams, J.A. Lovegrove, Meal ingestion provokes entry of lipoproteins containing fat from the previous meal: possible metabolic implications, Eur J Nutr 44(6) (2005) 377-83.

[10]   D.G. Burrin, Y. Petersen, B. Stoll, P. Sangild, Glucagon-like peptide 2: a nutrient-responsive gut growth factor, J Nutr 131(3) (2001) 709-12.

[11]   S. Dash, C. Xiao, C. Morgantini, P.W. Connelly, B.W. Patterson, G.F. Lewis, Glucagon-like peptide-2 regulates release of chylomicrons from the intestine, Gastroenterology 147(6) (2014) 1275-1284.e4.

[12]   C. Xiao, P. Stahel, G.F. Lewis, Regulation of Chylomicron Secretion: Focus on Post-Assembly Mechanisms, Cell Mol Gastroenterol Hepatol 7(3) (2019) 487-501.

[13]   C. Xiao, P. Stahel, A. Nahmias, G.F. Lewis, Emerging Role of Lymphatics in the Regulation of Intestinal Lipid Mobilization, Front Physiol 10 (2019) 1604.

[14]   P. Stahel, C. Xiao, X. Davis, P. Tso, G.F. Lewis, Glucose and GLP-2 (Glucagon-Like Peptide-2) Mobilize Intestinal Triglyceride by Distinct Mechanisms, Arterioscler Thromb Vasc Biol 39(8) (2019) 1565-1573.

[15]   J. Pedersen, N.B. Pedersen, S.W. Brix, K.V. Grunddal, M.M. Rosenkilde, B. Hartmann, C. Ørskov, S.S. Poulsen, J.J. Holst, The glucagon-like peptide 2 receptor is expressed in enteric neurons and not in the epithelium of the intestine, Peptides 67 (2015) 20-8.

[16]   B. Yusta, D. Matthews, J.A. Koehler, G. Pujadas, K.D. Kaur, D.J. Drucker, Localization of Glucagon-Like Peptide-2 Receptor Expression in the Mouse, Endocrinology 160(8) (2019) 1950-1963.

[17]   C. Ørskov, B. Hartmann, S.S. Poulsen, J. Thulesen, K.J. Hare, J.J. Holst, GLP-2 stimulates colonic growth via KGF, released by subepithelial myofibroblasts with GLP-2 receptors, Regul Pept 124(1-3) (2005) 105-12.

[18]   C. Xiao, R.H. Bandsma, S. Dash, L. Szeto, G.F. Lewis, Exenatide, a glucagon-like peptide-1 receptor agonist, acutely inhibits intestinal lipoprotein production in healthy humans, Arterioscler Thromb Vasc Biol 32(6) (2012) 1513-9.

[19]   A.J. Barabas, U.K. Aryal, B.N. Gaskill, Proteome characterization of used nesting material and potential protein sources from group housed male mice, Mus musculus, Sci Rep 9(1) (2019) 17524.

[20]   A.S. Zembroski, K.K. Buhman, U.K. Aryal, Proteome and phosphoproteome characterization of liver in the postprandial state from diet-induced obese and lean mice, J Proteomics 232 (2021) 104072.

[21]   J. Cox, M. Mann, MaxQuant enables high peptide identification rates, individualized p.p.b.-range mass accuracies and proteome-wide protein quantification, Nat Biotechnol 26(12) (2008) 1367-72.

[22]   J. Cox, N. Neuhauser, A. Michalski, R.A. Scheltema, J.V. Olsen, M. Mann, Andromeda: a peptide search engine integrated into the MaxQuant environment, J Proteome Res 10(4) (2011) 1794-805.

[23]   Y. Zhou, B. Zhou, L. Pache, M. Chang, A.H. Khodabakhshi, O. Tanaseichuk, C. Benner, S.K. Chanda, Metascape provides a biologist-oriented resource for the analysis of systems-level datasets, Nat Commun 10(1) (2019) 1523.

[24] D. Szklarczyk, A.L. Gable, D. Lyon, A. Junge, S. Wyder, J. Huerta-Cepas, M. Simonovic, N.T. Doncheva, J.H. Morris, P. Bork, L.J. Jensen, C.V. Mering, STRING v11: protein-protein association networks with increased coverage, supporting functional discovery in genome-wide experimental datasets, Nucleic Acids Res 47(D1) (2019) D607-d613.

[25] K.J. Wijesinghe, L. McVeigh, M.L. Husby, N. Bhattarai, J. Ma, B.S. Gerstman, P.P. Chapagain, R.V. Stahelin, Mutation of Hydrophobic Residues in the C-Terminal Domain of the Marburg Virus Matrix Protein VP40 Disrupts Trafficking to the Plasma Membrane, Viruses 12(4) (2020) 482.

[26] C.A. Schneider, W.S. Rasband, K.W. Eliceiri, NIH Image to ImageJ: 25 years of image analysis, Nat Methods 9(7) (2012) 671-5.

[27] J. Zhu, B. Lee, K.K. Buhman, J.X. Cheng, A dynamic, cytoplasmic triacylglycerol pool in enterocytes revealed by ex vivo and in vivo coherent anti-Stokes Raman scattering imaging, J Lipid Res 50(6) (2009) 1080-9.

[28] K. Bulut, C. Pennartz, P. Felderbauer, J.J. Meier, M. Banasch, D. Bulut, F. Schmitz, W.E. Schmidt, P. Hoffmann, Glucagon like peptide-2 induces intestinal restitution through VEGF release from subepithelial myofibroblasts, Eur J Pharmacol 578(2-3) (2008) 279-85.

[29] H. Nurmi, P. Saharinen, G. Zarkada, W. Zheng, M.R. Robciuc, K. Alitalo, VEGF-C is required for intestinal lymphatic vessel maintenance and lipid absorption, EMBO Mol Med 7(11) (2015) 1418-25.

[30] J. Hsieh, K.E. Trajcevski, S.L. Farr, C.L. Baker, E.J. Lake, J. Taher, J. Iqbal, M.M. Hussain, K. Adeli, Glucagon-Like Peptide 2 (GLP-2) Stimulates Postprandial Chylomicron Production and Postabsorptive Release of Intestinal Triglyceride Storage Pools via Induction of Nitric Oxide Signaling in Male Hamsters and Mice, Endocrinology 156(10) (2015) 3538-47.

[31] X. Guan, H.E. Karpen, J. Stephens, J.T. Bukowski, S. Niu, G. Zhang, B. Stoll, M.J. Finegold, J.J. Holst, D. Hadsell, B.L. Nichols, D.G. Burrin, GLP-2 receptor localizes to enteric neurons and endocrine cells expressing vasoactive peptides and mediates increased blood flow, Gastroenterology 130(1) (2006) 150-64.

[32] C. Xiao, P. Stahel, C. Morgantini, A. Nahmias, S. Dash, G.F. Lewis, Glucagon-like peptide-2 mobilizes lipids from the intestine by a systemic nitric oxide-independent mechanism, Diabetes Obes Metab 21(11) (2019) 2535-2541.

[33] T. D'Aquila, D. Sirohi, J.M. Grabowski, V.E. Hedrick, L.N. Paul, A.S. Greenberg, R.J. Kuhn, K.K. Buhman, Characterization of the proteome of cytoplasmic lipid droplets in mouse enterocytes after a dietary fat challenge, PLoS One 10(5) (2015) e0126823.

[34] T.A. Bowman, K.R. O'Keeffe, T. D'Aquila, Q.W. Yan, J.D. Griffin, E.A. Killion, D.M. Salter, D.G. Mashek, K.K. Buhman, A.S. Greenberg, Acyl CoA synthetase 5 (ACSL5) ablation in mice increases energy expenditure and insulin sensitivity and delays fat absorption, Mol Metab 5(3) (2016) 210-220.

[35] C.L. Yen, D.W. Nelson, M.I. Yen, Intestinal triacylglycerol synthesis in fat absorption and systemic energy metabolism, J Lipid Res 56(3) (2015) 489-501.

[36] M.M. Hussain, J. Shi, P. Dreizen, Microsomal triglyceride transfer protein and its role in apoB-lipoprotein assembly, J Lipid Res 44(1) (2003) 22-32.

[37] E. Wei, M. Alam, F. Sun, L.B. Agellon, D.E. Vance, R. Lehner, Apolipoprotein B and triacylglycerol secretion in human triacylglycerol hydrolase transgenic mice, J Lipid Res 48(12) (2007) 2597-606.

[38] E. Wei, Y. Ben Ali, J. Lyon, H. Wang, R. Nelson, V.W. Dolinsky, J.R. Dyck, G. Mitchell, G.S. Korbutt, R. Lehner, Loss of TGH/Ces3 in mice decreases blood lipids, improves glucose tolerance, and increases energy expenditure, Cell Metab 11(3) (2010) 183-93.

[39] D. Gilham, S. Ho, M. Rasouli, P. Martres, D.E. Vance, R. Lehner, Inhibitors of hepatic microsomal triacylglycerol hydrolase decrease very low density lipoprotein secretion, Faseb J 17(12) (2003) 1685-7.

[40] J. Lian, E. Wei, S.P. Wang, A.D. Quiroga, L. Li, A. Di Pardo, J. van der Veen, S. Sipione, G.A. Mitchell, R. Lehner, Liver specific inactivation of carboxylesterase 3/triacylglycerol hydrolase decreases blood lipids without causing severe steatosis in mice, Hepatology 56(6) (2012) 2154-62.

[41] L.K. Maresch, P. Benedikt, U. Feiler, S. Eder, K.A. Zierler, U. Taschler, S. Kolleritsch, T.O. Eichmann, G. Schoiswohl, C. Leopold, B.I. Wieser, C. Lackner, T. Rülicke, J. van Klinken, D. Kratky, T. Moustafa, G. Hoefler, G. Haemmerle, Intestine-Specific Overexpression of Carboxylesterase 2c Protects Mice From Diet-Induced Liver Steatosis and Obesity, Hepatol Commun 3(2) (2019) 227-245.

[42] S. Siddiqi, C.M. Mansbach, 2nd, Phosphorylation of Sar1b protein releases liver fatty acid-binding protein from multiprotein complex in intestinal cytosol enabling it to bind to endoplasmic reticulum (ER) and bud the pre-chylomicron transport vesicle, J Biol Chem 287(13) (2012) 10178-88.

[43] E. Levy, Insights from human congenital disorders of intestinal lipid metabolism, J Lipid Res 56(5) (2015) 945-62.

[44] D. Jensen, R. Schekman, COPII-mediated vesicle formation at a glance, J Cell Sci 124(Pt 1) (2011) 1-4.

[45]   S.A. Siddiqi, F.S. Gorelick, J.T. Mahan, C.M. Mansbach, 2nd, COPII proteins are required for Golgi fusion but not for endoplasmic reticulum budding of the pre-chylomicron transport vesicle, J Cell Sci 116(Pt 2) (2003) 415-27.

[46]   S. Siddiqi, S.A. Siddiqi, C.M. Mansbach, 2nd, Sec24C is required for docking the prechylomicron transport vesicle with the Golgi, J Lipid Res 51(5) (2010) 1093-100.

[47]   M. Ouimet, T.J. Barrett, E.A. Fisher, HDL and Reverse Cholesterol Transport, Circ Res 124(10) (2019) 1505-1518.

[48]   A. Kontush, M. Lindahl, M. Lhomme, L. Calabresi, M.J. Chapman, W.S. Davidson, Structure of HDL: particle subclasses and molecular components, Handb Exp Pharmacol 224 (2015) 3-51.

[49]   F. Blanco-Vaca, J.C. Escolà-Gil, J.M. Martín-Campos, J. Julve, Role of apoA-II in lipid metabolism and atherosclerosis: advances in the study of an enigmatic protein, J Lipid Res 42(11) (2001) 1727-39.

[50]   E. Rassart, F. Desmarais, O. Najyb, K.F. Bergeron, C. Mounier, Apolipoprotein D, Gene 756 (2020) 144874.

CHAPTER 5 PROTEOME AND PHOSPHOPROTEOME CHARACTERIZATION OF LIVER IN THE POSTPRANDIAL STATE FROM DIET-INDUCED OBESE AND LEAN MICE

5.1 Abstract

A metabolic consequence of obesity is hepatosteatosis, which can develop into more serious diseases in the non-alcoholic fatty liver disease (NAFLD) spectrum. The goal of this study was to identify the protein signature of liver in the postprandial state in obesity compared to leanness. The postprandial state is of interest due to the central role of the liver in regulating macronutrient and energy homeostasis during the fed-fast cycle and lack of previously reported controlled studies in the postprandial state. Therefore, we assessed the proteome and phosphoproteome of liver in the postprandial state from diet-induced obese (DIO) and lean mice using untargeted LC-MS/MS analysis. We identified significant alterations in the levels of proteins involved in fatty acid oxidation, activation, and transport, as well as proteins involved in energy metabolism including ketogenesis, tricarboxylic acid cycle, and electron transport chain in liver of DIO compared to lean mice. Additionally, phosphorylated proteins in liver of DIO and lean mice reflect possible regulatory mechanisms controlling fatty acid metabolism and gene expression that may contribute to hepatic metabolic alterations in obesity. Our data indicates PPARα-mediated transcriptional regulation of lipid metabolism and adaptation to hepatic lipid overload. The results of this study expand our knowledge of the molecular changes that occur in liver in the postprandial state in obesity compared to leanness.

5.2 Introduction

Overweight and obesity are associated with abnormal lipid accumulation in the liver, or hepatosteatosis, which is a component of non-alcoholic fatty liver disease (NAFLD) [1]. NAFLD is a broad term for a series of conditions in the liver including steatosis, inflammation, and fibrosis, and can progress to more serious disorders such as non-alcoholic steatohepatitis (NASH) and liver

failure [2]. As the obesity rate in the United States continues to rise, the prevalence of NAFLD has increased accordingly, making it the most prevalent chronic liver disease in the United States [3]. In addition, NAFLD contributes to obesity-associated metabolic disorders such as type 2 diabetes and cardiovascular disease [4], in part by contributing to elevated postprandial blood glucose and lipid concentrations [5–7]. NAFLD is a significant health issue and understanding liver metabolism in NAFLD during phases of the fed-fast cycle is important.

We spend a significant amount of time during the day in the postprandial state and the liver's response in macronutrient metabolism during this time impacts both hepatic and systemic health. In the postprandial state, the liver catabolizes glucose through glycolysis, which produces biosynthetic building blocks and cellular energy through the tricarboxylic acid (TCA) cycle and mitochondrial electron transport chain (ETC) [8]. In addition, fatty acids (FA) are used to build cellular components such as membranes, and amino acids are used for protein synthesis. Excess nutrients not immediately used are stored, for example amino acids can be used for *de novo* FA synthesis, glucose is packaged in glycogen or used for *de novo* FA synthesis, and excess FA are incorporated into triacylglycerol (TAG) and stored in cytoplasmic lipid droplets (CLDs) [9]. Regulation of the metabolic pathways involved in these processes is required to maintain cellular and systemic energy and nutrient homeostasis. During obesity, the liver's utilization of macronutrients in the postprandial state is disrupted [5, 10]; however, the molecular characteristics of liver in the postprandial state in obesity that may contribute to these effects are undefined.

Examining the postprandial state in obesity interrogates the nutrient processing capabilities of the liver during obesity-associated hepatosteatosis. Hepatosteatosis is a lipid storage disorder, arising from an imbalance in hepatic lipid utilization, secretion, and storage. Therefore, whether hepatic metabolism in the postprandial state in obesity, where liver is already overladen with fat, differs from hepatic metabolism in the postprandial state in leanness, with no fat accumulation, has not been assessed. As information on the contribution of dietary factors such as degree of fat consumption to hepatosteatosis is lacking [11], comparing liver in the postprandial state in obesity and leanness may reveal key differences in hepatic metabolism as well as generate hypotheses as to how dietary factors contribute to obesity-associated hepatosteatosis.

Mass spectrometry-based proteomics has become an increasingly powerful tool to identify both differentially expressed proteins in a complex protein mixture and regulated protein modifications such as phosphorylation [12], and these techniques have recently been applied to

studying obesity-associated hepatosteatosis. Continuous improvements in methodologies, instrumentation and versatility of the techniques to perform shotgun proteomics and phosphoproteomics, including sample preparation, chromatographic separation, peptide ionization, mass spectrometry detection, and data analysis methods, have made it possible to identify and quantify a few thousand proteins and phosphoproteins from a limited amount of sample in a single experiment [13, 14]. In regards to studying obesity-associated hepatosteatosis, proteome and phosphoproteome analyses have been performed on livers isolated from multiple models of obesity, including obese humans [15–18], diet-induced obese (DIO) mice [19–23], or genetically-induced obese mice [24, 25], which have provided new insights into cellular mechanisms of obesity-associated hepatosteatosis. However, these studies were performed using liver in the fasted or *ad libitum* fed state. To our knowledge, quantitative proteomic and phosphoproteomic analyses of liver in a controlled postprandial state of DIO compared to lean mice has not been previously reported.

To understand the molecular characteristics of liver in the postprandial state in obesity compared to leanness, we assessed the proteome and phosphoproteome of liver in the postprandial state from lean and DIO mice and identified unique features defining obesity and leanness.

5.3 Materials and methods

5.3.1 Mouse husbandry and diets

Animal experiments were carried out in accordance with the National Institute of Health Guide for the Care and Use of Laboratory Animals and approved by the Purdue Animal Care and Use Committee. C57BL/6 male mice were housed in a temperature- and humidity-controlled facility with a 12-h light/dark cycle with *ad libitum* access to food and water. Mice were fed a chow diet consisting of 62.1% of calories from carbohydrate (starch), 24.7% from protein, and 13.2% from fat (PicoLab 5053, Lab Diets, Richmond, IN, United States) from weaning to 5 weeks of age. At 5 weeks of age, mice were switched to either a low-fat (10% calories from fat, D12450J) or high-fat (60% calories from fat, D12492) diet (Research Diets, Inc.; New Brunswick, NJ, United States) for 12 additional weeks. Body weight was recorded weekly. Fasting blood glucose was measured using OneTouch glucometer (LifeScan, Milpitas, CA). Fat pad weight was measured at time of euthanasia.

5.3.2 Triacylglycerol concentration

Triacylglycerol concentration of liver homogenates was measured using Wako L-Type Triglyceride M test (FUJIFILM Wako Diagnostics U. S.A).

5.3.3 Liver isolation and preparation for proteomics

Seven mice from the lean group and seven from the DIO group were fasted for four hours at the beginning of the light cycle. To model the postprandial state that occurs after a lipid meal, mice from both diet groups were administered 200 µL olive oil by oral gavage and euthanized two hours later. We chose to compare the liver of lean and DIO mice at the two hour time point, as this is the middle of the triglyceridemic response in mice [26–28]. Livers were isolated, flash frozen, and stored at -80°C until processing. Liver samples were washed three times with 100 mM ammonium bicarbonate to remove traces of blood. Samples were homogenized in 100 mM ammonium bicarbonate in reinforced tubes containing ceramic beads (Precellys CK28-R Hard Tissue Homogenizing Kit) using the Precellys 24 homogenizer (Bertin Technologies) set at 6500 rpm, 3 cycles of 30 s each. Protein concentration of liver homogenates was determined by bicinchoninic acid (BCA) assay (Pierce^{TM} BCA Protein Assay Kit, Thermo Fisher Scientific #23225). An aliquot of each sample containing approximately 50 µg protein was prepared for proteomic analysis. Samples were separated into soluble and insoluble fractions by centrifugation at 55,000 rpm for 30 min at 4°C. The supernatant and pellet represent the soluble and insoluble fractions, respectively. Proteins in the soluble fraction were precipitated using ice-cold acetone overnight, then pelleted by centrifugation and dried. Proteins in both fractions were reduced and solubilized using 10 mM dithiothreitol and 8 M urea, then alkylated with iodoethanol. Proteins were digested with 4 µg Trypsin/Lys-C Mix, Mass Spec Grade (Promega) using a barocycler set at 50°C, 20 kpsi for 60 cycles (Pressure Biosciences Inc., Barocycler NEP2320). Samples were cleaned using MacroSpin^{TM} C18 reversed phase spin columns (The Nest Group, Inc.) then dried.

5.3.4 Phosphopeptide enrichment

Livers from one DIO mouse and one lean mouse isolated two hours after the olive oil gavage were homogenized with a cocktail of protease and phosphatase inhibitors (final concentration of 20 mM sodium fluoride, 10 mM sodium molybdate, 10 mM sodium

orthovanadate, 10 mM β-glycerolphosphate, 1 mM phenylmethylsulfonyl fluoride) as described above. From each homogenate, two aliquots each containing approximately 500 μg protein were independently prepared for phosphopeptide enrichment, and this preparation was repeated for a total of four technical replicates for each lean and DIO. Lipids were extracted from each sample using chloroform/methanol. Proteins were precipitated with four volumes of cold (-20°C) acetone overnight. Proteins were pelleted by centrifugation then dried. Proteins were reduced and solubilized with 10 mM dithiothreitol/8 M urea and alkylated with iodoethanol. Proteins were digested with 10 μg Trypsin/LysC Mix, Mass Spec Grade (Promega) using a barocycler set at 50°C, 20 kpsi, for 60 cycles (Pressure Biosciences Inc., Barocycler NEP2320). Samples were cleaned using MacroSpin^{TM} C18 reversed phase spin columns (The Nest Group, Inc.) then dried. Phosphopeptide enrichment was performed using the Spin-Tip PolyMac-Ti Phosphopeptide Enrichment kit following the manufacturer's protocol (Tymora Analytical) [29].

5.3.5 Liquid chromatography-tandem mass spectrometry (LC-MS/MS)

Peptide samples were analyzed using a Dionex UltiMate 3000 RSLC nano System (Thermo Fisher Scientific, Odense, Denmark) coupled on-line to Orbitrap Fusion Lumos Mass Spectrometer (Thermo Fisher Scientific, Waltham, MA, USA) as described previously [30]. Reverse phase peptide separation was accomplished using a trap column (300 mm ID × 5 mm) packed with 5 mm 100 Å PepMap C18 medium coupled to a 50-cm long × 75 μm inner diameter analytical column packed with 2 μm 100 Å PepMap C18 silica (Thermo Fisher Scientific). The column temperature was maintained at 50°C. Mobile-phase solvent A consisted of purified water and 0.1% formic acid and mobile-phase solvent B consisted of 80% acetonitrile and 0.1% formic acid. Sample was loaded to the trap column in a loading buffer (3% acetonitrile, 0.1% formic acid) at a flow rate of 5 μL/min for 5 min and eluted from the analytical column at a flow rate of 300 nL/min using a 120-min LC gradient. Data were acquired in the Orbitrap mass analyzer and data were collected using an HCD fragmentation. Full scan MS data were collected from 350 to 1600 m/z at a resolution of 120,000 at 200 m/z with automatic gain control target at 4×10^5, maximum injection time set at 50 ms, dynamic exclusion 30 s and intensity threshold 5.0×10^4. MS data were acquired in Data Dependent mode with cycle time of 5 s/scan. MS/MS data were collected at 15,000 resolutions. The MS/MS scans were acquired at a resolution of 15,000 at m/z 200 with an ion-target value of 1×10^5 and a maximum injection of 60 milliseconds.

5.3.6 Data analysis

LC-MS/MS data were analyzed using MaxQuant software (version 1.6.0.16) [31–33] against the UniProtKB *Mus musculus* protein database (85,159 sequences as of February 29, 2019) for protein identification and label-free relative quantitation. Soluble and insoluble fractions of samples for the global analysis were searched together and results combined. Default settings were used except the following parameters: 10 ppm precursor mass (MS) tolerance, 20 ppm fragment mass (MS/MS) tolerance, enzyme specificity for trypsin/Lys-C, allowing up to two missed cleavages. Oxidation of methionine (M) and phosphorylation of serine, threonine and tyrosine (pSTY) were defined as a variable modification, and iodoethanol of cysteine (C) was defined as a fixed modification for database searches. The 'unique plus razor peptides' were used for peptide quantitation and the false discovery rate (FDR) of both peptides spectral match (PSM) and proteins identification was set at 0.01. Proteins labeled either as contaminants or reverse hits were removed from the analysis. Similarly, proteins identified without any quantifiable peak (0 intensity) and those identified by a single MS/MS count were also removed from downstream analyses. Label-free quantification (LFQ) intensity values were transformed by log2. For the global proteomic analysis, proteins that were detected in at least four of the seven biological replicates in at least one condition were included for further analysis. For phosphoproteomic analysis, phosphopeptides present in at least two out of four replicates in at least one diet group were used for analysis. Phosphopeptides present in at least two out of four replicates in one diet group and none in the other were considered identified in only DIO or only lean samples. Phosphopeptides containing sites with a probability score < 0.4 or those without a detected site were removed. Sites without a matching phosphopeptide were also removed.

For the global proteomic analysis, a two-sample t-test was performed using the transformed LFQ values of those proteins that were identified in at least four of the seven biological replicates per diet group. Statistical significance considered $p < 0.05$. Uniprot ID numbers in the "Majority protein IDs" column were used for functional annotation. Functional annotation and statistical enrichment was conducted using Metascape using the default settings [34]. PCA scores plot was generated using Metaboanalyst [35].

5.3.7 Data availability

All raw LC-MS/MS data are available on the Mass Spectrometry Interactive Virtual Environment (MassIVE) data repository at ftp:// massive.ucsd.edu/MSV000085612.

5.4 Results

5.4.1 Mice fed a high-fat diet develop obesity and hepatosteatosis

To induce obesity-associated hepatosteatosis, mice were fed a 60% high-fat diet for 12 weeks. Mice fed a high-fat diet gained more weight compared to mice fed a low-fat diet (Figure 5-1A). In addition, fasting blood glucose concentrations (Figure 5-1B) and adipose tissue deposition (Figure 5-1C) were more than doubled in mice fed a high-fat diet compared to mice fed a low-fat diet. Lastly, mice fed a high-fat diet accumulated about five-fold more liver TAG compared to mice fed a low-fat diet (Figure 5-1D). These results are consistent with previously reported studies where mice were fed the same high-fat and low-fat diets [36, 37].

5.4.2 Proteins and phosphorylated proteins are differentially present in livers of DIO compared to lean mice

To determine the molecular characteristics of liver in the postprandial state of DIO compared to lean mice, lean and DIO mice were administered 200 μL olive oil by oral gavage and livers were isolated two hours later for proteome and phosphoproteome analysis (Figure 5-2). We identified 29,460 peptides corresponding to 2554 proteins distributed across the two conditions by LC-MS/MS analysis (Figure 5-3A). Of the 2257 proteins common to livers of lean and DIO mice, 478 proteins were present at significantly lower levels in DIO compared to lean mice, and 358 proteins were present at significantly higher levels in DIO compared to lean mice. 194 proteins were identified only in livers of lean mice, and 103 proteins were identified only in livers of DIO mice. The similarity of biological replicates and distinction between lean and DIO samples was confirmed by principal component analysis (Figure 5-3B).

After phosphopeptide enrichment, we identified 1420 unique phosphopeptides containing 2345 phosphosites derived from 824 phosphorylated proteins (Figure 5-3C). Of the 824 phosphorylated proteins, 749 were common to livers of both lean and DIO mice, 11 were identified only in livers of lean mice and 64 were identified only in livers of DIO mice. Similarly, of the

1420 unique phosphopeptides, 1264 were common to livers of both lean and DIO mice, 23 were identified only in livers of lean mice and 133 were identified only in livers of DIO mice. Of the 2345 phosphosites, 86.3% were phosphoserine (pS), 12.7% were phosphothreonine (pT), and 1.07% were phosphotyrosine (pY), which is in line with the general phosphorylation site pattern of mouse tissues [38]. To note, 353 of the 824 proteins identified as phosphorylated were also identified in the global analysis, while the other 471 proteins were only identified upon phosphopeptide enrichment. In addition, 22 proteins that were not present in our global list were detected exclusively with phosphopeptide enrichment, but were modified by either oxidation, acetylation, or their modification could not be confirmed. Overall, phosphopeptide enrichment not only helped to characterize phosphoproteins but also identified hundreds of low-abundant proteins otherwise not identified in the global analysis, allowing for better depth of proteome coverage.

5.4.3 Functional annotation analysis indicates increased FA oxidation, ketogenesis and altered energy and glucose metabolism in livers of DIO compared to lean mice

We performed functional annotation enrichment analysis of proteins differentially present in livers of DIO compared to lean mice in the global analysis (Figures 5-4 and 5-5). Proteins present at significantly higher levels or identified only in livers of DIO mice are enriched in Kyoto Encyclopedia of Genes and Genomes (KEGG) pathways and Gene Ontology Biological Process (GO_BP) terms involving monocarboxylic acid metabolism, peroxisome, cofactor metabolism, and branched chain amino acid (BCAA) degradation (Figure 5-4). Seven of the nine proteins with the greatest fold change increase in livers of DIO mice are involved in FA metabolism and transport (Figure 5-6), including Acss3 (2.86 fold), Cd36 (2.19 fold), and Aldh3a2 (1.99 fold), as well as those in peroxisomal fatty acid oxidation (FAO) such as Acaa1a (1.6 fold) and Acaa1b (1.77 fold). In contrast, Fabp5 was the most significantly downregulated protein in livers of DIO mice (4.14 fold).

Consistent with the upregulation of proteins involved in FA metabolism, peroxisome proliferator-activated receptor (PPAR) signaling was also one of the most enriched KEGG pathways of proteins higher in livers of DIO compared to lean mice (Figure 5-4A). In fact, Vnn1, a marker of PPARα activation in the liver [39, 40], was identified only in livers of DIO mice. We identified PPARα-responsive proteins present at higher levels in livers of DIO mice, including those in FA binding and transport (Fabp2, Fabp4, Cd36) and those in mitochondrial and

peroxisomal FAO. For example, proteins in every step of the mitochondrial FAO cycle were present at higher levels in livers of DIO mice, including FA entry into the mitochondria (Acsl1, Cpt1a, Cpt2, Crat (1.7 fold)), and the first through fourth steps (dehydrogenation, hydration, oxidation, thiolytic cleavage) of the FAO cycle (Acads, Acadm, Acadvl, Acox1; Hadh, Hadha, Hadb, Eci1). Interestingly, in contrast to the other enzymes catalyzing the first dehydrogenation step in the FAO cycle that were present at higher levels in livers of DIO mice, one enzyme specific for long-chain fatty acids, Acadl, was present at lower levels in livers of DIO mice.

Three potential fates of excess acetyl-CoA produced from FAO include conversion into ketones, *de novo* FA synthesis, or *de novo* cholesterol synthesis. The four enzymes that catalyze ketogenesis (Acat1, Hmgcs2, Hmgcl, Bdh1) were present at higher levels in livers of DIO mice. However, enzymes involved in *de novo* fatty acid synthesis were present at lower (Acly, Fasn) or unchanged (Acaca) levels in livers of DIO compared to lean mice. In addition, enzymes involved in *de novo* cholesterol synthesis were present in only livers from lean mice (Acat2) or present at higher levels in livers of DIO mice (Hmgcs1). We did not identify the enzyme catalyzing the rate-limiting step in cholesterol synthesis, Hmgcr.

Proteins present at significantly lower levels in livers of DIO mice or identified only in livers of lean mice are enriched in related pathways and processes (Figure 5-5B) involved in drug metabolism, nucleobase metabolism, and generation of metabolites and energy (Figure 5-5). Proteins in these categories include enzymes of almost every step of the TCA cycle (Dlat, Cs, Aco1, Idh3g, Idh3b, Ogdh, Sdha, Sdhb, Sdhc, Sucla2, Mdh, Pck1), and enzymes regulating glucose homeostasis including glycolysis (Pgk1, Gpi1, Pgam1, Pklr), gluconeogenesis (Pck1, Fbp2, G6pc), glycogen synthesis (Gys2, Ppp1ca, Ppp1cb, Gyg) and glycogen breakdown (Phkg2, Pygl). Interestingly, Mlxipl, encoding the Carbohydrate Response Element Binding Protein (ChREBP) transcription factor which regulates the expression of genes involved in glucose and lipid metabolism [41], was identified only in livers of lean mice.

In addition to a decrease in the levels of proteins involved in cellular energy homeostasis, proteins involved in oxidative phosphorylation were present at lower levels in livers of DIO mice. These include subunits in all five complexes of the mitochondrial ETC, for example eleven proteins in Complex I, the rate-limiting step of mitochondrial respiration [42]: mt-Nd1, mt-Nd2, mt-Nd4, mt-Nd5, Ndufa8, Ndufa9, Ndufb6, Ndufs5, Ndufv2, Ndufv3, Ndufaf3. In addition, three out of the four subunits of Complex II (Sdha, Sdhb, Sdhc), as well as subunits in Complex III

(Uqcr10, Uqcrc2, Uqcrq), Complex IV (mt-Co1, Cox20, Cox4i1) and five subunits of Complex V/ATP synthase (Atp5b, Atp5l, Atp5f1, mt-Atp6, mt-Atp8) were present at lower levels in livers of DIO mice. In fact, mt-Atp8 was one of the most significantly downregulated proteins in livers of DIO mice (Figure 5-6), and mt-Atp6 was identified in only livers of lean mice. Interestingly, one subunit of Complex V (Atp5a1) was present at higher levels in livers of DIO mice.

Enzymes that neutralize cellular reactive oxygen species (ROS) including Cat, Prdx1, Prdx3, were present at higher levels, while Sod2, Prdx4, Prdx5, Prdx6 were present at lower levels in livers of DIO compared to lean mice. In addition, glutathione S-transferase family members were present at higher (Gsta1, 1.97 fold) and lower (Gstp1, 1.62 fold) levels in livers of DIO mice (Figure 5-6).

Enzymes involved in bile acid homeostasis, including Cyp7b1 and Slco1a1, were present at 3.26 and 3.43 fold lower levels, respectively, in livers of DIO compared to lean mice (Figure 5-6). Other enzymes involved in bile acid homeostasis were present at both higher (Cyp8b1, Hsd3b7, Akr1d1, Amacr, Baat, Abcc2) and lower (Cyp2c70, Abcb11, Slc10a1, Slco1a1), levels in livers of DIO mice.

Other proteins that were present at significantly different levels are those involved in lipid droplet and lipoprotein metabolism (higher in DIO), members of the cytochrome P450 family (both higher and lower in DIO), ribosomal subunits and translational proteins (lower in DIO), proteasomal subunits (lower in DIO), and those involved in mRNA splicing (lower in DIO).

5.4.4 Differential phosphorylation of proteins involved in mRNA splicing and FA metabolism in livers of DIO compared to lean mice

To determine changes in the liver phosphoproteome, we analyzed the proteins identified as phosphorylated in livers of only DIO or lean mice by functional annotation. Interestingly, more proteins were phosphorylated in livers of only DIO mice (65 proteins) compared to only lean mice (11 proteins) (Figure 5-3C). To note, the most enriched functional annotation category of the 749 proteins identified as phosphorylated in livers of both DIO and lean mice was mRNA metabolism (Figure 5-8), which includes members of the heterogeneous nuclear ribonucleoprotein (Hnrnp) family and the serine/arginine-rich (Sr) family of proteins involved in mRNA splicing.

Due to the low number of proteins identified as phosphorylated in livers of only lean mice, no functional annotation terms were specifically enriched in this group of proteins. However, the

most enriched terms of proteins identified as phosphorylated in livers of only DIO mice include long-chain fatty acid metabolism and saturated monocarboxylic acid metabolism (Figure 5-7), which is attributable to the identification of the Acot3 and Cyp2d10 protein groups. Another enriched term of proteins phosphorylated in livers of only DIO mice is negative regulation of mRNA splicing, which includes Dyrk1a (Y283, localization probability: 0.97), Hnrnpa2b1 (S259, 0.999), and Srsf6 (S303, 0.93). Interestingly, Irs1, a component of the insulin signaling pathway, was phosphorylated on S887 (0.91) in livers of only DIO mice. In fact, other mediators of insulin signaling were differentially present in livers of DIO and lean mice in the global analysis. For example, Enpp1 was identified in livers of only DIO mice, and Grb14 was identified in livers of only lean mice.

To determine differences in phosphorylation sites of proteins phosphorylated in livers of both DIO and lean mice, we used the following criteria: site identification in at least three out of four replicates in one group and none in the other, and site localization probability of at least 0.9. We identified 15 peptides mapping to 14 proteins with 19 phosphorylation sites identified in livers of only DIO or only lean mice (Table 5-1). Consistent with the general phosphorylation results, many proteins with differential phosphorylation sites in livers of DIO or lean mice are involved in mRNA splicing, for example, Rnmt, Prpf4b, and Hnrnpc. Interestingly, Hnrnpc was phosphorylated in livers of DIO mice at S241 (Table 5-1) and was also present at significantly lower levels in livers of DIO compared to lean mice in the global analysis. Other proteins differentially phosphorylated in livers of DIO or lean mice include those involved in fatty acid metabolism. For example, Acbd5 was phosphorylated at S208 in livers of DIO mice and also present at significantly higher levels in livers of DIO mice in the global analysis (Table 5-1). In addition, Acss2 was phosphorylated at S263 and S267 in livers of lean mice and also present at significantly lower levels in livers of DIO mice in the global analysis (Table 5-1).

5.5 Discussion

5.5.1 Summary of results

To determine the molecular characteristics of liver in the postprandial state of DIO compared to lean mice, we performed untargeted shotgun proteome and phosphoproteome analysis on livers of DIO and lean mice isolated two hours after an olive oil oral gavage. About 30% of the

proteins identified in the global analysis were present at significantly different levels in livers of DIO compared to lean mice, which were associated with multiple macronutrient and energy pathways. In addition, differential phosphorylation of proteins in livers of DIO or lean mice may indicate regulatory changes in proteins involved in gene expression and FA metabolism. Based on the functional annotation enrichment data and the identification of proteins in the enriched metabolic pathways, we hypothesize that in liver in the postprandial state of DIO mice, FA uptake, metabolism, and oxidation is increased, while flux through the TCA cycle and ETC is decreased. The excess acetyl-CoA that results from this response is preferentially shuttled into ketogenesis. Glucose homeostasis is also altered, including release into the blood, storage, and catabolism. In addition, splicing factors in the nucleus are differentially phosphorylated, influencing gene expression, and insulin signaling may be altered. Therefore, the molecular characteristics of liver in the postprandial state of DIO compared to lean mice may contribute to altered liver metabolism in obesity-associated hepatosteatosis (Figure 5-9).

5.5.2 PPARα activation, elevated FAO, and ketogenesis in livers of DIO compared to lean mice is similar to other proteomic studies

Our results are similar to other proteomic studies of livers from DIO compared to lean mice. A common observation in other proteomic studies of livers from DIO mice is an increase in the levels of proteins involved in FAO [19-21, 23], suggesting an upregulation of FAO is a compensatory response to liver lipid accumulation. PPARα is a transcription factor that regulates the expression of enzymes involved in FAO and other lipid metabolic pathways [43, 44]. It is possible that increased levels of PPARα-responsive proteins in livers of DIO mice in this study may be exacerbated by increased cellular availability of oleic acid (18:1), the primary fatty acid present in the olive oil gavage and potent activator of PPARα [45]. However, since an increase in the levels of proteins involved in FAO is consistently observed in livers of DIO compared to lean mice, the activation of PPARα and upregulation of proteins involved in FAO may be a standard response to liver lipid accumulation to increase fatty acid catabolism.

The identification of Vnn1 in livers of only DIO mice in our study supports PPARα activation but also suggests Vnn1 has a unique role in livers of DIO mice. Although Vnn1 mRNA and protein levels are higher in livers of obese compared to lean mice [46–48], conflicting reports for the influence of Vnn1 on lipid and glucose metabolism [39, 47, 48] have made its exact role in

nutrient metabolism difficult to delineate. Instead, Vnn1 may contribute to hepatosteatosis by modulating the oxidative stress response. For example, mice lacking Vnn1 had increased glutathione levels and antioxidant capacity in the liver due to a decrease in cellular cysteamine concentrations and subsequent activation of glutathione synthesis by glutamate cysteine ligase, the rate-limiting enzyme [49]. Although the two subunits of glutamate cysteine ligase, Gclc and Gclm, and the enzyme catalyzing the second step in glutathione synthesis, Gss, [50] were present in livers of both DIO and lean mice at similar levels in our study, the identification of Vnn1 in livers of only DIO mice in our study may indicate a disruption in cellular redox status in livers of DIO mice, which can exacerbate cell damage and perpetuate NAFLD.

Consistent with the results of other proteomic studies of livers from DIO mice [19, 20] our results indicate an increase in ketone production. Although ketogenesis is most often activated under fasting conditions when insulin levels are low, ketone synthesis also occurs in insulin resistant states due to increased FA catabolism and elevated cellular acetyl-CoA levels which exceed the oxidative capacity of the TCA cycle [51, 52]. As the liver is the primary organ responsible for ketone synthesis, it is possible that overproduction of acetyl-CoA from elevated FAO may lead to an increase in cellular and systemic ketone levels in DIO mice.

Our results suggest changes in glucose metabolism in livers of DIO mice. For example, we observed a decrease in the levels of proteins involved in glycolysis and gluconeogenesis in livers of DIO mice. Interestingly, gluconeogenesis is often upregulated in insulin resistant states such as NAFLD [53]. In addition to altered glucose breakdown and synthesis, glucose storage may also be dysregulated in livers of DIO mice. Proteins regulating glycogen synthesis and breakdown were lower in livers of DIO mice. Together, these results suggest that DIO mice may have reduced glucose metabolism during the postprandial state.

5.5.3 Decreased TCA cycle flux and lower oxidative energy production in livers of DIO compared to lean mice

Our results suggest reduced oxidative energy production in livers of DIO mice, as we identified proteins involved in the TCA cycle and oxidative phosphorylation present at lower levels in livers of DIO mice. This is in contrast to other proteomic studies of livers from DIO mice [19, 20, 23] in that proteins in the TCA cycle and oxidative phosphorylation were higher in livers of DIO compared to lean mice. These differences may be attributable to the administration of an olive

oil oral gavage in our study, indicating a lower TCA cycle flux and disrupted ATP synthesis in liver in the postprandial state of DIO mice. A connection between dysregulated mitochondrial metabolism and NAFLD has been well established, however inconsistencies on the effect of NAFLD on mitochondrial function exist [54, 55]. Interestingly, a decline in mitochondrial function is generally observed in the development of more serious liver conditions such as NASH [56, 57]. This suggests that obesity may exacerbate NAFLD progression by negatively influencing the liver's mitochondrial energy metabolism.

5.5.4 Other altered metabolic pathways in livers of DIO compared to lean mice

Our results suggest bile acid homeostasis is altered in livers of DIO mice. In addition to their role in dietary fat absorption, bile acids are signaling molecules that bind transcription factors such as the farnesoid X receptor (FXR), in turn regulating genes involved in lipid, glucose, and bile acid metabolism [58]. Changes in the cellular concentration or composition of bile acids can therefore influence the expression of certain genes in macronutrient and energy homeostasis, and can also contribute to cell damage, as bile acids have strong detergent properties [59]. Since we observed changes in the levels of proteins involved in bile acid synthesis, modification, and transport in livers of DIO compared to lean mice in our study, it is possible that bile acid signaling is altered in livers of DIO mice, which may contribute to dysregulated nutrient metabolism or bile acid and cholesterol accumulation.

Elevated FAO and defective mitochondrial energy metabolism in livers of DIO mice can generate increased levels of ROS. Enzymes that neutralize cellular ROS, including those in the glutathione S-transferase family, were present at both higher and lower levels in livers of DIO compared to lean mice, which may reflect differences in substrate specificity [60]. A consequence of elevated levels of ROS is endoplasmic reticulum (ER) stress, which can activate the uncoupled protein response (UPR) and contribute to inflammation and ultimately apoptosis [61, 62]. One response of the UPR is autophagy, which degrades damaged proteins and cellular organelles in an attempt to regain cellular homeostasis [63]. Interestingly, we identified Tex264, a receptor for the autophagic turnover of ER [64, 65] in livers of only DIO mice, suggesting an activation of ER turnover, which may reflect an increase in ER stress that often occurs with lipid accumulation in NAFLD.

5.5.5 Differential phosphorylation in livers of DIO and lean mice may regulate FA metabolism or alter gene expression

Protein phosphorylation mediates a wide variety of cellular processes in the liver [66], and altered phosphorylation is linked to metabolic disorders such as insulin resistance which contributes to NAFLD. The phosphorylation of proteins involved in FA metabolism in livers of DIO mice may reflect metabolic regulation contributing to altered metabolic pathways. For example, Acot3, Acbd5, and Acss2 were differentially phosphorylated between livers of DIO and lean mice. Acbd5 is involved in the transport of very-long chain FA into peroxisomes for FAO [67], while Acot3 is thought to release FA for their transport out of peroxisomes [68]. In addition, Acss2 synthesizes acetyl-CoA from acetate which can be used for *de novo* FA synthesis [69], and is implicated in maintaining lipid homeostasis in mice [70]. Although the phosphorylation sites we detected for Acbd5, Acss2, Acot3 have been previously reported [71], the functional significance of these modifications, for example whether the phosphorylation of Acot3 and Acbd5 influences peroxisomal FAO or is related to the change in relative levels of Acss2 or Acbd5 in livers of DIO compared to lean mice in the global analysis, is not clear. However, phosphorylation of Acss2 was shown to influence its cellular localization, as phosphorylation at S659 stimulates the translocation of Acss2 to the nucleus to regulate gene expression in nucleoblastoma cells [72]. Future studies of the metabolic consequences of differential phosphorylation of these proteins in livers of DIO or lean mice are warranted.

The majority of phosphorylated proteins we identified are involved in mRNA metabolism and splicing. The phosphorylation of splicing factors is thought to regulate their activity, localization, and formation of the spliceosome complex [73, 74], which in turn can influence alternative splicing and gene expression. This suggests changes in phosphorylation and/or expression of splicing factors may influence gene expression and contribute to dysregulated metabolic pathways [75]. In fact, knockdown of the splicing factor SFRS10 in human hepatoma HepG2 cells results in an increase in the mRNA expression of lipogenic genes, *de novo* lipogenesis and TAG accumulation [76]. These effects were attributed to altered splicing of a gene involved in TAG synthesis, *Lpin1*, which changed the cellular ratio of *Lpin1* isoforms. Notably, we identified proteins involved in mRNA splicing phosphorylated in livers of only DIO mice. Therefore, altered regulation of alternative splicing by phosphorylation may contribute to the

metabolic disturbances that occur in livers of DIO mice by affecting the expression of genes involved in nutrient and energy metabolism.

5.6 Conclusion

In conclusion, we characterized the proteome and phosphoproteome of liver in the postprandial state of DIO and lean mice to identify the molecular characteristics of liver in obesity compared to leanness. Combining proteomics and phosphoproteomics allowed for the identification of hundreds of altered proteins and phosphoproteins that are involved in critical metabolic processes, mainly in macronutrient and energy metabolism. In particular, identification of more phosphorylated proteins in livers of DIO mice compared to livers of lean mice highlight a potential role of phosphorylation in obesity-associated hepatosteatosis. Our data will help generate new hypotheses to focus future studies in order to elucidate the roles of these altered proteins and phosphoproteins in obesity-associated hepatosteatosis. Overall, this study expands our knowledge of the molecular mechanisms that contribute to the metabolic disturbances that occur in the liver during obesity and the consideration of dietary factors contributing to disease progression.

A limitation of this study is that we did not determine the difference in response before and after the olive oil gavage as we compared livers of DIO and lean mice only after the olive oil gavage in the postprandial state. It is important to note that the livers of lean and DIO mice are likely different before the olive oil gavage and that the olive oil gavage may differentially impact the liver proteome and phosphoproteome in DIO and lean mice; however, this difference in response cannot be determined from the current study design. It is of interest in future studies to determine this difference in response.

5.7 Funding

Bioscience Center (assistantship to A.S.Z). LC-MS/MS analysis was performed at the Purdue Proteomics Facility in the Bindley Bioscience Center at Purdue University.

5.8 Acknowledgments
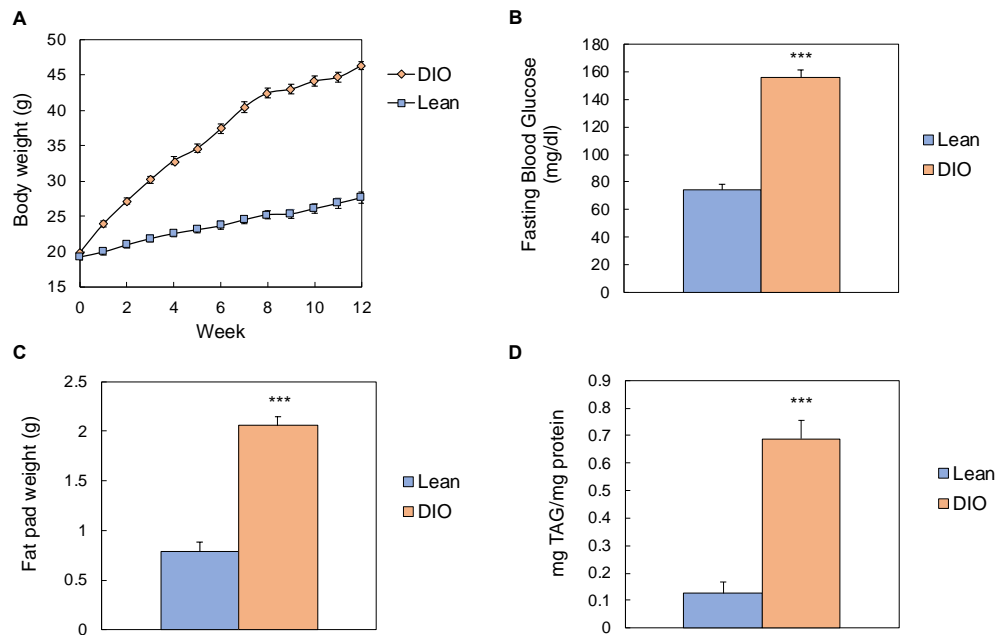
Figure 5-1. Mice fed a chronic high-fat diet develop obesity and hepatosteatosis. To induce obesity, mice were fed a 60% high-fat diet for 12 weeks. Lean mice were fed a control 10% low-fat diet for 12 weeks. (A) Body weight over time. (B) Fasting blood glucose at 12 weeks. (C) Fat pad weight at 12 weeks. (D) Liver triacylglycerol (TAG) concentration. ***$P<0.001$. Data shown as mean ± SEM. n=25 DIO, n=20 lean mice for body weight and fasting blood glucose data; n=14 each DIO and lean mice for fat pad data; n=7 each DIO and lean mice for liver TAG concentration. Body weight data previously published in: D'Aquila T, Zembroski AS, Buhman KK, 2019. Diet Induced Obesity Alters Intestinal Cytoplasmic Lipid Droplet Morphology and Proteome in the Postprandial Response to Dietary Fat. Front Physiol, 10:180. https://doi.org/10.3389/fphys.2019.00180.
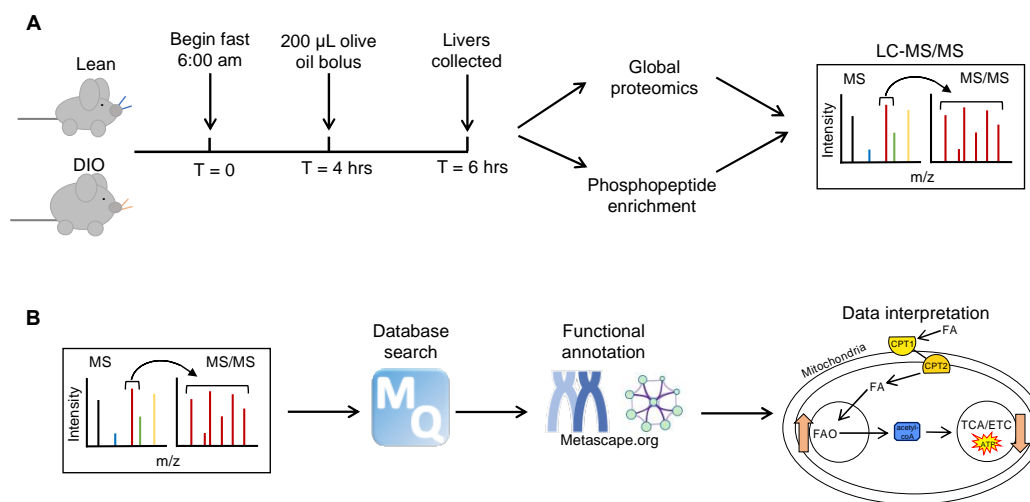
Figure 5-2. Experimental design and data analysis workflow. (A) Experimental design. Seven lean and seven DIO mice were fasted at the beginning of the light cycle (6:00 am). Four hours later, mice from both groups were administered a 200 µL olive oil bolus by oral gavage. Two hours post gavage, mice were euthanized and livers isolated and flash frozen. All samples were prepared for global proteomics, while one sample from each diet group was enriched for phosphopeptides. Proteins were detected by LC-MS/MS. (B) Data analysis workflow. Mass spectral data was searched and proteins identified using Maxquant software. Functional annotation of identified proteins was assigned using Metascape software. Data was interpreted in a biological context.
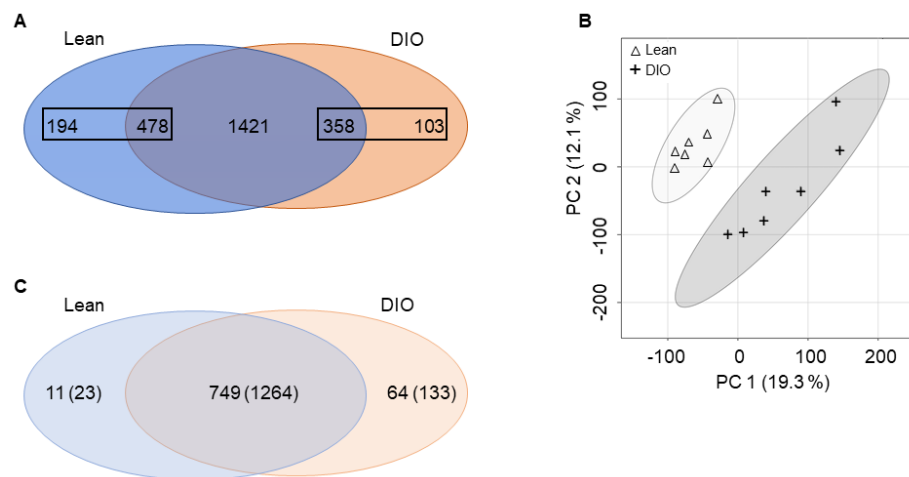
Figure 5-3. Proteins and phosphopeptides are differentially present in livers of diet-induced obese (DIO) mice. (A) Distribution of proteins identified in the global analysis. The boxed-in regions are the number of proteins identified only in or higher in one condition. (B) Scores plot of DIO and lean biological replicates used in the global analysis. Principal components 1 and 2 are shown. Figure generated in Metaboanalyst. (C) Distribution of identified phosphorylated proteins. Numbers in parentheses are the number of phosphopeptides mapping to phosphorylated proteins in each condition.
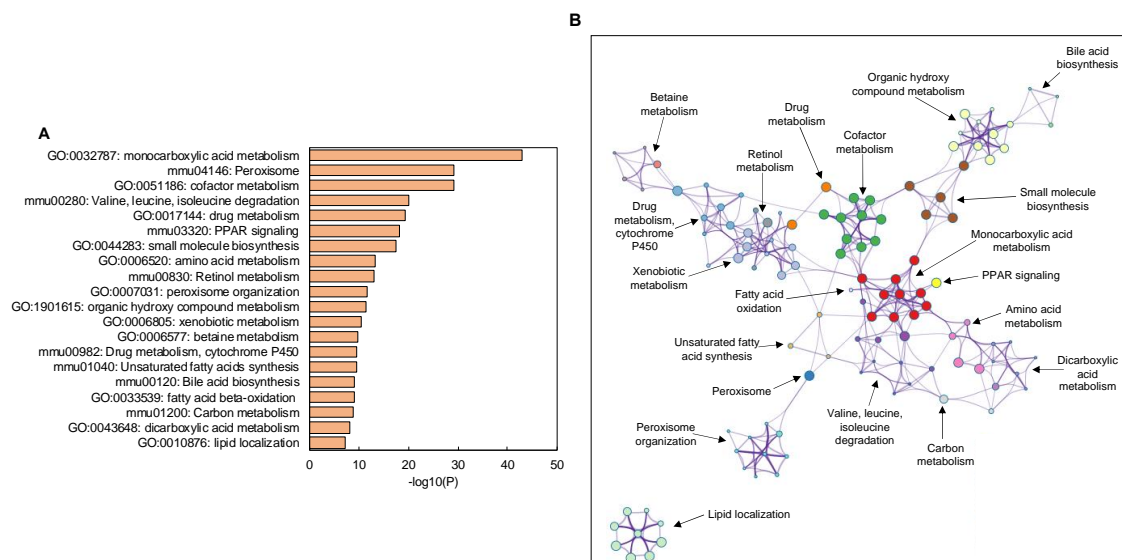
Figure 5-4. Functional annotation analysis of proteins present at significantly higher levels or identified only in livers of diet-induced obese (DIO) compared to lean mice. (A) Top 20 clusters of statistically enriched Kyoto Encyclopedia of Genes and Genomes (KEGG) pathways and Gene Ontology Biological Process (GO_BP) terms higher in DIO. A higher -log10(P-value) indicates more enriched. (B) Enriched clusters of KEGG pathways and GO_BP terms higher in DIO presented in network format. Statistically enriched similar terms are organized into clusters and colored based on the representative term for that cluster. Each circle within a colored cluster represents one term, and the size of the circle correlates with the number of proteins within that term. Similar terms are connected by a line, with a thicker line indicating higher similarity between terms. Enrichment values and cluster networks calculated in Metascape.
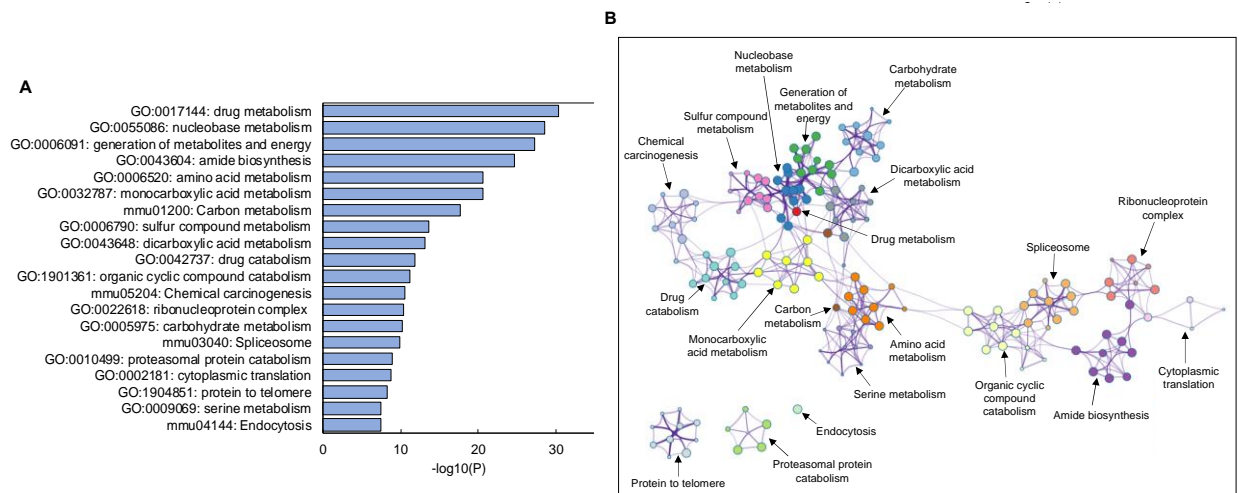
Figure 5-5. Functional annotation analysis of proteins present at significantly lower levels in livers of diet-induced obese (DIO) compared to lean mice or proteins identified only in livers of lean mice. (A) Top 20 clusters of statistically enriched Kyoto Encyclopedia of Genes and Genomes (KEGG) pathways and Gene Ontology Biological Process (GO_BP) terms lower in DIO. A higher -log10(P-value) indicates more enriched. (B) Enriched clusters of KEGG pathways and GO_BP terms lower in DIO presented in network format. Statistically enriched similar terms are organized into clusters and colored based on the representative term for that cluster. Each circle within a colored cluster represents one term, and the size of the circle correlates with the number of proteins within that term. Similar terms are connected by a line, with a thicker line indicating higher similarity between terms. Enrichment values and cluster networks calculated in Metascape.
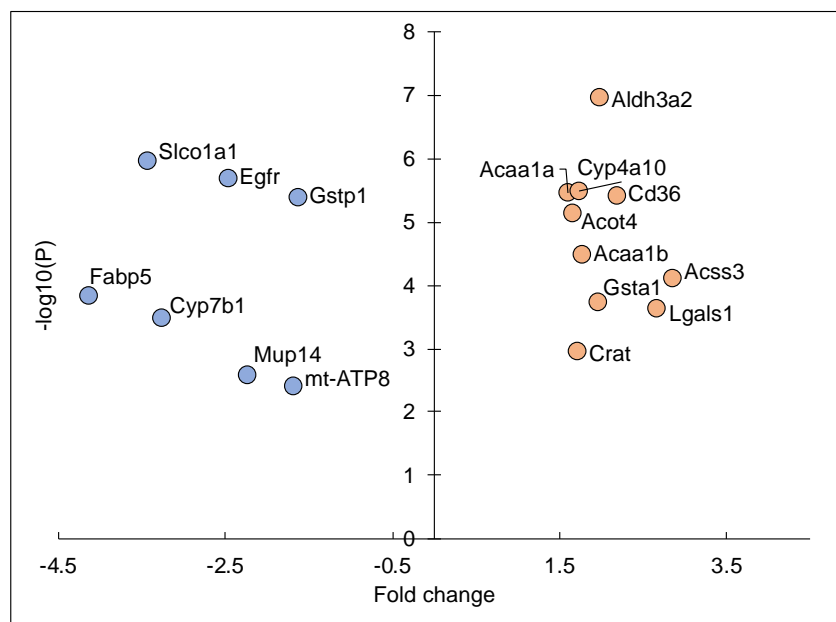
Figure 5-6. Proteins with the largest fold change difference between livers of diet-induced obese (DIO) and lean mice are both up- and down-regulated. Proteins significantly higher (orange) or lower (blue) in DIO present in at least four out of seven samples in both conditions with a T-test p-value less than 0.05 and a Log2 fold change value greater than +/- 1.5 (DIO/lean). Log2 fold change values plotted against -log10 P-values.
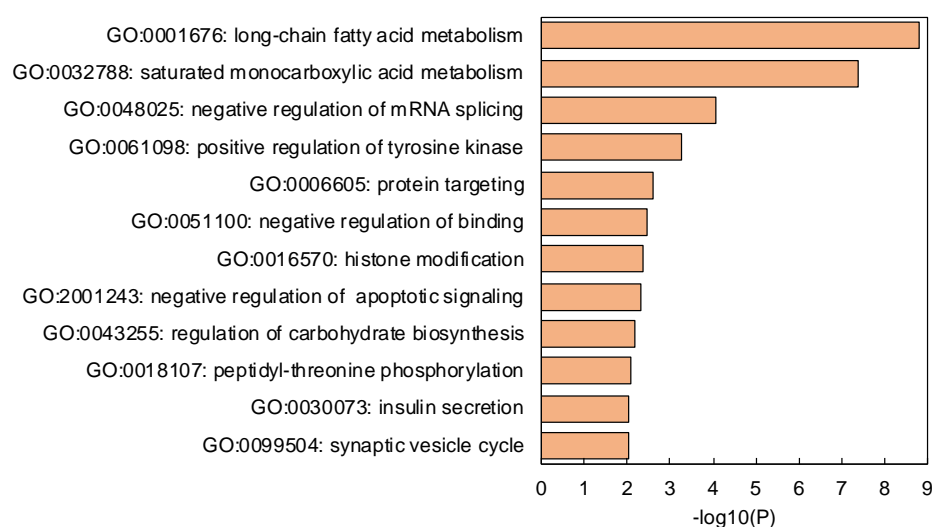
Figure 5-7. Proteins are differentially phosphorylated in livers of diet-induced obese (DIO) mice. Most enriched Kyoto Encyclopedia of Genes and Genomes (KEGG) pathways and Gene Ontology Biological Process (GO_BP) terms of proteins phosphorylated only in livers of DIO mice. A higher -log10(P-value) indicates more enriched.
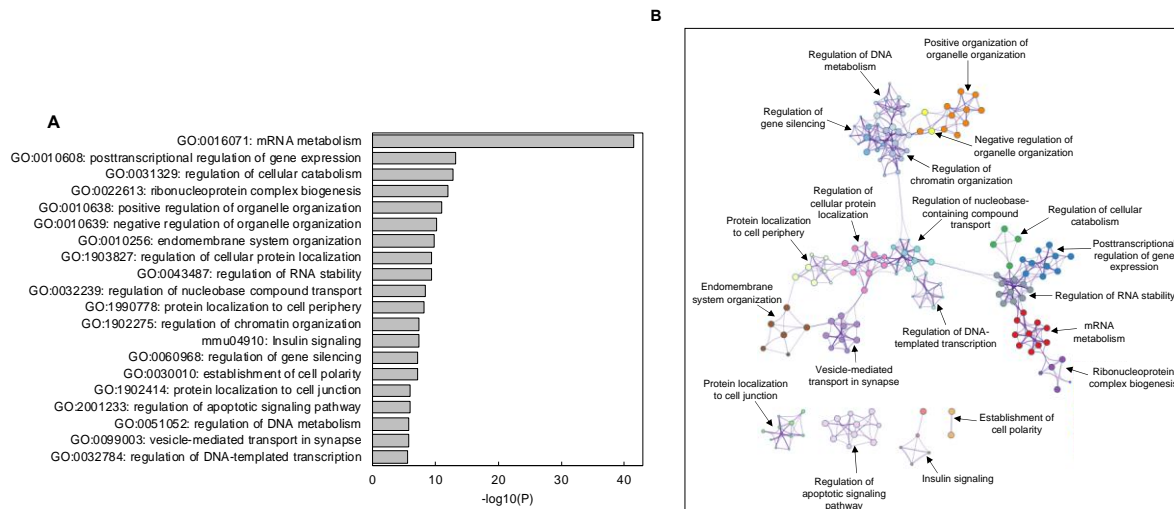
Figure 5-8. Functional annotation analysis of proteins phosphorylated in livers of both diet-induced obese (DIO) and lean mice. (A) Top 20 clusters of statistically enriched Kyoto Encyclopedia of Genes and Genomes (KEGG) pathways and Gene Ontology Biological Process (GO_BP) terms of proteins phosphorylated in livers of both DIO and lean mice. A higher -log10(P-value) indicates more enriched. (B) Enriched clusters of KEGG pathways and GO_BP terms of proteins phosphorylated in livers of both DIO and lean mice presented in network format. Statistically enriched similar terms are organized into clusters and colored based on the representative term for that cluster. Each circle within a colored cluster represents one term, and the size of the circle correlates with the number of proteins within that term. Similar terms are connected by a line, with a thicker line indicating higher similarity between terms. Enrichment values and cluster networks calculated in Metascape.

Figure 5-9. Graphical representation of a hepatocyte in the postprandial state from diet-induced obese (DIO) mice after a lipid meal. Interpretation of proteomic results in a biological context based on enriched functional annotation terms of proteins present at higher or lower levels in livers of DIO compared to lean mice. Proteins belonging to enriched metabolic pathways in fatty acid (FA) metabolism and transport, energy metabolism, and glucose metabolism are listed below the graphic. (1) lipoprotein and FA uptake; (2) FA activation/deactivation; (3) fatty acid oxidation (FAO); (4) tricarboxylic acid (TCA) cycle, electron transport chain (ETC), and ketogenesis; (5) gluconeogenesis and de novo FA, triacylglycerol, and cytoplasmic lipid droplet (CLD) synthesis; (6) glycogenesis; (7) glycogenolysis; (8) glycolysis; (9) transcription and mRNA splicing; (10) insulin signaling. ATP, adenosine triphosphate; CMr, chylomicron remnant; CoA, coenzyme A; PPARα, peroxisome proliferator-activated receptor alpha.

215

Table 5-1. Differential phosphosites between livers of DIO and lean mice. Of the proteins phosphorylated in livers of both DIO and lean mice, phosphosites identified in at least three out of four replicates per group and none in the other with a site localization probability of at least 0.9 were considered identified only in that condition. The specific peptide sequence and phosphorylation site for each protein are listed.

Uniprot ID	Protein names	Gene names	Site	Sequence	Localization probability	ID in
A0A2I3BRB9	Acyl-CoA-binding domain-containing protein 5	Acbd5	S208	Gp**S**FVQDIQSDIHTDSSR	0.999889	DIO
A2AQN5	Acetyl-coenzyme A synthetase, cytoplasmic	Acss2	S263	AELGMND**p**SPSQSPPVK	0.967351	Lean
A2AQN5	Acetyl-coenzyme A synthetase, cytoplasmic	Acss2	S267	AELGMNDSPSQ**p**SPPVK	0.993513	Lean
B1AZ15	Cordon-bleu protein-like 1	Cobll1	S761	QD**p**SNPKPKPSNEITR	0.999996	DIO
Q9CQV4	Protein FAM134C	Fam134c	T307	GQ**p**TPLTEGSEDLDGHSDPEESFAR	0.999949	DIO
A0A571BFA7	Protein FAM83H	Fam83h	S1126	RG**p**SPTTGLMEQK	0.981419	DIO
Q9Z204	Heterogeneous nuclear ribonucleoproteins C1/C2	Hnrnpc	S241	**p**SEEEQSSASVK	0.99998	DIO
B1B1A8	Myosin light chain kinase, smooth muscle	Mylk	S364	VPAIGSF**p**SPGEDRK	0.977889	DIO
E9Q3G8		Nup153	S339	RIPSAVSSPLN**p**SPLDR	0.963496	Lean
Q61136	Serine/threonine-protein kinase PRP4 homolog	Prpf4b	S278	K**p**SPIVNER	1	DIO
D3Z4K1	mRNA cap guanine-N7 methyltransferase	Rnmt	S11	ASVA**p**SDPESPPGGNEPAAASGQR	0.90046	DIO
Q6NZR5		Skiv2l	S253	AS**p**SLEDLVLK	0.994042	DIO
A2A8V9	Serine/arginine repetitive matrix protein 1	Srrm1	S669	RRSP**p**SLSSK	0.990717	DIO
Q8BTI8	Serine/arginine repetitive matrix protein 2	Srrm2	S882	SSTPPRQ**p**SPSR	0.942625	DIO
Q8BTI8	Serine/arginine repetitive matrix protein 2	Srrm2	S875	VK**p**SSTPPRQSPSR	0.931743	DIO
Q64511	DNA topoisomerase 2-beta	Top2b	S1324	RNPW**p**SDDESKSESDLEEAEPVVIPR	1	DIO
Q64511	DNA topoisomerase 2-beta	Top2b	S1328	RNPWSDDE**p**SKSESDLEEAEPVVIPR	1	DIO
Q64511	DNA topoisomerase 2-beta	Top2b	S1330	RNPWSDDESK**p**SESDLEEAEPVVIPR	1	DIO
Q64511	DNA topoisomerase 2-beta	Top2b	S1332	RNPWSDDESKSE**p**SDLEEAEPVVIPR	1	DIO

5.9 References

[1]   S.A. Polyzos, J. Kountouras, C.S. Mantzoros, Obesity and nonalcoholic fatty liver disease: From pathophysiology to therapeutics, Metabolism 92 (2019) 82-97.

[2]   S.L. Friedman, B.A. Neuschwander-Tetri, M. Rinella, A.J. Sanyal, Mechanisms of NAFLD development and therapeutic strategies, Nat Med 24(7) (2018) 908-922.

[3]   Z.M. Younossi, Non-alcoholic fatty liver disease - A global public health perspective, J Hepatol 70(3) (2019) 531-544.

[4]   A. Lonardo, F. Nascimbeni, A. Mantovani, G. Targher, Hypertension, diabetes, atherosclerosis and NASH: Cause or consequence?, J Hepatol 68(2) (2018) 335-352.

[5]   N. Matikainen, S. Mänttäri, J. Westerbacka, S. Vehkavaara, N. Lundbom, H. Yki-Järvinen, M.R. Taskinen, Postprandial lipemia associates with liver fat content, J Clin Endocrinol Metab 92(8) (2007) 3052-9.

[6]   A. Leon-Acuña, J.F. Alcala-Diaz, J. Delgado-Lista, J.D. Torres-Peña, J. Lopez-Moreno, A. Camargo, A. Garcia-Rios, C. Marin, F. Gomez-Delgado, J. Caballero, B. Van-Ommen, M.M. Malagon, P. Perez-Martinez, J. Lopez-Miranda, Hepatic insulin resistance both in prediabetic and diabetic patients determines postprandial lipoprotein metabolism: from the CORDIOPREV study, Cardiovasc Diabetol 15 (2016) 68.

[7]   M.C. Moore, K.C. Coate, J.J. Winnick, Z. An, A.D. Cherrington, Regulation of hepatic glucose uptake and storage in vivo, Adv Nutr 3(3) (2012) 286-94.

[8]   I. Martínez-Reyes, N.S. Chandel, Mitochondrial TCA cycle metabolites control physiology and disease, Nat Commun 11(1) (2020) 102.

[9]   P. Nguyen, V. Leray, M. Diez, S. Serisier, J. Le Bloc'h, B. Siliart, H. Dumon, Liver lipid metabolism, J Anim Physiol Anim Nutr (Berl) 92(3) (2008) 272-83.

[10]   G.F. Lewis, N.M. O'Meara, P.A. Soltys, J.D. Blackman, P.H. Iverius, A.F. Druetzler, G.S. Getz, K.S. Polonsky, Postprandial lipoprotein metabolism in normal and obese subjects: comparison after the vitamin A fat-loading test, J Clin Endocrinol Metab 71(4) (1990) 1041-50.

[11]   C.J. Green, L. Hodson, The influence of dietary fat on liver fat accumulation, Nutrients 6(11) (2014) 5018-33.

[12]   R. Aebersold, M. Mann, Mass spectrometry-based proteomics, Nature 422(6928) (2003) 198-207.

[13]   B. Aslam, M. Basit, M.A. Nisar, M. Khurshid, M.H. Rasool, Proteomics: Technologies and Their Applications, J Chromatogr Sci 55(2) (2017) 182-196.

[14] Y. Zhu, R. Zhao, P.D. Piehowski, R.J. Moore, S. Lim, V.J. Orphan, L. Paša-Tolić, W.J. Qian, R.D. Smith, R.T. Kelly, Subnanogram proteomics: impact of LC column selection, MS instrumentation and data analysis strategy on proteome coverage for trace samples, Int J Mass Spectrom 427 (2018) 4-10.

[15] E. Rodriguez-Suarez, J.M. Mato, F. Elortza, Proteomics analysis of human nonalcoholic fatty liver, Methods Mol Biol 909 (2012) 241-58.

[16] A. Valle, V. Catalán, A. Rodríguez, F. Rotellar, V. Valentí, C. Silva, J. Salvador, G. Frühbeck, J. Gómez-Ambrosi, P. Roca, J. Oliver, Identification of liver proteins altered by type 2 diabetes mellitus in obese subjects, Liver Int 32(6) (2012) 951-61.

[17] S. Caira, A. Iannelli, R. Sciarrillo, G. Picariello, G. Renzone, A. Scaloni, P. Addeo, Differential representation of liver proteins in obese human subjects suggests novel biomarkers and promising targets for drug development in obesity, J Enzyme Inhib Med Chem 32(1) (2017) 672-682.

[18] J. Wattacheril, K.L. Rose, S. Hill, C. Lanciault, C.R. Murray, K. Washington, B. Williams, W. English, M. Spann, R. Clements, N. Abumrad, C.R. Flynn, Non-alcoholic fatty liver disease phosphoproteomics: A functional piece of the precision puzzle, Hepatol Res 47(13) (2017) 1469-1483.

[19] N. Krahmer, B. Najafi, F. Schueder, F. Quagliarini, M. Steger, S. Seitz, R. Kasper, F. Salinas, J. Cox, N.H. Uhlenhaut, T.C. Walther, R. Jungmann, A. Zeigerer, G.H.H. Borner, M. Mann, Organellar Proteomics and Phospho-Proteomics Reveal Subcellular Reorganization in Diet-Induced Hepatic Steatosis, Dev Cell 47(2) (2018) 205-221.e7.

[20] E. Sabidó, Y. Wu, L. Bautista, T. Porstmann, C.Y. Chang, O. Vitek, M. Stoffel, R. Aebersold, Targeted proteomics reveals strain-specific changes in the mouse insulin and central metabolic pathways after a sustained high-fat diet, Mol Syst Biol 9 (2013) 681.

[21] O. Benard, J. Lim, P. Apontes, X. Jing, R.H. Angeletti, Y. Chi, Impact of high-fat diet on the proteome of mouse liver, J Nutr Biochem 31 (2016) 10-9.

[22] I.A. Kirpich, L.N. Gobejishvili, M. Bon Homme, S. Waigel, M. Cave, G. Arteel, S.S. Barve, C.J. McClain, I.V. Deaciuc, Integrated hepatic transcriptome and proteome analysis of mice with high-fat diet-induced nonalcoholic fatty liver disease, J Nutr Biochem 22(1) (2011) 38-45.

[23] Y. Guo, M. Darshi, Y. Ma, G.A. Perkins, Z. Shen, K.J. Haushalter, R. Saito, A. Chen, Y.S. Lee, H.H. Patel, S.P. Briggs, M.H. Ellisman, J.M. Olefsky, S.S. Taylor, Quantitative proteomic and functional analysis of liver mitochondria from high fat diet (HFD) diabetic mice, Mol Cell Proteomics 12(12) (2013) 3744-58.

[24] U. Edvardsson, H.B. von Löwenhielm, O. Panfilov, A.C. Nyström, F. Nilsson, B. Dahllöf, Hepatic protein expression of lean mice and obese diabetic mice treated with peroxisome proliferator-activated receptor activators, Proteomics 3(4) (2003) 468-78.

[25] J.M. Guzmán-Flores, E.C. Flores-Pérez, M. Hernández-Ortíz, S. López-Briones, J. Ramírez-Emiliano, S. Encarnación-Guevara, V. Pérez-Vázquez, Comparative Proteomics of Liver of the Diabetic Obese *db/db* and Non-Obese or Diabetic Mice, Current Proteomics 13 (2016) 231.

[26] A. Uchida, M.C. Whitsitt, T. Eustaquio, M.N. Slipchenko, J.F. Leary, J.X. Cheng, K.K. Buhman, Reduced triglyceride secretion in response to an acute dietary fat challenge in obese compared to lean mice, Front Physiol 3 (2012) 26.

[27] A. Uchida, H.J. Lee, J.X. Cheng, K.K. Buhman, Imaging cytoplasmic lipid droplets in enterocytes and assessing dietary fat absorption, Methods Cell Biol 116 (2013) 151-66.

[28] A. Uchida, M.N. Slipchenko, T. Eustaquio, J.F. Leary, J.X. Cheng, K.K. Buhman, Intestinal acyl-CoA:diacylglycerol acyltransferase 2 overexpression enhances postprandial triglyceridemic response and exacerbates high fat diet-induced hepatic triacylglycerol storage, Biochim Biophys Acta 1831(8) (2013) 1377-85.

[29] A.C. Searleman, A.B. Iliuk, T.S. Collier, L.A. Chodosh, W.A. Tao, R. Bose, Tissue phosphoproteomics with PolyMAC identifies potential therapeutic targets in a transgenic mouse model of HER2 positive breast cancer, Electrophoresis 35(24) (2014) 3463-9.

[30] A.J. Barabas, U.K. Aryal, B.N. Gaskill, Proteome characterization of used nesting material and potential protein sources from group housed male mice, Mus musculus, Sci Rep 9(1) (2019) 17524.

[31] J. Cox, M.Y. Hein, C.A. Luber, I. Paron, N. Nagaraj, M. Mann, Accurate proteome-wide label-free quantification by delayed normalization and maximal peptide ratio extraction, termed MaxLFQ, Mol Cell Proteomics 13(9) (2014) 2513-26.

[32] J. Cox, N. Neuhauser, A. Michalski, R.A. Scheltema, J.V. Olsen, M. Mann, Andromeda: a peptide search engine integrated into the MaxQuant environment, J Proteome Res 10(4) (2011) 1794-805.

[33] J. Cox, M. Mann, MaxQuant enables high peptide identification rates, individualized p.p.b.-range mass accuracies and proteome-wide protein quantification, Nat Biotechnol 26(12) (2008) 1367-72.

[34] Y. Zhou, B. Zhou, L. Pache, M. Chang, A.H. Khodabakhshi, O. Tanaseichuk, C. Benner, S.K. Chanda, Metascape provides a biologist-oriented resource for the analysis of systems-level datasets, Nat Commun 10(1) (2019) 1523.

[35] J. Chong, O. Soufan, C. Li, I. Caraus, S. Li, G. Bourque, D.S. Wishart, J. Xia, MetaboAnalyst 4.0: towards more transparent and integrative metabolomics analysis, Nucleic Acids Res 46(W1) (2018) W486-w494.

[36] S.E. Ehrlicher, H.D. Stierwalt, S.A. Newsom, M.M. Robinson, Skeletal muscle autophagy remains responsive to hyperinsulinemia and hyperglycemia at higher plasma insulin concentrations in insulin-resistant mice, Physiol Rep 6(14) (2018) e13810.

[37] F.P. la Fuente, L. Quezada, C. Sepúlveda, M. Monsalves-Alvarez, J.M. Rodríguez, C. Sacristán, M. Chiong, M. Llanos, A. Espinosa, R. Troncoso, Exercise regulates lipid droplet dynamics in normal and fatty liver, Biochim Biophys Acta Mol Cell Biol Lipids 1864(12) (2019) 158519.

[38] E.L. Huttlin, M.P. Jedrychowski, J.E. Elias, T. Goswami, R. Rad, S.A. Beausoleil, J. Villén, W. Haas, M.E. Sowa, S.P. Gygi, A tissue-specific atlas of mouse protein phosphorylation and expression, Cell 143(7) (2010) 1174-89.

[39] J.A. van Diepen, P.A. Jansen, D.B. Ballak, A. Hijmans, G.J. Hooiveld, S. Rommelaere, F. Galland, P. Naquet, F.P. Rutjes, R.P. Mensink, P. Schrauwen, C.J. Tack, M.G. Netea, S. Kersten, J. Schalkwijk, R. Stienstra, PPAR-alpha dependent regulation of vanin-1 mediates hepatic lipid metabolism, J Hepatol 61(2) (2014) 366-72.

[40] S. Rommelaere, V. Millet, T. Gensollen, C. Bourges, J. Eeckhoute, N. Hennuyer, E. Baugé, L. Chasson, I. Cacciatore, B. Staels, G. Pitari, F. Galland, P. Naquet, PPARalpha regulates the production of serum Vanin-1 by liver, FEBS Lett 587(22) (2013) 3742-8.

[41] P. Ortega-Prieto, C. Postic, Carbohydrate Sensing Through the Transcription Factor ChREBP, Front Genet 10 (2019) 472.

[42] L.K. Sharma, J. Lu, Y. Bai, Mitochondrial respiratory complex I: structure, function and implication in human diseases, Curr Med Chem 16(10) (2009) 1266-77.

[43] M. Rakhshandehroo, B. Knoch, M. Muller, S. Kersten, Peroxisome proliferator-activated receptor alpha target genes, PPAR Res 2010 (2010) 612089.

[44] L. Fang, M. Zhang, Y. Li, Y. Liu, Q. Cui, N. Wang, PPARgene: A Database of Experimentally Verified and Computationally Predicted PPAR Target Genes, PPAR Res 2016 (2016) 6042162.

[45] H.E. Popeijus, S.D. van Otterdijk, S.E. van der Krieken, M. Konings, K. Serbonij, J. Plat, R.P. Mensink, Fatty acid chain length and saturation influences PPARα transcriptional activation and repression in HepG2 cells, Mol Nutr Food Res 58(12) (2014) 2342-9.

[46] W. Motomura, T. Yoshizaki, N. Takahashi, S. Kumei, Y. Mizukami, S.J. Jang, Y. Kohgo, Analysis of vanin-1 upregulation and lipid accumulation in hepatocytes in response to a high-fat diet and free fatty acids, J Clin Biochem Nutr 51(3) (2012) 163-9.

[47]   J.A. van Diepen, P.A. Jansen, D.B. Ballak, A. Hijmans, F.P.J.T. Rutjes, C.J. Tack, M.G. Netea, J. Schalkwijk, R. Stienstra, Genetic and pharmacological inhibition of vanin-1 activity in animal models of type 2 diabetes, Sci Rep 6 (2016) 21906.

[48]   S. Chen, W. Zhang, C. Tang, X. Tang, L. Liu, C. Liu, Vanin-1 is a key activator for hepatic gluconeogenesis, Diabetes 63(6) (2014) 2073-85.

[49]   C. Berruyer, F.M. Martin, R. Castellano, A. Macone, F. Malergue, S. Garrido-Urbani, V. Millet, J. Imbert, S. Duprè, G. Pitari, P. Naquet, F. Galland, Vanin-1-/- mice exhibit a glutathione-mediated tissue resistance to oxidative stress, Mol Cell Biol 24(16) (2004) 7214-24.

[50]   S.C. Lu, Regulation of glutathione synthesis, Mol Aspects Med 30(1-2) (2009) 42-59.

[51]   P. Puchalska, P.A. Crawford, Multi-dimensional Roles of Ketone Bodies in Fuel Metabolism, Signaling, and Therapeutics, Cell Metab 25(2) (2017) 262-284.

[52]   J.D. McGarry, D.W. Foster, Regulation of hepatic fatty acid oxidation and ketone body production, Annu Rev Biochem 49 (1980) 395-420.

[53]   R.B. Bazotte, L.G. Silva, F.P. Schiavon, Insulin resistance in the liver: deficiency or excess of insulin?, Cell Cycle 13(16) (2014) 2494-500.

[54]   K. Begriche, J. Massart, M.A. Robin, F. Bonnet, B. Fromenty, Mitochondrial adaptations and dysfunctions in nonalcoholic fatty liver disease, Hepatology 58(4) (2013) 1497-507.

[55]   Z. Chen, R. Tian, Z. She, J. Cai, H. Li, Role of oxidative stress in the pathogenesis of nonalcoholic fatty liver disease, Free Radic Biol Med 152 (2020) 116-141.

[56]   M. Léveillé, J.L. Estall, Mitochondrial Dysfunction in the Transition from NASH to HCC, Metabolites 9(10) (2019) 233.

[57]   N.E. Sunny, F. Bril, K. Cusi, Mitochondrial Adaptation in Nonalcoholic Fatty Liver Disease: Novel Mechanisms and Treatment Strategies, Trends Endocrinol Metab 28(4) (2017) 250-260.

[58]   T. Li, J.Y. Chiang, Bile acid signaling in metabolic disease and drug therapy, Pharmacol Rev 66(4) (2014) 948-83.

[59]   M.J. Perez, O. Briz, Bile-acid-induced cell injury and protection, World J Gastroenterol 15(14) (2009) 1677-89.

[60]   D.M. Townsend, K.D. Tew, The role of glutathione-S-transferase in anti-cancer drug resistance, Oncogene 22(47) (2003) 7369-75.

[61]   C. Lebeaupin, D. Vallée, Y. Hazari, C. Hetz, E. Chevet, B. Bailly-Maitre, Endoplasmic reticulum stress signalling and the pathogenesis of non-alcoholic fatty liver disease, J Hepatol 69(4) (2018) 927-947.

[62]   D. Senft, Z.A. Ronai, UPR, autophagy, and mitochondria crosstalk underlies the ER stress response, Trends Biochem Sci 40(3) (2015) 141-8.

[63]   S. Deegan, S. Saveljeva, A.M. Gorman, A. Samali, Stress-induced self-cannibalism: on the regulation of autophagy by endoplasmic reticulum stress, Cell Mol Life Sci 70(14) (2013) 2425-41.

[64]   H. Chino, T. Hatta, T. Natsume, N. Mizushima, Intrinsically Disordered Protein TEX264 Mediates ER-phagy, Mol Cell 74(5) (2019) 909-921.e6.

[65]   H. An, A. Ordureau, J.A. Paulo, C.J. Shoemaker, V. Denic, J.W. Harper, TEX264 Is an Endoplasmic Reticulum-Resident ATG8-Interacting Protein Critical for ER Remodeling during Nutrient Stress, Mol Cell 74(5) (2019) 891-908.e10.

[66]   Y. Bian, C. Song, K. Cheng, M. Dong, F. Wang, J. Huang, D. Sun, L. Wang, M. Ye, H. Zou, An enzyme assisted RP-RPLC approach for in-depth analysis of human liver phosphoproteome, J Proteomics 96 (2014) 253-62.

[67]   S. Ferdinandusse, K.D. Falkenberg, J. Koster, P.A. Mooyer, R. Jones, C.W.T. van Roermund, A. Pizzino, M. Schrader, R.J.A. Wanders, A. Vanderver, H.R. Waterham, ACBD5 deficiency causes a defect in peroxisomal very long-chain fatty acid metabolism, J Med Genet 54(5) (2017) 330-337.

[68]   M.A. Westin, S.E. Alexson, M.C. Hunt, Molecular cloning and characterization of two mouse peroxisome proliferator-activated receptor alpha (PPARalpha)-regulated peroxisomal acyl-CoA thioesterases, J Biol Chem 279(21) (2004) 21841-8.

[69]   H. Sone, H. Shimano, Y. Sakakura, N. Inoue, M. Amemiya-Kudo, N. Yahagi, M. Osawa, H. Suzuki, T. Yokoo, A. Takahashi, K. Iida, H. Toyoshima, A. Iwama, N. Yamada, Acetyl-coenzyme A synthetase is a lipogenic enzyme controlled by SREBP-1 and energy status, Am J Physiol Endocrinol Metab 282(1) (2002) E222-30.

[70]   Z. Huang, M. Zhang, A.A. Plec, S.J. Estill, L. Cai, J.J. Repa, S.L. McKnight, B.P. Tu, ACSS2 promotes systemic fat storage and utilization through selective regulation of genes involved in lipid metabolism, Proc Natl Acad Sci U S A 115(40) (2018) E9499-e9506.

[71]   P.V. Hornbeck, B. Zhang, B. Murray, J.M. Kornhauser, V. Latham, E. Skrzypek, PhosphoSitePlus, 2014: mutations, PTMs and recalibrations, Nucleic Acids Res 43(Database issue) (2015) D512-20.

[72]   X. Li, W. Yu, X. Qian, Y. Xia, Y. Zheng, J.H. Lee, W. Li, J. Lyu, G. Rao, X. Zhang, C.N. Qian, S.G. Rozen, T. Jiang, Z. Lu, Nucleus-Translocated ACSS2 Promotes Gene Transcription for Lysosomal Biogenesis and Autophagy, Mol Cell 66(5) (2017) 684-697.e9.

[73]   C. Naro, C. Sette, Phosphorylation-mediated regulation of alternative splicing in cancer, Int J Cell Biol 2013 (2013) 151839.

[74]   T. Misteli, RNA splicing: What has phosphorylation got to do with it?, Curr Biol 9(6) (1999) R198-200.

[75]   N.J.G. Webster, Alternative RNA Splicing in the Pathogenesis of Liver Disease, Front Endocrinol (Lausanne) 8 (2017) 133.

[76]   J. Pihlajamäki, C. Lerin, P. Itkonen, T. Boes, T. Floss, J. Schroeder, F. Dearie, S. Crunkhorn, F. Burak, J.C. Jimenez-Chillaron, T. Kuulasmaa, P. Miettinen, P.J. Park, I. Nasser, Z. Zhao, Z. Zhang, Y. Xu, W. Wurst, H. Ren, A.J. Morris, S. Stamm, A.B. Goldfine, M. Laakso, M.E. Patti, Expression of the splicing factor gene SFRS10 is reduced in human obesity and contributes to enhanced lipogenesis, Cell Metab 14(2) (2011) 208-18.

CHAPTER 6 SUMMARY AND FUTURE DIRECTIONS

6.1 Summary

The ever-increasing incidence of MetS and its associated disorders has led to greater prevalence of metabolic diseases including CVD, NAFLD/MAFLD, and cancer. Therefore, identifying contributing factors to the development or progression of these diseases is critical for their prevention or treatment. The accumulation of neutral lipid in CLDs is a characteristic feature and contributing factor to metabolic disease and therefore may serve as a therapeutic target. The research included in this dissertation utilized proteomic methods to examine the role of CLDs in metabolic diseases including cancer, NAFLD/MAFLD, and enterocytes during the process of dietary fat absorption, a determinant of CVD risk and development.

We determined that CLDs in human metastatic breast cancer cells display novel associated proteins that may serve as contributing factors to disrupted cellular metabolism and metastasis. This first report of the CLD proteome from metastatic breast cancer cells created a hypothesis-generating list of proteins that can be further examined in functional studies to determine their role in metastasis. This research is important to both the CLD and cancer field as it widens our knowledge about the proteins that associate with CLDs in disease states and also provides insight as to how CLDs and their proteins contribute to cancer aggressiveness.

We determined differences in dietary fat processing and storage in enterocyte CLDs along the length of the small intestine in lean and DIO mice in response to dietary fat. This study was the first to characterize CLDs in each intestine region and helped to characterize the physiological response to dietary fat in enterocytes during the process of dietary fat absorption in lean and obese states. The data we generated can be applied to the understanding of distal intestine lipid metabolism as well as how CLDs may be differentially metabolized in each region or in obesity based on their characteristics and associated proteins. This allows for the identification of novel factors regulating CLD metabolism and dietary fat absorption in each region, which may be utilized for the development of therapeutic strategies targeting intestinal fat absorption, hypertriglyceridemia, and CVD.

We identified potential molecular mediators of the intestinal response to GLP-2 and helped define the intestinal TAG pool mobilized by GLP-2. This is the first study analyzing human

enterocytes by TEM as well as the intestinal tissue proteome in the response to GLP-2. The results from this study support the mobilization of post-enterocyte TAG pools by GLP-2 and identified proteins that may be contributing to the response. This research extends our knowledge on where dietary fat can be stored in the intestine as well as the physiological factors that stimulate intestinal dietary fat absorption. Overall, this insight may help in the development of therapies targeting the intestine or GLP-2 to reduce TAG secretion, hyperlipidemia, and CVD.

Lastly, we identified differentially expressed proteins and phosphoproteins in livers of DIO compared to lean mice in the postprandial state, reflecting altered activity of hepatic metabolic pathways and nutrient utilization in obesity-associated hepatosteatosis. This study was the first to characterize the liver proteome in DIO and lean mice in a controlled postprandial state, and by using comparative proteomic analysis we were able to identify potentially disrupted energy and nutrient metabolism pathways in liver of DIO mice. The data we generated can be used in future studies to confirm the consequence of altered proteins and phosphoproteins on cellular metabolism in NAFLD and how this may influence systemic homeostasis during obesity.

In conclusion, this dissertation research furthers our understanding of the role of CLDs in metabolic disease and has uncovered candidate factors regulating CLD and/or cellular metabolism. These factors have potential to be exploited for the development of targeted therapies that modulate cellular lipid storage in order to prevent or treat metabolic disease.

6.2 Future directions

6.2.1 Determining the function of CLD proteins

Although CLD proteomic studies allow for the untargeted identification of hundreds if not thousands of proteins, the function of many of these proteins on CLDs remains elusive. Appreciating the function of CLD proteins is required in order to understand the role or utilization of CLDs in different cell types and disease states. However, determining the function of a CLD protein is a daunting task, as many proteins identified in CLD proteomic studies are due to contamination of the isolated CLD fraction with other organellar proteins [1] and must be validated at the CLD by imaging images, and choosing a relevant protein of interest out of a large list of potential options is often an educated guess. However, several methods of analyzing CLD proteome datasets may help to uncover novel CLD proteins worth pursuing, including comparison

to other cell types or disease states, performing functional annotation and metabolic pathway analysis, and literature searching to determine the general role and cellular localization of specific proteins.

6.2.1.1 CLD proteins in cancer and metastasis

Determining the function of proteins that associate with CLDs in metastatic breast cancer cells is necessary to understand the function of CLDs in cancer and metastasis. One method to determine how CLDs and their proteins contribute to metastasis is to perform a comparative proteomic analysis of the CLD proteins isolated from non-metastatic and metastatic breast cancer cells. The presence or absence of certain proteins, or differences in their relative levels, may implicate a specific CLD protein in metastasis promotion or may indicate how CLDs may be differentially utilized in more aggressive metastatic cancers. A challenge with this method is the lack of CLDs in non-metastatic cancer cells [2, 3], making the choice of an adequate control for comparison difficult. Another method to determine how CLDs and their proteins contribute to breast cancer metastasis is to prevent CLD formation by inhibiting TAG synthesis enzymes or PLIN proteins and assess cellular factors known to be influenced by CLDs, including cell migration [4], ER and oxidative stress [5], FAO [6], and activation of proliferative and/or lipid-mediated signaling pathways [7]. This may reveal a core role of CLDs in one or more features of cancer that facilitate breast cancer progression. Similarly, inhibiting the localization of certain proteins of interest identified in CLD proteomic studies to CLDs and assessing the above parameters will help determine how CLD proteins contribute to the survival advantage conferred by CLDs in cancer cells.

6.2.1.2 CLD proteins in enterocytes during dietary fat absorption

Determining the function of CLD proteins in enterocytes is critical to identify regulators of CLD metabolism and CM secretion. As CLDs are thought to be mobilized over time and used for CM assembly and secretion, identifying factors regulating the balance between TAG storage and secretion establishes them as molecular targets that can be modulated in order to reduce or inhibit the absorption of dietary fat for the treatment of metabolic diseases associated with elevated CM secretion and hypertriglyceridemia. Although several proteins have been validated on CLDs

from mouse enterocytes [8, 9] and the human Caco-2 cell model of enterocytes [10, 11], most notably those involved in lipid metabolism, only some have been functionally investigated. For example, proteome analysis of CLDs isolated from Caco-2 cells identified 17β-hydroxysteroid dehydrogenase type 2 (DHB2), an enzyme involved in the metabolism of steroid hormones, which was confirmed to localize to CLDs and prevent TAG secretion in part by controlling cellular testosterone concentrations [10]. Therefore, future research in the intestinal CLD field should be directed towards determining the function of CLD proteins and their effects on TAG storage and secretion in order to better understand and target the complex process of dietary fat absorption. These studies would entail modulating the localization of specific proteins of interest to CLDs in enterocytes and assessing CLD metabolism and CM secretion.

6.2.2 Molecular mechanisms of triacylglycerol mobilization by physiological factors

Several studies, including Chapter 4 of this dissertation, have confirmed a role for physiological factors such as glucose and GLP-2 in intestinal TAG mobilization [12], however the molecular mechanisms responsible for initiating or mediating their effects are unknown. Adding to the complication is that each factor potentially acts by different mechanisms; such appears the be the case for glucose and GLP-2 [13]. Identifying how physiological factors stimulate intestinal TAG mobilization is critical in understanding how the process of dietary fat absorption is regulated, how disease states may differentially activate these physiological factors to contribute to abnormal lipid metabolism and blood lipid concentrations, and to identify molecular targets that can be modified to reduce the absorption of dietary fat and prevent or treat metabolic diseases including CVD.

Physiological factors may stimulate intestinal TAG mobilization by several mechanisms. First, they may activate cellular signaling pathways that increase the activity of lipolytic enzymes at the CLD surface to release FA to be used for CM assembly. Alternatively, they may directly activate lipolysis enzymes or other unidentified intracellular factors that mediate the mobilization of TAG stores. A major unanswered question in the intestinal lipid metabolism field is the identity of the enzyme responsible for directing FA released from CLDs to the ER for CM assembly, as well as the factors or enzymes that partition TAG into separate pools for CM assembly or CLD formation. Identifying these factors may be key in determining the molecular action of physiological factors that mobilize CLDs for CM secretion, such as glucose [14]. Physiological

factors may instead stimulate extracellular elements that are responsible for TAG mobilization, including activating blood or lymph flow which in turn stimulates CM movement through the pathway. Although the actions of GLP-2 on intestinal TAG mobilization are associated with these mechanisms [15], how exactly it does this has not been defined. One place to start investigating the molecular actions of GLP-2 may be examining known mediators of GLP-2 on the intestinal absorption of other nutrients, including the enteric nervous system and mTORC1 pathway involved in GLP-2 mediated amino acid absorption [16], or the PI3K pathway involved in GLP-2 mediated glucose absorption [17]. To determine whether these pathways are involved in GLP-2 mediated TAG release, we would inhibit these pathways then assess intestinal TAG release upon stimulation with GLP-2. Future studies focused on identifying intra- and extra-cellular targets of physiological factors and their molecular mechanisms of intestinal TAG mobilization will lead to a greater understanding the dynamics of dietary fat absorption and potential areas for regulation.

6.2.3 Role of CLDs and bile acid metabolism in the distal intestine

In Chapter 3, we identified Fabp6 as a novel CLD protein that localizes to CLDs in the distal region of the small intestine. As Fabp6 is involved in bile acid metabolism, we hypothesized that CLDs may regulate or interfere with bile acid signaling or trafficking in the distal intestine during the enterohepatic circulation. This is significant for several regions. First, since lipid reaches the distal region of the small intestine generally only with consumption of large amounts of dietary fat, lipid may continually be stored in CLDs in distal enterocytes with chronic high fat diets, in turn interfering with bile acid signaling, reabsorption, and modification. These changes may alter the bile acid pool and systemic bile acid homeostasis, which can affect factors regulated by bile acids including nutrient and energy metabolism, dietary fat absorption, and the gut microbiota [18]. Therefore, altered bile acid signaling due to the presence of CLDs in the distal intestine may contribute to the negative health consequences of chronic high fat diets. On the other hand, the distal region of the intestine is exposed to greater levels of dietary fat with certain types of bariatric surgery, including Roux-en-Y gastric bypass. Whether CLDs form in enterocytes of the distal intestine in response to consumption of dietary fat in patients who have undergone Roux-en-Y gastric bypass has not been examined. However, bariatric surgery is associated with positive health outcomes, including weight loss and increased insulin sensitivity [19, 20]. Whether this is mediated by altered bile acid signaling due to the presence of CLDs is unknown. Alternatively,

the localization of Fabp6 on CLDs in the distal region also suggests CLDs may instead store bile acids, which would uncover a novel aspect of enterohepatic circulation of bile acids.

In order to determine whether CLDs present in enterocytes of the distal region of the small intestine influence bile acid metabolism, several experiments are needed. First, we would assess the expression of bile-acid regulated genes in distal enterocytes and the liver of fasted mice (without CLDs in distal enterocytes) and mice administered an oil gavage (with CLDs in distal enterocytes) to determine whether the presence of CLDs interferes with bile acid signaling. If CLDs do inhibit the transport of bile acids through the cell and therefore prevent them from activating proper gene expression, we would expect a decrease or increase in the mRNA levels of proteins normally positively or negatively regulated by bile acids in enterocytes such as FGF15, ASBT, or OSTα/β [21]. In addition, we would analyze the composition and concentration of the bile acid pool to determine whether bile acid modification or reabsorption is influenced by CLDs in the distal region. Finally, to determine whether bile acids are stored in CLDs in enterocytes of the distal intestine, we would either perform lipidomic analysis on CLDs isolated from distal enterocytes or administer mice an oral gavage containing labeled bile acids and assess CLD formation and composition in distal enterocytes. Overall, these future studies aim to determine the role of CLDs in bile acid metabolism distal enterocytes, which may provide new insight as to the effect of high fat diets and lipid processing in the distal intestine on bile acid signaling and metabolism.

6.2.4 Hepatic proteome and phosphoproteome in the postprandial response to a lipid meal

In Chapter 5, we compared the proteome and phosphoproteome of liver from DIO and lean mice in the postprandial state, which provided new insight as to the molecular adaptations that occur in the liver in obesity-associated hepatosteatosis. However, we were unable to determine how livers in DIO mice may differentially respond to incoming nutrients compared to livers of lean mice, which would expand upon our previous study in the understanding of liver metabolism during different states of the fed/fast cycle in obesity. In fact, the postprandial response to a lipid meal is exacerbated in obesity, contributing to elevated blood TAG levels [22-24]. The molecular landscape present in the liver during obesity that contributes to these effects are not clear.

In order to determine the influence of obesity on the hepatic proteome and phosphoproteome in the postprandial response to dietary fat, we would collect liver samples from

lean and DIO mice in the fasting state, administer an olive oil gavage, then collect liver samples in the postprandial state from lean and DIO mice two hours after the gavage. Comparison of the liver proteome and phosphoproteome in the fasted and postprandial state in lean mice would be the control molecular response to a lipid meal. We would then compare the proteome and phosphoproteme of DIO mice in the fasted and postprandial state to that of lean mice. This will allow us to investigate differences in the relative levels of proteins involved in nutrient and energy metabolism pathways in order to identify how liver in obesity may differentially respond to and process a lipid meal. Based on our previous study of DIO and lean liver in the postprandial state, we expect altered levels of proteins involved in nutrient and energy metabolism pathways in the hepatic response to dietary fat in obesity, including lipid and glucose metabolism, indicating abnormal nutrient utilization. In addition, we expect an altered hepatic protein phosphorylation pattern in obesity which may indicate how metabolic pathways are differentially regulated to contribute to changes in nutrient and energy metabolism. Overall, this study would better define the molecular factors responsible for abnormal liver metabolism during obesity and may identify potential areas to target for the treatment of obesity-associated hepatosteatosis and its related conditions.

6.2.5 Future directions in proteomic research

Despite breakthroughs in proteomic instrumentation and methods, several challenges inherent in proteome research remain. These include characterizing every aspect of a protein, including its proteoforms [25], structure, folding properties, interacting partners, and cellular localization in order to better understand a protein's function [26]. Understanding the functional significance of these features is key in appreciating how cellular systems work and are regulated, as well as how dysfunctional protein interactions, modifications, or mislocalization contribute to disease states. Due to the sheer number and dynamic nature of biological proteins, determining these protein features on a large scale is a great feat. However, as proteomics is a rapidly developing field, it is likely these challenges will be addressed in the coming years and advance our understanding of the complexities of protein biology and their influence on metabolic disease.

6.3 References

[1]   K. Bersuker, C.W.H. Peterson, M. To, S.J. Sahl, V. Savikhin, E.A. Grossman, D.K. Nomura, J.A. Olzmann, A Proximity Labeling Strategy Provides Insights into the Composition and Dynamics of Lipid Droplet Proteomes, Dev Cell 44(1) (2018) 97-112.e7.

[2]   H. Abramczyk, J. Surmacki, M. Kopec, A.K. Olejnik, K. Lubecka-Pietruszewska, K. Fabianowska-Majewska, The role of lipid droplets and adipocytes in cancer. Raman imaging of cell cultures: MCF10A, MCF7, and MDA-MB-231 compared to adipocytes in cancerous human breast tissue, Analyst 140(7) (2015) 2224-35.

[3]   C. Nieva, M. Marro, N. Santana-Codina, S. Rao, D. Petrov, A. Sierra, The lipid phenotype of breast cancer cells characterized by Raman microspectroscopy: towards a stratification of malignancy, PLoS One 7(10) (2012) e46456.

[4]   C.J. Antalis, A. Uchida, K.K. Buhman, R.A. Siddiqui, Migration of MDA-MB-231 breast cancer cells depends on the availability of exogenous lipids and cholesterol esterification, Clin Exp Metastasis 28(8) (2011) 733-41.

[5]   P. Shyu, Jr., X.F.A. Wong, K. Crasta, G. Thibault, Dropping in on lipid droplets: insights into cellular stress and cancer, Biosci Rep 38(5) (2018) BSR20180764.

[6]   A. Pucer, V. Brglez, C. Payré, J. Pungerčar, G. Lambeau, T. Petan, Group X secreted phospholipase A(2) induces lipid droplet formation and prolongs breast cancer cell survival, Mol Cancer 12(1) (2013) 111.

[7]   A.L.S. Cruz, E.A. Barreto, N.P.B. Fazolini, J.P.B. Viola, P.T. Bozza, Lipid droplets: platforms with multiple functions in cancer hallmarks, Cell Death Dis 11(2) (2020) 105.

[8]   T. D'Aquila, D. Sirohi, J.M. Grabowski, V.E. Hedrick, L.N. Paul, A.S. Greenberg, R.J. Kuhn, K.K. Buhman, Characterization of the proteome of cytoplasmic lipid droplets in mouse enterocytes after a dietary fat challenge, PLoS One 10(5) (2015) e0126823.

[9]   T. D'Aquila, A.S. Zembroski, K.K. Buhman, Diet Induced Obesity Alters Intestinal Cytoplasmic Lipid Droplet Morphology and Proteome in the Postprandial Response to Dietary Fat, Front Physiol 10 (2019) 180.

[10]   F. Beilstein, J. Bouchoux, M. Rousset, S. Demignot, Proteomic Analysis of Lipid Droplets from Caco-2/TC7 Enterocytes Identifies Novel Modulators of Lipid Secretion, Plos One 8(1) (2013) 17.

[11]   J. Bouchoux, F. Beilstein, T. Pauquai, I.C. Guerrera, D. Chateau, N. Ly, M. Alqub, C. Klein, J. Chambaz, M. Rousset, J.M. Lacorte, E. Morel, S. Demignot, The proteome of cytosolic lipid droplets isolated from differentiated Caco-2/TC7 enterocytes reveals cell-specific characteristics, Biology of the Cell 103(11) (2011) 499-517.

[12]   C. Xiao, P. Stahel, A.L. Carreiro, K.K. Buhman, G.F. Lewis, Recent Advances in Triacylglycerol Mobilization by the Gut, Trends Endocrinol Metab 29(3) (2018) 151-163.

[13]   P. Stahel, C. Xiao, X. Davis, P. Tso, G.F. Lewis, Glucose and GLP-2 (Glucagon-Like Peptide-2) Mobilize Intestinal Triglyceride by Distinct Mechanisms, Arterioscler Thromb Vasc Biol 39(8) (2019) 1565-1573.

[14]   C. Xiao, P. Stahel, A.L. Carreiro, Y.H. Hung, S. Dash, I. Bookman, K.K. Buhman, G.F. Lewis, Oral Glucose Mobilizes Triglyceride Stores From the Human Intestine, Cell Mol Gastroenterol Hepatol 7(2) (2019) 313-337.

[15]   C. Xiao, P. Stahel, A. Nahmias, G.F. Lewis, Emerging Role of Lymphatics in the Regulation of Intestinal Lipid Mobilization, Front Physiol 10 (2019) 1604.

[16]   J. Lee, J. Koehler, B. Yusta, J. Bahrami, D. Matthews, M. Rafii, P.B. Pencharz, D.J. Drucker, Enteroendocrine-derived glucagon-like peptide-2 controls intestinal amino acid transport, Mol Metab 6(3) (2017) 245-255.

[17]   C.I. Cheeseman, Upregulation of SGLT-1 transport activity in rat jejunum induced by GLP-2 infusion in vivo, Am J Physiol 273(6) (1997) R1965-71.

[18]   T. Li, J.Y. Chiang, Bile acid signaling in metabolic disease and drug therapy, Pharmacol Rev 66(4) (2014) 948-83.

[19]   B. Laferrère, F. Pattou, Weight-Independent Mechanisms of Glucose Control After Roux-en-Y Gastric Bypass, Front Endocrinol (Lausanne) 9 (2018) 530.

[20]   A.H. Affinati, N.H. Esfandiari, E.A. Oral, A.T. Kraftson, Bariatric Surgery in the Treatment of Type 2 Diabetes, Curr Diab Rep 19(12) (2019) 156.

[21]   P.A. Dawson, T. Lan, A. Rao, Bile acid transporters, J Lipid Res 50(12) (2009) 2340-57.

[22]   N. Matikainen, S. Mänttäri, J. Westerbacka, S. Vehkavaara, N. Lundbom, H. Yki-Järvinen, M.R. Taskinen, Postprandial lipemia associates with liver fat content, J Clin Endocrinol Metab 92(8) (2007) 3052-9.

[23]   G.F. Lewis, N.M. O'Meara, P.A. Soltys, J.D. Blackman, P.H. Iverius, A.F. Druetzler, G.S. Getz, K.S. Polonsky, Postprandial lipoprotein metabolism in normal and obese subjects: comparison after the vitamin A fat-loading test, J Clin Endocrinol Metab 71(4) (1990) 1041-50.

[24]   A. Leon-Acuña, J.F. Alcala-Diaz, J. Delgado-Lista, J.D. Torres-Peña, J. Lopez-Moreno, A. Camargo, A. Garcia-Rios, C. Marin, F. Gomez-Delgado, J. Caballero, B. Van-Ommen, M.M. Malagon, P. Perez-Martinez, J. Lopez-Miranda, Hepatic insulin resistance both in prediabetic and diabetic patients determines postprandial lipoprotein metabolism: from the CORDIOPREV study, Cardiovasc Diabetol 15 (2016) 68.

[25]   L.M. Smith, N.L. Kelleher, Consortium for Top Down Proteomics, Proteoform: a single term describing protein complexity, Nat Methods 10(3) (2013) 186-7.

[26]   J.R. Yates, 3rd, Recent technical advances in proteomics, F1000Res 8 (2019) F1000 Faculty Rev-351.